DISSERTATION

CHARACTERIZATION OF THE INSTABILITY ELEMENTS PRESENT WITHIN THE 3' UTR OF THE GLUTAMINASE mRNA IN WKPT KIDNEY CELLS

Submitted by

Yeon Jean Lee

Department of Biochemistry and Molecular Biology

In partial fulfillment of the requirements

For the Degree of Doctor of Philosophy

Colorado State University

Fort Collins, Colorado

Fall 2006

COLORADO STATE UNIVERSITY

October 26, 2006

WE HEREBY RECOMMEND THAT THE DISSERTATION PREPARED UNDER OUR SUPERVISION BY YEON J. LEE ENTITLED CHARACTERIZATION OF THE INSTABILITY ELMENTS PRESENT WITHIN THE 3' UTR OF THE GLUTAMINASE mRNA IN WKPT KIDNEY CELLS BE ACCEPTED AS FULFILLING IN PART REQUIREMENTS FOR THE DEGREE OF DOCTOR OF PHILOSOPHY.

Committee on Graduate Work

James Bamburg

Paul Laybourn

Erica Suchman

Jeffrey Wilusz

Advisor- Norman Curthoys

Department Head- Marvin Paule

ABSTRACT OF DISSERTATION

CHARACTERIZATION OF THE INSTABILITY ELEMENTS PRESENT WITHIN THE 3' UTR OF THE GLUTAMINASE mRNA IN WKPT KIDNEY CELLS

During metabolic acidosis, the level of glutaminase (GA) is increased 8-fold within the renal proximal convoluted tubule. This adaptation contributes to the ability of the kidney to generate NH_4^+ and HCO_3^- ions from glutamine to facilitate the excretion of acids and partially restore acid-base balance. The increased GA expression results from increased stability of the GA mRNA that is mediated by two 8-base AU-sequences that function as pH-response elements (pHRE). This sequence binds ζ-cryst and p40-AUF1 with high affinity and specificity. An *in vitro* mRNA decay assay was developed using cytosolic extracts of WKPT cells, a line of rat renal proximal tubule cells.

A 28-nt segment containing the pHRE of GA mRNA was cloned into pGem-A_0 and pGem-A_{60} vectors. The two plasmids were transcribed in the presence of [α-^{32}P]-UTP and 500 μM ^{7met}GpppG to produce mRNAs that either lack or contain a 60-nt poly-A tail. The GemGA-A_{60} mRNA was used as a substrate for an *in vitro* mRNA turnover assay. As controls, *in vitro* decay of Gem-A_{60} and GemARE-A_{60} were also analyzed. The latter mRNA contains the AU-rich element that mediates the rapid turnover of TNFα mRNA. The turnover of GemGA-A_{60} mRNA was enhanced by addition of poly-A RNA and inhibited by p40-AUF1 and HuR. By contrast, the Gem-A_{60} mRNA was relatively stable when incubated with the WKPT extracts and its decay was not affected by addition of various RNA binding proteins. The addition of tristetraprolin (TTP) greatly enhanced deadenylation and degradation of GemARE-A_{60} mRNA, but only slightly stimulated the

decay of GemGA-A_{60} mRNA. The turnover rate of GemGA-A_{60} was greatly enhanced in a cytosolic extracts of a clonal line of WKPT cells that over express ζ-cryst by 36-fold. Omission of ATP and phosphocreatine also increased the rate of deadenylation and resulted in the accumulation of the fully deadenylated product. The data indicate that *in vitro* decay of GemGA-A_{60} mRNA is initiated by deadenylation and that this reaction is enhanced by endogenously expressed ζ-cryst and TTP and inhibited by p40-AUF1 and HuR. Subsequent degradation of the deadenylated RNA required ATP and thus, may be mediated by the exosome.

An i*n vitro* decapping assay demonstrated that both the 5'→3' and 3'→5' degradation pathways are involved in the turnover of the GA mRNA. Determination of whether 5'→3' or 3'→5' decay pathway predominates *in vivo* will require further analysis. Antibodies against ζ-cryst, total eIF2α and phospho-eIF2α were used in immunostaining experiments to reveal that phospho-eIF2α and ζ-cryst may co-localize in stress granules. The treatment of WKPT-ζ^+ cells with pH 6.9 medium activated the ER stress signaling pathway and resulted in the initial, but transient, association of ζ-cryst with stress granules. The completed experiments demonstrated the differential role of ARE binding proteins on the regulation of the GA mRNA, and the importance of localization of RNA:protein complexes as a possible determining factor of mRNA turnover.

Yeon Jean Lee
Department of Biochemistry
and Molecular Biology
Fort Collins, CO 80523
Fall 2006

ACKNOWLEDGMENTS

First and foremost, I would like to thank my advisor, Dr. Norman Curthoys, for being a wonderful mentor and for his patience and guidance throughout my graduate career. My achievement today would not have been accomplished without his support and guidance.

I would also like to thank my committee, Dr. James Bamburg, Dr. Paul Laybourn, Dr. Erica Suchman, and Dr. Jeff Wilusz, for their advice and guidance as well. I would especially like to thank Dr. James Bamburg and Laurie Minamide for taking me as an honorary member of their laboratory. And I would like to thank Dr. Jeff Wilusz and Dr. Carol Wilusz for helping to set up the *in vitro* systems and for the guidance they have provided throughout the project.

I would like to thank all of the Curthoys lab members, both past and present, for their friendship and support. I would like to thank Sachin Hajarnis, Moran O'Hayre and Jill Schroeder for their friendship throughout the graduate years. I would like Lynn Taylor and Hend Ibrahim for all the help they have given. I would also like to thank Mary Robinson for purifying some of the recombinant proteins used in my projects, and Sarah Lee for her work during her rotation in the lab.

I would like to express my gratitude to all of my friends in the department, especially the members of Bamburg lab, including Mike Maloney, Janice Gonzales, Kevin Flynn, Chi Pak, and Hilary Bowden for their friendship throughout the years and for all memories we shared. I would like to thank Chi Pak and Richard Davis for helping me with my immunostaining experiment. I also want to thank Vidya Subramanian and David Goldstrohm for their friendship and support. I would like to express my gratitude for Young-Mi Kim, who has treated me as I were her own sister, and provided enormous support throughout the years.

I would also like to thank Mateusz Opyrchal for helping me to set up the *in vitro* system and for his friendship. My friends, Jen Barth and Adam Guli, whom I have known for nearly a decade, have provided enormous support throughout the years. Words can not describe the depth of my gratitude for their friendship.

Special thanks must be made to my family for support, and encouragement throughout my life. My older sister, Hyong, was always there for me to help me to get through the hardships and to share the joys and happiness. My younger brother, Ki, always made me smile. My parents were always my inspiration to succeed, they always taught us to pursue our goals and dreams, and provided us with love and support. I would like to dedicate my hard work and accomplishment to my father, who has always been there for me and reminded me that I was loved.

Table of Contents

List of Figures and Tables

Abbreviations

8C - LLC-PK_1-F^+-8C

3' UTR – 3' untranslated region

5' cap – 5' 7-methyl-guanosine cap

ADH - alcohol dehydrogenase

AP-1 - activating protein-1

ARE –AU-rich element

ATP - activating transcription factor

ATP/PC – ATP/phosphocreatine

bp – base pair

βG – β-globin

bGH – bovine growth hormone

BME - β-mercaptoethanol

Brf - butyrate response factor

BSA – bovine serum albumin

CAT - chloramphenicol acetyltransferase

CHOP - CCAAT/enhancer-binding protein homologues protein

CMV – cytomegalovirus

DEPC – diethyl pyrocarbonate

DNA – deoxyribonucleic acid

DRB – 5,6-dichlorobenzimidazole 1-β-D-ribofuranoside

DTT – dithiothreitol

EDTA – ethylenediaminetetraacetic acid

eIF - eukaryotic translation initiation factor

EMSA – electrophoretic mobility shift assay

ER - endoplasmic reticulum

FBPase – fructose-1,6-bisphosphatase

FPLC – fast protein liquid chromatography

G418 – geneticin

GADD153 - growth arrest and DNA-damage-inducible protein

GAPDH – glyceraldehyde-3-phosphate dehydrogenase

GCN2 - general control non-derepressible-2

GDH – glutamate dehydrogenase

GA – glutaminase

GFP - green fluorescence protein

GM-CSF – granulocyte-macrophage colony-stimulating factor

His - histidine

HNF-1 - hepatic nuclear factor-1

hnRNP – heterogenous nuclear ribonucleoprotein

HRI - haem-regulated inhibitor or EIF2AK1

IGF-II - insulin-like growth factor II

IPTG – isopropyl-β-D-thiogalactopyranoside

JNK – c-jun N-terminal kinase

Kb – kilobase

kDa – kilodalton

LLC-PK_1-F^+ cells – LLC-PK_1-$FBPase^+$ cells

Luc – luciferase

MAPK – mitogen-activated protein kinase

MK2 - MAPK-activated kinase 2

MKK – mitogen-activated protein kinase kinase

MOPS – 3-(N-morpholino)propanesulfonic acid

mRNA – messenger ribonucleic acid

mRNP – messenger ribonucleoprotein

NHE3 - Na^+/H^+ exchanger NHE3

nt – nucleotide

oligo – oligodeoxynucleotide

P-bodies - processing-bodies

PABP – poly-A binding protein

PC - phosphocreatine

PCV – packed cell volume

PBS – phosphate buffered saline

pBSSK – pBluescript II SK (-)

PCR – polymerase chain reaction

PEPCK – phospho*enol*pyruvate carboxykinase

PERK - RNA-dependent protein kinase-like ER kinase

pHi – intracellular pH

pHRE – pH-responsive element

PI3-K – phosphatidylinositol-3-kinase

pol II – polymerase II

PKR - protein kinase R

PMR1 - Polysomal ribonulcease 1

PMSF - Phenylmethylsulfonylfluoride

RNA – ribonucleic acid

RNase – ribonuclease

RRM - RNA recognition motif

RSV – Rous sarcoma virus long terminal repeat promoter

SAM – S-adenosyl methionine

SDS – sodium dodecyl sulfate

$t_{1/2}$ – half-life

TCA - tricarboxylic acid

tet – tetracycline

tetO – tetracycline operator sequence

tetR – tet repressor

TIA-1 - T cell restricted intracellular antigen

TIAR - TIA-related protein

TNF-α – tumor necrosis factor alpha

TRE – tetracycline-responsive element

TTP – tristetraprolin

UPR - unfolded protein response

UV – ultraviolet

ζ-cryst - ζ-crystallin/NADPH:quinone reductase

CHAPTER 1

INTRODUCTION

1.1 Glutamine

The maintenance of blood acid-base balance is essential for survival. The normal pH of arterial blood is 7.4, whereas the pH of venous blood and interstitial fluids is about 7.35. The difference is due to the accumulation of CO_2 from tissues that forms H_2CO_3. Fluctuations in excess of 0.5 pH units from these values are usually lethal. A person is considered to be acidotic when the arterial blood pH falls below 7.35 [Guyton-Arthur, 1996]. The kidneys play a key role in regulating hydrogen ion removal. Under normal acid-base balance, the kidney extracts and metabolizes a small amount of glutamine [Squires, 1996]. The acute onset of metabolic acidosis causes the kidneys to extract more glutamine from the blood [Hughey et al, 1980]. This results in increased glutamine flux through the glutaminase and glutamate dehydrogenase, as an adaptive response to partially restore acid-base balance during the metabolic acidosis [Guyton-Arthur et al, 1996].

Glutamine is synthesized by the glutamine synthetase, which catalyzes the ATP-dependent ligation of an ammonium ion and glutamate to form glutamine. The glutamine synthetase is a cytosolic enzyme that is expressed most abundantly in muscle, lungs, and adipose tissues. In the rat kidneys, glutamine synthetase is expressed solely in the straight portion or S3 segment of the proximal tubule [Burch et al, 1978].

$$\text{L-Glutamate}^- + NH_4^+ + \text{ATP} \rightarrow \text{L-Glutamine} + \text{ADP} + P_i$$

The catabolism of glutamine is initiated by a mitochondrial glutaminase that catalyzes the hydrolytic cleavage of glutamine to form glutamate and an ammonium ion. Glutamine can be both synthesized and catabolized in liver, kidneys, and brain.

$$\text{L-Glutamine} + H_2O \rightarrow \text{L-Glutamate}^- + NH_4^+$$

Glutamine is the most abundant amino acid in the human body [Labow et al, 2000], accounting for over 20-25% of the free α-amino acids. It is present in the arterial plasma at a concentration of 0.5 - 0.8 mM. It also functions as the primary metabolic fuel for rapidly dividing cells, including intestinal epithelial cells [Mithieux et al, 2001], lymphocytes [Newsholme, 2001], and various transformed cells [Medina et al, 2001]. Glutamine metabolism plays a crucial role in metabolic pathways such as ureagenesis, ammoniagenesis, and gluconeogenesis [Curthoys et al, 1995]. The metabolism of glutamine provides precursors for transamination reactions, the γ-glutamyl cycle, the purine nucleotide cycle, the tricarboxylic acid (TCA) cycle, and the hepatic urea cycle. Glutamine is used in these pathways to synthesize glucose, urea, purines, pyrimidines, glucosamine, and other amino acids [Curthoys et al, 1995]. Glutamine is classified as a conditionally essential amino acid, since it is effective in treating critically ill patients. Patients recovering from trauma, major surgery, or sepsis do not synthesize or store sufficient glutamine to meet their metabolic needs [Neu et al, 1996].

1.2 Renal adaptations following acute metabolic acidosis

In normal acid-base balance, the kidneys extract and catabolize very little of the plasma glutamine [Brosnan et al, 1998]. The measured rat renal arterial-venous difference is less than 3% arterial concentration of glutamine. Approximately 20% of the

plasma glutamine is filtered by the glomeruli and enters the lumen of the nepheron. The filtered glutamine is reabsorbed by the epithelial cells of the proximal convoluted tubule [Silbernagl, 1980]. Reabsorbed glutamine is then transported across the apical brush border membrane and returned to the blood via transport across the basolateral membrane.

Metabolic acidosis can result from a high protein diet, prolonged fasting, or cachexia associated with severe burns, trauma, or sepsis. It is also associated with genetically determined acidurias, defects in renal reabsorption of HCO_3^-, and excessive diarrhea [Taylor et al, 2004]. Additionally, the overproduction of normal metabolic acids, such as lactate during anaerobic exercise or acetoacetate and β-hydroxybutyrate in diabetes mellitus, also cause a decease in plasma HCO_3^- concentration.

Increased renal ammoniagenesis and gluconeogenesis from plasma glutamine contribute to the adaptive response that partially restores acid-base balance during metabolic acidosis [Brosnan et al, 1988]. The renal catabolism of glutamine is significantly increased following the onset of metabolic acidosis. Net extraction reaches 30-40% of the plasma glutamine, and therefore exceeds the percent filtered by the glomeruli [Hughey et al, 1980]. The direction of basolateral glutamine transport must be reversed to allow the proximal convoluted tubular cells to extract glutamine from both the glomerular filterate and the venous blood. Furthermore, the apical Na^+/H^+ exchanger (NHE3) is activated to produce a prompt acidification of the urine [Peng et al, 2001], which facilitates the rapid excretion of cellular ammonium ions in the urine [Tannen et al, 1979]. Finally, a pH-induced activation of α-ketoglutarate dehydrogenase reduces the intracellular concentrations of α-ketoglutarate and glutamate [Lowry et al, 1980].

Therefore, increased catabolism of glutamine initially results from activation of the key transporters, an increased glutamine availability, and a decreased concentration of the product of the glutaminase (GA) and glutamate dehydrogenase (GDH) reactions.

1.3 Renal adaptations following chronic metabolic acidosis

During chronic metabolic acidosis, most of the acute adaptations are partially compensated. However, the kidney continues to extract more than one-third of the total plasma glutamine [Squires et al, 1976]. Renal catabolism of glutamine is sustained during chronic acidosis, at least in part, by increased expression of the genes that encode the cytoplasmic phospho*enol*pyruvate carboxykinase (PEPCK) [Burch et al, 1978], the mitochondrial glutaminase [Curthoys et al, 1973], and glutamate dehydrogenase [Wright et al, 1990]. All three activities are increased solely within the proximal tubules [Burch et al, 2001].

Following onset of acidosis, the decrease in the plasma pH and HCO_3^- concentration produces a comparable and sustained decrease in the intracellular pH (pH_i) of the proximal convoluted tubules [Ackerman et al, 1981; Sahai et al, 1990]. The adaptive increase in GA and PEPCK activities may be initiated by a decrease in pH_i. Both adaptations result from increased rates of synthesis of the proteins [Iynedjian et al, 1975; Tong et al, 1986] that correlate with comparable increases in the levels of their respective mRNAs [Cimbala et al, 1982; Hwang et al, 1991b]. However, the increase in GA results from selective stabilization of the GA mRNA [Hansen et al, 1996], while the increase in PEPCK results from enhanced transcription of the *PCK1* gene [Hanson et al, 1997].

The levels of the mitochondrial glutamine transporter [Sastrasinh et al, 1990], the apical Na^+/H^+ exchanger NHE3 [Horie et al, 1990], the basolateral NA^+-$3HCO_3^-$ cotransporter [Preisig et al, 1998], and the apical Na^+-dicarboxylate cotransporter NaDC-1 [Aruga et al, 2000] are also increased during chronic acidosis. The increased renal ammoniagenesis provides an expendable cation that facilitates the excretion of titratable acids while conserving sodium and potassium ions. The increased apical Na^+/H^+ exchanger also promotes the tubular reabsorption of HCO_3^- ions. In addition, the generated α-ketoglutarate is converted to glucose, generating 2 HCO_3^- ions per α-ketoglutarate. The increase in basolateral NA^+-$3HCO_3^-$ cotransporter facilitates the translocation of reabsorbed HCO_3^- ions into the renal venous blood. Thus the combined adaptation creates a net release of HCO_3^- ions that partially compensates the systemic acidosis (**Fig. 1-1**).

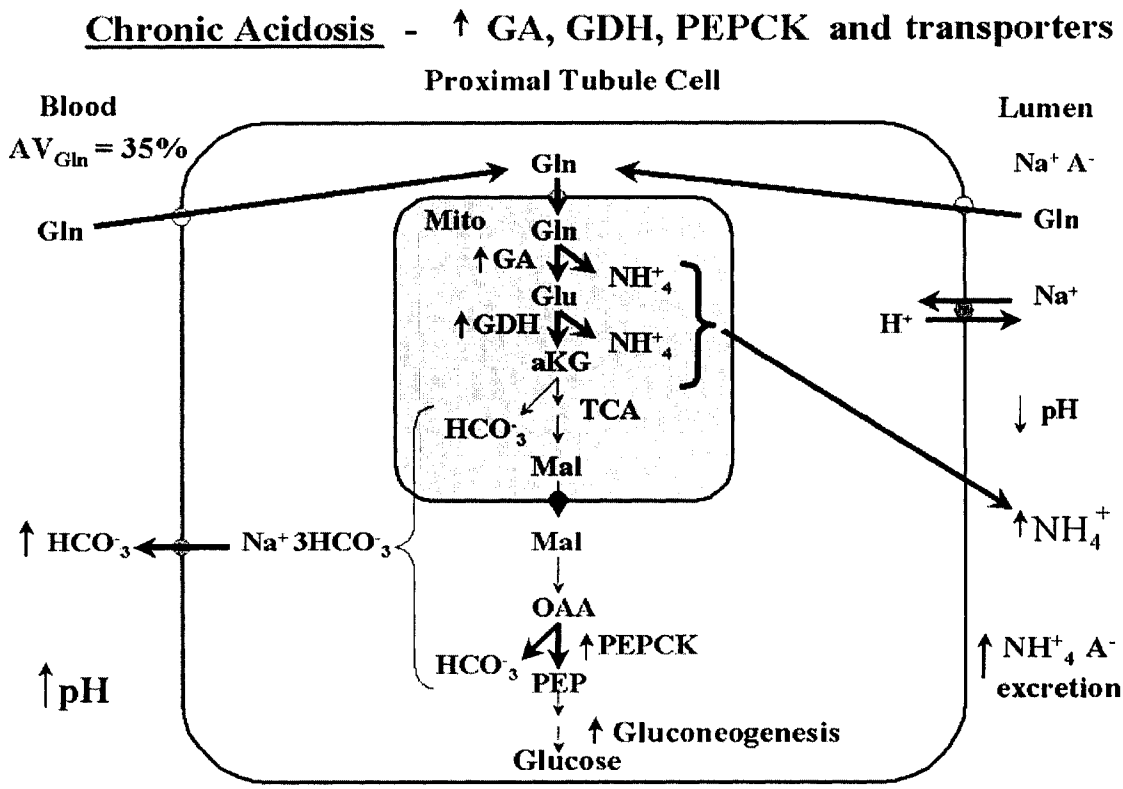

Fig. 1-1. Renal proximal tubular catabolism of glutamine. During chronic acidosis, increased renal ammonia and glucose synthesis are sustained by increased expression of glutaminase (GA), glutamate dehydrogenase (GDH), phospho*enol*pyruvate carboxykinase (PEPCK), the mitochondrial glutamine transporter, the apical Na+/H+ exchanger, and the basolateral glutamine transporter and Na+-3HCO3- cotransporter.

1.4 Glutaminase

The mitochondrial glutaminase (GA) catalyzes the initial reaction in the primary pathway for the renal catabolism of glutamine [Tannen et al, 1993].

$$\text{L-Glutamine} + H_2O \rightarrow \text{L-Glutamate}^- + NH_4^+$$

There are two isoforms of phosphate-dependent glutaminase. In the rat, the liver-type GA is expressed only in adult liver tissue, whereas the kidney type GA is expressed at high levels in kidney, brain, intestine, fetal liver, the cells of the immune system, and in many transformed cells [Taylor et al, 2004]. The changes in the relative levels of GA mRNA were determined in order to characterize the mechanism responsible for the adaptive increase in renal GA activity. The rat kidney-type glutaminase cDNA was isolated by screening a rat brain cDNA library [Banner et al, 1988]. The full-length rat kidney GA cDNA contains 58 bp of 5' untranslated sequence, 2022 bp of an open reading frame, and 2446 bp of 3' untranslated sequence. When transcribed and translated *in vitro*, the cDNA produced a 74-kDa protein, which corresponded to the protein size observed in *in vivo* pulse-chase experiments [Perera et al, 1990; Perera et al, 1991]. This 74-kDa precursor protein composed of 674 amino acids, which included an N-terminal sequence of 16 residues that has propensity to form an amphipathic α-helix mitochondrial targeting signal. The 3' untranslated region (3'-UTR) of the glutaminase mRNA contained two polyadenylation sites.

1.4.1 pH-responsive stabilization of GA mRNA

In the rat, the onset of acidosis leads to a gradual increase in the mitochondrial GA activity. To achieve a 7- to 20-fold adaptation within the proximal convoluted tubule

requires 5 – 7 d [Curthoys et al, 1995]. The GA cDNA hybridized to 4.7 kb and 3.4 kb mRNAs in total or poly-A RNA isolated from rat kidney [Hwang et al, 1991]. During onset of acute acidosis, the two GA mRNAs are increased following a 6- to 8- hour lag and reached a 5-fold increase within 1 d and a maximal 8-fold increase after 5 d. Acute recovery from chronic acidosis occurred with first-order kinetics, and an apparent $t_{1/2}$ of 4 h. Nuclear run off assays indicated that the rate of transcription of the renal GA mRNA is unaffected by changes in acid-base balance. Therefore, the increase in glutaminase activity during chronic acidosis results from an increased level of total and translatable GA mRNA, which may result from an increased stability of the GA mRNAs.

The selective stabilization of the GA mRNA was initially demonstrated using various β-globin (βG) constructs that were transfected into LLC-PK_1-F^+ cells [Hansen et al, 1996]. Expression of pβG produced a very stable mRNA ($t_{1/2}$ > 30 h) that was not affected by transfer of cells to acidic medium. On the other hand, the pβG-GA plasmid that contains the 956-bp of 3'-untranslated region (UTR) produced βG-GA mRNA with a decreased $t_{1/2}$ of 4.6 h. Transfer of the cells to acidic medium (pH 6.9) resulted in a pronounced stabilization of GA mRNA, indicating that the 3'-UTR contains a pH-responsive instability element (pHRE).

1.4.2 Identification and analysis of a pH-responsive element in the GA 3' UTR

Further mapping of the 3'-UTR of the GA mRNA using various βG constructs in LLC-PK_1-F^+ cells identified two adjacent 8-base AU-sequence (UUAAAAUA and UUUAAAUA) within the 3' UTR of the GA mRNA, that function as a pH-response element (pHRE) in a chimeric reporter mRNA [Laterza et al, 1997]. Site-directed

mutation of both eight-base AU sequences completely abolished the pH-responsive stabilization of the βG-GA mRNA. Previous experiments indicated that either the direct repeat or a single copy of the eight-base AU sequence is both necessary and sufficient to function as a pHRE. In addition, a S100 cytoplasmic extract prepared from the rat renal cortex that were made acutely acidotic exhibit an increased protein binding to the direct repeat of the pHRE [Laterza et al, 2000].

1.4.3 pH-response element binding proteins

1.4.3.1 Identification and purification of ζ-cryst

A biotinylated oligoribonucleotide containing the pHRE was used as an affinity ligand to purify a 36-kDa protein from rat renal cortex [Tang et al, 2001]. Microsequencing of the purified protein by mass spectroscopy identified the protein as ζ-crystallin/NADPH:quinone reductase (ζ-cryst). The addition of antibody against ζ-cryst blocked the formation of the RNA:protein complex produced by the pHRE and the purified protein.

ScanProsite analysis indicated that ζ-cryst has a zinc-containing alcohol dehydrogenase (ADH) signature domain. ζ-cryst has NADPH-dependent quinone reductase activity that is distinct from other known quinone reductases. It lacks alcohol dehydrogenase activity even though it has a high degree of similarity to the zinc-containing alcohol dehydrogenase family [Jornvall et al, 1993]. Zinc-containing ADH's are dimeric or tetrameric enzymes that bind two atoms of zinc per subunit [Jornvall et al, 1987; Sun et al, 1992].

ζ-cryst was not previously known to function as an RNA binding protein. However, bovine ζ-cryst binds to Z-DNA and to single-strand DNA [Gagna et al, 1998; Rao et al, 1997]. The interaction is effectively competed by the addition of NADPH, indicating that the DNA may interact with the dinucleotide binding site. Hence, the nucleotide binding site of metabolic enzymes may function both in catalysis and gene regulation [Hentze, 1994].

1.4.3.2 Identification of AUF1 as a pHRE binding protein

A tetracycline-responsive promoter system was developed in LLC-PK_1-F^+ cells to perform pulse-chase analysis of the turnover of a chimeric βG mRNA that contained 960-bp of the 3'-UTR of GA mRNA (βG-GA) [Schroeder et al, 2005]. βG-GA mRNA degraded with a $t_{1/2}$ of 2.9 h when LLC-PK_1-F^+ cells were grown under normal condition and exhibited a 14-fold stabilization when the cells were transferred to an acidic medium. The total RNAs isolated from the transcriptional pulse analysis were also used to determine the mechanism of decay of the βG mRNA. RNase H cleavage and northern blot analysis demonstrated that rapid deadenylation occurred concomitantly with the rapid decay of the βG mRNA in cells grown in normal medium. In contrast, stabilization of the βG mRNA in acidic medium produced a pronounced decrease in the rate of deadenylation. Thus, the factors that normally bind to the instability elements within the GA mRNA are either modified or displaced during acidosis.

ARE-mediated decay of mRNA is usually preceded by rapid deadenylation [Ross, 1995]. The AUF1 is a known *trans*-acting factor that binds to AU-rich element [Demaria et al, 1996, Wilson et al, 1999]. Previous western blot analysis using LLC-PK_1-F^+ cells

demonstrated the presence of AUF1 in the extracts [Schroeder et al, 2005]. RNA gel-shift assays demonstrated that the recombinant p40-AUF1 binds to the pHRE with high affinity and specificity. The addition of antibody against AUF1 produced a slight supershift of the GA(R2-I) RNA/protein complex that is formed using a cytosolic extract of LLC-PK_1-F^+ cells. Analysis using the mutated GA(R2-I) also indicated that a single 8-base AU-element was sufficient for AUF1 binding. These data suggest that AUF1 may mediate the rapid turnover of the GA mRNA, whereas increased binding of ζ-cryst during acidosis may inhibit degradation and result in selective stabilization.

1.4.4 Proposed model for the stabilization of GA mRNA

In normal acid-base balance, AUF1 may preferentially bind to the pHRE and recruit protein complexes that are involved in mRNA turnover, leading to the rapid deadenylation and subsequent decay of the GA mRNA. In contrast, the onset of metabolic acidosis may activate a specific signaling mechanism that results in covalent modification of ζ-cryst and/or AUF1 to affect their interaction with the pHRE of the GA mRNA. As a result, interaction of the deadenylase with the poly-A tail is reduced, leading to stabilization of the GA mRNA (**Fig. 1-2**).

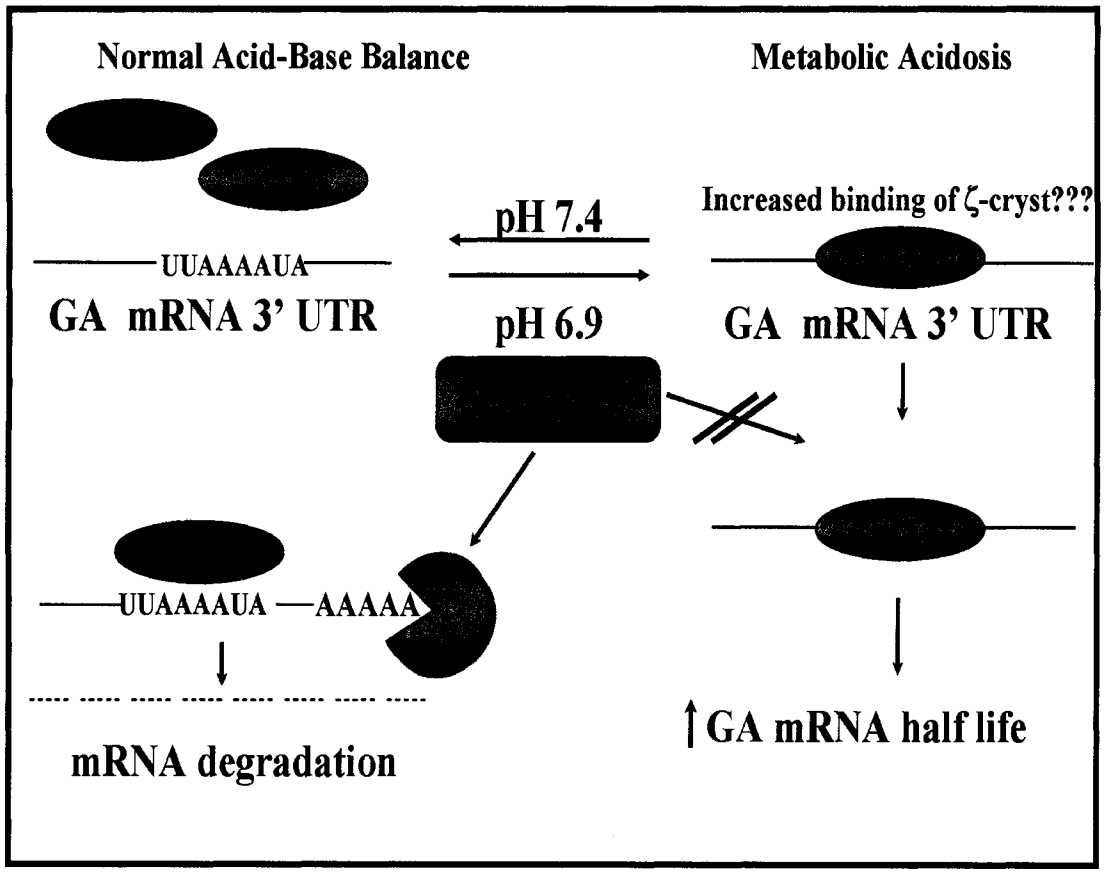

Fig. 1-2 Proposed model for the mechanism by which the onset of metabolic acidosis leads to stabilization of the renal GA mRNA. An 8-base AU-rich pHRE serves as a binding site for ζ-cryst. The resulting complex prevents the binding of destabilizing ARE-binding proteins. In normal acid-base balance, the weak binding of the ζ-cryst allows for the more rapid deadenylation and degradation of the GA mRNA. However, during metabolic acidosis, the increased binding of ζ-cryst blocks recruitment of the deadenylase (DAN) and exosome and leads to selective stabilization.

1. 5 Phospho*enol*pyruvate carboxykinase (PEPCK)

The cytosolic form of phospho*enol*pyruvate carboxykinase (PEPCK-C) catalyzes the committed step in hepatic and renal gluconeogenesis [Rognstad, 1979].

$$\text{Oxaloacetate} + \text{GTP} \leftrightarrow \text{PEP} + CO_2 + \text{GDP}$$

This activity is a key regulator of the increased renal metabolism of glutamine that occurs in response to metabolic acidosis. Analysis of the pH-responsive induction of PEPCK expression and the associated signal transduction pathway provide an excellent paradigm to characterize the molecular mechanism by which the cell specific transcription of a gene is activated during metabolic acidosis.

The cytosolic form of PEPCK is expressed predominantly in liver, kidney, and adipose tissues. In kidney, the PEPCK gene is expressed solely within the convoluted and straight segments of the proximal tubule [Burch et al, 1978]. The level of PEPCK is increased in response to glucocoticoids, parathyroid hormone or angiotensin II [Hanson et al, 1994]. The latter hormones increase cAMP levels within the proximal tubule. Since renal gluconeogenesis is primarily coupled to renal ammoniagenesis and the maintenance of acid-base balance, renal PEPCK gene expression is also induced by acidosis

cDNAs that encode the cytoplasmic form of rat PEPCK have been isolated from both kidney and liver libraries [Beale et al, 1985]. The primary structure of the rat cytosolic PEPCK mRNA was determined by sequencing of both the cDNA and the genomic DNA. It encodes a 2.6-kb mRNA including 143 and 615 nucleotides of 5'- and 3'-nontranslated sequences, respectively. The –490 to +73 bp region of the PEPCK gene

contains 13 distinct *cis*-regulatory elements [Hanson et al, 1995]. Sequencing of the genomic DNA established that the entire gene is composed of 10 exons and 9 introns, spanning 6-kb in length.

Various segments of the PEPCK promoter, as well as the core promoter (-460 to +73 bp) containing specific block mutations in regulatory elements, have been extensively analyzed in transgenic animals to determine their role in controlling PEPCK gene expression [Hanson et al, 1994]. The wild type core promoter fused to the bovine growth hormone (bGH) gene contains all of the information necessary to insure appropriate expression and hormonal regulation in liver [McGrane et al, 1990; McGrane et al, 1988]. A larger 2.3-kb segment of the PEPCK promoter was required to drive expression of the transgene in adipose tissue [McGrane et al, 1990; McGrane et al, 1988]. However, both of these constructs were expressed at low levels in the kidney.

In contrast, the CRC362 transgene, that contains only 362 bp of the promoter but all of the downstream exons and introns of the rat PEPCK gene, was expressed with the correct developmental profile and at normal levels in the kidney [Eisenberger et al, 1992]. This transgene differed from the endogenous gene only by the substitution of a segment of the chicken PEPCK gene into the portion of the final exon that encodes the 3'-untranslated region of the PEPCK mRNA. Furthermore, only the latter construct exhibited a significant renal-specific induction when the transgenic mice were made acidotic [Cassuto et al, 2003]. Previous experiments demonstrated marked differences in the foot-printing patterns observed with nuclear extracts prepared from rat liver and kidney [Roesler et al, 1989], suggesting that kidney and liver may utilize different *trans*-acting factors to regulate the PEPCK gene. These data suggest that the PEPCK gene may

contain a downstream element that is essential for full expression and pH-responsive induction in the kidney.

1.5.1 pH-responsive induction of PEPCK

The level of PEPCK mRNA in rat kidney is rapidly increased following acute onset of acidosis [Hwang et al, 1991b]. The increase is initiated within 1 h and reaches a maximum within 7 h at a level that is 6-fold greater than normal. The 6-fold induced level of PEPCK mRNA is sustained in rats that are made chronically acidotic for 7 d [Hwang et al, 1991b]. Transcription run off experiments were conducted using isolated rat renal nuclei [Hwang et al, 1991b]. The relative rate of transcription of the PEPCK gene increased 3-fold within 2 h after acute onset of acidosis, reached a maximum of 4-fold induction by 6 h, and then decreased slightly by 20 h. The initial increase in transcription exceeded the initial increase in PEPCK mRNA. Therefore, enhanced transcription can account for the initial induction of PEPCK mRNA. The observed changes in PEPCK mRNA levels closely correlated with earlier data that measured changes in the relative rates of PEPCK protein synthesis in normal and acidotic rats [Iynedjian et al, 1975]. Thus, regulation of the translation of the PEPCK mRNA is unlikely to contribute to the observed changes in PEPCK gene expression.

Initial experiments were performed using available promoter/chloramphenicol acetyltransferase (CAT) reporter constructs [Holcomb et al, 1996] to characterize the increase in transcription of the PEPCK gene caused by changes in acid-base balance. Confluent cultures transfected with PEPCK$_{-490}$CAT exhibited a 2- to 3- fold increase in CAT activity when shifted to acidic medium for 48 h [Holcomb et al, 1996]. Mutation of

the P3(II) or CRE1 element caused a 50% decrease in the pH-response, whereas mutation of the other well-characterized elements in the PEPCK promoter had no effect on this response. Cassuto, *et al.* [Cassuto et al, 1997] generated a PEPCK$_{-597}$CAT construct along with various deletions and site-specific mutations. It was determined that the wild type construct exhibited a 2.5-fold increase in CAT activity when the cells were transferred to acidic medium. However, this response was retained in a deletion construct that lacked the entire P3 region suggesting that the P3(II) element was not necessary. A mutation in CRE-1 again caused a partial reduction in the fold response. Mutation of the P2 element significantly reduced basal activity and also had a lower pH-response (1.6-fold). Thus, they concluded that the binding of hepatic nuclear factor-1 (HNF-1) to the P2 element contributes to both basal and pH-responsive activation of PEPCK expression in kidney cells. Finally, Drewnowsk, *et al.* [Drewnowsk et al, 2002] compared the pH-response of PEPCK$_{-490}$CAT and PEPCK$_{-2300}$CAT constructs in subconfluent LLC-PK$_1$-F$^+$ cells. A 2.7-fold pH-response was observed only with the construct containing the longer promoter element, suggesting that an element upstream of the shorter -490-bp segment was essential for the pH-response.

Given the divergence of these results and the fact that the measured CAT activity approached the lower limits of the sensitivity of this assay, the -490 and -2300 promoter segments were cloned into pGL2-Basic (Promega), a firefly luciferase (Luc) expression vector. The activity of the resulting PEPCK$_{-490}$Luc construct in LLC-PK$_1$-F$^+$ cells was activated 30-fold by co-expression of the catalytic subunit of PKA [Liu et al, 2001]. In contrast, neither PEPCK$_{-490}$Luc nor PEPCK$_{-2300}$Luc exhibited a pH-responsive activation [unpublished data]. Stable cell lines that express integrated copies of the PEPCK

promoter/luciferase gene were also isolated and tested for a pH-response. Again, none of these constructs exhibited a pH-responsive increase in luciferase activity even though the level of the endogenous PEPCK mRNA was still increased 3-fold following transfer to acidic medium. Similar experiments were performed using adenovirus constructs to infect LLC-PK_1-F^+ cells with the $PEPCK_{-2300}$Luc gene. Control experiments using a green fluorescent protein construct indicated that nearly all the LLC-PK_1-F^+ cells are rapidly infected with the adenovirus. This protocol also produced very high luciferase activity in the LLC-PK_1-F^+ cells but again this activity was not pH-responsive. These observations and the finding that a transgene containing only 362 bp of the promoter along with the downstream exons and introns is sufficient to recapitulate the pH-responsive induction [Cassuto et al, 2003] suggest that the PEPCK gene may require a downstream element that is essential for the pH-responsive increase in transcription.

1.5.2 Signaling pathway that activates for transcription of the PEPCK gene

The potential involvement of known mitogen-activated protein kinase (MAPK) was examined by determining the effects of specific MAPK activators and inhibitors on the PEPCK mRNA levels in LLC-PK_1-F^+ cells grown under normal condition or transferred to acidic medium. Anisomycin, a protein synthesis inhibitor, is a potent activator of the p38 mitogen-activated protein kinase (MAPK). Anisomycin caused an increase in PEPCK mRNA comparable to that observed by treatment with acidic medium. In addition, the p38 MAPK is phosphorylated when LLC-PK_1-F^+ cells are transferred to acidic medium. ATF-2 is a basic leucine zipper transcription factor that is activated by p38 MAPK. Phosphorylation of ATF-2 was also observed in LLC-PK_1-F^+

cells following transfer to acidic medium. Furthermore, the addition of SB-203580, a p38 MAPK inhibitor, blocked the phosphorylation of ATF2 and prevented the pH-responsive increase in PEPCK mRNA. The combined data suggest that the p38 MAPK/ATF-2 signaling pathway contributes to the pH-responsive induction of PEPCK mRNA transcription in renal LLC-PK_1-F^+ cells.

Western blot analysis demonstrated LLC-PK_1-F^+ cells express high levels of the upstream kinase MAPK kinase-3 (MKK), but relatively low levels of the alternative upstream kinase MKK6 [O'Hayre et al, 2006]. Expression of caMKK6, but not caMKK3, caused an increase in phosphorylation of p38 MAPK and a comparable increase in the level of PEPCK mRNA observed with treatment with acidic medium. Co-expression of both dnMKKs block the increases in phosphorylation of p38 MAPK and PEPCK mRNA, an effect that closely mimicked the effect of the p38 MAPK inhibitor SB203580. The expression of either dnMKK3 or dnMKK6 was less effective than co-expression of both dnMKKs, indicating that the pH-responsive increase in the PEPCK mRNA is mediated by the activation of MKK3 and/or MKK6 of p38 MAPK signaling pathway (**Fig. 1-3**).

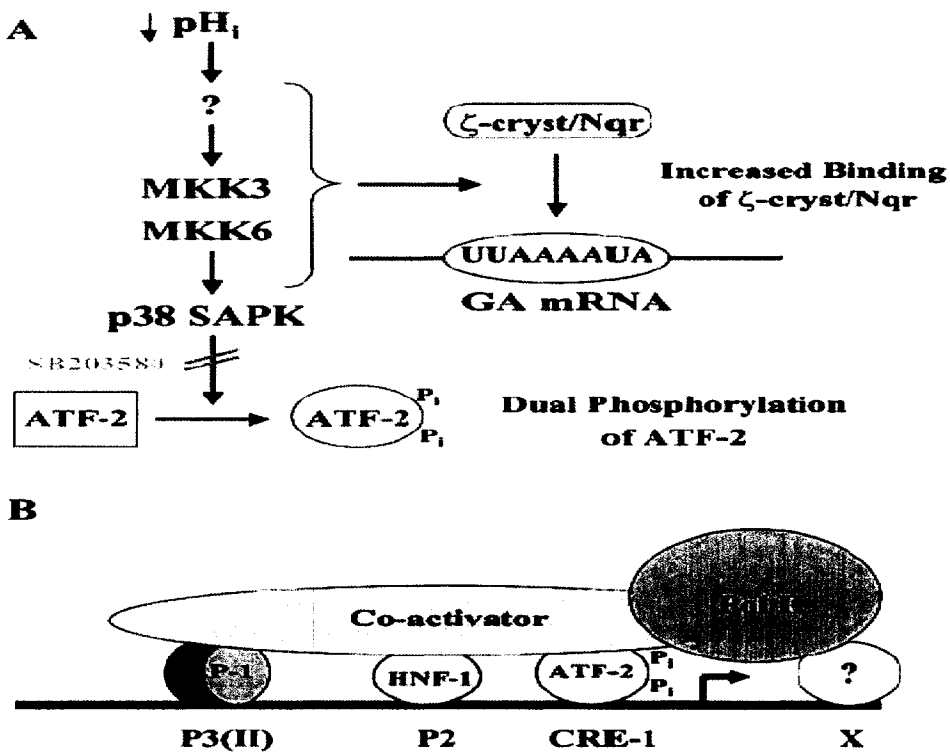

Fig.1-3 Hypothesis for the coordinate induction of PEPCK and GA gene expression during metabolic acidosis. Panel A – A decrease in intracellular pH (pHi) leads to activation of the p38 stress-activated protein kinase (p38 SAPK) pathway and the phosphorylation of activating transcription factors (ATF)-2. A kinase upstream of p38 SAPK modifies ζ-cryst to enhance its binding to the pHRE within the GA mRNA. MKK, mitogen-activated protein kinase kinase. **Panel B** – Hepatic nuclear factor (HNF-1), and possibly activating protein (AP)-1, binding to the P2 and P3(II) elements within the proximal promoter, respectively, may account for basal transcription of the PEPCK gene. The binding of phosphorylated ATF2 to the CRE-1 element along with the binding of an unidentified factor (?) to an element that is downstream of the initiation site may enhance the recruitment of a coactivator and polymerase II (Pol II), leading to activated transcription.

1.5.3 Identification and analysis of the instability element in the PEPCK 3' UTR

Previous studies demonstrated that the $t_{1/2}$ of the PEPCK mRNA is increased in the liver in response to cAMP [Liu J. et al, 1991] and glucocorticoids [Petersen et al, 1988]. This indicated that increased stability of PEPCK mRNA may also contribute to the sustained induction of the PEPCK mRNA in the kidney [Hwang et al, 1991b]. The presence of a destabilizing element within the 3'-UTR of the PEPCK mRNA was previously demonstrated using DRB, a polymerase II inhibitor, to determine the $t_{1/2}$ of a chimeric βG-PEPCK mRNA in LLC-PK_1-F^+ cells. The βG mRNA produced a $t_{1/2}$ of >30 h, compared to a $t_{1/2}$ of 5 h for the βG-PCK1 mRNA that contained the entire 3'-UTR of PEPCK mRNA. RNA gel shift assay also demonstrated two protein binding interactions using a S100 cytosolic extracts of rat renal cortex [Laterza et al, 2000].

Mapping analysis using a Tet-regulated promoter system demonstrated that the 3'-UTR of the PEPCK mRNA contains multiple instability elements [Hajarnis et al, 2005]. AUF1 was shown to bind with high affinity and specificity to PCK-2, PCK-6 and PCK-7 RNAs segments of the 3' UTR that contribute to the rapid turnover of the PEPCK mRNA. It was also determined that the primary destabilizing elements are located within the PCK6/7 segment that constituted the final 73-nt of the PEPCK 3'-UTR. Detailed mapping studies indicated that AUF1 binds to the AU-rich and CU-rich region within the PCK6/7 segment. More recent studies demonstrated that ζ-cryst also binds to the 3'-UTR of the PEPCK mRNA and that this binding occurs within a highly conserved stem-loop structure in the PCK6/7 segment [Ph.D. Thesis, S. Harjarnis]. In addition, a chimeric βG-PEPCK mRNA exhibited a 2.5-fold stabilization upon transfer of LLC-PK_1-

F^+ cells to an acidic medium. These findings indicate that stabilization of the PEPCK mRNA contributes to its increased expression.

1.6 LLC-PK1-F^+ cell line

Characterization of the specific *cis/trans* interactions that mediate the pH-responsive activation of the GA and PEPCK genes required the identification of a renal cell line that accurately models the two adaptations. LLC-PK_1 cells exhibit a number of properties characteristics of renal proximal tubular cells [Gstraunthaler et al, 1987], including a pH-responsive increase in glutamine metabolism [Gstraunthaler et al, 1987]. The parent LLC-PK_1 cells are unable to synthesize glucose from pyruvate due to a lack of fructose-1,6-bisphosphate (FBPase). In order to derive a gluconeogenic subline, LLC-PK_1 cells were grown in low glucose medium (<0.5 mM) and then selected with essentially glucose-free medium supplemented with 10 mM pyruvate. The selected cells expressed significant FBPase activity, and were designated as LLC-PK_1-F^+ cells. Compared to the parental LLC-PK_1 cells, LLC-PK_1-F^+ cells exhibited enhanced level of oxidative metabolism, an increase level of mitochondrial density [Gstraunthaler et al, 1987], with an increase in basal GA activity. As a result, the LLC-PK_1-F^+ cells exhibit an enhanced rate of glutamine catabolism [Gstraunthaler et al, 1987] and a higher basal rate of ammonia production [Gstraunthaler et al, 2000]. In addition, the level of the pH-responsive cytosolic PEPCK mRNA was increased 2- to 3-fold while the level of the constitutively expressed mitochondrial PEPCK mRNA was unchanged [Holcomb et al, 1995]. Thus, the gluconeogenic LLC-PK_1-F^+ strain is a pH-responsive renal proximal tubule-like cell line.

1.7 WKPT and WKPT-ζ+ cell line

The rat renal proximal tubular epithelial cell line was established by SV40 transformation of isolated cells from the proximal tubules. The cells were initially isolated by microdissection, then cultured and immortalized using a replication defective recombinant retrovirus encoding SV40 large T-antigen gene using a vector that co-expresses a neomycin resistance gene [Woost et al, 1996]. WKPT cells were not previously characterized as a pH-responsive line of renal proximal tubules. Hence, it was important to determine if the WKPT cells are pH-responsive prior to performing molecular analysis of the mechanism mediating the enhanced expression of the GA gene during the onset of metabolic acidosis. It should be also noted that endogenous PEPCK mRNA is not detected in WKPT cells. A line of WKPT cells that over expresses ζ-cryst was produced by stable transfection of WKPT with pcDNA 3.1/Hygro-ζ-cryst and designated as WKPT-ζ^+ cells. Western blot analysis demonstrated that the clonal WKPT-ζ^+ cells over-express ζ-cryst by 36-fold compared to WKPT cells [unpublished data, Chapter 5].

1.8 mRNA turnover in eukaryotes

The abundance of an mRNA is determined by regulation of transcription and the post-transcriptional regulation of mRNA turnover. The rate of mRNA turnover is determined by the presence of *cis*-acting elements within the mRNA, including the $^{7'met}$guanosine cap at the 5'-end, stem-loop structures, adenylate- and uridylate-rich elements (AREs), and the poly-A tail. Stabilization or destabilization is regulated by *trans*-acting factors, usually mRNA binding proteins, which interact with the *cis*-acting

elements [Ross, 1995]. Specific AU-rich elements within the coding sequence or the 3'-untranslated region of the mRNAs function as instability elements [Chen, C. et al, 1995]. Turnover of mRNA in mammalian cells involves deadenylation, decapping, and exonucleolytic decay (**Fig. 1-4**).

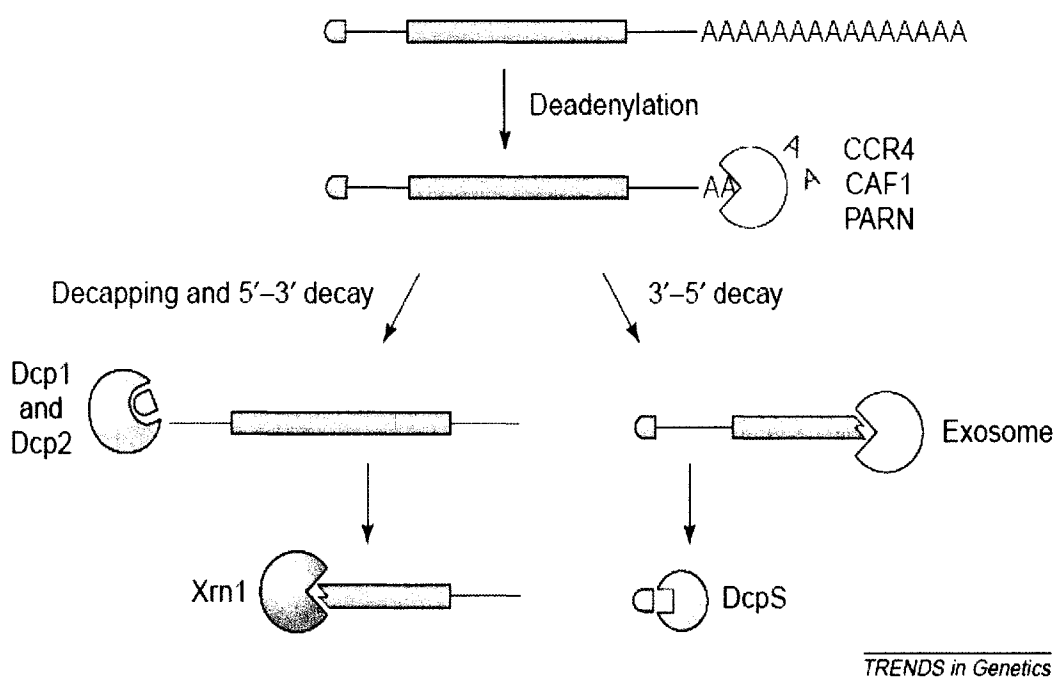

Wilusz CJ, Wilusz J. *Trends Genet.* 2004 Oct;20(10):491-7.

Fig. 1-4 Decay pathways in mammalian cells. Removal of poly-A tail initiates the first step in decay of mRNAs, catalyzed by several different enzymes. Following deadenylation, the mRNA undergoes a exonucleolytic decay from either the 5' or 3' ends. A 5'→3' decay pathway is initiated by removal of the cap structure by the decapping enzymes Dcp1/2. The 5'→3'exonuclease, Xrn1, then degrades the body of the mRNA. A 5'→3' decay pathway is catalyzed by the exosome, a 3'→5'exonuclease, leading to production of ^{7met}GpppG, that is released as ^{7met}GMP by DcpS, the scavenger decapping protein. CAF1, CCR4, and PARN are deadenylases involved in mRNA deadenylation.

1.8.1 Deadenylation

The poly-A tail is a major determinant of translation efficiency and stability, hence deadenylation simultaneously modulates both translation and decay [Chen, CY, et al 1995]. Deadenylation is also the only reversible step in the decay pathway. Partial deadenylation can lead to translational silencing, followed by subsequent polyadenylation [de Moor et al, 2001]. There are at least four different deadenylases that have been identified, including PAN2/PAN3, CCR4 and nocturnin, CAF1, and PARN. PAN2/PAN3 is a cytoplasmic deadenylase that is activated by Pab1p [Uchida et al, 2004]. PAN2 has an intrinsic 3'→5' exoribonuclease activity and requires Mg^{+2} for activity, whereas PAN3 interacts with PABP to simulate the PAN2 nuclease activity. It was suggested that PAN2/PAN3 may play a role in the synchronous poly-A shortening of mammalian mRNAs [Yamashita et al, 2005]. In contrast to other deadenylases, PAN2/PAN3 activity is stimulated by interaction with PABP [Brown et al, 1996].

CCR4-NOT complex includes CCR4p, Pop2p/Caf1p, Caf40p, Caf130p, and Not1-5p [Chen J. et al, 2001]. CCR4p is the major catalytic subunit of the complex, and exhibits homology to *E. Coli* exonuclease III [Tucker et al, 2002]. Pop2p/Caf1p subunit is a member of the RNase D-like DEDD family of nucleases [Bianchin et al, 2005]. CCR4-NOT complexes have been shown to have a distinct spatial and temporal expression from PARN, and are localized to P-bodies [Baggs et al, 2003]. In addition, CCR4-NOT may have a role in transcriptional regulation [Denis et al, 2003]. CCR4-NOT may be associated with translational regulation, since PABP, a positive *trans*-acting factor in translation initiation, acts as a negative regulator of CCR4-NOT [Tucker et al, 2002]. CAF1 is a component of the CCR4-NOT complex, that has

3'→5'exoribonulcease activity with a preference for poly-A substrates *in vitro*. However, in yeast the deadenylase activity of CAF1 is not required for poly-A removal function [Viswanathan et al, 2004].

PARN is a cap-dependent deadenylase [Dehlin et al, 2000] that has been shown to be modulated by ARE-binding proteins [Lai et al, 2003]. PARN exhibits homology to RNase D-like enzymes of the DEDD superfamiliy family of 3'→5' RNA and DNA exonucleases. This motif is essential for the binding of divalent metal ions [Ren et al, 2004]. PARN activity is stimulated by the cap structure at 5'-end of the mRNA and inhibited in *trans* by the addition of cap analog [Martinez et al, 2001]. It was also demonstrated that enhanced mRNA turnover correlated with a decrease in cap-associated eIF4E and an increase in cap binding of PARN in HepG2 cells [Seal et al, 2005].

1.8.2 3'→5' mRNA decay

The exosome-mediated 3'→5' mRNA decay appears to be the predominant pathway in mammalian cell extracts. The core exosome consists of six RNase PH domain-containing exonuclease (Pm/Scl-75/Rrp45, Rrp41, Rrp42, Rrp26, OIP2, and Mtr3) and three proteins containing S1 and/or KH-type RNA-binding domains (Csl4, Rrp4, Rrp40). The three core proteins, Rrp4, Rrp40, Csl4, may play a role in RNA substrate recognition whereas the other six subunits appear to comprise the enzymatic core [Raijmakers et al, 2002]. The exosome complex is also associated with several accessory factors, including the hSki2w RNA helicase, MPP6, and Pm/Scl-100 [Raijmakers et al, 2002]. In the nucleus, the exosome mediates the processing of rRNAs, snRNAs, and snoRNAs and in mRNA turnover, while in cytoplasm, the exosome is

involved in mRNA turnover only [Raijmakers et al, 2004]. Following the exosome-mediated 3'→5' mRNA decay, DcpS, a scavenger mRNA decapping enzyme, acts as a pyrophosphatase to cleave ^{7met}GpppG to release ^{7met}GMP [Liu, H. et al, 2002].

1.8.3 5'→3' mRNA decay

An alternative pathway that occurs following deadenylation involves decapping of the transcript, followed by 5'→3' mRNA decay mediated by the Xrn1 ribonuclease. Even though 5'→3' mRNA decay is the major pathway in yeast, it appears that 5'→3' mRNA decay may be a minor pathway in mammalian cells [Gao et al, 2001]. The decapping enzyme is a complex of three proteins, Dcp1a, Dcp2, and Hedls. Dcp2 is the catalytic subunit, while Dcp1a plays a regulatory role. The third subunit, Hedls, is shown to enhance the decapping activity of Dcp2 and acts as a bridging factor between Dcp1a and Dcp2 [Fenger-Gron et al, 2005]. Together these proteins form a functional enzyme that is localized in the cytoplasm and associates with several auxiliary factors [Lykke-Andersen et al, 2002; Wang et al, 2002]. Among the auxiliary factors, the Lsm proteins, that bind to the 3' end of mRNAs, are essential for the decapping process [Tharun et al, 2005]. In HeLa cells, the dedenylation-dependent decapping of a transcript is regulated by both cap binding proteins and PABP. eIF4E, a cap binding protein, has been shown to inhibit decapping [Gao et al, 2001]. Decapping is also repressed by interaction of the PABP with the cap and poly-A tail [Khanna et al, 2004]. Once the mRNA is decapped, it is rapidly degraded by the Xrn1, a 5'→3' ribonuclease. Recently, it was demonstrated that the decapping enzme and Xrn1 are localized in P-bodies, indicating that P-bodies are the cytoplasmic loci where 5'→3' mRNA decay occurs [Kedersha et al, 2005].

1.8.4 ARE mediated Decay

AREs, or AU-rich elements, were first discovered in the 3'-UTR of several cytokines and oncogenes [Caput et al, 1986]. There are three classes of AREs based on the number and the distribution of the AUUUA pentamers [Chen et al, 1995]. Class I AREs contain one to three pentamers within a U-rich region in the 3'-UTR (e.g. c-myc and c-fos). Class II AREs contain at least two overlapping copies of the UUAUUUA(U/A)(U/A) nonamer sequence within a U-rich region (e.g. TNF-α and GM-CSF). Class III AREs do not contain the AUUUA pentamers, but contain a U-rich region (e.g. c-jun). Stabilization or destabilization of ARE-containing mRNAs is regulated by *trans*-acting factors, e.g. mRNA binding proteins. Biochemical approaches using RNA electrophoretic mobility shift assays (EMSA) and UV-crosslinking experiments have indicated that the same ARE-containing mRNA can bind to multiple ARE-binding proteins [Barreau et al, 2006]. ARE-binding protein mediated decay occurs by various mechanism, including recruitment of the exosome [Chen CY et al, 2001] or decapping complexes [Gao et al 2001], and stimulating deadenylation by PARN [Gao et al, 2000].

1.8.5 ARE binding proteins

Tristetraprolin (TTP) and its homolog, butyrate response factor 1 (Brf1) are members of the Tis11 family of Cys-Cys-Cys-His (CCCH) tandem zinc-finger proteins, shown to have a destabilizing role on ARE-containing mRNAs [Carballo et al, 1998]. TTP binds to class II AREs including those presenting TNF-α [Carballo et al, 1998], IL-3 [Raghavan et al, 2001] and COX-2 [Sully G. et al, 2004] mRNAs. TTP is a nuclear-cytoplasmic shuttling protein that is translocated to the cytoplasm in response to certain

environmental stimuli [Kedersha et al, 2005]. TTP requires an intact tandem zinc finger domain but not RNA binding ability for nuclear accumulation [Phillips et al, 2002]. TTP was also shown to stimulate deadenylation of ARE-containing mRNA by PARN, and that the deadenylation required Mg^{+2}, but not ATP or capping of the RNA substrate [Lai et al, 2003]. It was speculated that TTP may compete with a stabilizing *trans*-acting factor bound in the 3' UTR of ARE-containing mRNAs and recruit PARN indirectly by interacting with other factors.

AUF1/hnRNP D or ARE/poly-U-binding /degradation factor 1, exists as four different isoforms, p37, p40, p42, and p45 that are produced by differential splicing of exons 2 and 7 [Wagner et al, 1998]. Many studies that have characterized the function of AUF1 have utilized a single recombinant isoform. Both stabilizing and destabilizing roles of AUF1 have been suggested from the results of over-expression experiments. AUF1 was identified as a part of the α-globin mRNA stability complex [Kiledjian et al, 1997]. Over-expression of p37 and p40 were shown to destabilize the ARE reporters in hemin-treated cells [Loflin et al, 1999]. The same group also reported that all four isoforms stabilized class II ARE mRNAs in NIH 3T3 cells [Chen et al, 2004; Xu et al, 2001]. By contrast, over-expression of p37 and p40 lead to the destabilization of β-Gal-GM-CSF reporter in 293, NIH 3T3, HeLa, and COS cells [Sarkar et al, 2003]. Thus, it is difficult to draw conclusions from these data. The resulting data should be interpreted as the effect of over-expression of one isoform in a particular cell line. AUF1 may have different functions in different cells, or different over-expression effects of AUF1 may be obtained due to the differential expression of stabilizing and destabilizing factors in the

cells. It was also suggested that *in vivo* the differential effects of AUF1 may result from changes in the relative abundance of the multiple isoforms [Raineri et al, 2004].

HuR is a member of the embryonic lethal abnormal vision (ELAV)-like family of RNA binding proteins. HuR has shown to bind and stabilize p38-regulated AREs of GM-CSF [Fan et al, 1998], TNF-α [Dean et al, 2001], IL-3 [Ming et al, 2001], and COX-2 [Sully et al, 2004]. HuR is predominantly a nuclear protein [Peng, S. et al, 1998]. Translocation of HuR to the cytoplasm in response to various environmental stimuli correlates with ARE-mediated mRNA stabilization [Wang et al, 2000; Yaman et al, 2002].

T cell restricted intracellular antigen (TIA-1) and TIA-related protein (TIAR) bind to U-rich regions of RNA [Dember et al, 1996]. TIA-1 and TIAR are members of the RNA recognition motif (RRM) family of RNA binding proteins. It was demonstrated that TIA-1 and TIAR are shuttling proteins that are involved in the regulation of stress-induced translation arrest. Under certain environmental stress conditions, these proteins bind to the 3'-UTR of the ARE-containing mRNAs and lead to their recruitment into the stress granules, preventing translation initiation [Kedersha et al, 1999]. It should be noted that unlike other ARE-binding proteins discussed previously, TIA-1 functions in translational regulation rather than mRNA stability.

1.8.6 P-bodies and stress granules

RNA granules are the cytoplasmic loci that play an important role in the posttranscriptional regulation of gene expression. ARE-binding proteins such as TTP, TIA-1, TIAR, and HuR localize to stress granules and P-bodies. Stress granules appear

in the cytoplasm of mammalian cells that were exposed to environmental stress, including heat, oxidative conditions, UV irradiation, and hypoxia [Anderson et al, 2006]. Specific mRNAs are selectively recruited to stress granules, while mRNAs encoding stress-induced heat shock proteins, e.g. HSP70, are excluded from stress granules. RNA-binding proteins, such as TIA-1, TIAR, TTP, and PABP, were shown to rapidly shuttle in and out of the stress granules and P-bodies, suggesting the RNA granules are the sites where the fate of mRNA may be decided [Anderson et al, 2006]. The translation initiation factor, eIF2α, is phosphorylated under environmental stress conditions by a family of stress-activated kinases, such as protein kinase R (PKR), PKR-like ER kinase, GCN2, and heme-regulated inhibitors [Anderson et al, 2006]. Phosphorylation of eIF2α decreases the availability of the eIF2-GTP-$tRNA_i^{met}$ ternary complex, leading to the binding of TIA-1 and TIAR to the 48S complex, thereby blocking translation initiation and promoting polysome disassembly. The formation of stress granules occurs upon auto-aggregation of the prion-like C-termini of TIA-1 proteins [Kedersha et al, 2002].

The P-bodies are the discrete cytoplasmic RNA granules that contain the components of the 5'→3' decay pathway, the non-sense mediated decay pathway, and the RNA-induced silencing complex [Anderson et al, 2006]. P-bodies contain the proteins involved in mRNA turnover, including CCR4, the decapping enzyme complex (Dcp1/2, Hedls, hEdc3, and p54/RCK) [Fenger-Gron et al, 2005; Yu et al, 2005], an Lsm1-7 heptamer [Ingelfinger et al, 2002], and a 5'→3'exonuclease, Xrn1 [Kedersha et al, 2005]. P-bodies were also shown to contain the components of the RNA-induced silencing complex such as argonatue and microRNA [Liu J. et al, 2005a; Sen et al, 2005], the eIF4E-binding protein 4-ET [Anderson et al, 2006], and GW182 [Liu J. et al, 2005b],

an RNA-binding protein required for microRNA-dependent silencing. In addition, P-bodies also contain several ARE-binding proteins, including TTP, Brf1, CPEB, 4-ET, and Smaug [Anderson et al, 2006]. It should be noted that the components of 3'→5' decay pathway and ARE-binding proteins such as hnRNPA1, hnRNPD, and AUF1/hnRNPD [Kedersha et al, 2002] are excluded from P-bodies, indicating 3'→5' decay may occur at a different site compared to the 5'→3' decay [Wilusz, C. et al, 2004].

1.8.7 Endoribonucleolytic cleavage

The major pathway of mRNA turnover in *E. coli* involves endoribonucleolytic cleavage of the recognition sequence or structural element within the mRNA [Kushner et al, 2004]. It is hypothesized that under certain condition these elements are bound by *trans*-acting factors that prevents mRNAs from the endonucleolytic cleavage. However, when stimulated by extracellular and/or developmental stimuli, these stabilizing factors dissociate from mRNAs, allowing endonucleolytic cleavage to occur. It should also be noted that deadenylation does not necessarily occur prior to endonucleolytic cleavage [Binder et al, 1994]. The characterization of endonucleolytic decay is difficult due to the extremely rapid decay of the cleavage products. Polysomal ribonuclease I (PMR1), an endonuclease, that is activated upon estrogen stimulation in *Xenopus* hepatocytes, accomplishes the rapid degradation of the albumin mRNA [Pastori et al, 1991]. PMR1 does not contain an RNA binding domain, hence it may not bind to the mRNAs directly [Yang et al, 2004]. Instead, it is likely that PMR1 is recruited to mRNAs by other RNA-binding proteins when it is activated by external stimuli to initiate the endonucleolytic

cleavage of mRNAs. In eukaryotic cells, PMR1 is shown to be distributed throughout cytoplasm, but is excluded from P-bodies [Yang et al, 2004].

1.9 Role of the p38/MK2 pathway in mRNA turnover

It has been proposed that TTP-mediated mRNA destabilization is down-regulated by activation of p38 signaling pathway. The p38 pathway has been shown to up-regulate TTP expression by stabilizing TTP mRNA in RAW 264.7 macrophage-like cells via an ARE within the 3'-UTR of TTP [Tchen et al, 2004]. It was proposed that the induction of TTP following p38 activation serves as a negative feed back regulation to destabilize the TTP mRNA, preventing further gene regulation of ARE-containing mRNAs. TTP is post-translationally modified by phosphorylation [Taylor, G. et al, 1995]. Hence, phosphorylation of TTP by p38 may inactivate destabilization by preventing the binding of the protein to ARE-containing mRNAs.

It was also demonstrated that p38 MAPK/MK2-mediated phosphorylation of TTP induced the binding of TTP to 14:3:3 proteins, resulting in exclusion from stress granules and inhibition of the destabilizing effect [Stoecklin et al, 2004]. In addition, the over-expression of HuR, along with activation of the p38 MAPK/MK2 pathway, further inhibited the destabilizing effect of TTP [Ming et al, 2001]. However, the regulation of TTP remains controversial. Other groups failed to detect an association of TTP with 14:3:3, and also found activation of MK2 pathway did not have an effect on TTP function [Rigby et al, 2005].

Rigby demonstrated that p38 activation alters TTP entry into the stress granule, but it does not alter TTP function. Moreover, the interaction of TTP with 14-3-3, which

regulates the entry of TTP into the stress granule, may not be involved in mRNA stabilization. Another group also demonstrated that the activation Iκβ kinase and protein kinase C-δ is involved in phosphorylation of 14-3-3-β, and found MK2 does not play a role in TTP regulation [Gringuis et al, 2005]. Thus, the signaling pathway involved in the regulation of TTP is not clear at present. It is likely that different environmental stimuli may differentially regulate TTP and downstream degradation of ARE-containing mRNAs. Accumulated experiments demonstrated that the regulation of mRNAs by ARE-binding proteins may involve nuclear-cytoplasmic shuttling and binding of a member of 14-3-3 scaffolding proteins to regulate the cytoplasmic levels of ARE-binding proteins.

1.10 ER stress signaling pathway

The endoplasmic reticulum (ER) is the site of synthesis, folding and modification of secretory and cell-surface proteins. The unfolded protein response (UPR) is induced by the accumulation of unfolded proteins in the lumen of the ER. The UPR alleviates stress by up-regulating protein folding and degradation pathways in the ER and inhibiting the protein synthesis. There are three ER-resident transmembrane proteins that sense ER stress. These include the IRE1 (α and β), PERK (RNA-dependent protein kinase-like ER kinase) and ATP6 (activating transcription factor 6, α and β) [Rutkowski et al, 2004]. Both IRE1 and PERK contain cytoplasmic serine/threonine kinase domains. ER stress induces homodimerization of the luminal domain of the IRE1 and PERK that leads to autophosphorylation and activation. In contrast, the accumulation of unfolded proteins

leads to the translocation of ATF6 to the Golgi complex, where it is cleaved by S1P and S2P proteases to release activated transcription factor [Rutkowski et al, 2004].

The activation of all three components of the UPR depends on the dissociation from the ER-luminal chaperone BiP. It is proposed that the luminal domains of IRE1, PERK, and ATF6 associate readily with BiP in the absence of the ER stress [Rutkowski et al, 2004]. In contrast, the accumulation of unfolded proteins during ER stress leads to the dissociation of BiP from IRE1, PERK, and ATF6, and preferentially association with the unfolded proteins. This dissociation of BiP leads to homodimerization and autophosphorylation of of IRE1 and PERK. On the other hand, dissociation of ATF6 from BiP allows the protein to translocate to Golgi complex where it undergoes proteolytic cleavage by proteases [Rutkowski et al, 2004].

Phosphorylation of eIF2α occurs not only in response to activation of PERK eIF2α kinase, but also by other kinases such as GCN2 (general control non-derepressible-2), PKR (pancreatic eIF2α kinase), and HRI (haem-regulated inhibitor or EIF2AK1) [Rutkowski et al, 2004]. Phosphorylation of eIF2α reduces global translation of proteins, while it induces translation of selective mRNAs such as ATF4 mRNA (activating transcription factor 4) [Wek et al, 2006]. Subsequently, ATF4 enhances the expression of additional transcription factors, including ATF3, CHOP (CCAAT/enhancer-binding protein homologues protein), and GADD153 (growth arrest and DNA-damage-inducible protein) [Wek et al, 2006]. The activated transcription factors enhance expression of genes involved in metabolic pathways, the redox reactions of the cells, and apoptosis. eIF2 kinases may function in conjunction with other stress-response pathway, such as

mitogen-activated protein kinases, to elicit gene expression for a specific stress condition [Wek et al, 2006].

CHAPTER 2

STATEMENT OF PROBLEM

The maintenance of blood acid-base balance is essential for survival. Under normal acid-base conditions, the kidney metabolizes very little of the plasma glutamine. However, during metabolic acidosis, the kidneys extract and catabolize about one-third of the plasma glutamine. The mitochondrial glutaminase (GA) catalyzes the initial reaction in the primary pathway of the increased renal catabolism of glutamine. The resulting glutamate is then oxidatively deaminated by glutamate dehydrogenase (GDH), yielding a second ammonium ion. The increased renal ammoniagenesis provides an expendable cation that facilitates the excretion of titratable acid, while conserving sodium and potassium ions. In rats and humans, the resulting α-ketoglutarate is primarily converted to glucose via gluconeogenesis, generating bicarbonate ions that partially compensate the systemic acidosis.

In rat kidney, this adaptation is sustained by the cell specific induction of multiple enzymes and various transport systems. Increased expression of the mitochondrial GA results from stabilization of the GA mRNA. The 3'-untranslated region (3'-UTR) of the GA mRNA contains a direct repeat of eight base AU-sequences (UUAAAAUA and UUUAAAUA) that function as a pH-responsive element (pHRE). These sequences exhibit a high affinity and specificity for the pHRE binding proteins, ζ-cryst and AUF1. Previous experiments indicated that chronic acidosis may lead to enhanced binding of ζ-cryst to the pHRE within GA. Thus, it was hypothesized that this interaction contributed to the increased stabilization of the GA mRNA. Recent studies indicated that rapid

deadenylation of the 3'-poly(A) tail precedes the normal turnover of the GA mRNA and that selective stabilization is associated with a decreased rate and extent of deadenylation. These data demonstrated that multiple ARE binding proteins can bind to the pHRE. However, RNA gel shift analysis only determines the binding affinity and specificity of the ARE binding to the pHRE. Hence, it was important to further characterize the roles of the ARE binding proteins in the regulation of GA mRNA in order to establish how the various ARE binding proteins contribute to the stabilization of GA mRNA during the metabolic acidosis.

Western blot analysis will be performed to identify and to characterize the nuclear and cytoplasmic distribution of the *trans*-acting RNA binding proteins that may be involved. UV-crosslinking and RNA electromobility shift assays will be performed to characterize the binding of the identified *trans*-acting ARE binding proteins to the pHRE of the GA mRNA. An *in-vitro* degradation assays will be developed to determine whether turnover of GemGA-A_{60} mRNA involves the 3'→5'degradation pathway. These assays can be also utilized to characterize the effect of each ARE binding proteins on the rate of deadenylation and turnover of GemGA-A_{60} mRNA. Extracts from cells treated with either normal or acidic medium for 24 h will be tested in *in vitro* deadenylation assay to investigate whether the stabilization of GA mRNA during metabolic acidosis is due to a slower deadenylation rate of GA mRNA. These experiments may reveal whether the deadenylation is the rate limiting step in stabilization of GA mRNA.

An alternative pathway following deadenylation is the decapping of the transcript followed by 5'→3'degradation decay mediated by the Xrn1 ribonuclease. Hence, an *in vitro* decapping assay will be performed to investigate whether 5'→3'degradation

pathway is also involved in GA mRNA turnover. Finally, immunostaining experiments can be utilized to investigate the localization of ζ-cryst. Previous 2D gel electrophoresis experiment indicated that ζ-cryst may be post-translationally modified. Therefore, phosphoprotein purification will be performed to determine if ζ-cryst is a phosphoprotein.

Previous experiments using a Tet-regulated promoter system demonstrated that the 3'-UTR of the PEPCK mRNA contains multiple instability elements [Hajarnis et al, 2006] that contribute to the pH-responsive stabilization of the PEPCK mRNA during metabolic acidosis. AUF1 was shown to bind with high affinity and specificity to the PCK-2, PCK-6, and PCK-7 segments of the 3'-UTR that contribute to the rapid turnover of the PEPCK mRNA. It was determined that the primary destabilizing elements are located within the PCK6/7 segment that constitutes the final 73-nt of the PEPCK 3'-UTR. In order to investigate the potential role of the proteins that bind to the PCK6/7 segment in stabilization of PEPCK mRNA, an *in vitro* deadenylation analysis using GemPCK6/7-A_{60} mRNA will be performed.

Appendix: Downstream elements contribute to the pH-responsive induction of renal phospho*enol*pyruvate carboxykinase

Metabolic acidosis causes increased expression of numerous proteins in the kidney that participate in the catabolism of glutamine, partially restore acid-base balance, and promote hypertrophy. Transcription of the phospho*enol*pyruvate carboxykinase (PEPCK) gene is rapidly activated following the onset of acidosis and thus serves as a paradigm to identify the elements that mediate this response. Luciferase (Luc) constructs

containing either 490 or 2300 bp of the PEPCK promoter were expressed in LLC-PK_1-$FBPase^+$ cells. Neither construct exhibited increased activity when the cells were transferred to acidic medium (pH 6.9, 10 mM HCO_3^-). Integrated copies of both chimeric constructs and adenovirus constructs of PCK_{-2300}Luc also failed to exhibit a pH-responsive increase even though the endogenous PEPCK mRNA was increased 2- to 3-fold. However, Eisenberger, *et al.* [Eisenberger et al, 1992] demonstrated that the CRC362 transgene that contains only 362 bp of the PEPCK promoter, is expressed with a normal developmental profile and at normal adult levels in kidney and is induced when the transgenic mice were made acidotic [Cassuto et al, 2003]. Hence, an element located downstream of the proximal promoter may also contribute to the pH-responsive expression of the PEPCK gene. Therefore, the CRC362 transgene will be stably expressed LLC-PK_1-F^+ cells. A quantitative real-time RT-PCR assay will be developed using specific primer sets and differentially labeled Taqman probes to quantify the CRC362 and GAPDH mRNAs in order to determine if the chimeric CRC362 transgene exhibits a pH-responsive induction and to map the region containing the pH-responsive downstream element.

CHAPTER 3

MATERIALS

3.1 Materials

Geneticin (G418) and Hygromycin B were obtained from Mediatech. Dulbecco's modified Eagle's medium/F-12 base medium, cloning rings, poly-A RNA, phosphocreatine, and β-tubulin antibody were obtained from Sigma-Aldrich. Tissue culture plates were purchased from Dow Corning. Cell scrapers were from Sarstedt. TRIzol Reagent, Platium qPCR SuperMix-UDG, Hoechst and ER track Blue-White DPX dyes, and Prolong Gold antifade reagents were purchased from Invitrogen. Formazol was purchased from Molecular Research Center. Mini-RNA isolation kit was ordered from Zymo Research. The avian myeloblastosis virus-reverse transcriptase and DNA purification MiniPrep System were purchased from Promega. Dual-labeled Taqman Probes were ordered from Biosearch Technologies.

Various restriction enzymes were purchased from New England Biolabs. GENECLEAN kits were obtained from Q-Biogene. QIAquick Gel Purification Kit and Qiagen Maxi Kit were purchased from Qiagen. The PCRScript cloning kit and *E. coli* strain BL21 codon plus competent cells were obtained from Stratagene.

[α-^{32}P]-UTP (800 Ci/mmol), [α-^{32}P]-GTP (800 Ci/mmol), [α-^{32}P]-dCTP (3000 Ci/mmol) purchased from ICN Biochemicals or Amersham Pharmacia Biotech. dNTPs, rNTPs, ^{m7}G(5')ppp(5')G, HiTrap 5 ml Chelating Sepharose High Performance column and HiTrap 1 ml Heparin HP column were purchased from Amersham. RNase T1, RNase I, RNase A, SP6 RNA polymerase, and yeast tRNA were acquired from Roche

and MBI Fermentas. RNasin was obtained from Fisher. Guanylyl transferease, vaccinia virus capping enzyme, and DECA prime II oligolabelling kit were purchased from Ambion. tRNA was purchased from Roche. Microtiter plates were purchased from VWR International, Inc. Buffer-saturated phenol was purchased from USB. GelBond PAG films were purchased from Intermountain Scientific. GeneScreen Plus was purchased from New England Nuclear.

Vivaspin 500 (MWCO 10000) and Vivaspin 20 (MWCO 3000) were purchased from VivaSciences. Phosphatase inhibitor and protease inhibitor cocktail, and NE-Per Nuclear and Cytoplasmic Extraction Reagent were purchased from Pierce. Chemicals for acrylamide gels, Micro Bio-spin chromatography columns, Bradford reagent and protein standards, Econo-Pac® Serum IgG Purification Kit were purchased from Bio-Rad.

Glass bottom culture plates were obtained from MatTek. IRDye® goat-anti-rabbit antibody was from Odyssey. Alexa-fluor 680 goat-anti-mouse antibody, Texas-red 595 goat-anti-rabbit, Fluorescein 494 goat-anti-rabbit, Fluorescein 494 goat-anti-mouse antibodies were purchased from Molecular Probes.

α-HuR antibody was obtained from Santa Cruz Biotechnology. α-AUF1 antibody was purchased from Upstate Technology. Dcp2 antibody was generously provided by Dr. Megerditch Kiledjian (Rutgers University, Department of Cell Biology and Neurosciences, Piscataway, NJ). DcpS and Dcp1a antibodies were provided by Dr. Jens Lykke-Andersen (University of Colorado, MCD Biology, Boulder, CO). PARN antisera was provided by Dr. Anders Virtanen (Uppsala University, Department of Cell and Molecular Biology, Uppsala, Sweden), which was purified using Econo-Pac® Serum IgG Purification Kit (Bio-Rad). Brf1 antibody was a generous gift from Dr. Christoph

Moroni (Institute of Medical Microbiology, University of Basel, Basel, Switzerland). TTP antibodies were provided by Dr. Perry Blackshear (Director of Clinical Research, NIEHS, RTP, NC) and Dr William Rigby (Department of Medicine, Dartmouth Medical School, Lebanon, NH). eIF2α antibody was purchased from Abcam. Phopho-eIF2α and BiP antibodies were purchased from Cell Signaling. eIF4 antibody was purchased from Santa Cruz. PM-Scl75 antiserum was provided by Dr. Jeffrey Wilusz (Department of Microbiology, Immunology, and Pathology, Colorado State University, Fort Collins, CO)

The expression vectors for $(His)_6$ tagged-p38, p40, p42, and p45 AUF1 were received from Dr. Jeffrey Wilusz and Dr. Robert Schneider (Department of Microbiology, New York University, School of Medicine, New York, NY). His_6-TTP expression vector was also received from Dr. Jeffrey Wilusz.. The expression vector for pET21a-$(His)_6$-HuR was received from Dr. Joan Steitz (Molecular Biophysics and Biochemistry, Yale University, New Haven, CT). pQE-$(His)_6$-Brf1 was received from Dr. Christoph Moroni (Institute of Medical Microbiology, University of Basel, Basel, Switzerland).

3.2 Buffers and Solutions

Krebs-Henseleit Saline Buffer (KHS)

118 mM Sodium Chloride

4.8 mM Potassium Chloride

1.2 mM Sodium Phosphate

1.2 mM Magnesium Phosphate

2.5 mM Calcium Chloride

25 mM Sodium Bicarbonate

5.5 mM Glucose

1.0 mM Acetoacetate

1.0 mM Alanine

0.1 mM Myoinositol

1.0 mM Glutamine

pH to 7.4

Rat Renal Cortex Cytoplasmic Extraction Buffer

40 mM HEPES

100 mM Potassium Acetate

10 mM Magnesium Acetate

1 mM Dithiothreitol (DTT)

0.01 mM Leupeptin

0.01 mM Antipain

5 μg/ml Phenylmethylsulfonylfluoride (PMSF)

pH to 7.4

1X Binding Buffer for FPLC

10 mM HEPES

1 mM DTT

0.5% Igepal CA630

pH to 7.4

100X Binding Buffer for FPLC

10 mM HEPES

1 mM DTT

0.5% Igepal CA630

0.5 M Potassium Acetate

50 mM Magnesium Acetate

pH to 7.4

1X Dialysis Buffer, pH 7.4

10 mM HEPES

25 mM Potassium Acetate

2.5 mM Magnesium Acetate

1 mM DTT

pH to 7.4

Lower Tris Stock

18.17 g Tris Base

4 ml 10% Sodium Dodecylsulfate (SDS)

pH to 8.6, adjust to 100 ml

Upper Tris stock

6.06 g Tris Base

4 ml 10% SDS

pH to 6.6, adjust to 100 ml

2X Sample Buffer

10 ml Glycerol

5 ml β-Mercaptoethanol (BME)

30 ml 10% SDS

12.5 ml Upper Tris Stock

5 ml 0.05% Bromophenol Blue

Adjust to 100 ml

4X Reservoir Buffer Stock

12 g Tris Base

57.6 g Glycine

pH to 8.5, adjust to 1 L

After dilution add 1/100 volume of 10% SDS

Annealing Buffer

50 mM Sodium Chloride

66 mM Tris-HCl

6.6 mM Magnesium Chloride

pH to 7.5

50X TAE Buffer

2.0 M Tris-acetate, pH 8.0

100 mM Ethylenediaminetetraacetic acid (EDTA)

10X Stop Buffer

2 ml 0.25 M EDTA

2.5 ml Glycerol

0.5 ml Nanopure Water

25 mg Bromophenol Blue

5X TBE Buffer

450 mM Tris, pH 8.2

550 mM Boric Acid

10 mM EDTA

5X TB Buffer

450 mM Tris, pH 8.2

550 mM Boric Acid

Type III Buffer (6X)

0.25% Bromophenol Blue

0.25% Xylene Cyanol

30% Glycerol

Elution Buffer

0.5 M Ammonium Acetate

10 mM Magnesium Acetate

1 mM EDTA

0.1% SDS

DEPC-treated Water

0.1% (v/v) Diethyl Pyrocarbonate (DEPC)

Incubate at 37 °C overnight and autoclave

10X Binding Buffer

100 mM HEPES

25 mM Magnesium Acetate

250 mM Potassium Acetate

pH to 7.4

2X HBSP, pH 7.0

1.5 mM Sodium Phosphate

10 mM Potassium Chloride

280 mM Sodium Chloride

12 mM Glucose

50 mM HEPES

65 μM 5,6-Dichlorobenzimidazole 1-β-D-ribofuranoside (DRB)

4.2 mg/ml dissolved in 95% ethanol

Use 40 µl 4.2 mg/ml DRB / 8 ml medium to obtain 65 µM

10X MOPS Buffer

0.2 M MOPS (3-(N-morpholino)propanesulfonic acid)

10 mM Sodium Acetate

10 mM EDTA, pH to 7.0

Northern Loading Buffer

33.75% Formaldehyde (37% v/v)

10% Glycerol

10% 0.1 % Bromophenol Blue

20% 10X MOPS

RNA Agarose Gel Running Buffer

10% v/v 10X MOPS

8% v/v Formaldehyde (37% v/v)

20X SSC

3.0 M Sodium Chloride

0.1 M Sodium Citrate

Hybridization Buffer

250 mM Sodium Chloride

50% v/v Formamide

25 mM Sodium Phosphate, pH 7.2

1 mM EDTA

7% w/v SDS

Northern Wash Solutions

Wash 1: 2X SSC

0.5% w/v SDS

Wash 2: 25 mM Sodium Phosphate, pH 7.2

0.5% w/v SDS

1 mM EDTA

Wash 3: 25 mM Sodium Phosphate, pH 7.2

5% w/v SDS

1 mM EDTA

10X RNA polymerase buffer

400 mM Tris-Cl, pH 7.9

60 mM Magnesium chloride

20 mM Spermidine

100 mM Dithiothreitol

15X capping buffer

750 mM Tris-Cl, pH 7.9

90 mM Potassium chloride

37.5 mM Dithiothreitol

18.8 mM Magnesium chloride

1.5 mg/ml Iodoacetylated bovine serum albumin (BSA)

8 M Urea RNA gel loading buffer

20 mM Tris-Cl, pH 7.6

8 M Urea

1 mM Ethylenediamine tetraacetic acid (EDTA)

0.02% w/v Xylene cyanol

0.02% w/v Bromophenol blue

HSCB

25 mM Tris-Cl, pH 7.6

400 mM Sodium chloride

0.1% SDS

5X NTP mixture for *in vitro transcription*

5 mM NTPs (5 mM each ATP, GTP, UTP, CTP)

5X NTP mixture for labeled *in-vtiro* transcription

5 mM each ATP, GTP, CTP

0.5 mM rUTP

10X CE buffer

500 mM Tris-Cl, pH 7.9

300 mM Ammonium sulfate

10 mM Magnesium chloride

Phosphate-buffered saline (PBS), pH 7.4

137 mM Sodium chloride

2.7 mM Potassium chloride

10 mM Sodium phosphate

2 mM Potassium phosphate

Buffer A for cytoplasmic extracts preparation, pH 7.4

10 mM HEPES, pH 7.4

1.5 mM Magnesium chloride

10 mM Potassium chloride

Phosphatase inhibitors

Protease inhibitors

Buffer B for cytoplasmic extracts preparation, pH 7.4

0.3M HEPES, pH 7.4

1.4 M Potassium chloride

30 mM Magnesium chloride

Phosphatase inhibitors

Protease inhibitors

Buffer A for cytoplasmic extracts preparation, pH 6.9

10 mM HEPES, pH 6.9

1.5 mM Magnesium chloride

10 mM Potassium chloride

Phosphatase inhibitors

Protease inhibitors

Buffer B for cytoplasmic extracts preparation, pH 6.9

0.3M HEPES, pH 6.9

1.4 M Potassium chloride

30 mM Magnesium chloride

Phosphatase inhibitors

Protease inhibitors

T4 DNA ligase buffer

50 mM Tris-Cl, pH 7.5

10 mM Magnesium chloride

10 mM DTT

1 mM ATP

25 μg/ml Bovine serum albumin (BSA)

Starting buffer for HiTrap Chelating HP resin

10 mM Tris-Cl, pH 8.0

300 mM Potassium chloride

10% Glycerol

Elution buffer for HiTrap Chelating HP resin

10 mM Tris-Cl, pH 8.0

300 mM Potassium chloride

10% Glycerol

1M Imidazole

Starting buffer for HiTrap Chelating HP resin for recom. ζ-cryst purification

20 mM Tris-Cl, pH 7.9

500 mM Sodium chloride

10% Glycerol

Elution buffer for HiTrap Chelating HP resin for recom. ζ-cryst purification

20 mM Tris-Cl, pH 7.9

500 mM Sodium chloride

10% Glycerol

1M Imidazole

Stripping buffer for HiTrap Chelating HP resin

10 mM Tris-Cl, pH 8.0

300 mM Potassium chloride

0.1M EDTA

10% Glycerol

Chelating buffer for HiTrap Chelating HP resin

0.3M Nickel sulfate

Buffer A for HiTrap Heparin resin

50 mM Tris-Cl, pH 8.0

100 mM Sodium chloride

2.5 mM DTT

10% Glycerol

Buffer B for HiTrap Heparin resin

50 mM Tris-Cl, pH 8.0

500 mM Sodium chloride

2.5 mM DTT

1 mM EDTA

0.01% Triton X-100

10% Glycerol

Dialysis buffer for HiTrap Heparin resin

10 mM HEPES, pH 7.4

25 mM Potassium Acetate

2.5 mM Magnesium Acetate

1 mM DTT

250 mM phosphocreatine/12.5 mM ATP

Phenol saturated with 10 mM Tris-Cl, pH 8.0

Phenol:Chloroform:isoamyl alcohol 25:24:1

40% Acylamide/bis-acrylamide (37.5:1)

40% Acylamide/bis-acrylamide (19:1)

30% Acylamide/bis-acrylamide (29:1)

10M ammonium acetate

10% w/v ammonium persulfate

10% w/v polyvinyl alcohol

CHAPTER 4

METHODS

4.1 Plasmids

pGem-A_{60}, pGem-A_0, pGem-ARE-A_{60}, and pGem-ARE-A_0 plasmids were obtained from Dr. Jeffrey Wilusz (Department of Microbiology, Immunology, and Pathology, Colorado State University, Fort Collins, CO). A 28-nt segment containing the pHRE of GA mRNA ($^{5'}$CTAGTGCTAGCTC**TTTAAATA**AA**TTAAAATA**ATTACT AAT$^{3'}$) was cloned into XbaI site of pGem-A_0 and pGem-A_{60} vectors to yield pGemGA-A_0 and pGemGA-A_{60}, respectively. The inserted sequence also contains a unique NheI restriction enzyme site that was used confirm the insertion of the segment into the vectors. A 73-nt segment containing the AU- and CU-rich PCK6/7 segment ($^{5'}$GTACCGTATGTTTAAATTATTTTTATACACTGCCCTTTCTTACCTTTCTTTAC TAATTGAAATAGGTATCCTGACCAG$^{3'}$) was cloned into XbaI site of pGem-A_0 and pGem-A_{60} vectors to yield pGemPCK-A_0 and pGemPCK-A_{60}, respectively.

pGem-A_{60}, pGemARE-A_{60}, pGemGA-A_{60}, and pGemPCK-A_{60} were digested with SspI restriction enzyme to generate a DNA template that encodes a polyadenylated tail of 60 nt. pGem-A_0, pGemARE-A_0, pGemGA-A_0 and pGemPCK-A_0 were digested with HindIII restriction enzyme to generate a DNA template without a polyadenylated tail. The plasmids were transcribed using SP6 RNA polymerase in the presence of [α-^{32}P]-UTP and 500 μM ^{7met}GpppG to produce mRNAs that contain a 5' cap. The labeled RNAs were purified by electrophoresis on a 5% denaturing polyacylamide gel containing 8 M urea.

4.2 Cell culture

LLC-PK_1-FBPase$^+$ cells (LLC-PK_1-F^+ cells)

The porcine renal proximal tubular epithelial cells were maintained at 37 °C in a humidified atmosphere with 5% CO_2. The cells were cultured in DMEM/F12 medium supplemented with fetal bovine serum (10%), penicillin (10 U/ml), streptomycin (10 μg/ml). Sub-confluent and confluent LLC-PK_1-F^+ cells, that were grown for 2-14 post split days were treated with either normal medium (pH 7.4, 25 mM HCO_3^-) or acidic medium (pH 6.9, 10 mM HCO_3^-) before isolating total RNA for real-time RT-PCR analysis.

WKPT cells

The rat renal proximal tubular epithelial cell line was cultured as described previously (Brandsch, 1995). The cells were maintained at 37 °C in a humidified atmosphere with 5% CO_2. The cells were cultured in DMEM/F12 medium supplemented with fetal bovine serum (10%), penicillin (10 U/ml), streptomycin (10 μg/ml), insulin (5 μg/ml), dexamethasone (4 μg/ml), apotransferrin (5 μg/ml), and epidermal growth factor (10 ng/ml). Sub-confluent and confluent WKPT cells were treated with either normal medium (pH 7.4, 25 mM HCO_3^-) or acidic medium (pH 6.9, 10 mM HCO_3^-) for 1-5 days before isolating total RNA for real-time RT-PCR analysis.

WKPT-ζ^+cells

pcDNA 3.1/Hygro-ζ-cryst was used to select clonal lines of WKPT cells that over-express ζ-crystallin. At 2 d post splitting, cells were transfected with calcium

phosphate precipitated DNA. The transfected cells were selected for growth in standard medium supplemented with 0.8 mg/ml hygromycin. The cells were allowed to select for 2-3 weeks. The resulting colonies were isolated with cloning rings and the clonal lines were expanded in medium containing 0.2 mg/ml hygromycin. 90% confluent WKPT-ζ^+ cells were treated with either normal medium (pH 7.4, 25 mM HCO_3^-) or acidic medium (pH 6.9, 10 mM HCO_3^-) for 24 h for preparation of nuclear and cytoplasmic extracts.

4.3 RNA extraction and reverse transcription

Total cellular RNA was isolated using the TRIzol® reagent or Mini-RNA Isolation Kit and the RNA concentration was determined by measuring the absorbance at 260 nm. The initial strand of cDNA was synthesized in 20 μl solution containing 5 mM $MgCl_2$, 1X reverse transcription buffer (10 mM Tris-Hcl, pH 9.0, 50 mM KCl, 0.1% Triton X-100), 1 mM of each dNTP, 40 U of RNasin, 14 U of avian myeloblastosis virus-reverse transcriptase, 0.5 μg Oligo-dT_{18} primer, and 1μg total RNA, and incubated for 60 min at 42 °C. The cDNAs prepared from the reverse transcription reactions were used directly for quantitative real-time RT-PCR analysis.

4.4 Quantitative real-time RT-PCR

The purified 475-bp fragment of porcine GAPDH plasmid was serially diluted from 1 ng/μl to 10^{-5} ng/μl. A primer set was designed to amplify from 731 bp to 875 bp within the coding region. The forward primer, $^{5'}$GATGGGCATGAACCATGAGA$^{3'}$, and the reverse primer, $^{5'}$GGCATGGACTGTGGTCATGA$^{3'}$, were used in real-time RT-PCR along with a Taqman Probe, $^{5'}$CAL-Red™-TGCCTCCTGTACCACCAACTGCTTGG-

BHQ2[3'], that is complementary to region from 783 bp to 807 bp of the porcine GAPDH coding region.

Porcine KGA cDNA was amplified using a forward primer, [5']AAAAGCCTTTTGGACTGACG[3'], and a reverse primer, [5']AATGACACTGTCCCAA GGTATAGC [3'], that amplify the region from 2775 bp to 2981 bp within the unique coding region of porcine KGA mRNA. The purified 207-bp porcine KGA PCR product were used as a standard. It was serially diluted from 10^{-2} ng/μl to 10^{-5} ng/μl. The real-time RT-PCR reaction also included a [5']FAM-TAAGTTCCTCTGATGGACAGATGC ATATCCTAAC–BHQ1[3'] that is complementary to the region from 2886 bp to 2899 bp of porcine KGA cDNA.

Porcine GAC cDNA was amplified using a forward primer, [5']TCCTTTCCTACTCCAACAGCC[3'], and a reverse primer, [5']CCTGATGCAGCTCAGT TAAGG[3'], that amplify the region from 3167 bp to 3311 bp within the unique coding region of porcine GAC mRNA. The purified 145-bp porcine GAC PCR product were used as a standard. It was serially diluted from 10^{-2} ng/μl to 10^{-5} ng/μl. The real-time RT-PCR reaction also included a [5']Tet-TCACTTCTGGTCTAAATCAGTGGCTTCA GC–BHQ2[3'] that is complementary to the region from 3205 bp to 3234 bp of porcine GAC cDNA.

Rat GAPDH cDNA was amplified using a forward primer, [5']GATGGGTGTGAACCACGAGA[3'], and a reverse primer, [5']GGCATGGACTGTGG TCATGA[3'], that amplify the region from 1238 bp to 1382 bp of the rat GAPDH coding region. The 145-bp GAPDH PCR product was cloned into pGem-T-easy vector. The purified 165-bp EcoRI fragment from the resulting plasmid was used as a standard. It

was serially diluted from 1 ng/μl to 10^{-5} ng/μl. The real-time RT-PCR reaction also included a $^{5'}$CAL-Red^{TM}-AATGCATCCTGCACCACCAACTGCTTAG–BHQ2$^{3'}$ that is complementary to the region from 1287 bp to 1314 bp of rat GAPDH cDNA.

The purified 507-bp EcoRI/HindIII fragment of pGA105, a rat GAC plasmid, was serially diluted from 10^{-2} ng/μl to 10^{-7} ng/μl. A primer set was designed to amplify the region from 1911 bp to 2033 bp within the unique coding region of the GAC mRNA. The forward primer, $^{5'}$TTGGACTATGAGAGTCTCCAGC$^{3'}$, and the reverse primer, $^{5'}$TCTCCCCCAGACTTTCCATTC$^{3'}$, were used in real-time RT-PCR along with a Taqman Probe, $^{5'}$FAM-CACAGTGTGGAAAAAAGTGTCACCTGAGTCAAG–BHQ1$^{3'}$, that is complementary to region from 1952 bp to 1984 bp of the GAC coding region.

The purified 338-bp PstI fragment of pGA104, a rat KGA plasmid, was serially diluted from 10^{-2} ng/μl to 10^{-7} ng/μl. A primer set was designed to amplify the region from 2061 bp to 2245 bp within the unique coding region of the KGA mRNA. The forward primer, $^{5'}$TGGAAGCTTGCAAAGTTAACCC$^{3'}$, and the reverse primer, $^{5'}$ CCCGTCAAGATTCTTGTGGAC$^{3'}$, were used in real-time RT-PCR along with a Taqman Probe, $^{5'}$HEX-TTCCCCAAGGACAGGTGGAATAACACCC–BHQ1$^{3'}$, that is complementary to region from 2084 bp to 2111 bp of the GAC coding region.

The quantitative real-time PCR reaction was performed using Platinum qPCR Supermix-UDG in the presence of 100 nM primers, 200 nM Taqman Probes, and 9 mM $MgCl_2$. The induction was calculated using a mathematical model of relative expression in real-time PCR (Pfaffl, 2001) to quantify the relative levels of the GAC and KGA

mRNA in comparison to the GAPDH mRNA. The reported values are the mean ± S.E. of data obtained from triplicate samples that were assayed in triplicate.

4.5 Preparation of S10 and S100 cytoplasmic extracts

For the *in vitro* deadenylation assay, cytoplasmic S10 and S100 extracts were prepared. WKPT and WKPT-ζ^+ cells were grown at 37 °C in a humidified atmosphere with 5% CO_2. 90% confluent WKPT cells were treated with either normal medium (pH 7.4, 25 mM HCO_3^-) or acidic medium (pH 6.9, 10 mM HCO_3^-) for 24 h before harvesting. The cells were washed 2 times with PBS, then trypsinized and centrifuged at 1500 xg for 10 min at 4 °C. The pellet was resuspended in cold PBS, then washed 2 times with cold PBS. The packed cell volume (PCV) was noted. The cells were resuspended in cold 5 packed cell volumes of buffer A (10 mM HEPES, pH 7.4 or pH 6.9, 1.5 mM $MgCl_2$, and 10 mM KCl, containing phosphatase and protease inhibitors) for 10 min on ice. The cells were then lysed using a pre-chilled Dounce homogenizer with 15 strokes of the pestle. The lysed cells were then spun at 1500 xg for 10 min at 4 °C. The supernatant was transferred to a new tube without transferring the pelleted nuclei, then 0.11 packed cell volumes of buffer B (0.3 M HEPES, pH 7.4 or pH 6.9, 1.4 M KCl, and 30 mM $MgCl_2$, containing phosphatase and protease inhibitors) was added. The cytoplasmic fraction was centrifuged either at 10,000 xg or at 100,000 xg for 1 h in an ultracentrifuge to produce the S10 and S100 supernatant, respectively. The supernatants were collected, and 0.25 volume of 80% glycerol was added before storing at -80 °C.

4.6 Western blot analysis

Samples containing 40 μg of protein were mixed with an equal volume of 2X SDS sample buffer (10% (w/v) glycerol, 5% (w/v) β-mercaptoethanol, 3% (w/v) SDS, 184 mM Tris-HCl, pH 6.8, and 0.2% (w/v) bromophenol blue). The samples were heated for 4 min at 95 °C, then loaded onto a 10% SDS-polyacrylamide gel. Following electrophoresis, the gel was then transferred to a PVDF membrane and after blocking the membrane was incubated with 1:500-1:1000 dilution of various purified IgG antibodies or antisera. The membrane was then incubated with a 1:10,000 dilution of secondary antibody conjugated to IRDye® goat-anti-rabbit antibody or Alexa-fluor^{680} goat-anti-mouse antibody. Images were then visualized and quantified using an Odyssey Infra-red imaging system.

4.7 *In vitro* transcription

DNA templates were digested with the desired restriction enzyme for 2 h at 37 °C, then extracted with phenol:chloroform:isoamyl alcohol (25:24:1). The pellet was resuspended in DEPC-treated H_2O. *In vitro* transcription of [^{32}P]-labeled, 5'-capped RNAs was performed as follows: 1 μg DNA template, 500 μM cap analog (^{7met}GpppG), 1X NTP mix (1 mM ATP, 1 mM CTP, 1 mM GTP, 0.1 mM UTP), 1X RNA polymerase buffer, 20 U RNasin, 10 μCi [α^{32}P]-UTP (800 Ci/mmol), 26 U SP6 RNA polymerase, in a 10 μl reaction volume. The products were then extracted with phenol:chloroform:isoamyl alcohol (25:24:1), and precipitated with a 1/10 volume of 10 M NH_4Ac. The pellet was resuspended in 8 M urea RNA gel loading buffer (20 mM Tris-Cl, pH 7.6, 8 M urea, 1 mM EDTA, 0.02% w/v xylene cyanol, 0.02% w/v

bromophenol blue) and heated at 95 °C for 1 min. The samples were loaded onto a 5% denaturing polyacrylamide gel containing 8 M urea. The labeled RNA was eluded with HSCB (25 mM Tris-Cl, pH 7.6, 400 mM NaCl, 0.1% SDS) and treated with 30 μg proteinase K (10 mg/ml). The extracted samples were precipitated with buffer-saturated phenol. The RNA pellet was resuspended in DEPC-treated H_2O. The [^{32}P]-labeled RNAs were quantified by scintillation counting and DEPC-treated H_2O was added to adjust the sample to the desired concentration.

4.8 *Purification of recombinant ARE binding proteins*

The recombinant $(His)_6$-tagged ζ-cryst proteins were expressed in Sf9 cells, grown with Grace's media. The recombinant ζ-cryst was purified using a HiTrap Chelating Column that was eluted with an increasing concentration of imidazole on a FPLC™ system.

All other recombinant $(His)_6$-tagged proteins were expressed in *E. coli* strain BL21 codon plus bacteria. The recombinant proteins were induced with 1 mM IPTG and purified using a HiTrap Chelating HP column that was eluted with an increasing concentration of imidazole on a FPLC™ System. For $(His)_6$-p40 AUF1 recombinant protein, the eluted proteins fractions were further purified using a HiTrap Heparin column, in order to eliminate a contaminating RNase activity. The $(His)_6$-Brf1 and $(His)_6$-p37-AUF1 recombinant proteins were found to be insoluble, hence the purification of the recombinant proteins were attempted in 8 M urea. The purity of the purified proteins were accessed by SDS-PAGE and Coomassie blue staining. Protein

concentrations were determined with the Bradford assay using bovine serum albumin (BSA) as the standard [Bradford, 1976].

4.9 *RNA Electrophoretic mobility shift (RNA-EMSA)*

Various amounts, 0.25-30 μg, of S10 post-nuclear or S100 cytoplasmic extracts of WKPT or WKPT-ζ^+ cells or 0.06-1.5 μM (final concentrations) of the recombinant proteins were pre-incubated for 10 min at room temperature in 1X binding buffer (0.5% Nonidet P-40, 1 mM dithiothreitol, 2 μg yeast t-RNA, 40 units of RNasin, 10% glycerol) with 20,000 cpm of [^{32}P]-labeled, capped RNA. For competition assays, 125-500 μM cap analog was added with the labeled RNA. The reaction mixture was incubated at room temperature for 20 min with or without addition of RNase T1. For the reactions with the RNase T1 addition, 10 U of RNase T1 was added to the reaction mixture and then incubated further for 10 min at 37 °C. The samples were separated on 5% native polyacrylamide gels and the gels were dried and exposed overnight to a PhosphorImager screen. In the supershift experiments, the various antibodies were pre-incubated with the recombinant proteins for 20 min at room temperature and then added to the binding buffer.

4.10 *UV-crosslinking experiment*

The following reagents were added in the reaction: 1X CE buffer, 1 mM $MgCl_2$, and 1 μl containing 100,000 cpm of [^{32}P]-labeled, capped RNA substrate were incubated with 23 μg WKPT or WKPT-ζ^+ S100 cytoplasmic extracts or 2 μM (final concentrations) recombinant proteins, in a 10 μl reaction volume. The reactions were incubated at 30 °C

for 5 min and then transferred to a microwell plate. The samples were UV-crosslinked for 10 min using a UV Stratalinker. Then 1.7 μl of RNase A (10 mg/ml) and 0.3 μl of RNase I (100 U/μl) were added to the reaction for poly-adenylated RNA substrates, or 2 μl of RNase A (10 mg/ml) for RNA substrates without the poly-A tail. The samples were incubated at 30 °C for 10 min. Finally, 10 μl of 2X SDS samples buffer was added and the samples were heated at 95 °C for 4 min and resolved on a 10% SDS-polyacrylamide gel. The gel was dried and exposed for 3 days to a PhosphorImager screen.

4.11 *In vitro* deadenylation assay

The following reagents were added in the following order: 4 μl 10% polyvinyl alcohol, 1 μl 250 mM phosphocreatine/15 mM ATP, 1 μl 500 ng/μl poly-A RNA, 0.5 μl RNase inhibitor (40 U/μl), 1 μl containing 100,000 cpm of RNA substrate, 16 μg WKPT or WKPT-ζ^+ S100 cytoplasmic extracts. The reactions were incubated at 30 °C for the desired time. HCSB buffer (25 mM Tris-Cl, pH 7.6, 400 mM NaCl, 0.1% SDS) was added to stop the reaction. The samples were phenol extracted and the RNA was precipitated by addition of a 1/10 volume of 10 M NH_4Ac and storing at -80 °C for 10 min in the presence of 2 μl of tRNA (10 μg/μl). The pelleted RNA was resuspended in urea RNA gel loading buffer, and then loaded onto a 5% denaturing polyacrylamide gel. In some reactions, the ATP/phosphocreatine (ATP/PC) and/or poly-A RNA was replaced by the addition of DEPC-treated H_2O. For competition assay, 5-50 μM cap analog was added with the labeled RNA, with or without the addition of poly-A RNA.

4.12 *In vitro* transcription for decapping assay

In order to generate RNA substrates that are radiolabeled within the cap structure, the following reactions were prepared: 1 μg linearized DNA template, 1X NTP mixtures (1 mM each ATP, GTP, UTP, CTP), 1X RNA polymerase buffer, 20 U of SP6 polymerase, 20 U of RNasin, and the total volume was brought up to 10 μl with DEPC-treated H_2O. The reaction was incubated at 37 ˚C for 2 h. The samples were then extracted with phenol:chloroform:isoamyl alcohol (25:24:1), and the RNA was precipitated with 1/10 volume of 10 M NH_4Ac. The pellet was lysophilized and resuspended in the following reaction mixture: 4.5 μl of [α-^{32}P]GTP (800 Ci/mmol), 0.5 μl of 15X capping buffer, and 0.5 μl of 10 mM S-adenosyl methionine. 20 U of RNasin was added and the reaction mixture was incubated at 37 ˚C for 30 min. Then the samples were extracted again with phenol:chloroform:isoamyl alcohol (25:24:1), and precipitated with a 1/10 volume of 10M NH_4Ac. The samples were resuspended in urea RNA gel loading dye, and then heated at 95 ˚C for 1 min before loading onto a denaturing 5% polyacrylamide gel. The labeled RNA was eluded with HSCB (25 mM Tris-Cl, pH 7.6, 400 mM NaCl, 0.1% SDS) and treated with 3 μg proteinase K. Then the samples were phenol extracted and the RNA was precipitated. The RNA pellet was resuspended in DEPC-treated H_2O. The [^{32}P]-cap labeled RNAs were quantified by scintillation counting and DEPC-treated H_2O was added to adjust the sample to the desired concentration.

4.13 *In vitro* decapping assay

The following reaction was assembled: 1X CE buffer and 1 μl containing 100,000 cpm of cap-labeled RNA were incubated with 28 μg of WKPT or WKPT-ζ^+ S10 post-nuclear or S100 cytoplasmic extracts, in a 10 μl reaction volume. The reactions were incubated at 30 ˚C for 30 min. The reactions were performed in the absence or presence of 200 μM of cap analog. Then, 20 μl of buffer saturated phenol was added to each reaction, and 10 μl of the reaction's aqueous phase was transferred to a new tube. 4 μl of urea RNA loading buffer was added and the samples were heated at 95 ˚C for 1 min before resolving on a 20% denaturing polyacrylamide gel.

4.14 *Preparation of nuclear and cytoplasmic extracts from WKPT and WKPT-ζ^+ cells*

Nuclear and cytoplasmic extracts were prepared according to the manufacturer's instruction of NE-Per Nuclear and Cytoplasmic Extraction Reagent. A hypotonic solution containing a mild detergent was used to lyse the cell membrane and release the cytoplasm. The intact nuclei were then subsequently lysed in a hypertonic solution.

4.15 *Immunostaining*

WKPT-ζ^+ cells were grown to 90% confluency on glass-bottom culture plates and then treated with normal medium (pH 7.4, 25 mM HCO_3^-) or acidic medium (pH 6.9, 10 mM HCO_3^-) for 24 h. The cells were washed 2 times with PBS and then fixed with 4% formaldehyde in PBS. The cells were incubated at 37 ˚C for 10 min then washed 5 times with PBS for 10 min. The cells were permeabilized by incubating in 0.2% Triton-X 100 for 10 min, followed by five 10-min washes with PBS. 2% Goat serum in TBS/1% BSA

was used to block for 1 h. The cells then incubated over night at 4 °C with 1:500-1:1000 dilutions of primary antibodies. The cells were then washed 5 times in TBS solution for 10 min, and then incubated with 1:400 dilution of secondary antibodies (Texas-red 595 goat-anti-rabbit, Fluorescein 494 goat-anti-rabbit, Fluorescein 494 goat-anti-mouse antibodies) for 1 h at room temperature. The cells were washed 5 times with TBS for 10 min. For the nuclear staining, a 1:200 dilution of Hoechst stain was added at the end of the incubation with secondary antibody. For the ER staining, a 1:400 dilution of ER track Blue-White DPX stain was added to the cells at the end of the incubation with the secondary antibody or added to the fixating solution at a 1:1000 dilution.

CHAPTER 5

DEVELOPMENT OF *IN VITRO* DEADENYLATION AND TURNOVER ASSAY

5.1. Comparison of LLC-PK$_1$-F$^+$ and WKPT cells

The mitochondrial glutaminase acts as a key regulator of the increased renal ammoniagenesis and gluconeogenesis in response to metabolic acidosis [Brosnan et al, 1988]. Glutamine extracted by the kidney is deamidated by a phosphate-activated glutaminase and then oxidatively deaminated by glutamate dehydrogenase (GDH), yielding two ammonium ions. This increased renal ammoniagenesis provides an expendable cation that facilitates the excretion of titratable acid, while conserving sodium and potassium ions. In rats, the resulting α-ketoglutarate is primarily converted to glucose, generating bicarbonate ions that partially compensate the systemic acidosis.

Following onset of acidosis, the decrease in the plasma pH and HCO_3^- concentration produces a comparable and sustained decrease in the intracellular pH (pH_i) of the proximal convoluted tubules [Ackerman et al, 1981]. Therefore, the adaptive increase in mitochondrial GA activity that results from the selective stabilization of the GA mRNA may be initiated by a decrease in pH_i [Curthoys et al, 1995].

A GA cDNA hybridizes to 4.7-kb and 3.4-kb mRNAs in total or poly-A RNA isolated from rat kidney [Hwang et al, 1991]. During the onset of acidosis, the two GA mRNAs level increase following a 6- to 8-h lag, reach a 5-fold increase within 1 d and attain a maximal 8-fold increase after 5 d. Acute recovery from chronic acidosis occurs with first-order kinetics and with an apparent half-life of 4 h. Nuclear run-on assays indicated that the rate of transcription of the renal GA mRNA is unaffected by changes in

acid-base balance. Therefore, the increase in glutaminase activity during chronic acidosis resulted from an increased level of GA mRNA that occurs through an increased stability of the GA mRNAs.

The rate of mRNA turnover is determined by the presence of *cis*-acting elements within the mRNA, including the $^{7\text{-met}}$guanosine cap at the 5'-end of the mRNA, stem-loop structures, adenylate- and uridylate-rich (AU-rich) elements, and the poly-A tail. Stabilization or destabilization is regulated by *trans*-acting factors, i.e., mRNA binding proteins that interact with the *cis*-acting elements [Ross, 1995]. Specific AU-rich elements within the coding sequence or the 3'-untranslated region of the mRNA may function as instability elements [Chen, C-Y et al, 1995]. The AREs recruit proteins that remove the poly-A binding proteins and enhance 3'-deadenylation, leading to the rapid exonucleolytic degradation of the mRNA. Alternatively, the turnover of a mRNA may be initiated by a site-specific endonucleolytic cleavage, which generates sites for rapid exonucleolytic degradation [Wang et al, 2000].

In order to identify and characterize the *trans*-acting factors that affect GA mRNA stability, an *in vitro* deadenylation assay was developed to compare the rates of deadenylation and degradation of the GA mRNA in cytosolic extracts prepared from cells grown in normal and acidic medium. The cytoplasmic extracts from rat WKPT and porcine LLC-PK_1-FBPase$^+$ (LLC-PK_1-F^+), two lines of renal proximal tubule cells, were analyzed to characterize the mechanism of pHRE-mediated mRNA decay and the role of ζ-cryst in the pH-responsive stabilization of the GA mRNA.

An *in vitro* mRNA deadenylation assay using HeLa cell extracts has been used to reproduce ARE-regulated mRNA deadenylation and degradation [Ford et al, 1997; Ford

et al, 1999]. A [P^{32}]-labeled RNA containing a 5'-cap and a precisely positioned 3'-poly-A tail was used as the substrate. The key aspect of this assay is activation by the addition of a poly-A RNA to sequester the poly-A binding proteins. The addition of poly-A RNA activates both a sequence-specific 3'-deadenylase activity and an ATP-dependent ribonucleolytic activity in HeLa cytoplasmic S100 extracts. The rate of RNA turnover was enhanced by the inclusion of an ARE in the RNA substrate.

As a control, an *in vitro* deadenylation of Gem-A_{60} RNA was analyzed. pGem-A_{60} and pGem-A_0 plasmids were obtained from Dr. Jeffrey Wilusz (Department of Microbiology, Immunology, and Pathology, Colorado State University, Fort Collins, CO). The two plasmids were digested with SspI or HindIII, respectively, and the resulting templates were transcribed using SP6 RNA polymerase in the presence of [α-^{32}P]-UTP and 500 μM ^{7met}GpppG to produce 5'-capped mRNAs that either lack or contain a 60-nt poly-A tail.

An *in vitro* decay of Gem-A_{60} RNA substrate was first analyzed using HeLa or LLC-PK_1-F^+ cytoplasmic extracts. With the addition of 500 ng of poly-A RNA, most of the control substrates were deadenylated within 30 min time-course in HeLa cytoplasmic extracts (**Fig. 5-1**). In contrast, the Gem-A_{60} RNA was completely degraded without detectable formation of the deadenylated Gem-A_0 RNA in LLC-PK_1-F^+ cytoplasmic extracts. Different conditions were tested to optimize the decay assay, including titration of poly-A RNA, varying $MgCl_2$ concentration, preparing the cytoplasmic extracts with 10 mM or 50 mM KCl, and adding protease and phosphatase inhibitors to the cytoplasmic extracts. In all cases, S100 cytoplasmic extracts of LLC-PK_1-F^+ cells failed to accumulate the deadenylated Gem-A_0 product.

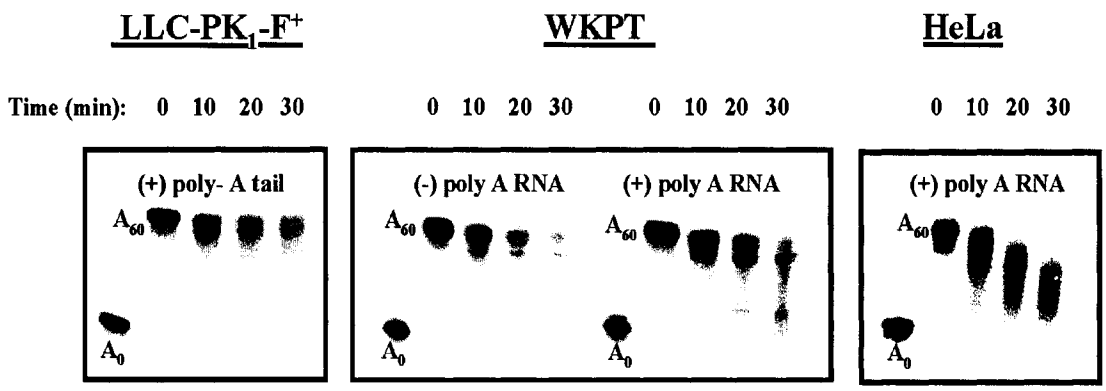

Fig. 5-1 Deadenylation and subsequent decay of the Gem-A_{60} RNA in extracts of HeLa, LLC-PK_1-F^+ and WKPT cells. The Gem-A_{60} mRNA substrate (A_{60}) was incubated with S100 cytoplasmic extracts of HeLa, LLC-PK_1-F^+ or WKPT cells for the indicated times in the absence or presence of 500 ng Poly-A RNA. The reaction products were analyzed on a 5% denaturing acrylamide gel. An aliquot of Gem-A_0 (A_0) was used to indicate the mobility of the fully deadenylated product.

Therefore, cytoplasmic extracts of WKPT cell lines, a line of rat renal proximal tubule cells, were tested in the *in vitro* decay assay **(Fig. 5-1)**. In the absence of poly-A RNA, the Gem-A_{60} mRNA was again degraded without the intermediated formation of the deadenylated Gem-A_0 RNA. In contrast, with the addition of poly-A RNA, the formation of deadenylated Gem-A_0 RNA was observed, indicating that the turnover of the Gem-A_{60} mRNA was initiated by deadenylation. Hence, it was important to determine if the WKPT cells are a pH-responsive line of renal proximal tubules, prior to performing molecular analysis of the mechanism mediating the enhanced expression of the GA gene during the onset of metabolic acidosis.

5.2 Quantitative real-time RT-PCR analysis of GA induction in WKPT cells

The induction of endogenous level of kidney-type GA mRNA was measured in WKPT and LLC-PK_1-F^+ cells using quantitative real-time RT-PCR. Both cell lines express a 4.5-kb GAC mRNA and a 5.0-kb KGA mRNA. In the rat, both GA mRNAs contain one or more pHREs, whereas in pig only the GAC isoform is pH-responsive [Porter et al, 2002].

A quantitative real-time RT-PCR assay was developed using specific primer sets and differentially labeled Taqman probes to quantify the GAC, KGA and glyceraldehyde 3-phosphate dehydrogenase (GAPDH) mRNAs in LLC-PK_1-F^+- cells (**Fig. 5-2**). The excitation and emission wavelengths of the three Taqman fluorescent probes do not overlap. Comparison of the ratio of GAC and KGA mRNAs to GAPDH mRNA in the total RNA samples isolated from triplicate plates of LLC-PK_1-F^+ cells treated with

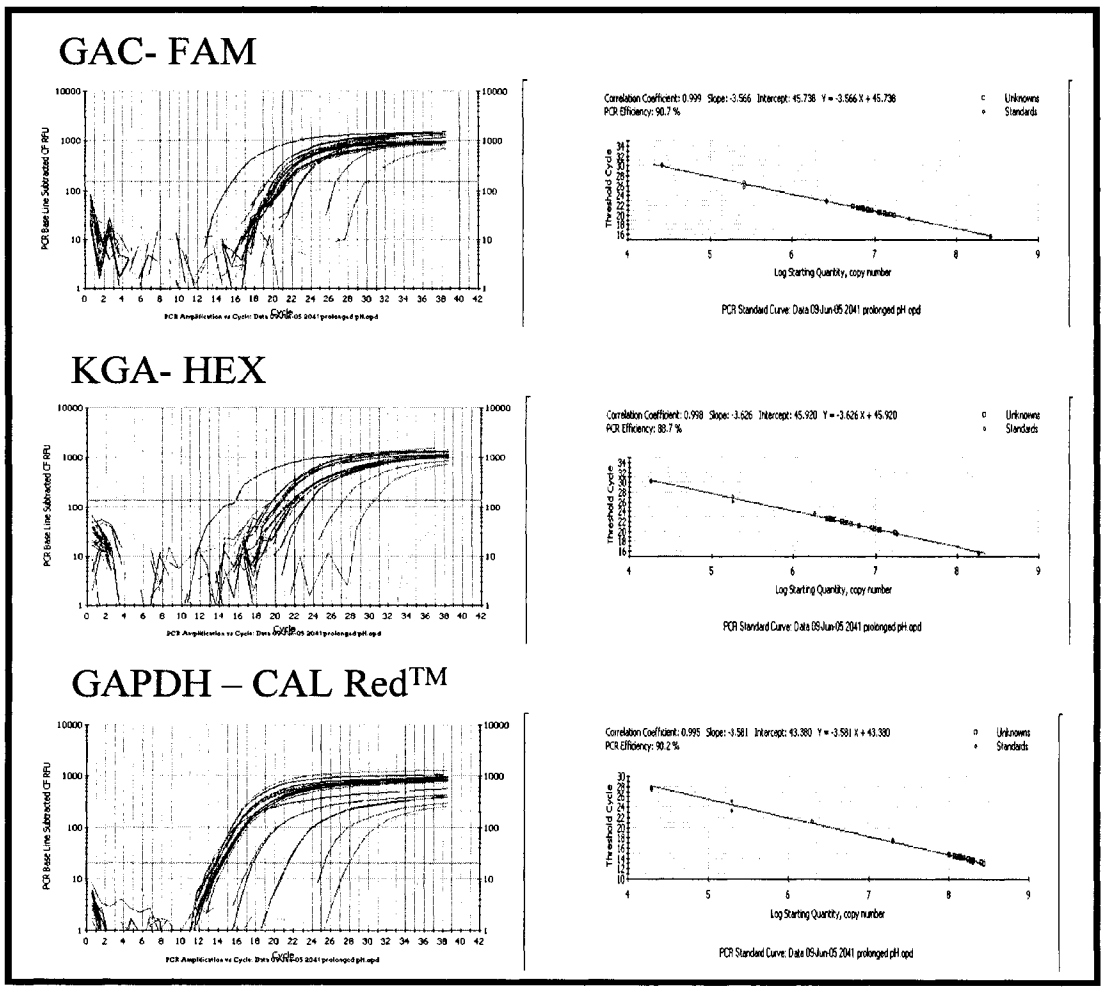

Fig. 5-2 Quantitative real-time RT-PCR assay. Standard curves for calculating the concentration of KGA, GAC and GAPDH mRNAs. Two template specific primers define the endpoints of the amplicon and provide an initial level of specificity. The Taqman probe is also complementary to the target sequence. Therefore, a fluorescence signal is obtained only when the correct segment is amplified. The resulting signal is directly proportional to the number of molecules present at the end of the cycle.

normal or acidic medium were used to calculate the fold induction of the two GA mRNAs. The analysis of the LLC-PK$_1$-F$^+$ cells harvested at 2 to 14 d post-split demonstrated that expression of the GAC mRNA was increased 2-fold, but only when 2-d post split LLC-PK$_1$-F$^+$ cells were transferred to acidic medium for 24 h (**Fig. 5-3**). On the other hand, KGA mRNA was not affected when the cells were transferred to acidic medium at various stages of confluency.

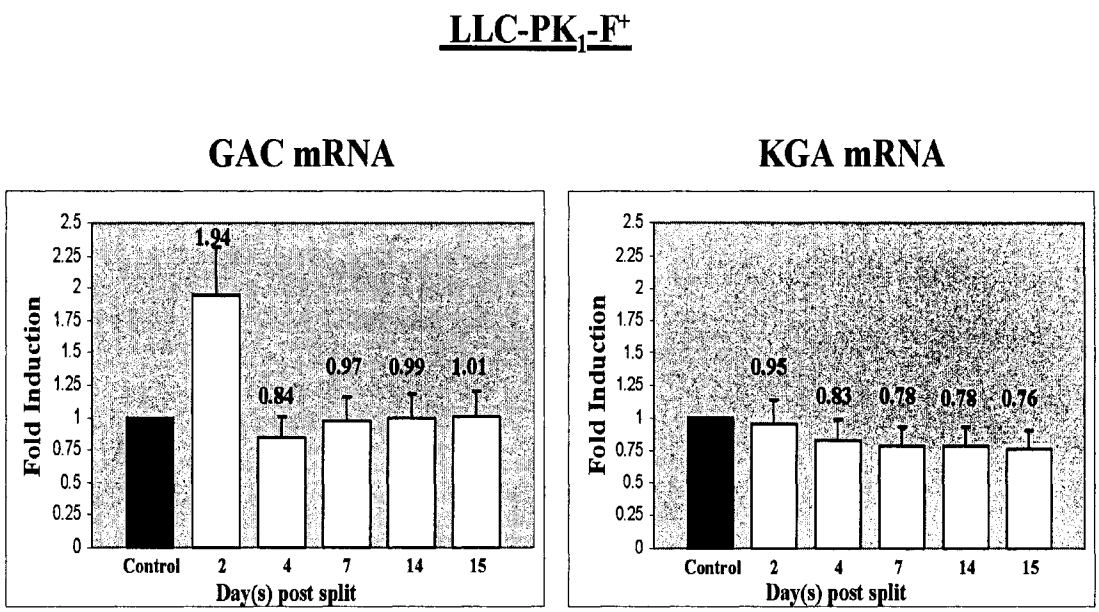

Fig. 5-3 pH-Responsive increase in GAC and KGA mRNAs in LLC-PK$_1$-F$^+$ cells. RNAs isolated from cells treated with pH 7.4 or pH 6.9 medium were analyzed for GAC, KGA, and GAPDH mRNA levels in 2-15 d post-split LLC-PK$_1$-F$^+$cells.. The ratio of GA to GAPDH mRNAs were normalized to the mean of samples obtained from cells grown at pH 7.4. The data are the mean ± the standard error for 3 samples.

In WKPT cells, the induction of KGA and GAC mRNAs was also measured using differentially labeled Taqman probes, by quantifying the KGA, GAC and GAPDH mRNAs. The pH-responsiveness of the GAC isoform has not been previously characterized in rat kidney or in rat kidney cells. The analysis of the WKPT cells harvested at different stages of confluency demonstrated that both KGA (1.9X) and GAC mRNA (1.5X) are increased when subconfluent (25%) cells are transferred to acidic medium for 24 h (**Fig. 5-4**).

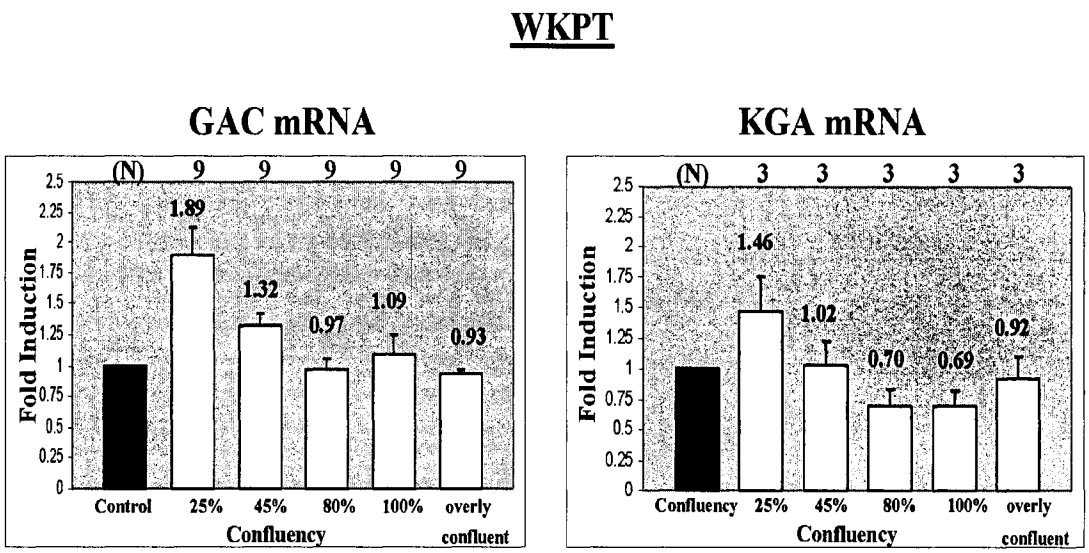

Fig. 5-4 pH-Responsive increase in GAC and KGA mRNAs in WKPT cells. RNAs were isolated from cells treated with pH 7.4 or pH 6.9 medium, and analyzed for KGA, GAC, and GAPDH mRNA levels at different confluency. The ratios of KGA or GAC mRNAs were normalized to the mean of samples from cells grown at pH 7.4. The data are the mean ± the standard error for "N" samples.

An increase in KGA mRNA was also observed in subconfluent WKPT cells that were transferred to acidic medium for a prolonged period. The cells were treated for different number of days in acidic medium, but harvested at 45% confluency (**Fig. 5-5**). The WKPT cells transferred to acidic medium for 4 or 5 d demonstrated 1.9X induction of KGA mRNA. This correlates with the observation that the in crude homogenates of whole kidney, the total renal GA activity increased gradually and reached a plateau after 7 d of acidosis. Hence, a prolonged treatment of WKPT cells may reflect the physiological changes of renal GA activity in rat kidneys under metabolic acidosis. On the other hand, with prolonged treatment in acidic medium, GAC mRNA was not increased when subconfluent cells were transferred to acidic medium.

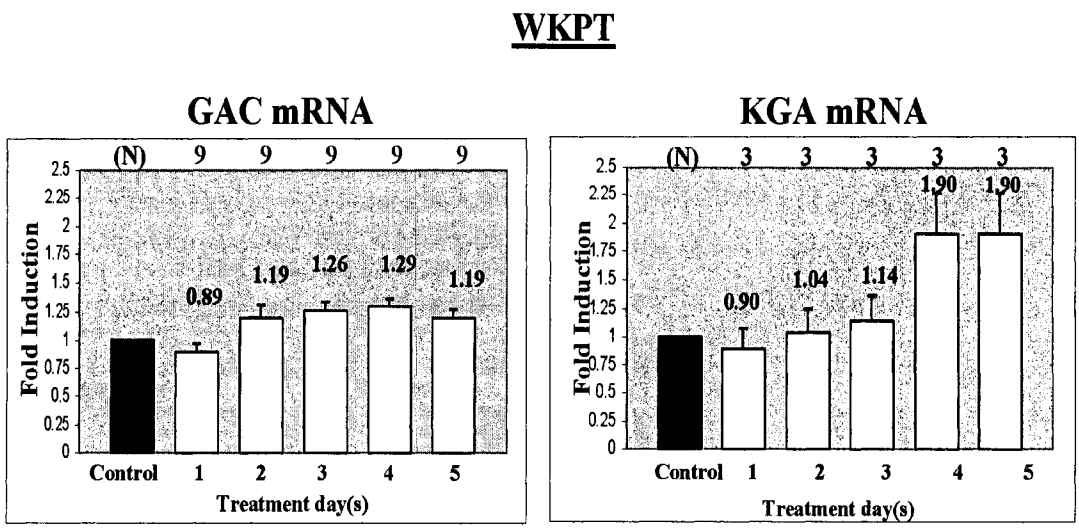

Fig. 5-5 pH-Responsive increase in KGA and GAC mRNAs in WKPT cells following prolonged treatment with acidic medium. RNAs isolated from control cells and cells treated with acidic medium (pH 6.9, 10 mM HCO_3^-) for 1-5 d were analyzed for KGA, GAC, and GAPDH mRNA levels. The ratios of KGA or GAC mRNAs were normalized to the mean of samples from cells grown at pH 7.4. The data are the mean ± the standard error for "N" samples.

5.3 Western blot analysis of RNA binding proteins

Once it was established WKPT cells are a pH-responsive renal proximal tubule cell line, western blot analysis was performed to characterize the presence of various well-characterized RNA binding proteins that may play a role in GA mRNA turnover. S10 and S100 cytoplasmic extracts were harvested from WKPT cells that had been grown in normal medium (pH 7.4, 25 mM HCO_3^-) or transferred to acidic medium (pH 6.9, 10 mM HCO_3^-) for 24 h. The western analysis of Dcp1a (decapping enzyme 1a), Dcp2 (decapping enzyme 2), PARN (poly-A ribonuclease), Pm/Scl-75 (catalytic subunit of exosome, a 3'→5' exonuclease), and eIF4E (eukaryotic translation initiation factor 4E, a cap binding protein) are shown in **Fig. 5-6**. β-tubulin, which was determined not to be pH-responsive, was used as a loading control. The proteins of interest were detected using rabbit antibodies and a secondary goat-anti-rabbit antibody that fluoresces at 800 nm wavelength, while β-tubulin was detected using a mouse antibody and was detected using a secondary goat-anti-mouse antibody that fluoresces at 700 nm wavelength. Both images were quantified using the Odyssey® Infra-red imaging instrument. This allowed a direct quantification of the protein interest relative to the level of β-tubulin in each sample.

Western blot analysis indicated that Dcp1a was expressed at a higher level in both S10 and S100 WKPT cells that were grown in pH 7.4 medium than those obtained from cells treated with pH 6.9 medium. The observed decrease in Dcp1a expression may contribute to the decreased turnover or increased stabilization of the GA mRNA. A similar result was observed for Pm/Scl-75, where a slightly higher Pm/Scl-75 protein expression was detected in normal extracts compared to extracts of cells treated with

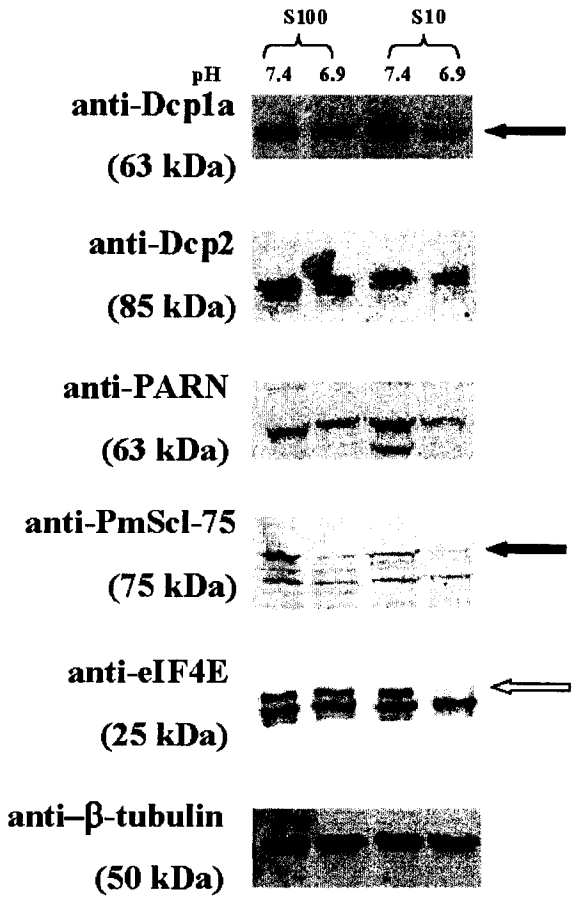

Fig. 5-6 Western blot analysis of RNA binding proteins in WKPT cells. S10 and S100 extracts of WKPT were subjected to western blot analysis using α-Dcp1a, α-Dcp2, α-PARN, α-PM/Scl-75, α-eIF4E, and α-β-tubulin antibodies. Arrows indicate pH-responsive decrease in total protein levels in WKPT cells treated with acidic medium (pH 6.9, 10 mM HCO3-) for 24 h.

acidic medium. Hence, a decrease in Pm/Scl-75 may also contribute to the selective stabilization of some mRNAs.

The relative Dcp2 protein level in extracts of WKPT cells grown in normal or acidotic medium are unaltered. However, it is interesting to note that a higher level of Dcp2 is recovered in the S100 extracts compared to the S10 extracts. Therefore, the RNA granules containing Dcp2 are recovered primarily in the S100 cytosolic fraction, rather than in S10 post-nuclear fraction that contains protein complexes with molecular weight >500 kDa.

The level of PARN in the WKPT S10 and S100 extracts appear to be relatively constant, regardless if the cells were grown in normal or acidotic medium. However, in the S10 post-nuclear fraction, a double band for PARN was observed in normal extracts, whereas a single (lower) band observed in extracts of cells treated with acidic medium. It was previously shown that PARN is a phosphoprotein [Seal et al, 2005], hence the lower band may reflect the unphosphorylated PARN. In contrast, a decreased amount of the phosphorylated form of eIF4E was observed in the S10 post-nuclear fraction of WKPT cells that were treated with pH 6.9 medium. This may indicate that under acidotic condition, there is diminished level of cap-dependent translation of some proteins due to decreased level of phosphorylated eIF4E, and increased level of phosphorylated PARN. Previous studies indicated that the increased expression of GA under acidotic condition is not due to regulation of translation [Hwang et al, 1991a]. Therefore, the possible decrease in cap-dependent translation may effect mRNAs, other than the GA mRNA.

5.4 Purification of recombinant ζ-cryst, p40-AUF1, TTP, and HuR

Specific *trans*-acting factors bind to AU-rich elements in the 3'-untranslated regions of a mRNA and thereby mediate control of mRNA degradation or stabilization. Among the RNA-binding proteins identified so far, HuR and its homologues have been associated with post-transcriptional stabilization of mRNA encoding GM-CSF [Fan et al, 1998], TNF_{α} [Dean et al, 2001], IL-3 [Ming et al, 2001] and COX-2, etc [Sully et al, 2004]. Both destabilizing [Loflin et al, 1999; Sarkar et al, 2003] and stabilizing [Chen, CY et al, 2004; Xu et al, 2001] roles of AUF1/hnRNP D have been suggested from the results of overexpression experiment. In contrast, a number of other RNA-binding proteins, including TTP, BRF1, and other hnRNP proteins, function in destabilization of the target mRNA [Kedersha et al, 2005; Lykke-Andersen et al, 2005]. In order to investigate the role of the various ARE-binding proteins on the decay of GA mRNA, recombinant $(His)_6$-tagged proteins, including ζ-cryst, p40-AUF1, TTP, and HuR, were purified and added to the decay reaction mixture to determine their effect on the rate of mRNA deadenylation and degradation.

The AUF1 transcript contain 10 exons that are alternatively spliced and translated to produce four protein isoforms, p37, p40, and p42, and p45 [Sarkar et al, 2003]. The p37 and p40 isoforms of AUF1 shuttle between the nucleus and the cytoplasm, whereas p42 and p45-AUF1 isoforms are retained in the nucleus. Plasmids encoding $(His)_6$-tagged recombinant p37, p40, p42, and p45-AUF1 were expressed in *E coli* strain BL21 codon plus bacteria cells and purified by nickel affinity chromatography. p37, p42, and p45-AUF1 isoforms were recovered in inclusion bodies and were insoluble, hence purification methods using denaturing condition need to be optimized. p40-AUF1 was

soluble and was readily purified. The p40-AUF1 fractions eluted from the chelating column were further purified using a Heparin column, in order to eliminate a contaminating RNase activity.

Recombinant $(His)_6$-tagged ζ-cryst purified from bacterial cells did not bind to the 28-nt GA RNA 3'-UTR segment containing the pH-responsive element (data not shown), suggesting that ζ-cryst may require post-translational modifications to bind to the pH-response element within GA 3' UTR. Therefore, a baculovirus was used to express His_6-tagged ζ-cryst in Sf9 cells. $(His)_6$-tagged-TTP and $(His)_6$-tagged-HuR were readily expressed in *E.coli* strain BL21 codon plus bacteria. The 3 proteins were purified using nickel affinity chromatography. Purified proteins were analyzed for purity by SDS-PAGE and Coomassie blue staining (**Fig. 5-7**). The concentrations of the purified recombinant proteins were determined using Bradford assay with bovine serum albumin (BSA) as the standard [Bradford, 1976].

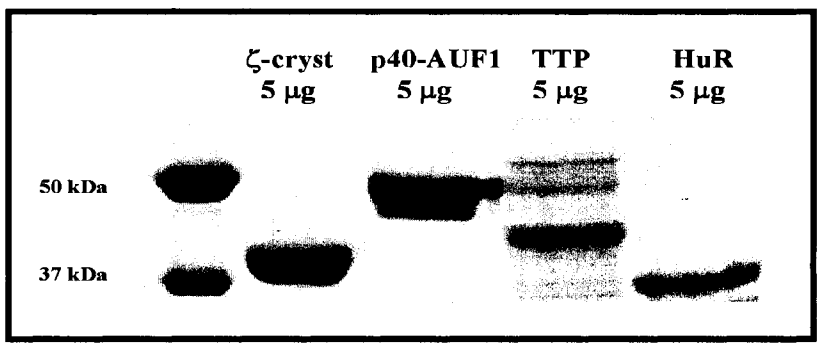

Fig. 5-7 Purity of recombinant RNA binding proteins. His_6-tagged recombinant ζ-cryst, p40-AUF1, TTP (tristetraprolin), and HuR were purified using HiTrap Ni^{+2}-chelating and HiTrap Heparin columns. Samples containing 5 μg of recombinant proteins were analyzed by SDS-PAGE and stained with Coomassie.

5.5 Decay profiles of Gem-A_{60} and GemARE-A_{60} in WKPT extracts

The purified recombinant proteins were added to the *in vitro* deadenylation assay, to determine the effect of ARE-binding proteins on the deadenylation and decay of the Gem-A_{60} and GemARE-A_{60} mRNAs in the absence or presence of poly-A RNA. The reactions were incubated at 30 °C for the indicated time and analyzed on a 5% denaturing polyacrylamide gel. A final concentration of 0.86 μM of recombinant ζ-cryst, 0.79 μM of p40-AUF1, or 0.20 μM of TTP was added to the reaction mixture.

When added individually, the recombinant RNA-binding proteins had little or no effect on the *in vitro* deadenylation or decay of the Gem-A_{60} RNA (**Fig. 5-8a**). It was expected that the purified recombinant proteins would not have an effect on the turnover rate of Gem-A_{60} RNA, since this substrate lacks an AU-rich element (ARE). The addition of poly-A RNA stimulated the turnover of the Gem-A_{60} substrate, in comparison to the absence of poly-A RNA.

The stimulatory effect of poly-A RNA was also observed in the *in vitro* deadenylation of GemARE-A_{60} (**Fig. 5-8b**). The addition of recombinant ζ-cryst had no effect on the deadenylation or decay of the GemARE-A_{60} RNA. This indicated that ζ-cryst may not effect the deadenylation and turnover of TNF-α mRNA. On the other hand, addition of recombinant p40-AUF1 had a slight stabilizing effect and produced a slower rate of disappearance of the GemARE-A_{60} compared to the control. In contrast, addition of recombinant TTP greatly enhanced the rate of deadenylation of the GemARE-A_{60}, resulting in the accumulation of the deadenylated GemARE-A_0 product. Therefore, the factors needed for the rapid turnover of deadenylated TNF-α mRNA may be limiting in WKPT cells.

(a)

Gem-A_{60} RNA

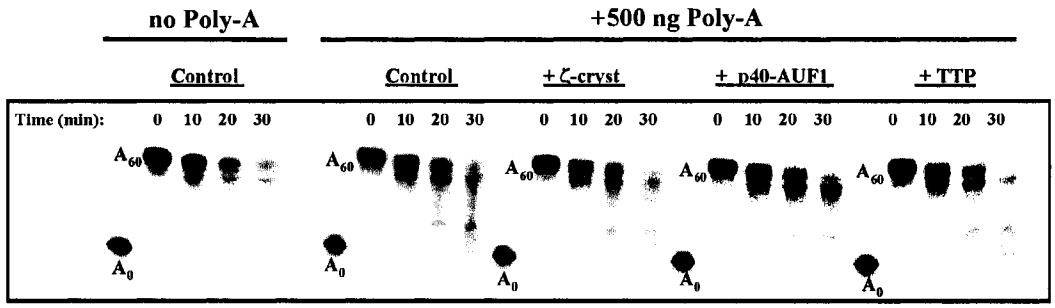

(b) GemARE-A_{60} RNA

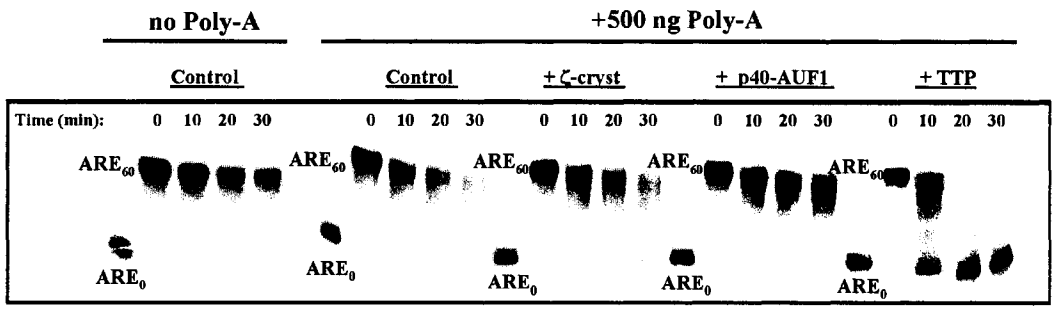

Fig. 5-8 Effect of recombinant proteins on the deadenylation and subsequent decay of the Gem-A_{60} and GemARE-A_{60} mRNAs in the absence or presence of poly-A RNA. The Gem-A_{60} (**Panel a**) and GemARE-A_{60} (**Panel b**) were incubated with S100 cytoplasmic extracts of WKPT cells for the indicated times in the absence or presence of the indicated amount of added proteins. The experiments were performed in the absence or presence of 500 ng Poly-A RNA. The reaction products were analyzed on a 5% denaturing acrylamide gel. The various additions had little effect on the deadenylation and decay of the Gem-A_{60} RNA. By contrast, addition of TTP greatly enhanced deadenylation of the GemARE-A_{60} RNA. Addition of p40-AUF1 stabilized the GemARE-A_{60} RNA.

5.6 WKPT-ζ^+ cells

The addition of recombinant ζ-cryst had no effect on the *in vitro* rate of deadenylation and turnover of the Gem-A_{60} and GemARE-A_{60} RNAs. To determine the effect of endogenously expressed ζ-cryst on mRNA turnover, a line of WKPT cells that over expresses ζ-cryst was produced by stable transfection of WKPT with pcDNA 3.1/Hygro-ζ-cryst. Western blot analysis of resulting WKPT-ζ^+ cells was performed using S100 cytoplasmic extracts. The analysis demonstrated that the clonal WKPT-ζ^+ cells over-express ζ-cryst by 36-fold compared to WKPT cells (**Fig. 5-9**).

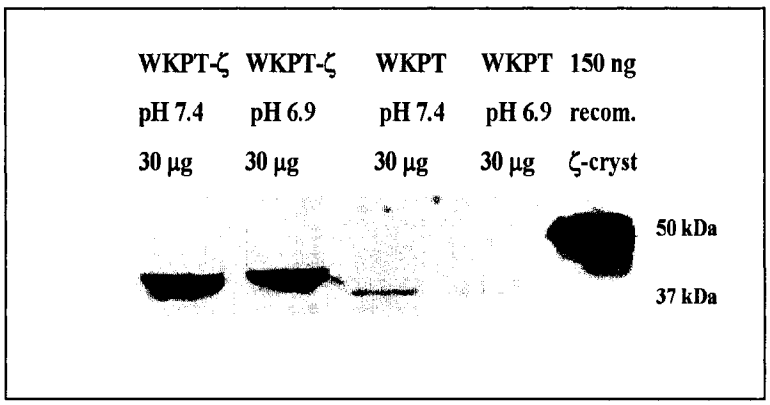

Fig. 5-9 Western blot analysis of ζ-cryst levels in WKPT and WKPT-ζ^+ cells. S100 Cytoplasmic extracts of WKPT and WKPT-ζ^+ cells were subjected to western blot analysis using α-ζ-cryst antibody. The WKPT-ζ^+ cells exhibit a 36-fold greater level of ζ-cryst.

5.7 Decay profiles of Gem-A_{60} and GemARE-A_{60} RNAs in WKPT-ζ^+ extracts

In vitro deadenylation assay was performed using WKPT-ζ^+ extracts with the control substrates, Gem-A_{60} and GemARE-A_{60} RNAs, in the presence of 0.86 μM of recombinant ζ-cryst, 0.79 μM of p40-AUF1, or 0.20 μM of TTP as described before.

Surprisingly, the rate of deadenylation and decay of the Gem-A_{60} and GemARE-A_{60} RNAs were greatly enhanced in WKPT-ζ^+extracts compared to WKPT extracts. The addition of recombinant proteins to the WKPT-ζ^+ extracts again had little effect the rate of turnover of the Gem-A_{60} RNA (**Fig. 5-10a**). Furthermore, the effect of poly-A RNA addition on the deadenylation reaction was minimal, probably due to the significant increase in the rate of turnover observed with the WKPT-ζ^+ extracts.

Similarly, the GemARE-A_{60} RNA also demonstrated a significant increase in the rate of turnover in WKPT-ζ^+ extracts (**Fig. 5-10b**). Addition of recombinant ζ-cryst to the reaction did not effect the deadenylation and turnover rate of GemARE-A_{60} RNA, since WKPT-ζ^+ cells already over-expressed ζ-cryst. The stabilizing effect of p40-AUF1 on GemARE-A_{60} RNA observed in WKPT extracts was no longer observed, due to the fact that the deadenylation process was significantly enhanced in WKPT-ζ^+ extracts. The addition of recombinant TTP greatly enhanced deadenylation of the GemARE-A_{60} RNA as observed in WKPT extracts. In WKPT-ζ^+ extracts, the GemARE-A_{60} RNA was fully deadenylated within 10 min compared to 20 min in WKPT extracts with the addition of recombinant TTP.

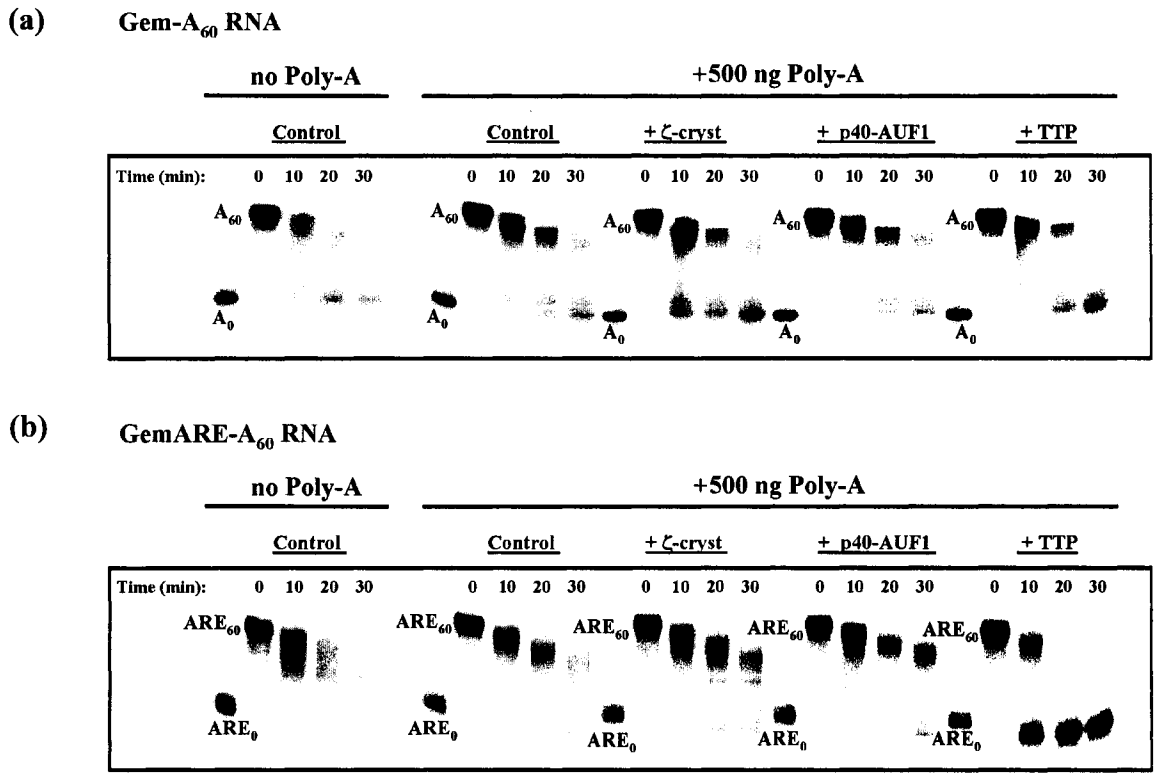

Fig. 5-10 Effect of recombinant proteins on the deadenylation and subsequent decay of the Gem-A_{60} and GemARE-A_{60} mRNAs in WKPT-ζ^+ cells. The Gem-A_{60} (Panel a) and GemARE-A_{60} (Panel b) were incubated with WKPT-ζ^+ S100 cytoplasmic extracts for the indicated times in the absence or presence of the indicated proteins. The experiments were performed in the absence or presence of 500 ng Poly-A RNA. The reaction products were analyzed on a 5% denaturing acrylamide gel. The deadenylation and subsequent decay of Gem-A_{60} and GemARE-A_{60} RNAs were enhanced in WKPT-ζ^+ cells. The various additions had little effect on the deadenylation and decay of the Gem-A_{60} RNA. By contrast, addition of TTP greatly enhanced deadenylation of the GemARE-A_{60} RNA.

The experiments performed in WKPT-ζ^+ cells demonstrated that ζ-cryst may act as a destabilizing ARE binding protein, that may stimulate the turnover of mRNA. Further experiments need to be performed in order to further characterize ζ-cryst as possible trans-acting instability factor. Overall, these experiments served as a control to demonstrate that the *in vitro* deadenylation assay can be used to characterize the role of various ARE binding proteins in the deadenylation and turnover rate of GA mRNA and in the stabilization of GA mRNA during metabolic acidosis.

CHAPTER 6

CHARACTERIZATION OF THE INSTABILITY ELEMENTS PRESENT WITHIN THE 3'-UTR OF THE GLUTAMINASE mRNA IN WKPT KIDNEY CELLS

The data in this chapter will be formatted as a manuscript for submission to the Journal of Biological Chemistry

Yeon J. Lee, Carol Wilusz, Jeffrey Wilusz, Norman Curthoys.

6.1 Cloning of pGemGA-A_{60} and pGemGA-A_0

The rate of mRNA turnover is determined by the presence of *cis*-acting elements within the mRNA, including the 5'-^{7met}guanosine cap, stem-loop structures, adenylate- and uridylate-rich (AU-rich) elements, and the poly-A tail. Stabilization or destabilization is regulated by *trans*-acting factors, i.e. mRNA binding proteins, that interact with the *cis*-acting elements [Ross, 1995]. Specific AU-rich elements (AREs) within the coding sequence or the 3'-untranslated region of the mRNA function as instability elements [Chen, C-Y et al, 1995]. The AREs recruit proteins that remove the poly-A binding proteins and enhance 3'-deadenylation, leading to the rapid exonucleolytic degradation of the mRNA. Alternatively, the turnover of a mRNA may be initiated by a site-specific endonucleolytic cleavage, which generates sites for rapid exonucleolytic degradation [Wang et al, 2000].

Previous studies (Hwang et al, 1991b) have indicated that the increase in GA activity during metabolic acidosis occurs through an increased stability of the GA mRNA. Chimeric β-globin reporter constructs (Hansen et al, 1996) were used to map the pH-response element (pHRE) of the rat kidney GA mRNA to a direct repeat of AU-sequence (Laterza et al, 1997) within the 3'UTR.

In order to perform a functional analysis of the pHRE and characterize the trans-acting factors responsible for the GA mRNA stabilization during metabolic acidosis, a 28-nt segment containing the pHRE of GA mRNA ($^{5'}$CTAGTGCTAGCTC<u>TTTAAATA</u>

AA**TTAAAATA**ATTACTAAT$^{3'}$) was cloned into the XbaI site of pGem-A_0 and pGem-A_{60} vectors to yield pGemGA-A_0 and pGemGA-A_{60}, respectively (**Fig. 6-1**). The templates were transcribed using SP6 RNA polymerase in the presence of [α-^{32}P]-UTP and 500 μM ^{7met}GpppG to produce capped mRNAs that either lack or contain a 60-nt poly-A tail.

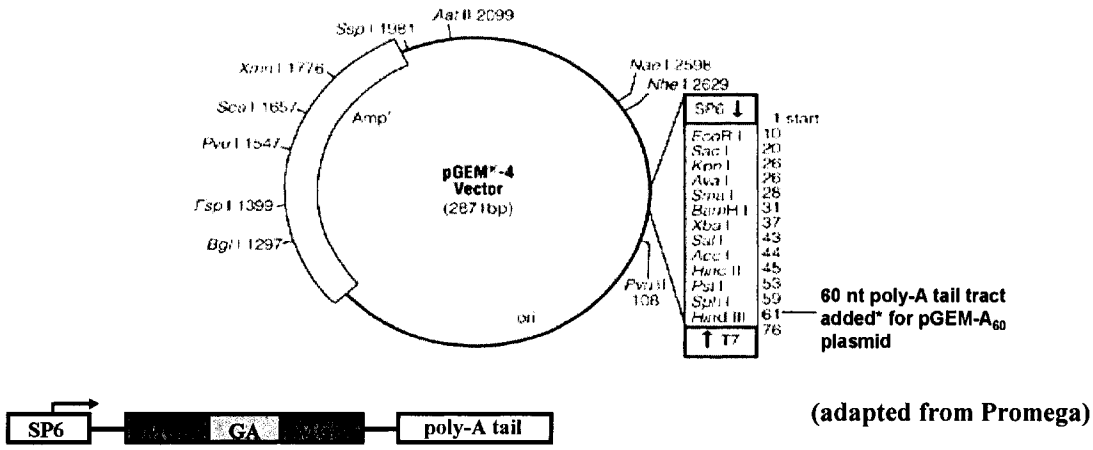

GA: 5'- UC**UUUAAAUA**AA**UUAAAAUA**AUUACUAA-3'

Fig. 6-1 Cloning of pGA-A_{60} and pGemGA-A_0. A 28-nt segment containing the AU-rich region of the GA mRNA was cloned into the pGemA_0 and pGemA_{60} vectors. The two plasmids were transcribed in the presence of [α-^{32}P]-UTP and 500μM ^{7met}GpppG to produce mRNAs that either lack or contain a 60-nt poly-A tail. The GemGA-A_{60} mRNA was used as the substrate for an *in vitro* mRNA deadenylation assay.

6.2. Identification of the proteins that bind to the pHRE within the 3' UTR of the GA mRNA

UV-crosslinking experiments were performed in order to identify the proteins that bind to the pHRE within the 3' UTR of the GA mRNA (**Fig. 6-2**). [^{32}P]-labeled, and capped GemGA-A_{60} and GemGA-A_0 mRNAs were incubated with 23 μg of S100 cytoplasmic extract from WKPT or WKPT-ζ^+ cells grown in normal medium or treated with acidic medium for 24 h. As controls, 2 μM recombinant ζ-cryst, TTP (tristetraprolin), or p40-AUF1 were incubated with GemGA-A_{60} and GemGA-A_0 mRNAs. RNA:proteins complexes with apparent molecular weights between 40-100 kDa were found to be associated with the Gem GA mRNAs. The observation that the two RNAs produce identical complexes indicates that the observed interactions do not result from binding to the A_{60} poly A tail. Bands corresponding to RNA:ζ-cryst and RNA:p40-AUF1 complexes were detected using either WKPT or WKPT-ζ^+ extracts. RNA:TTP complexes were not detected in the UV-crosslinking experiments. Whether this is an artifact of the high $MgCl_2$ concentration used in the experiment, that may hinder the binding of TTP to RNA substrates, needs to be determined. It is interesting to note that the abundance of RNA:p40-AUF1 complexes is similar between extracts from cells treated with pH 7.4 or pH 6.9 medium, whereas the RNA-ζ-cryst complex is decreased slightly using the WKPT-ζ^+ extract prepared from cells treated with acidic medium. Based on the previous western blot analysis, the steady state level of ζ-cryst does not change following treatment with acidic medium. Hence, the change in the formation of the RNA:ζ-cryst complex is not due to the changes of steady state level of ζ-cryst. Whether the decrease in RNA:ζ-cryst complex formation in pH 6.9 extracts of WKPT-ζ^+

is indicative of an effect of acidosis that contributes to the stabilization of the of GA mRNA needs to be determined. It is also interesting to note that RNA:protein complexes with a slightly different apparent molecular weight were found for RNA:p40-AUF1 complexes in the extracts of WKPT cells compared to the extracts of WKPT-z+ cells. It is not known at this time whether this is a result of post-translational modification of the corresponding protein or the binding of different pHRE binding proteins.

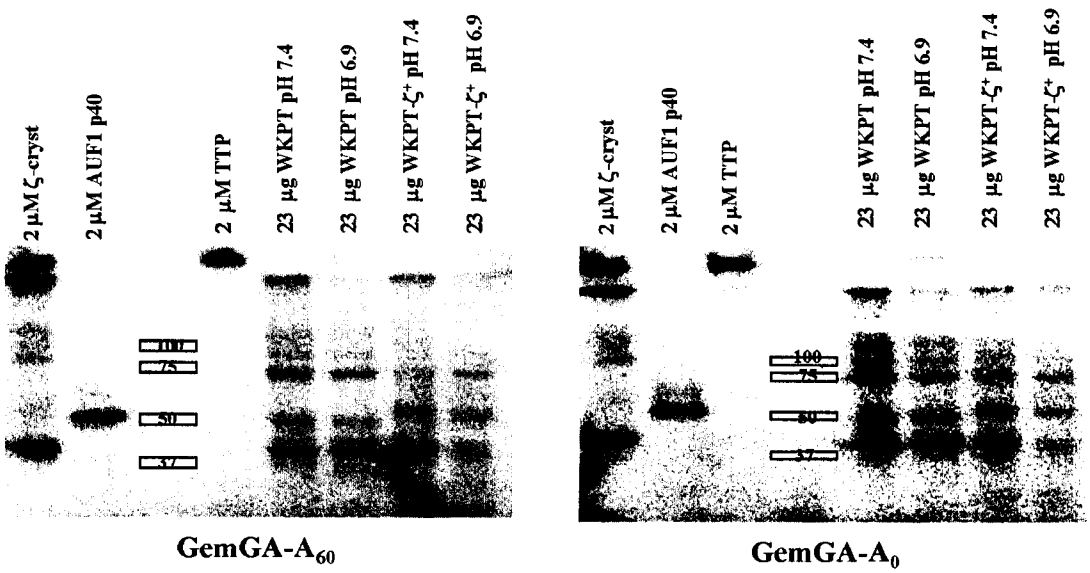

Fig. 6-2 UV-crosslinking. [^{32}P]-labeled and capped GemGA-A_{60} or GemGA-A_0 mRNA was incubated with S100 cytoplasmic extracts from WKPT or WKPT-ζ^+ cells grown in normal medium (pH 7.4) or treated with acidic medium (pH 6.9) for 24 h. As controls, of 2 μM of ζ-cryst, TTP, or p40-AUF1 were incubated with [^{32}P]-labeled, capped mRNAs. The reaction products were analyzed on a 10% SDS polyacrylamide gel. RNA:protein complexes corresponding to those formatted with ζ-cryst and AUF1 were found in the UV-crosslinking experiments with WKPT and WKPT-ζ^+ extracts. The bars represent the mobility of M_r standards.

6.3. S10 and S100 distribution of ARE binding proteins

UV-crosslinking experiments demonstrated the formation of RNA:protein complexes with apparent molecular weights ranging from 40-100 kDa (**Fig. 6-3**). In order to identify potential *trans*-acting RNA binding proteins that may be involved in GA mRNA turnover, western blot analysis was performed using S10 post-nuclear and S100 cytoplasmic extracts from WKPT and WKPT-ζ^+ cells that were treated with normal medium or transferred to acidic medium for 24 h. In **Fig.6-3 Panel A** shows a western blot for various ARE-binding proteins, and **panel B** shows a western blot for the proteins that are known to be involved in mRNA turnover. β-tubulin has been determined not to be pH-responsive and was used as a loading control.

The total protein levels of AUF1 and TTP in S10 and S100 extracts appear to be equivalent. On the other hand, HuR was recovered to a greater extent in S10 post-nuclear extracts that should contain protein complexes with molecular weight >500 kDa. Over-expression of ζ-cryst is observed in WKPT-ζ^+ cells compared to WKPT cells, but the level of ζ-cryst in the S10 and S100 extracts is not affected when the cells are grown in normal or acidic medium. On the other hand, it is interesting that the level of Brf1 (Butyrate response factor 1) is decreased in cells treated with pH 6.9 medium. Brf1 antibody also recognized a 51 kDa protein that may be the Brf2 isoform (Butyrate response factor 2). This protein is highly expressed in both WKPT and WKPT-ζ^+ cells, but again decreased in cells treated with acidic medium.

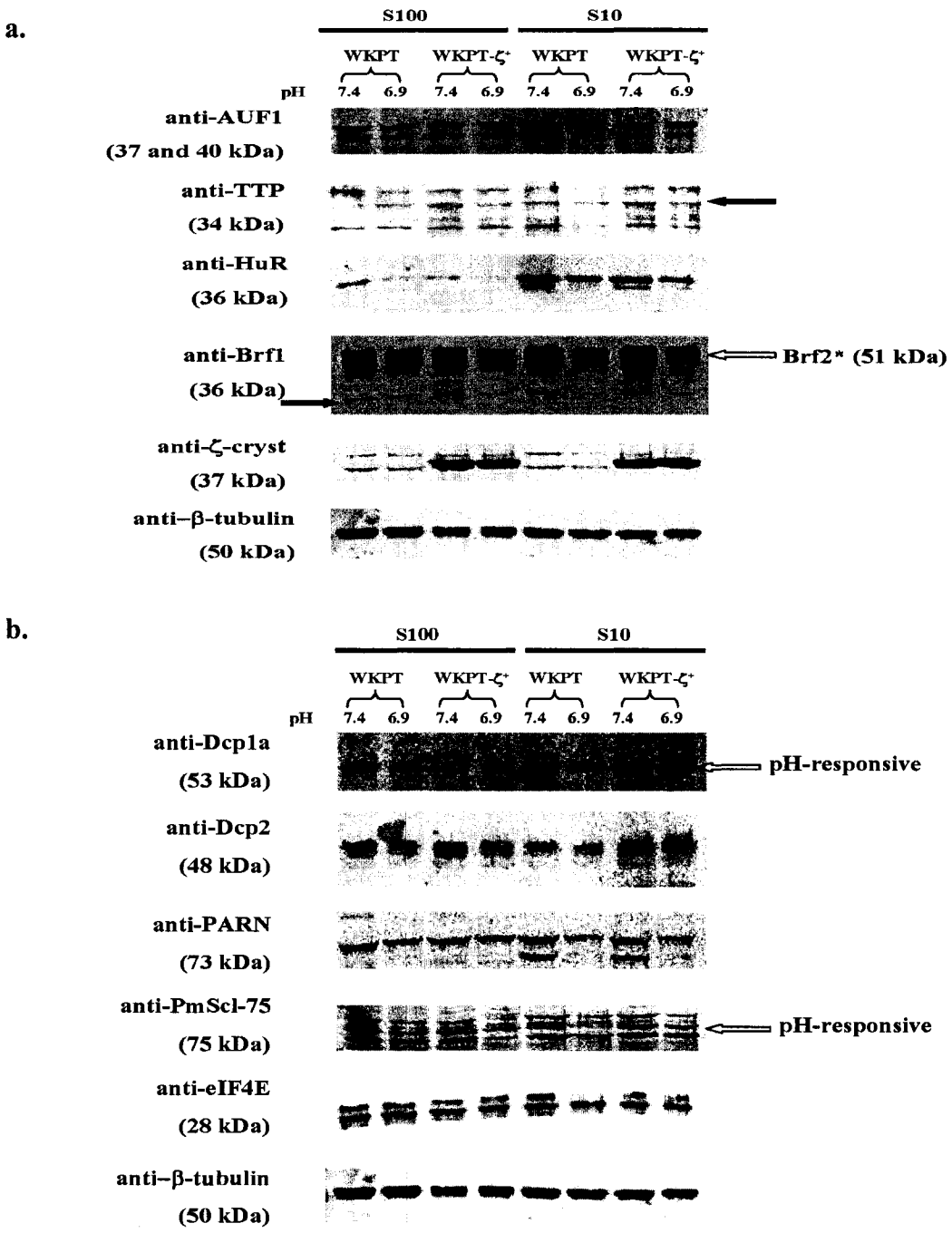

Fig.6-3 Steady state distribution of ARE binding proteins and proteins involved in mRNA turnover in S10 post-nuclear and S100 cytoplasmic extracts. S10 post-nuclear and S100 cytoplasmic extracts of WKPT and WKPT-ζ^+ were subjected to western blot analysis using antibodies to known ARE-binding proteins (**panel a**) and proteins involved in mRNA turnover process (**panel b**). β-Tubulin antibody was used as a loading control. The levels of Brf1, Brf2, Dcp1a, and Pm/Scl-75 were decreased in cells that were treated with acidic medium (pH 6.9, 10 mM HCO_3^-) for 24 h (open arrows).

In addition to various ARE binding proteins, western blot analysis was performed to identify the RNA binding proteins that may play a role in GA mRNA turnover. Western blot analysis indicated that Dcp1a was expressed at a higher level (1.6-fold +/- 0.1) in both S10 and S100 extracts from WKPT and WKPT-ζ^+ cells that were grown in normal medium than those obtained from cells treated with acidic medium. The observed decrease in Dcp1a expression may contribute to the increased stabilization of the GA mRNA. A similar result was obtained for Pm/Scl-75, where a slightly higher Pm/Scl-75 protein expression (2.6-fold +/- 0.6) was detected in normal extracts compared to extracts of cells treated with acidic medium. Hence, a decrease in Pm/Scl-75 may also contribute to the selective stabilization of the GA mRNA.

The relative levels of Dcp2 are unaltered in extracts of WKPT and WKPT-ζ^+ cells grown in normal medium or acidic medium. The levels of PARN in both S10 and S100 extracts also appear to be relatively constant regardless of the pH of the medium. However, in the S10 post-nuclear fraction, a double band was observed for PARN in normal extracts whereas a single (lower) band was observed in extracts of cells treated with acidic medium. It was previously shown that PARN is a phosphoprotein [Seal et al, 2005], hence the lower band may reflect the unphosphorylated PARN. In contrast, a decreased amount of the phosphorylated form of eIF4E was detected in S10 post-nuclear fraction of WKPT and WKPT-ζ^+ cells treated with acidic medium. The observed changes may indicate, that under acidotic condition, there is diminished level of cap-dependent translation of some proteins due to a decreased level of the phosphorylated eIF4E and an increased binding of phosphorylated PARN. Previous studies indicated that the increased expression of GA under acidotic condition is not due to regulation of

translation (Hwang et al, 1991a). Therefore, the possible decrease in cap-dependent translation may effect mRNAs other than the GA mRNA.

6.4 RNA EMSA (Electrophoretic Mobility Shift Assay) using WKPT and WKPT-ζ+ cells

RNA electrophoretic mobility shift assays (EMSA) were performed previously using cytoplasmic extracts prepared from rat kidney cortex and LLC-PK_1-F^+ cells. Since WKPT cells line were established as a pH-responsive rat proximal tubule cell line, it was important to examine whether the cytoplasmic extracts of WKPT cells form the same pHRE binding protein complexes. Various amounts (1.5-30 μg) of a S100 cytoplasmic extract from WKPT cells were incubated with a constant amount of [^{32}P]-labeled and capped GemGA-A_0 mRNA and then separated on a 5% native acrylamide gel. RNA gel shift assays demonstrated the formation of protein/RNA complexes similar to those observed using cytoplasmic extracts prepared from rat kidney cortex or LLC-PK_1-F^+ cells (**Fig. 6-4 panel a**).

A similar RNA electrophoretic mobility shift assay was performed using 0.25-4 μg of a S10 post-nuclear extract of WKPT-ζ^+ cells, a line of WKPT cells that over-expresses ζ-cryst by 36-fold. This experiment confirmed the presence of pHRE binding proteins in the WKPT cells (**Fig. 6-4 panel b**). A S10 post-nuclear extract was used in this assay because S100 cytoplasmic extracts may lack the stress granules and P-bodies that contain many of the proteins involved in mRNA turnover [Seal et al, 2005].

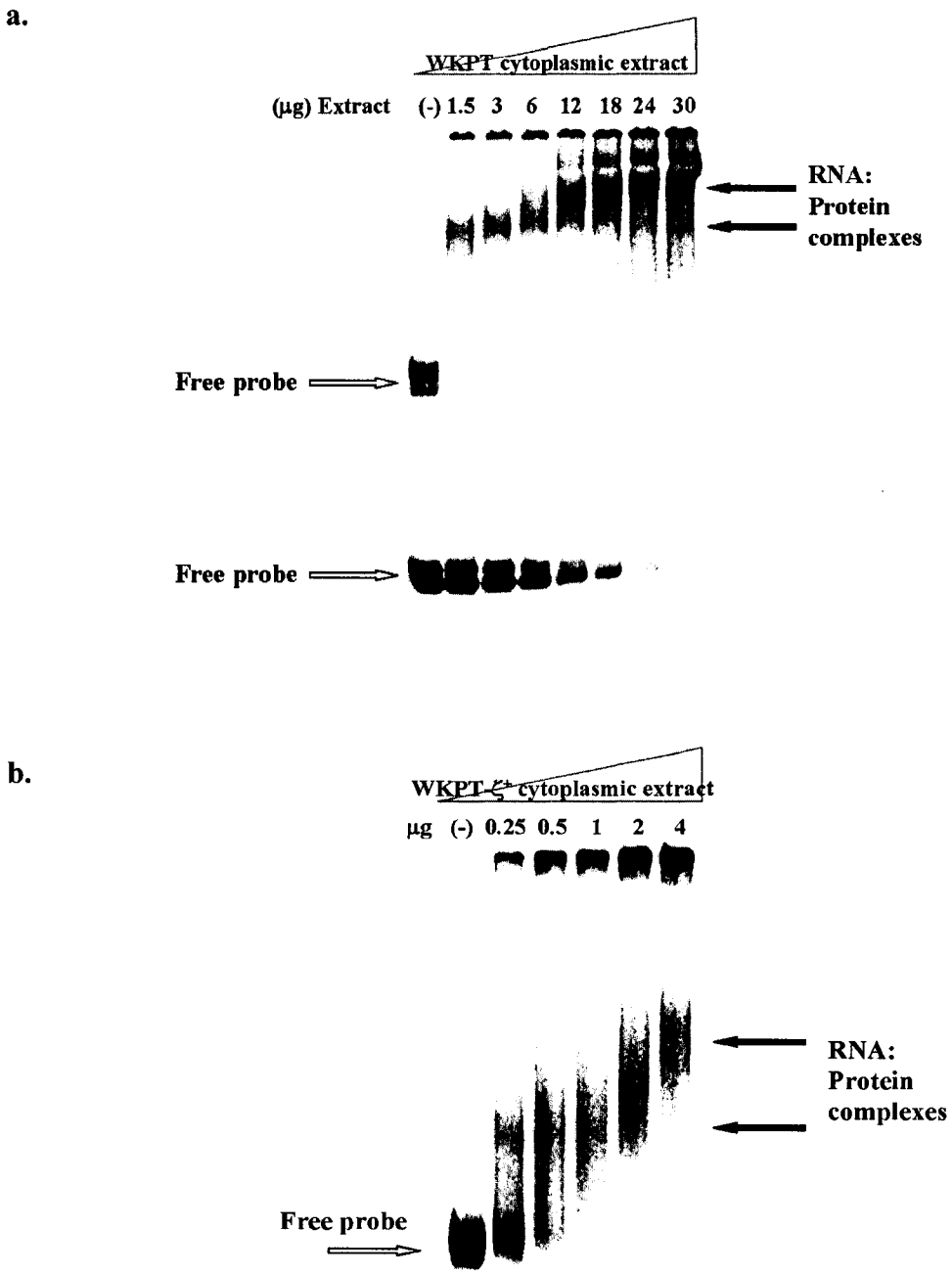

Fig. 6-4 Gel shift of pHRE binding proteins in WKPT cells. RNA electrophoretic mobility shift assay was performed using 20,000 cpm of [^{32}P]-labeled, capped GemGA-A_0 mRNA incubated with 1.5-30 μg of a S100 cytoplasmic extract from WKPT cells (**panel a**) or 0.25-4 μg of a S10 post-nuclear extract from WKPT-ζ^+ cells (**panel b**). Samples were resolved on a 5% native polyacrylamide gel. The gel was then dried and imaged on a PhosphorImager screen.

To identify the putative pHRE binding proteins in the WKPT-ζ^+ cells, antibodies to various RNA-binding proteins were used in a RNA gel super-shift assay. Pre-incubation of the WKPT-ζ^+ S10 post-nuclear extracts with ζ-cryst and HuR antibodies resulted in formation of RNA:protein complexes that were retained in the wells (**Fig. 6-5**). In contrast, the formation of minor bands that correspond to super-shifted RNA:protein complexes were observed with the addition of AUF1 and TTP antibodies (indicated by white arrows). Finally, antibody against Brf1 had little effect on RNA:protein complex formation. This experiment indicates that the observed RNA:protein complexes may contain ζ-cryst, AUF1, TTP, and HuR but not Brf1. It was previously demonstrated that ζ-cryst and AUF1 bind to the pHRE of the GA mRNA with high affinity and specificity. The current data demonstrate that ζ-cryst and AUF1 contained in WKPT cell extracts also bind to the pHRE. More importantly, this is the first demonstration that TTP and HuR, two well-characterized ARE binding proteins, also bind to the pHRE of the GA mRNA. Previous RNA gel shift experiments using S100 cytoplasmic extracts from kidney cortex failed to detect a super-shift when incubated with TTP and HuR antibodies [Ph. D. Thesis, H. Ibrahim]. However, western blot analysis demonstrated that HuR is highly enriched in S10 post-nuclear extracts, compared to S100 cytoplasmic extracts. Incubation of the pHRE containing RNA with S10 post-nuclear extracts of WKPT-ζ^+ cells clearly demonstrated the binding of HuR to the pHRE of GA mRNA. This is significant since HuR is a well-characterized stabilizing ARE binding protein and thus may play a role in the stabilization of the GA mRNA during metabolic acidosis.

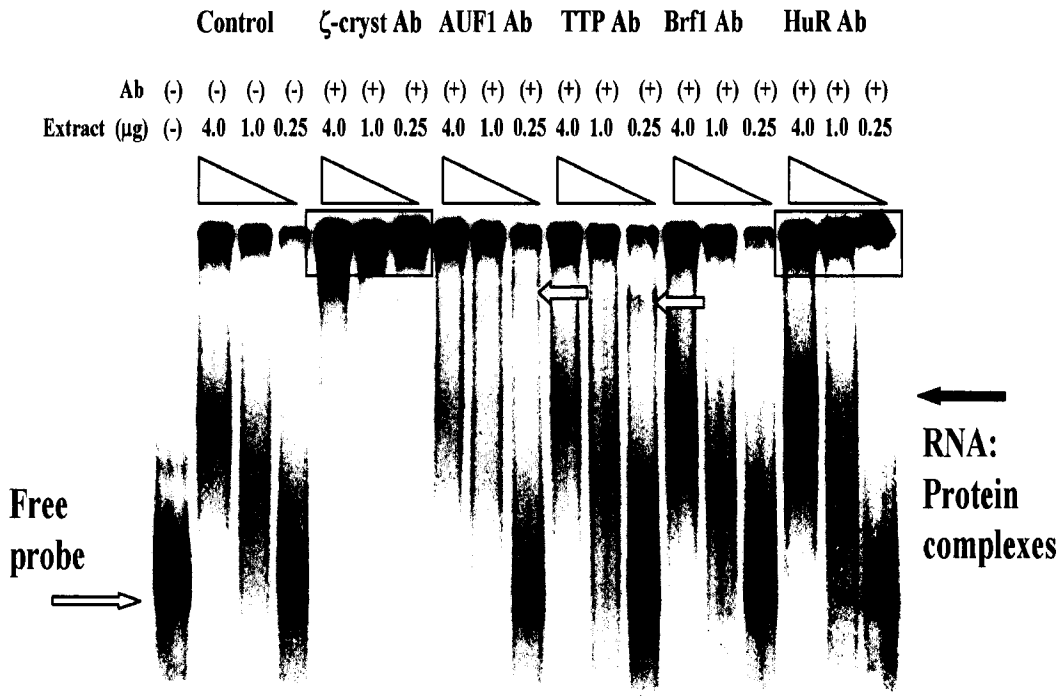

Fig. 6-5 Competition assay using antibodies against ARE binding proteins. Antibodies against well-characterized ARE-binding proteins were preincubated with 0.25-4 μg of S10 post-nuclear extracts and then mixed with 20,000 cpm of [^{32}P]-labeled, capped GemGA-A_0 mRNA to identify the possible pHRE binding proteins in WKPT-ζ^+ extracts. Samples were resolved on a 5% native polyacrylamide gel. The gel was then dried and exposed to a PhosphorImager screen.

6.5. RNA EMSA (Electrophoretic Mobility Shift Assay) using recombinant proteins

The RNA super-shift assays with antibodies against ARE binding proteins indicated that TTP and HuR may also bind to the pHRE of the GA mRNA. To test this hypothesis, recombinant $(His)_6$-tagged TTP and HuR were purified by Nickel column chromatography, and tested in RNA gel shift assays (**Fig. 6-6**). [^{32}P]-labeled, capped GemGA-A_0 RNA was incubated with increasing amounts of $(His)_6$-tagged ζ-cryst, p40-AUF1, TTP, and HuR, at a final concentrations ranging from 0.06-1.5 μM. The RNA electrophoretic mobility shift assay demonstrated the binding of ζ-cryst, p40-AUF1, TTP and HuR to the pHRE of the GA mRNA. The assays were performed in the absence of EDTA in running buffers, based on evidence that EDTA may chelate Zn^{+2} in solution and disrupt zinc-binding motifs [Nyborg and Peersen, 2004]. This experiment demonstrates the significant effect of EDTA on unfolding of the zinc-binding domain, since previous experiments performed in the presence of EDTA in running buffer failed to detect the pHRE:TTP interaction. However, with the omission of EDTA, there is a clear evidence of TTP binding to the pH-response element of GA mRNA. It is interesting to note that a population of RNA:protein complexes retained in the well when GemGA-A_0 RNA was incubated with recombinant ζ-cryst, TTP and HuR, compared to the absence of RNA:p40-AUF1 complexes in the well.

6.6 Competition assay using recombinant proteins

RNA electrophoretic mobility shift assays using [^{32}P]-labeled, capped RNA containing the pHRE of the GA mRNA indicate that multiple ARE binding proteins bind

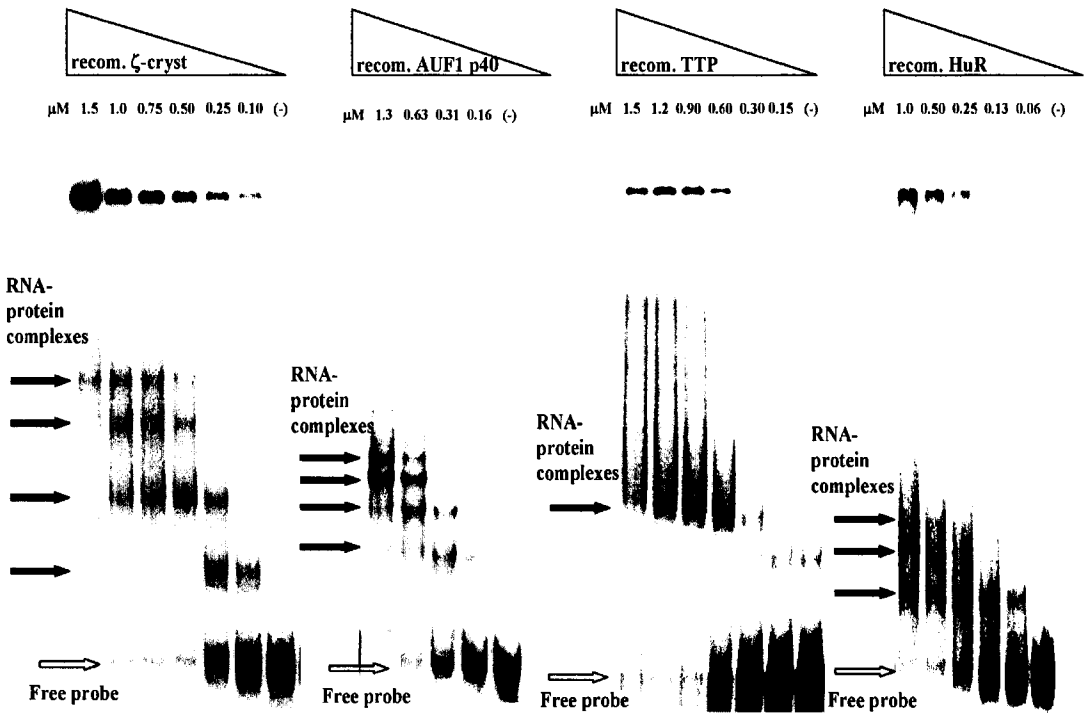

Fig. 6-6 Binding of recombinant ζ-cryst, p40-AUF1, TTP, and HuR to the pHRE of GA mRNA. RNA electrophoretic mobility shift assay was performed using 20,000 cpm [^{32}P]-labeled, capped GemGA-A_0 mRNA containing the pHRE of GA mRNA, incubated with varying amounts of recombinant ARE binding proteins at final concentration ranging from 0.06-1.5 μM. Samples were resolved on 5% native polyacrylamide gel. The gel was then dried and exposed to a PhosphorImager screen.

to the element. Competition assays were performed in order to examine if these ARE-binding proteins share the same binding site within the pHRE of GA mRNA. RNA gel shift assays were again performed in the absence of EDTA in the running buffer.

[^{32}P]-labeled, capped GemGA-A_0 RNA was incubated with a constant amount of ζ-cryst (0.50 μM) and with varying amounts of p40-AUF1 (0.0-1.3 μM) (**Fig. 6-7 panel a**). The resulting gel shift patterns demonstrate that the two ARE binding proteins do not share the same binding site. The RNA:ζ-cryst and RNA:p40-AUF1 form multiple complexes that exhibit slightly different mobilities. The addition of increasing amounts of p40-AUF1 result in increased formation of the RNA:p40-AUF1 complexes without loss of the RNA:ζ-cryst complex. In contrast, the titration of varying amounts of TTP (0.0-1.5 μM) with a constant amount of ζ-cryst (0.50 μM) resulted in the disappearance of RNA:ζ-cryst shift and the appearance of RNA:TTP complexes (**Fig. 6-7 panel b**). A similar disappearance of RNA:p40-AUF1 complexes was observed with the titration of TTP (0.0-1.5 μM) into samples containing 0.43 μM p40-AUF1 (**Fig. 6-7 panel c**). The data indicate that ζ-cryst and p40-AUF1 do not compete for the same site and therefore may bind simultaneously to different sites on the GemGA-A_0 mRNA. In contrast, TTP may bind to both sites and effectively displace both ζ-cryst and p40-AUF1 from their respective sites.

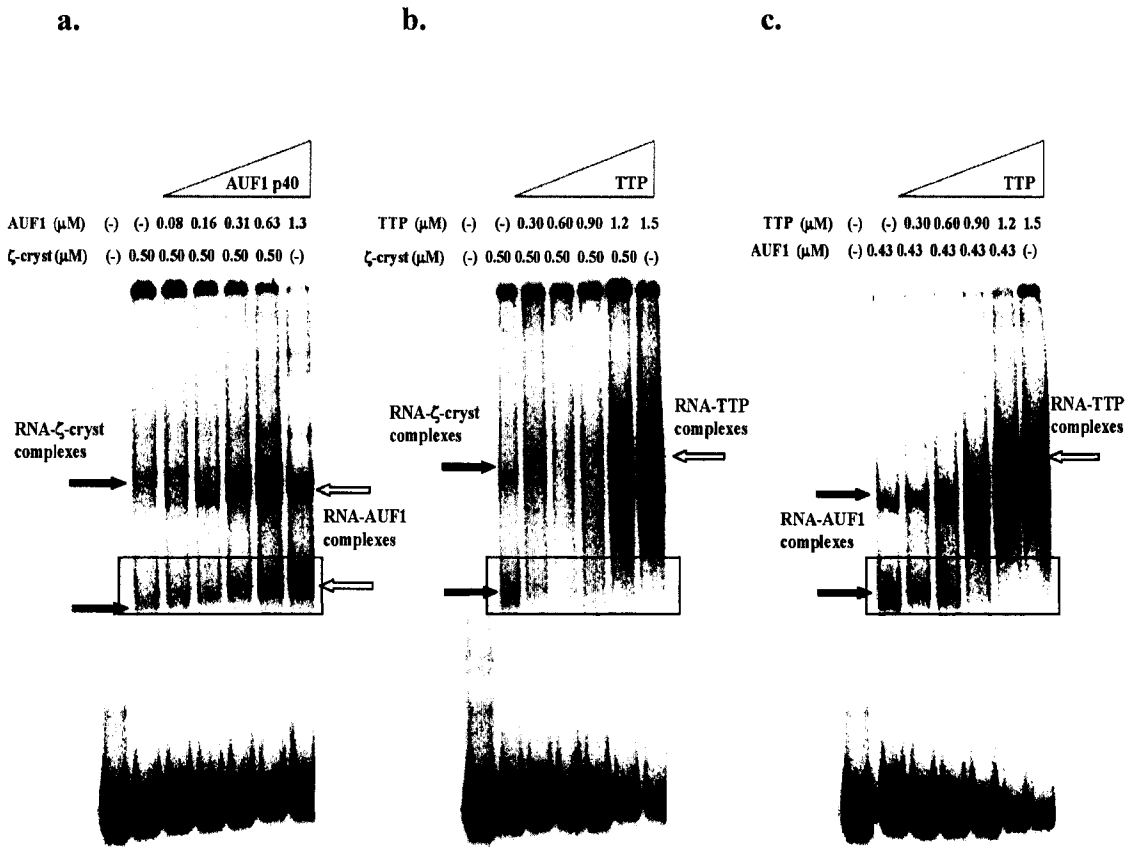

Fig. 6-7 Competitive binding of recombinant ζ-cryst, p40-AUF1, and TTP to the pHRE of GA mRNA. A competition assay was performed using 20,000 cpm [^{32}P]-labeled, capped GemGA-A_0 mRNA and various recombinant proteins. (a) 0.50 μM of ζ-cryst was incubated with increasing amounts of p40-AUF1, ranging from 0.08-1.3 μM. (b) 0.50 μM of ζ-cryst was incubated with increasing amounts of TTP (0.30-1.5 μM). (c) Varying amounts of TTP (0.30-1.5 μM) were titrated into reactions containing 0.45 μM of p40-AUF1. Samples were resolved on 5% native polyacrylamide gel. The gel was then dried and imaged on a PhosphorImager screen.

6.7. Competition assay with cap analog

Several findings were discovered by using purified recombinant proteins in the RNA electrophoretic mobility shift assays. [^{32}P]-labeled, capped or uncapped GemGA-A_0 formed different RNA:p40-AUF1 complexes (data not shown). This suggested that p40-AUF1 may also interact with the cap structure when bound to AU-rich element. Hence, different amounts of cap analog [^{met7}G(5')ppp(5')G] were titrated into the binding reactions to observe the effect of cap analog on the formation of RNA:protein complexes. It is interesting to note that the amount of ζ-cryst:RNA complex decreased slightly with the titration of cap analog, suggesting that ζ-cryst may also interact with 5' cap structure when bound to the pHRE (**Fig. 6-8**).

Similar experiments were performed using recombinant p40-AUF1. When 125-500 μM of cap analog was titrated into reactions containing 0.43 μM p40-AUF1 in the presence or absence of RNase T1, a decrease in the formation of the RNA:p40-AUF1 complex, with a corresponding increase in unbound probe, was observed (**Fig. 6-9**). Therefore, the binding of p40-AUF1 to the cap structure may increase the affinity of the interaction between p40-AUF1 and the pHRE within the GemGA-A_0 mRNA.

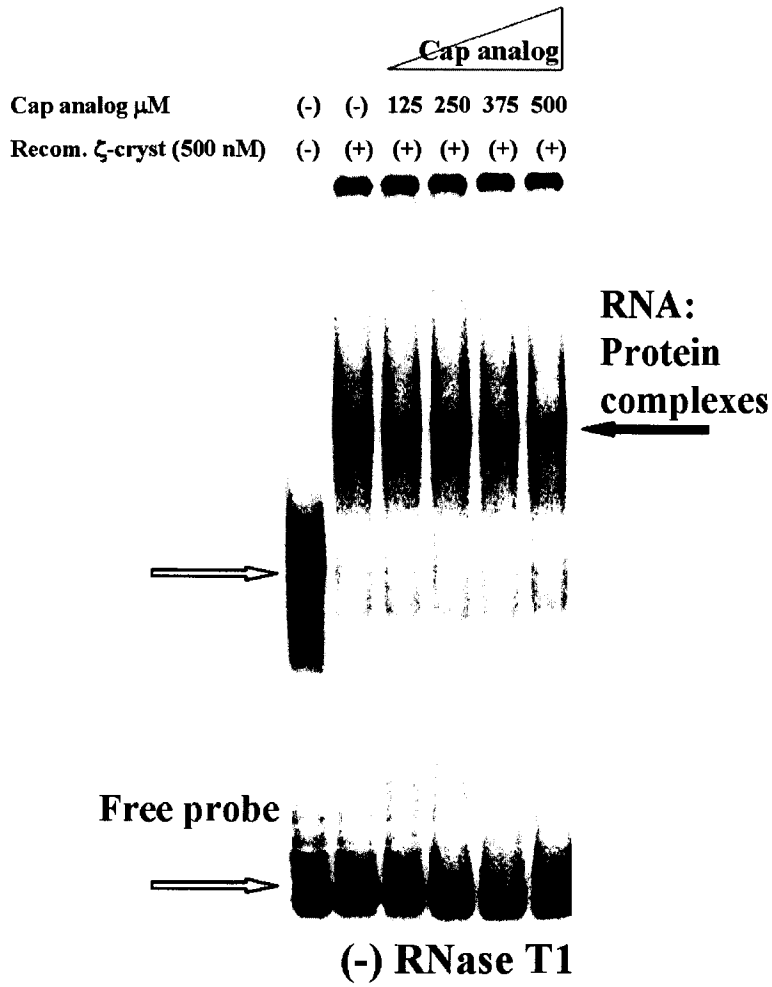

Fig. 6-8 Interaction of ζ-cryst with the 5' cap structure. Increasing amounts of cap analog [^{met7}G(5')ppp(5')G] were added in a RNA gel shift assay using 20,000 cpm [^{32}P]-labeled, capped GemGA-A_0 mRNA with 0.50 μM of ζ-cryst. Samples were resolved on 5% native polyacrylamide gel. The gel was then dried and exposed to a PhosphorImager screen.

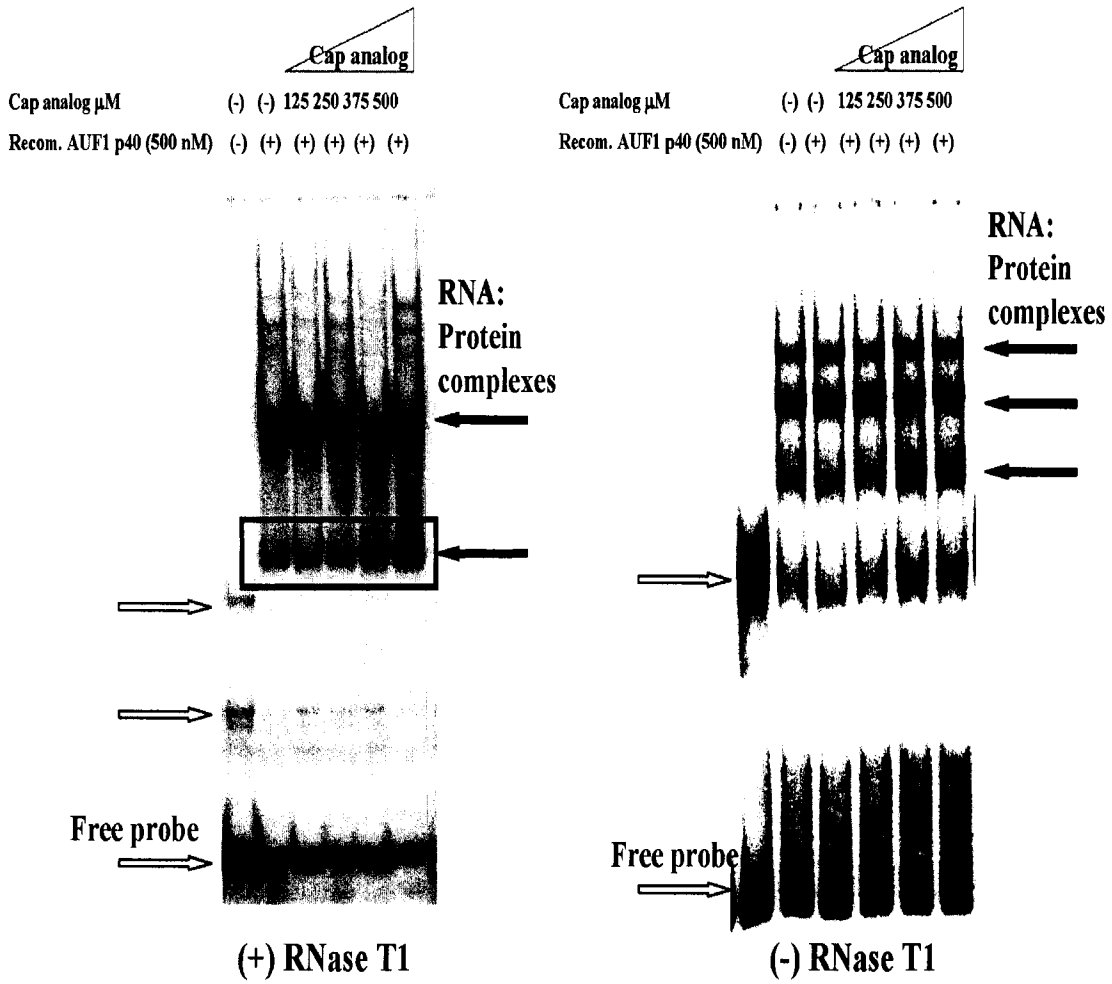

Fig. 6-9 Interaction between p40-AUF1 and the 5' cap structure. Increasing amounts of cap analog [^{met7}G(5')ppp(5')G] were added in a RNA gel shift assay using 20,000 cpm [^{32}P]-labeled, capped GemGA-A_0 mRNA with 0.50 μM of p40-AUF1. Samples were resolved on 5% native polyacrylamide gel. The gel was then dried and exposed to a PhosphorImager screen.

6.8 *In vitro* deadenylation of GemGA-A_{60}

RNA electrophoretic mobility shift assays demonstrated that various AU-rich binding proteins bind to the pHRE of the GA mRNA and provide an initial assessment of binding affinity and specificity. However, it is also important to investigate the potential roles of various ARE binding proteins in the stabilization of GA mRNA during the metabolic acidosis. Hence, an *in vitro* deadenylation assay was developed in order to characterize the differential effects of the various ARE binding proteins on the rate of deadenylation and turnover of GA mRNA.

Using WKPT cell extracts in the absence of poly-A RNA, the deadenylation and decay of the GemGA-A_{60} RNA was minimal (**Fig. 6-10 panel a**). The addition of recombinant TTP slightly stimulated the deadenylation of the GemGA-A_{60} RNA, whereas the addition of ζ-cryst and p40-AUF1 had little or no effect.

The addition of poly-A RNA to compete for the binding of poly-A binding proteins stimulated the deadenylation of the GemGA-A_{60} RNA (**Fig. 6-10 panel b**). The addition of ζ-cryst had a minimal effect on the deadenylation and turnover of GemGA-A_{60} mRNA. In contrast, the addition of p40-AUF1 had a significant stabilizing effect that is evident from the slower rate of disappearance of the GemGA-A_{60} RNA compared to the control. By contrast, the addition of TTP slightly stimulated the deadenylation of the GemGA-A_{60} RNA.

In order to investigate whether the exosome may play a role in the turnover process of GemGA-A_{60} mRNA, ATP and phosphocreatine (ATP/PC) were omitted from the reaction mixture. ATP is required by the catalytic subunit of the exosome, hence the omission of ATP/PC should inhibit the exosome and lead to the greater accumulation of

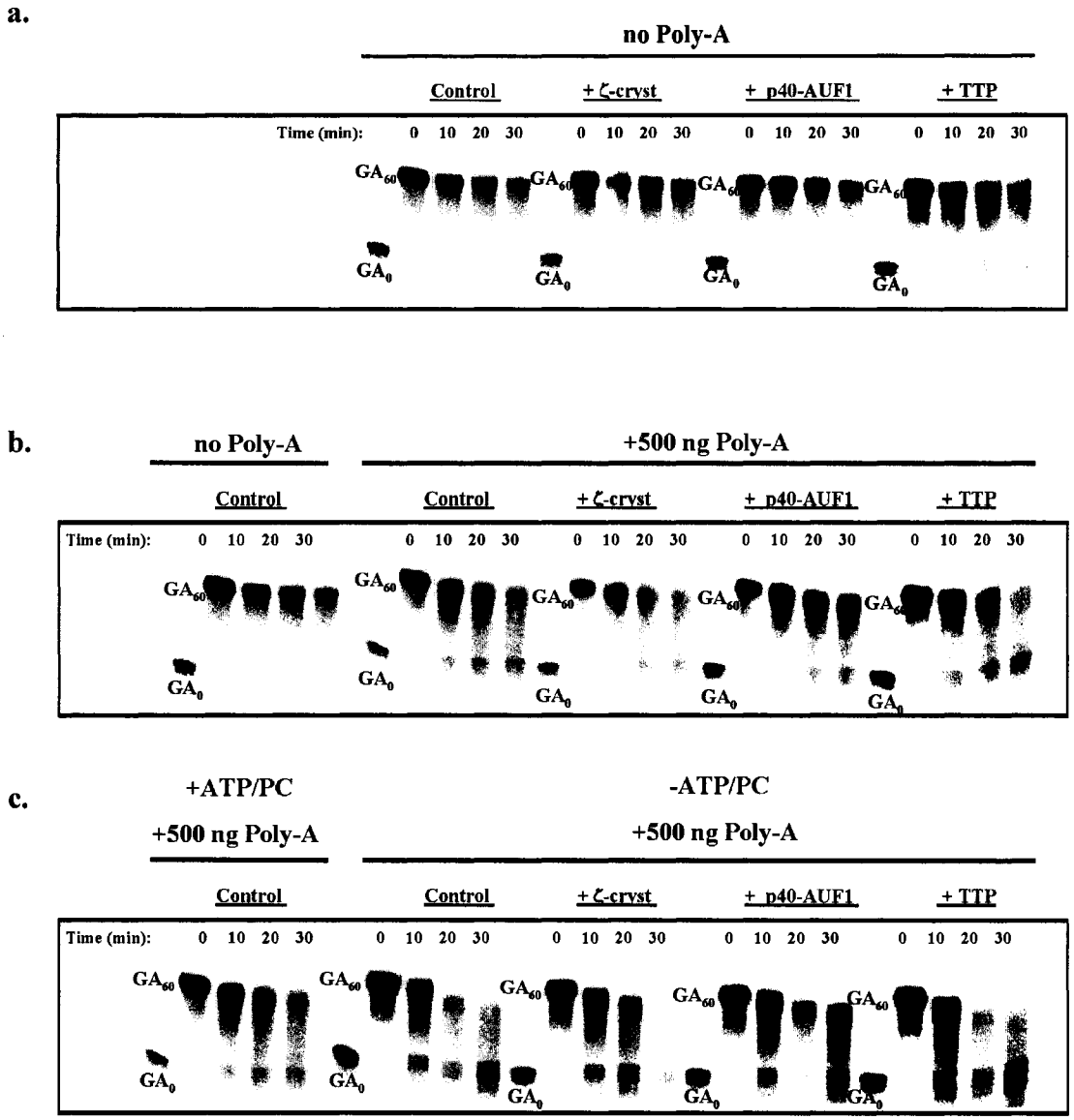

Fig. 6-10 Effect of recombinant proteins on the deadenylation and subsequent decay of GemGA-A_{60} mRNA in WKPT cells. The GemGA-A_{60} mRNA was incubated with a S100 cytoplasmic extract of WKPT cells for the indicated times in the absence or presence of the added recombinant proteins. The experiments were performed in the absence **(panel a)** or presence of 500 ng Poly-A RNA and ATP/phosphocreatine (PC). The reaction products were analyzed on a 5% acrylamide-urea gel. Addition of poly-A RNA enhanced the rate of mRNA turnover **(panel b)**. Slight stabilization of the GemGA-A_{60} substrate observed with the addition of p40-AUF1 in the absence of poly-A RNA. The addition of ζ-cryst and p40-ζ-crsyt had little effect on the deadenylation and decay of the GemGA-A_{60} RNA in the presence of ATP/PC **(panel b)**. By contrast, addition of TTP slightly enhanced deadenylation of the GemGA-A_{60} RNA. Subsequent mRNA turnover process of deadenylated products was inhibited in the absence of ATP/PC (**panel c**).

the deadenylated product. With the omission of ATP/PC, greater accumulation of deadenylated product was observed over the 30 min time course. This is most apparent with the addition of TTP (**Fig. 6-10 panel c**). This experiment demonstrates that the exosome is involved in the turnover of GemGA-A_{60} mRNA. Additionally, it also demonstrates that p40-AUF1 may act as a stabilizing *trans*-acting factor, while TTP may act as a destabilizing factor in the turnover of GA mRNA.

6.9 Decay profile of GemGA-A_{60} in WKPT-ζ^+ cells

The addition of recombinant ζ-cryst to the *in vitro* deadenylation assay using WKPT extracts had little or no effect on the rate of deadenylation and turnover of the GemGA-A_{60} RNA. However it is possible that the endogenous ζ-cryst requires a post-translational modification to function. In order to determine this possibility, extracts of WKPT-ζ^+ cells, a line of WKPT cells that over expresses ζ-cryst, were utilized.

The rate of deadenylation and turnover of the GemGA-A_{60} mRNA was significantly enhanced in WKPT-ζ^+ extracts compared to WKPT extracts, indicating ζ-cryst may function as a destabilizing *trans*-acting factor. In the absence of poly-A RNA, stabilizing effects of p40-AUF1 and HuR on the deadenylation and turnover of the GemGA-A_{60} mRNA were observed compared to the control (**Fig. 6-11 panel a**). Addition of ζ-cryst to the reaction did not further effect the deadenylation and turnover rate of the GemGA-A_{60} RNA. The addition of TTP slightly enhanced deadenylation of the GemGA-A_{60} RNA as observed in WKPT cells.

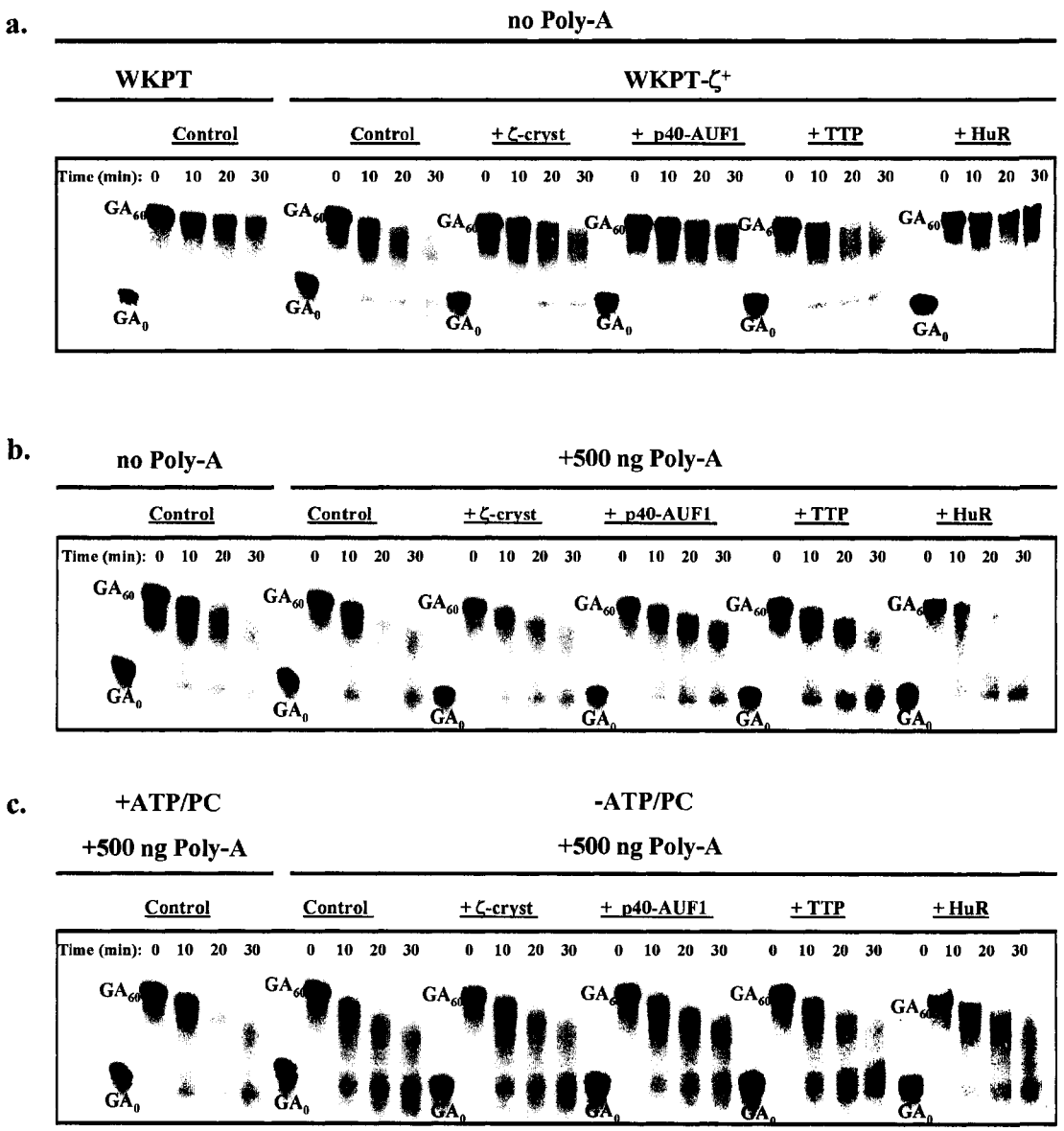

Fig. 6-11 Effect of recombinant proteins on the deadenylation and subsequent decay of GemGA-A_{60} mRNA in WKPT-ζ^+ cells. The GemGA-A_{60} mRNA was incubated with S100 cytoplasmic extracts of WKPT or WKPT-ζ^+ cells, for the indicated times in the absence **(panel a)** or presence of the indicated amount of added proteins. The experiments were performed in the absence or presence of 500 ng Poly-A RNA and ATP/phosphocreatine. The deadenylation and subsequent decay of the GemGA-A_{60} RNA was significantly enhanced in WKPT-ζ^+ cells. Addition of poly-A RNA slightly enhanced the rate of mRNA turnover **(panel b)**. Stabilization of the GemGA-A_{60} RNA observed with the addition of p40-AUF1 and HuR in the absence of poly-A RNA. TTP had slight destabilizing effect on the deadenylation and decay of the GemGA-A_{60} RNA, in presence or absence of poly-RNA polymer **(panel b)**. Subsequent mRNA turnover process of deadenylated products was inhibited in the absence of ATP/PC. The reaction products were analyzed on a 5% denaturing polyacrylamide gel **(panel c)**.

A slight increase in the rate of deadenylation and a greater accumulation of the deadenylated product were observed in the presence of 500 ng poly-A RNA (**Fig. 6-11 panel b**). However, the stabilizing effects of p40-AUF1 and HuR were no longer evident. Again, the addition of TTP slightly enhanced the rate of deadenylation and the accumulation of the deadenylated product. Omission of ATP/PC again resulted in the greater accumulation of the deadenylated product, indicating the exosome participates in the turnover of the GemGA-A_{60} (**Fig. 6-11 panel c**).

The experiments performed in WKPT-ζ^+ extracts demonstrate that ζ-cryst may act as a destabilizing ARE binding protein that may stimulate the turnover of mRNA. Further experiments need to be performed in order to further characterize ζ-cryst as possible *trans*-acting instability factor. *In vitro* deadenylation assay data suggest that TTP may also act as a destabilizing trans-acting factor that stimulates deadenylation and subsequent turnover of GA mRNA by the exosome. In contrast, p40-AUF1 and HuR may act as stabilizing *trans*-acting factors, increasing the stability of the GA mRNA. AUF1 has been demonstrated to function as either a stabilizing or destabilizing transacting factor. It has been suggested that the differential role of AUF1 may be regulated by the relative abundance of each AUF1 isoform [Raineri et al, 2004]. Hence it is possible that the stabilizing effect of p40-AUF1 on the deadenylation and turnover of GA mRNA may result from addition of just this isoform. The bacterially expressed recombinant p40-AUF1 lacks potential post-translational modifications. Therefore, the stabilizing effect of p40-AUF1 may reflect the effect of addition of unphosphorylated p40-AUF1. On the other hand, these experiments clearly demonstrate that the *in vitro* deadenylation assay can be used to characterize the stabilizing roles of p40-AUF1 and

HuR, and the destabilizing roles of ζ-cryst and TTP proteins on the deadenylation and turnover rate of GA mRNA, and that exosome may participate in the turnover of the GA mRNA.

6.10. The effects of cap analog and poly-A RNA polymers on the rate of deadenylation

The *in vitro* deadenylation assay demonstrated that the turnover of the GemGA-A_{60} mRNA involves deadenylation followed by subsequent 3'→5' degradation. There are at least four different deadenylases that have been identified, including Pan2 and Pan3, CCR4 and nocturnin, CAF1, and PARN. PAN2 and PAN3 are cytoplasmic deadenylases that are activated by Pab1p (**Table 6-1**). CCR4 and Noturnin complexes have been shown to be localized to P-bodies, while CAF1 has deadenylase activity in an *in vitro* assay. PARN is a cap-dependent deadenylase that is modulated by ARE-binding proteins.

Enzyme		Function
Deadenylases	PAN2 and PAN3	Cytoplasmic deadenylase activated by Pab1p
	CCR4 and Nocturnin	Localizes to P-bodies
	CAF1	Has deadenylase activity *in-vitro*
	PARN	Cap-dependent Modulated by ARE-binding proteins
Decapping Enzymes	DCP1 and DCP2	5'→ 3' decay pathway Localized to P-bodies
	DCPS	Scavenger enzyme Acts in both 5'→ 3' and 3'→ 5' pathways Nuclear
5'→ 3' exonuclease	XRN1	Localized to P-bodies
3'→ 5' exonuclease	Exosome	Modulated by ARE-binding proteins

Table 6-1 Summary of enzymes involved in mRNA turnover (adapted from Wilusz, CJ et al, 2004).

In order to test whether PARN is the deadenylase responsible for the deadenylation process in WKPT-ζ^+ cells, cap analog was titrated into the deadenylation reaction. **Fig. 6-12 panel a** illustrates the effect of increasing cap analog on deadenylation in the presence of 500 ng poly-A RNA. The rate of deadenylation and the subsequent decay of the deadenylated product were inhibited by the addition of cap analog, indicating that the cap-dependent PARN may be responsible for the deadenylation process in WKPT-ζ^+ extracts.

The inhibitory effect of poly-A binding proteins on deadenylation process is demonstrated in **Fig. 6-12 panel b**. In this experiment, increasing amounts of cap analog were titrated into the reaction in the absence or presence of poly-A RNA and all of the samples were incubated for 30 min. In the presence of poly-A RNA only the fully deadenylated product remained after 30 min regardless of the amount of cap analog added. Without the addition of poly-A RNA, there is a significant decrease in the rate of deadenylation. This is evident from the fact that much of the substrate is not fully deadenylated even after 30 min. The addition of increasing amounts of cap analog results in an increase in the amount of the partially deadenylated product. These data again demonstrate that PARN may be responsible for the deadenylase activity in the WKPT-ζ^+ extracts.

a.

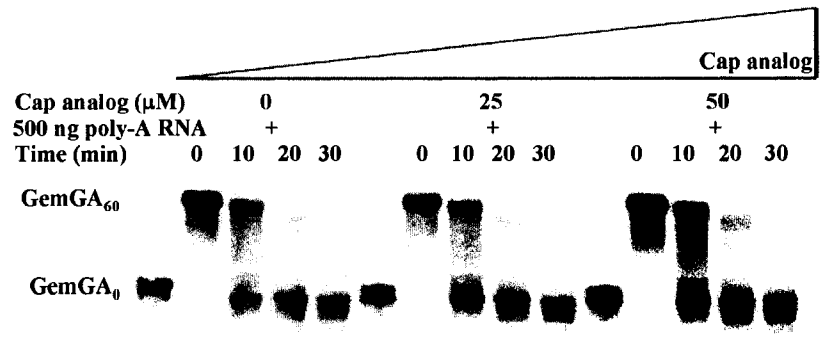

b.

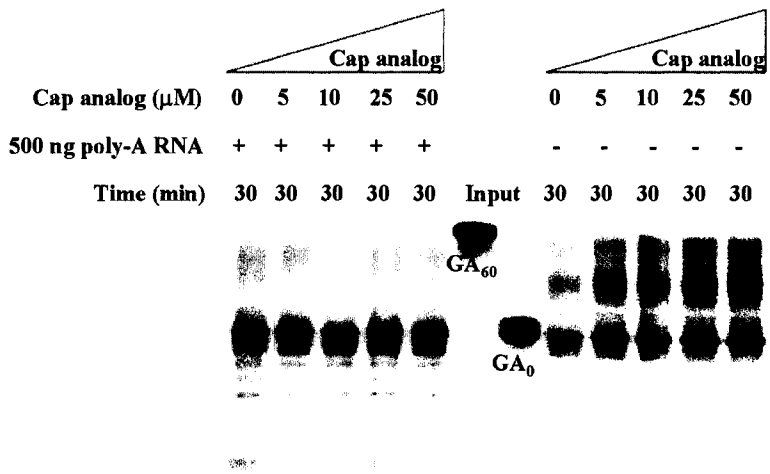

Fig. 6-12. The effect of cap analog on deadenylation of GemGA-A_{60} mRNA. (a) PARN is responsible for the deadenylation of GemGA-A_{60} mRNA. The [^{32}P]-labeled, capped GemGA-A_{60} mRNA was incubated with a S100 cytoplasmic extract of WKPT-ζ^+ cells various in the presence of 500 ng Poly-A RNA with increasing amounts of cap analog. Addition of cap analog decreased the rate of mRNA turnover of GemGA-A_{60} mRNA, indicating the cap-dependent deadenylation of the substrate. Hence, PARN maybe the deadenylase that is responsible for the observed deadenylation of GA mRNA. **(b) Effects of addition of poly-A RNA on a deadenylation.** The GemGA-A_{60} was incubated with a S100 cytoplasmic extract of WKPT-ζ^+ cells for 30 min in the absence or presence of 500 ng poly-A RNA with increasing amount of cap analog. The deadenylation of GemGA-A_{60} was stimulated by the addition of poly-A RNA. The reaction products were analyzed on a 5% denaturing polyacrylamide gel.

6.11. Decay profiles of GemGA-A_{60} mRNA at pH 6.9 versus pH 7.4

To investigate whether the stabilization of GA mRNA during metabolic acidosis is due to a decreased rate of deadenylation, WKPT and WKPT-ζ^+ extracts were prepared from cells that were maintained in normal medium or treated with acidic medium for 24 h. *In vitro* deadenylation assays were performed using S100 extracts in the presence of 500 ng poly-A RNA (**Fig. 6-13**). The rate of deadenylation observed with the extracts prepared from WKPT cells treated with acidic medium was comparable to that observed in extracts prepared from WKPT cells that were maintained normal medium. A significant increase in the rate of deadenylation and turnover rate was observed in WKPT-ζ^+ extracts compared to WKPT extracts. However, as observed with WKPT extracts, the rate of deadenylation observed with the extracts prepared from WKPT-ζ^+ cells treated with acidic medium was not significantly different from that observed in extracts prepared from WKPT-ζ^+ cells that were maintained normal medium. Therefore, the extracts prepared from cells treated with acidic medium do not reproduce the effect observed previously in experiments that measure the rate of deadenylation of the βG-GA reporter in LLC-PK_1-F^+ cells treated with acidic medium [Schroeder et al, 2006]. In contrast, the turnover rate of deadenylated GemGA-A_0 RNA is decreased with the extracts prepared from WKPT-ζ^+ treated with acidic medium, that may contribute to the stabilization of GA mRNA during the onset of metabolic acidosis. Based on the data obtained through *in vitro* deadenylation assays demonstrating differential roles of ARE binding proteins on the GemGA-A_{60} mRNA turnover, it is more likely the recruitment of either stabilizing or destabilizing ARE binding proteins to the pHRE determines the fate of GA mRNA.

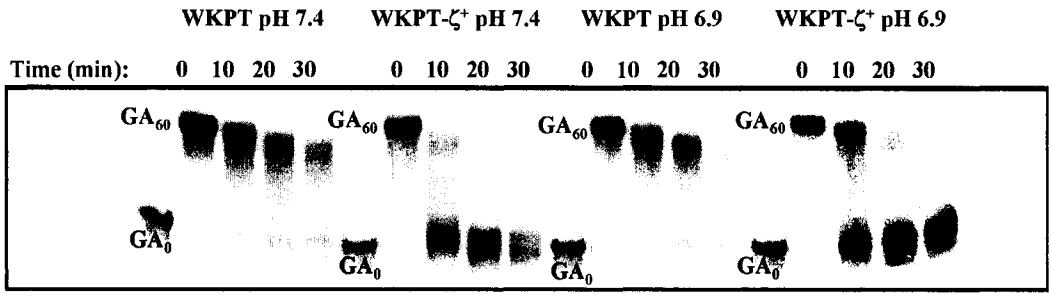

Fig. 6-13 Deadenylation and subsequent turnover of GemGA-A_{60} mRNA is not affected by preparing extracts from cells treated with acidic medium. The [^{32}P]-labeled, capped GemGA-A_{60} mRNA was incubated with S100 cytoplasmic extracts of WKPT or WKPT-ζ^+ cells that were maintained in normal medium or treated with acidic medium for 24 h. The reactions were performed in the presence of 500 ng Poly-A RNA and terminated at the indicated times. A significant increase in the deadenylation rate is observed in WKPT-ζ^+ cells. However, the rate of deadenylation occurs at a comparable rate in the extracts prepared from cells grown in normal medium (pH 7.4) or those with acidic medium (pH 6.9) for 24 h. The reaction products were analyzed on a 5% denaturing polyacrylamide gel.

6.12 *In vitro* decapping assay

The preceding *in vitro* studies demonstrate that the degradation of GemGA-A_{60} mRNA is initiated by deadenylation and may be followed by 3'→5'degradation pathway by the exosome. Recently, a cytoplasmic loci, named processing-bodies (P-bodies) has been identified [Sheth et al, 2003]. P-bodies contain the decapping enzymes, Xrn1, a 5'→3' exonuclease, and the Lsm1-7 heptamer [Kedersha et al, 2005]. ARE binding proteins such as HuR, TTP and Brf1 were shown to interact with both the exosome and the factors involved in decapping and 5'→3' degradation [Chen, C-Y et al, 20021; Kedersha et al, 2005]. Through the *in vitro* deadenylation assay, TTP was shown to enhance deadenylation and turnover of the GemGA-A_{60} mRNA, while HuR was shown to have a stabilizing effect. Western blot analysis demonstrated the presence of Brf1 in WKPT and WKPT-ζ^+ cells. Hence, it was important to investigate whether the 5'→3'degradation pathway is also involved in GemGA-A_{60} mRNA turnover.

[^{32}P]-Cap labeled GemGA-A_{60} and GemGA-A_0 RNAs were generated, and incubated with S10 and S100 extracts from WKPT and WKPT-ζ^+ cells (**Fig. 6-14**). Several decapping products were observed, including ^{7met}GpppG, ^{7met}GDP, and ^{7met}GMP. ^{7met}GpppG is produced by 3'→5' degradation of the transcript by the exosome. In this process, the scavenger decapping enzyme, DcpS, acts on the oligomeric product of exosomal decay to produce ^{7met}GMP. Alternatively following deadenylation, the direct hydrolysis of the 5'-cap by Dcp1a/Dcp2 generates ^{7met}GDP. The resulting decapped transcript is then subjected to 5'→3'degradation by Xrn1. In the absence of cap analog, the majority of the decapping products detected were ^{7met}GMP and ^{7met}GDP indicative of both pathways. Addition of cap analog to inhibit DcpS resulted in increased appearance

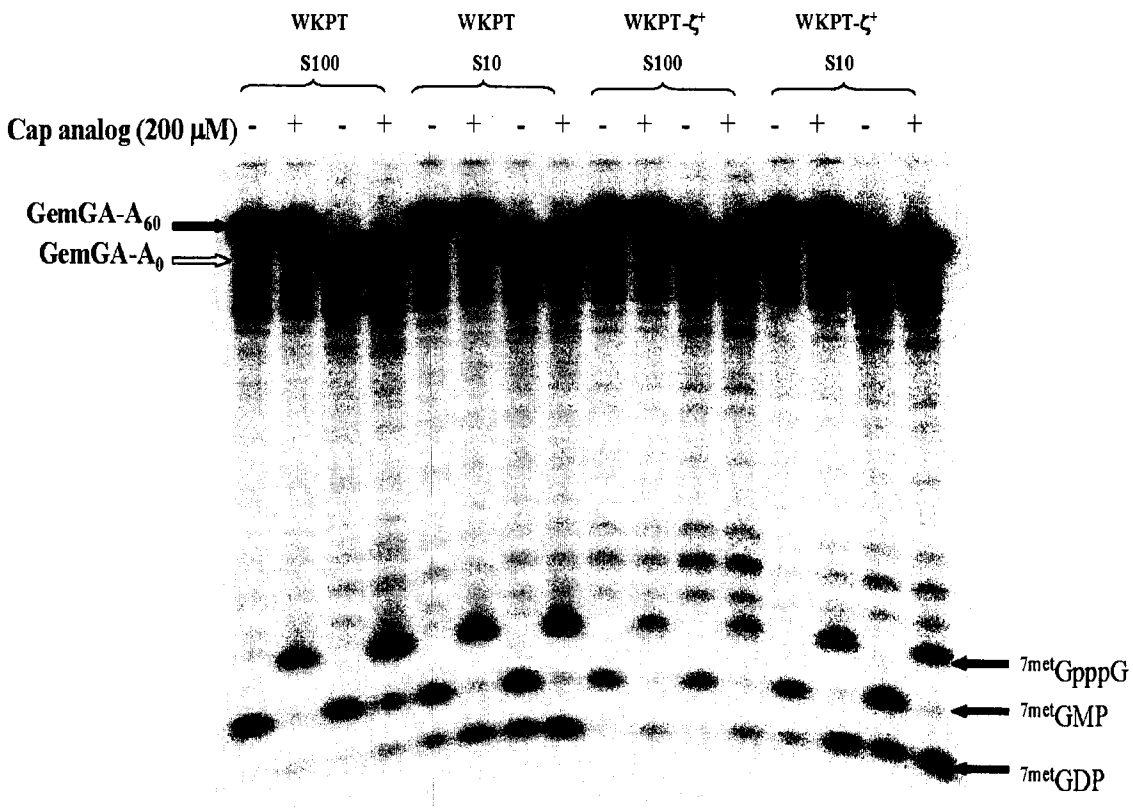

Fig. 6-14 Analysis of decapping products. The [^{32}P]-cap labeled GemGA-A_{60} and GemGA-A_0 mRNAs were incubated with S10 post-nuclear or S100 cytoplasmic extracts of WKPT and WKPT-ζ^+ cells grown in normal medium. The reactions were incubated at 30°C for 30 min. Accumulation of the Dcp1/Dcp2 decapping product ^{7met}GDP occurred to a higher extent with the S10 post-nuclear extract compared to the S100 cytoplasmic extract. The addition of cap analog inhibited the DcpS resulting in greater accumulation of the exosomal product, ^{7met}GpppG. The reaction products were analyzed on a 20% denaturing polyacrylamide gel.

of ^{7met}GpppG. It should be also noted that greater amount of ^{7met}GDP occurs at a faster rate in S10 post-nuclear extracts compared to S100 cytoplasmic extracts. It was previously reported that S100 cytoplasmic extracts may be deficient in the factors involved in 5'→3' degradation, since protein complexes >500 kDa are recovered in the S10 post-nuclear extracts [Seal, 2005]. Based on this observation, the S100 cytoplasmic extract contains the protein complexes necessary for 5'→3' degradation but to a lesser extent compared to the S10 post-nuclear extract. This experiment demonstrated the 5'→3'degradation pathway is also involved in the turnover of GemGA-A_{60} mRNA. Thus, it will be important to determine which pathway predominates in the proximal tubules in normal acid-base balance and during metabolic acidosis.

6.13 Nuclear and cytoplasmic distribution of ARE binding proteins

ARE binding proteins often display nuclear-cytoplasmic shuttling activity. TTP, Brf1, and AUF1 have been shown to bind 14-3-3 proteins that function to regulate of subcellular localization of the bound proteins [Stoecklin et al, 2004; He et al, 2006]. Hence it was important to characterize the distribution of ARE binding proteins involved in the GA mRNA turnover in WKPT-ζ^+ cells. Nuclear and cytoplasmic extracts were prepared using the NE-PER Nuclear and Cytoplasmic Extraction Kit. In this protocol, a hypotonic solution containing a mild detergent is used to lyse the cell membrane and to release the cytoplasm. The intact nuclei are subsequently lysed in a hypertonic solution.

The steady-state distribution of the ARE binding proteins was assessed by western blot analysis (**Fig. 6-15 panel a**). The p37, p40, p42, and p45 isoforms of AUF1 were detected in the nuclear fraction of WKPT-ζ^+ cells, while only the p37 and p40

a.

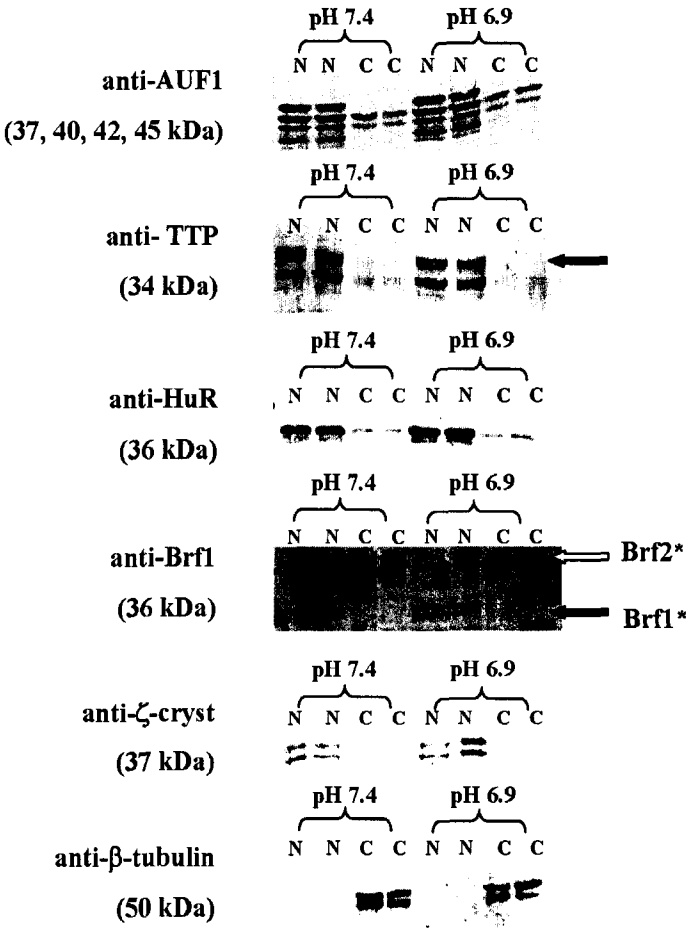

b.

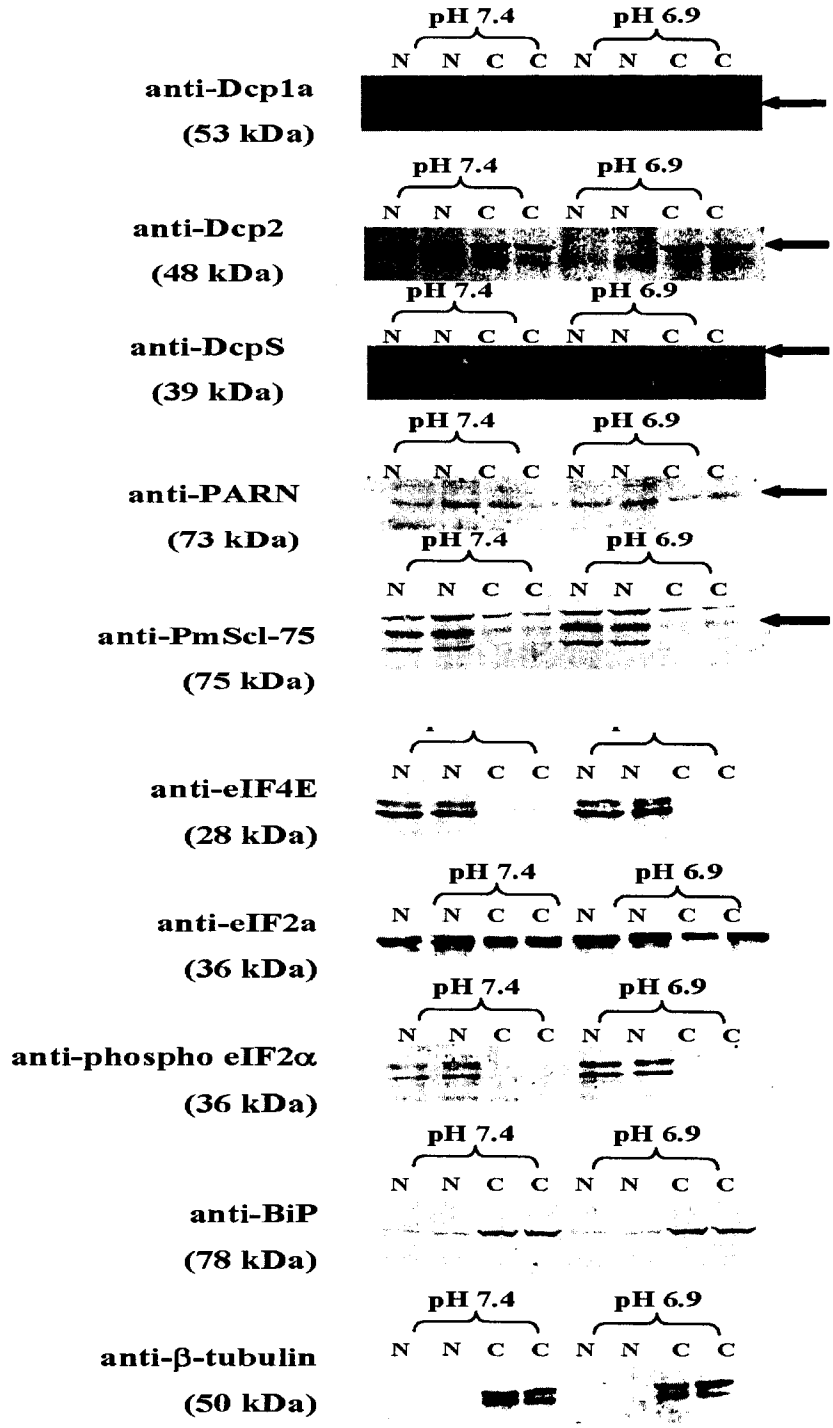

Fig. 6-15 Subcellular localization of the ARE binding proteins and proteins that participate in mRNA turnover. Nuclear and cytoplasmic fractions were separated using NE-PER Nuclear and Cytoplasmic Extraction Kit (Pierce). Samples containing 40 μg of protein from the two fractions were resolved on a 10% SDS-denaturing gel. Antibodies to well-characterized ARE binding proteins **(panel a)** and the proteins involved in mRNA turnover **(panel b)** were utilized to determine their subcellular distribution.

isoforms of AUF1 were detected in the cytoplasmic fraction. The majority of the TTP and HuR proteins were localized in the nuclear fraction, with less recovered in the cytoplasmic fraction, indicating the nuclear-cytoplasmic shuttling activity of the proteins. Brf1 localized in the nuclear fraction, in contrast to its homolog Brf2 that localized in the cytoplasmic extracts. Consistent with the previous data, the total amounts of Brf2 was decreased in the cytoplasmic extracts prepared from cells treated with acidic medium for 24 h. Interestingly, ζ-cryst was recovered only in the nuclear fraction, even though it was previously reported to be a cytoplasmic protein [Wang et al, 1998]. β-tubulin, a cytoplasmic protein served as a control, indicating that very little of the cytoplasmic proteins are present in the nuclear fraction.

It was expected that the ARE-binding proteins associated with P-bodies or cytoplasmic decay bodies would be recovered in the cytoplasmic and nuclear fractions, depending on their shuttling activity. This was demonstrated by western blot analysis of Dcp1a, Dcp2, DcpS, PARN, and PmScl-75 (**Fig. 6-15 panel b)**. The decapping proteins, Dcp1a and Dcp2 decapping proteins were found primarily in the cytoplasmic extracts, where the P-bodies reside. By contrast, the majority of DcpS was found in the nuclear fraction. PARN was present in both the nuclear and cytoplasmic fractions, while majority of the exosome as indicated by the α-Pm/Scl-75 protein, are found in the nuclear fraction and to a lesser extent in the cytoplasmic fraction. It should be noted that the components of 3'→5' decay pathway and ARE-binding proteins such as hnRNPA1, hnRNPD, and AUF1/hnRNPD [Kedersha et al, 2002] are excluded from P-bodies, indicating 3'→5' decay may occur at a different site compared to the 5'→3' decay [Wilusz, C. et al, 2004].

The localization of RNA binding proteins that are associated with stress granules were also analyzed by western blots (**Fig. 6-15 panel b**). Stress granules are the cytoplasmic loci, where stalled translation initiation complexes accumulate in cells that are subjected to the environmental stress. The phosphorylation of eIF2α serves as the initiator for the formation of stress granules. Hence it was surprising to find that while total eIF2α was recovered in both the nuclear and cytoplasmic fractions, phosphorylated eIF2α was found only in the nuclear fraction. eIF4E was also recovered solely in the nuclear fraction. Thus, it was hypothesized that the NE-PER Nuclear and Cytoplasmic Extraction Kit leaves the ER membrane associated proteins, including stress-granules, associated with intact nuclei. In contrast, soluble ER associated proteins, such as BiP, were released into the cytoplasmic fraction.

6.14 Immunostaining

Based on the western analysis of the distribution of the RNA binding proteins in the nuclear and cytoplasmic fractions, it became imperative to determine the localization of ζ-cryst. Hence immunostaining experiments were performed using ζ-cryst antibody and Hoechst stain to identify the nucleus (**Fig. 6-16**). Immunostaining of WKPT-ζ^+ cells grown with normal medium revealed that ζ-cryst is localized to both the nucleus and the cytoplasm, with the majority of the ζ-cryst present in the cytoplasm. A closer examination of the data revealed that a small population of ζ-cryst was clustered into cytoplasmic loci near the nucleus. Further experiments were performed to identify the peri-nuclear cytoplasmic loci where ζ-cryst localizes.

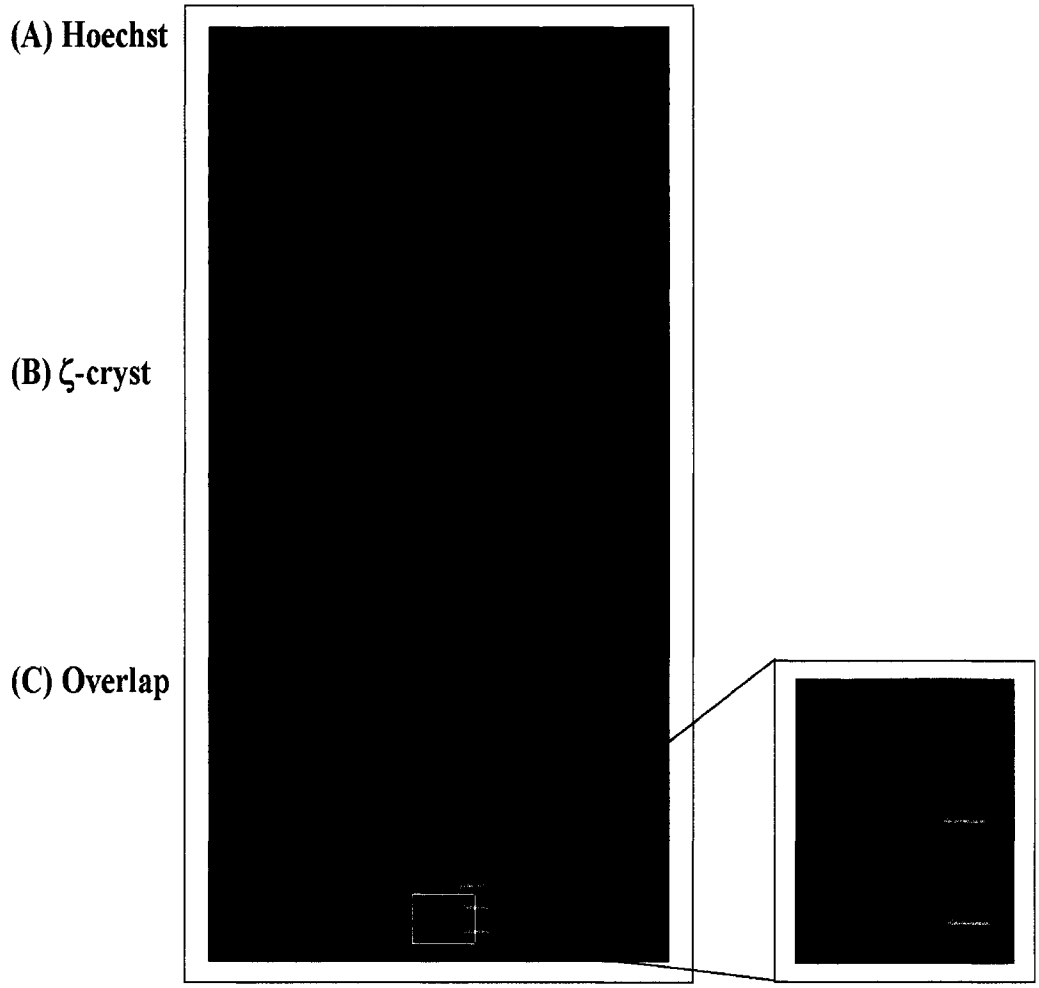

Fig. 6-16 Subcellular localization of ζ-cryst. WKPT-ζ^+ cells were grown in normal medium and then subjected to immunostaining using ζ-cryst antibody and the nuclear Hoechst stain. **(panel a)** Hoechst, **(panel b)** ζ-cryst antibody, and **(panel c)** merged image. ζ-cryst was present in both the nucleus and the cytoplasm.

The proximity to the nucleus suggested that the cytoplasmic loci might be stress granules. Hence, antibodies against ζ-cryst, total eIF2α, and phospho-eIF2α were used in immunostaining experiments along with the ER-tracker Blue/White DPX staining dye to examine if phospho-eIF2α and ζ-cryst may co-localize in stress granules. WKPT-ζ^+ cells were grown with normal medium, or treated with acidic medium for 2 h, 24 h, and for 5 d.

Immunostaining experiments (**Fig. 6-17**) using antibodies against ζ-cryst and total eIF2α revealed that ζ-cryst co-localized with total eIF2α within 24 h of treatment with acidic medium. The ER-tracker staining dye revealed that ζ-cryst and total eIF2α colocalize to the surface of the ER where stress granules are formed. Thus, metabolic acidosis may activate the ER stress signaling pathway. When treated for 5 d with acidic medium, ζ-cryst appeared to diffuse out of the stress granules and was again distributed in the cytoplasm. In contrast, total eIF2α localized in stress granules even after 5 d of treatment with acidic medium.

As a control, immunostaining experiments were performed using antibodies against total eIF2α and phospho-eIF2α along with the ER-tracker Blue/White dye in WKPT-ζ^+ cells that had been grown in normal medium or treated with acidic medium for 2 h, 24 h, and for 5 d (**Fig. 6-18**). Phosphorylation of eIF2α and its localization in stress granules was observed within 24 h of treatment with acidic medium. The stress granules detected with the total eIF2α antibody co-localized with phospho-eIF2α. This co-localization was evident even after 5 d in acidic medium. Thus, the transfer of WKPT-ζ^+ cells to pH 6.9 medium activates the ER stress signaling pathway that results in the initial but transient association of ζ-cryst with stress granules.

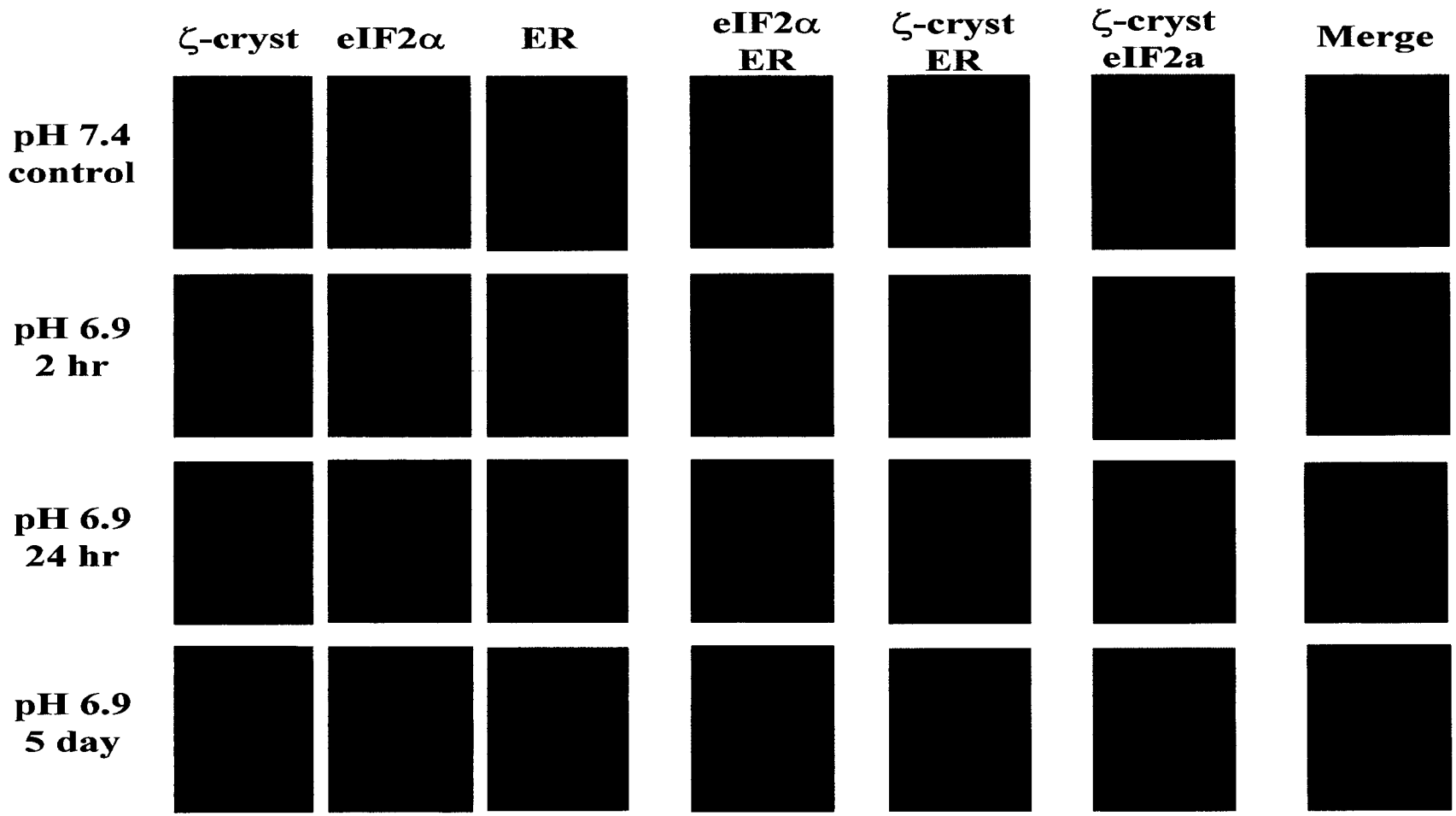

Fig. 6-17 Co-localization of ζ-cryst and eIF2α in stress granules. WKPT-ζ^+ cells were grown in normal medium (pH 7.4, 25 mM HCO_3^-) or treated with acidic medium (pH 6.9, 10 mM HCO_3^-) for 2 h, 24 h, and 5 d. Immunostaining was performed using ζ-cryst and total eIF2α antibodies along with the ER-tracker Blue/White DPX dye. ζ-cryst and eIF2α co-localized in stress granules after 24 h of acidic medium treatment.

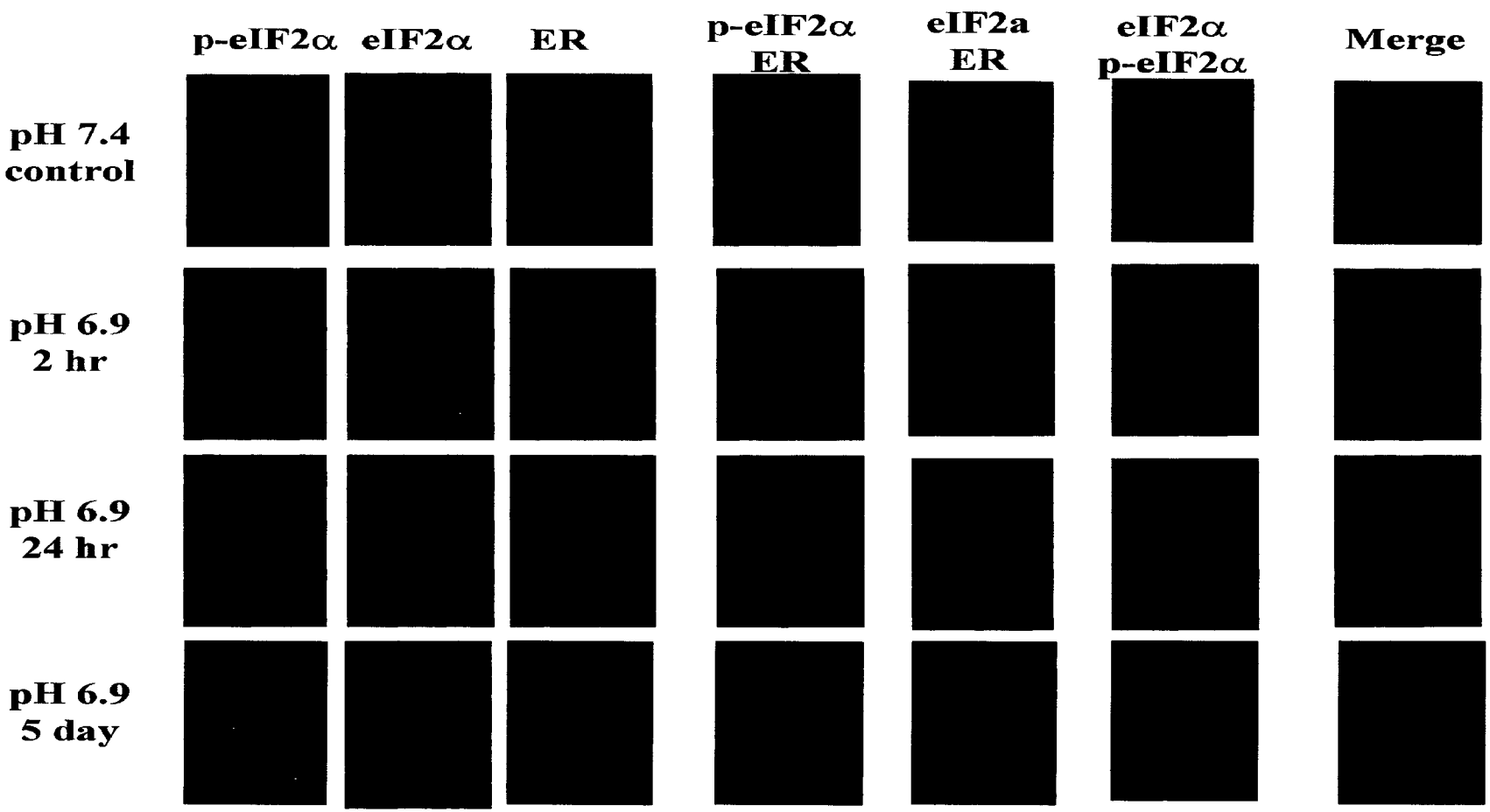

Fig. 6-18 Co-localization of phospho-eIF2α and total eIF2α in stress granules. WKPT-ζ^+ cells were grown in normal medium (pH 7.4, 25 mM HCO_3^-) or treated with acidic medium (pH 6.9, 10 mM HCO_3^-) for 2 h, 24 h, and 5 d. Immunostaining was performed using phospho- and total- eIF2α antibodies, along with the ER-tracker Blue/White DPX dye. Phosphorylated eIF2α localized in stress granules after 24 h of treatment with acidic medium, and was unchanged with prolonged (5 d) treatment with acidic medium.

6.15 Phophoprotein purfication

ARE binding proteins that contain nuclear-cytoplasmic shuttling activity are frequently regulated by post-translational modification. For example, MK2 phosphorylation of TTP results in the assembly of TTP:14-3-3 complexes that causes the exclusion of TTP from stress granules and inhibits TTP-dependent degradation of ARE-containing transcripts [Anderson et al, 2004]. Brf1, a homolog of TTP, was also shown to bind to the 14-3-3-β isoform in a phosphorylation-dependent manner [Schmidlin et al, 2004], whereas the interaction of p37-AUF1 with the 14-3-3-α isoform was found to be phosphorylation-independent [He et al, 2006]. It is not known if ζ-cryst also interacts with a member 14-3-3 family to regulate its subcellular localization o. Previous 2D gel analysis performed by H. Ibrahim (Ph.D. Thesis) indicated that ζ-cryst exists in multiple isoforms, indicating that it may be post-translationally modified.

The potential phosphorylation of ζ-cryst was assessed using the Qiagen PhosphoProtein Purification Kit. Extracts of WKPT-ζ^+ cells, that were grown in normal medium or transferred to acidic medium for 24 h, were separated into phosphorylated and unphosphorylated fractions. This experiment revealed that ζ-cryst is not a phosphoprotein, since ζ-cryst was recovered only in the unphosphorylated fraction (**Fig. 6-19**). By contrast, the majority of Brf2, detected using Brf1 antibody, was found to be in the phosphorylated fraction. AUF1 and HuR were found in both the phosphorylated and unphosphorylated fractions. It is interesting to note that phosphorylation of HuR may be increased following treatment with acidic medium. Potential conclusions from this data are speculative. Thus, further experiments need to be performed to determine the

potential role of phosphorylation of HuR and its possible association with 14-3-3 family protein in the stabilization of GA mRNA during metabolic acidosis.

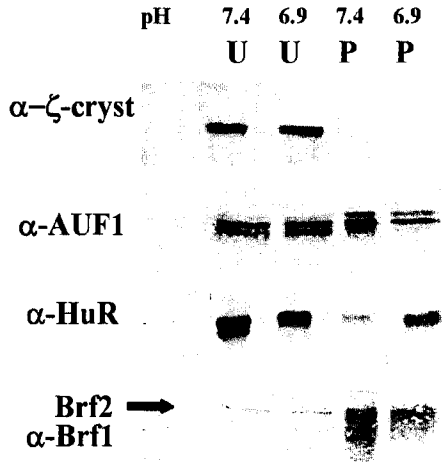

Fig. 6-19 Detection of Phosphoproteins. The PhosphoProtein Purification Kit was used to separate the phosphorylated and unphosphorylated protein fractions from WKPT-ζ^+ cell extracts. 30 μg of recovered samples were resolved on a 10% SDS-denaturing gel. Antibodies to ζ-cryst, AUF1, HuR, and Brf1 (which recognized both Brf1 and Brf2) were utilized to determine whether the proteins were post-translationally modified by phosphorylation.

CHAPTER 7

IN VITRO DEADENYLATION AND DECAY OF PEPCK mRNA REPORTER CONSTRUCTS

7.1 Cloning of pGemPCK6/7-A_{60} and pGemPCK6/7-A_0

Previous experiments using a tet-regulated promoter system demonstrated that the 3' UTR of the PEPCK mRNA contains multiple instability elements [Hajarnis et al, 2006] These findings were physiologically significant since the adaptive increase in PEPCK mRNA during metabolic acidosis is mediated by increased transcription and stabilization of PEPCK mRNA. AUF1 was shown to bind with high affinity and specificity to the PCK-2, PCK-6 and PCK-7 segments of the 3' UTR that contributed to the rapid turnover of the PEPCK mRNA. It was also determined that the primary destabilizing elements were located within the PCK6/7 segment that constituted the final 73-nt of the PEPCK 3'-UTR.

The 73-nt segment containing the AU- and CU-rich PCK6/7 RNA ($^{5'}$GTACCGTATGTTTAAATTATTTTTATACACTGCCCTTTCTTACCTTTCTTTAC ATAATTGAAATAGGTATCCTGACCAG$^{3'}$) was cloned into the XbaI site of pGem-A_0 and pGem-A_{60} vectors to yield pGemPCK-A_0 and pGemPCK-A_{60}, respectively (**Fig. 7-1**). pGemPCK-A_{60} was digested with SspI restriction enzyme to generate a DNA template that encodes the 60-nt poly-A tail. pGemPCK-A_0 was digested with HindIII restriction enzyme to generate a DNA template without a poly-A tail. The templates were transcribed using SP6 RNA polymerase in the presence of [α-^{32}P]-UTP and 500 μM ^{7met}GpppG to produce capped mRNAs that either lack or contain a 60-nt poly-A tail.

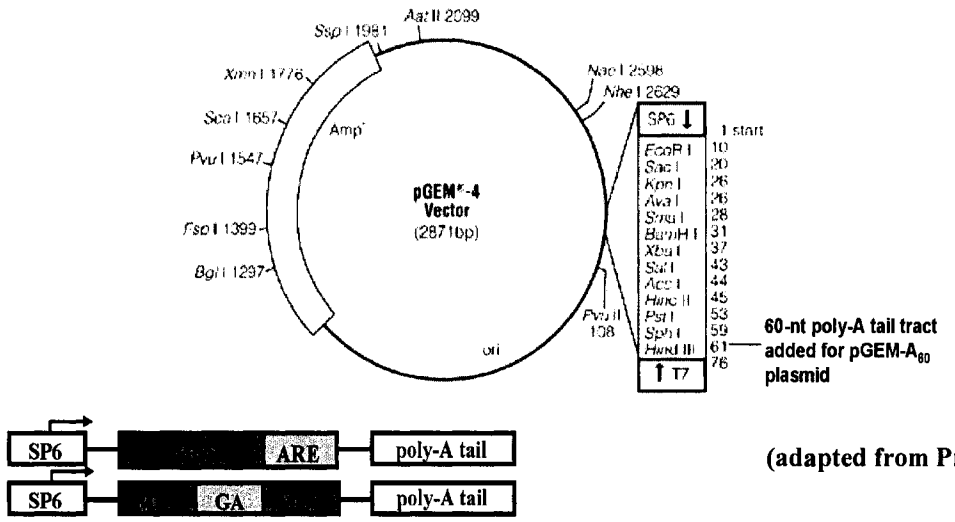

(adapted from Promega)

PCK6/7: 5'-GUAUGUUUAAAUU<u>AUUUUUA</u>UACACUGC<u>CCUUUCUUA</u><u>CCUUUCUUU</u>

<u>ACAUAAUUG</u>AAAUAGGUAUCCUGACCA-3'

By Sarah Lee

Fig. 7-1 Cloning of pGemPCK6/7-A_{60} and pGemPCK6/7-A_0. A 73-nt segment containing the AU- and CU-rich region of the PEPCK mRNA was cloned into the pGem-A_0 and pGem-A_{60} vectors. The two plasmids were transcribed in the presence of [α-^{32}P]UTP and 500 μM ^{7met}GpppG to produce mRNAs that either lack or contain a 60-nt poly-A tail. The GemPCK6/7-A_{60} mRNA was used as the substrate for an *in vitro* mRNA deadenylation assay.

7.2 Development of *in vitro* deadenylation assay

Purified recombinant ARE-binding proteins were added to the *in vitro* deadenylation assay, in the absence or presence of poly-A RNA, to determine their effect on the turnover of the GemPCK6/7-A_{60} mRNA. The *in vitro* deadenylation of the GemPCK6/7-A_{60} RNA was first analyzed using S100 cytoplasmic extracts of LLC-PK_1-F^+ cells, because the previous experiments using a tet-regulated promoter system to identify the instability elements within PEPCK 3' UTR were performed in LLC-PK_1-F^+ cells. In the presence of 16 μg of LLC-PK_1-F^+ S100 extract and poly-A RNA, the GemPCK6/7-A_{60} substrate was degraded in 10 min without accumulation of the deadenylated product (**Fig. 7-2**). Different conditions were tested to optimize the decay assay, including titration of various amounts of poly-A RNA, varying $MgCl_2$ concentration, and preparing the cytoplasmic extracts with 10 mM or 50 mM KCl. None of the conditions tested resulted in the formation of the fully deadenylated GemPCK6/7-A_0 product. Thus, it was determined that LLC-PK_1-F^+ cytoplasmic extracts were not suitable for an *in vitro* deadenylation assay for GemPCK6/7-A_{60} mRNA.

Extracts of WKPT cells, another well-characterized rat kidney proximal tubule cell line, were used previously to study the *in vitro* deadenylation of GemGA-A_{60} mRNA. Hence WKPT cell extracts were utilized to study the deadenylation and decay of GemPCK6/7-A_{60} mRNA. It should be noted that endogenous PEPCK mRNA is not detected in WKPT cells. However, the extracts may be useful to determine the effect of recombinant proteins on the PEPCK mRNA turnover.

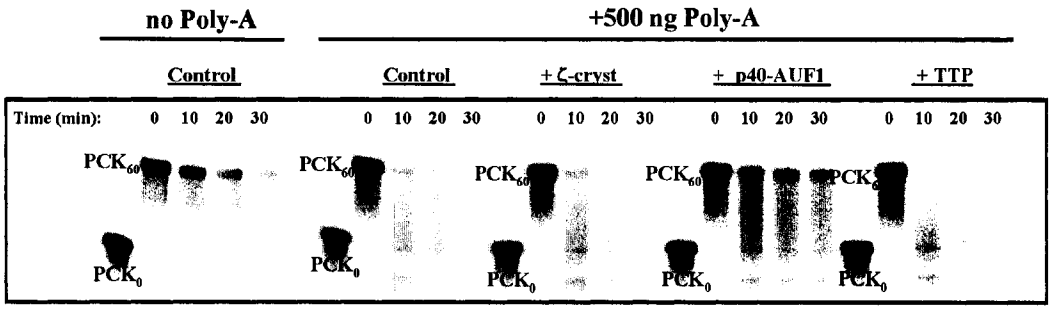

Fig. 7-2 Deadenylation and subsequent decay of the GemPCK6/7-A_{60} mRNA in LLC-PK_1-F^+ cells. The GemPCK6/7-A_{60} mRNA substrate was incubated with LLC-PK_1-F^+ S100 cytoplasmic extract for the indicated times in the absence or presence of 500 ng poly-A RNA. The reaction products were analyzed on a 5% denaturing acrylamide gel. Lack of formation of the GemPCK6/7-A_0 deadenylated product was observed.

The addition of poly-A RNA competed for the binding of poly-A binding proteins and stimulated the deadenylation of the GemPCK6/7-A_{60} RNA (**Fig. 7-3 panel a**). The addition of recombinant ζ-cryst or p40-AUF1 had little effect on the rate of decay of the GemPCK6/7-A_{60} mRNA. In addition, no accumulation of the deadenylated product was observed. Only the addition of TTP slightly stimulated the decay of the GemPCK6/7-A_{60} substrate, but again without the accumulation of deadenylated product. To determine if the deadenylated product was formed but was degraded too rapidly to accumulate, ATP and phosphocreatine (ATP/PC) were omitted from the reaction mixture. ATP is required for the catalytic activity of the exosome. Hence the omission of ATP/PC should inhibit the exosome from functioning and may lead to the accumulation of the deadenylated product of GemPCK6/7-A_{60} substrate.

Omission of ATP/PC increased the rate of decay of the GemPCK6/7-A_{60} RNA, and did result in accumulation of the deadenylated product (**Fig. 7-3 panel b**). Minimal effects of the addition of recombinant ζ-cryst and p40-AUF1 were observed on the decay pattern compared to the control. In contrast, the addition of recombinant TTP in the absence of ATP/PC resulted in accumulation of deadenylation product. Since the exosome should be non-functional in the absence of ATP/PC, this may indicate that other factors are also involved in the turnover of the GemPCK6/7-A_{60} mRNA. It is also possible that endogenous ATP present in the cell extracts allowed the exosome to function to a slight extent. Importantly, this experiment demonstrated that deadenylation and subsequent decay of GemPCK6/7-A_{60} mRNA may differ slightly from that of the GemGA-A_{60} RNA.

a.

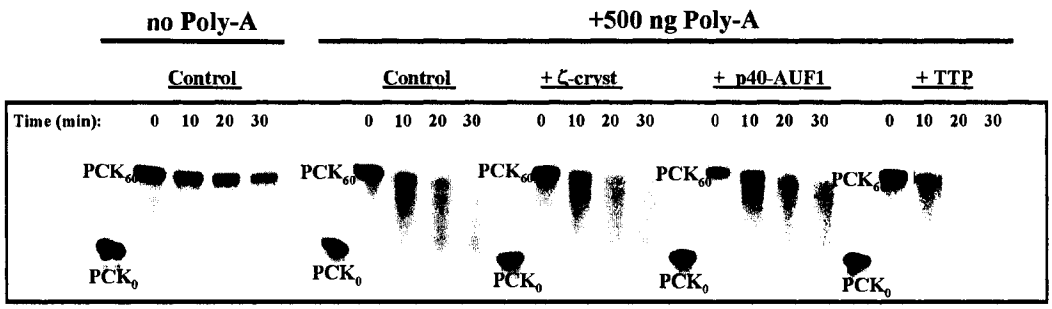

b.

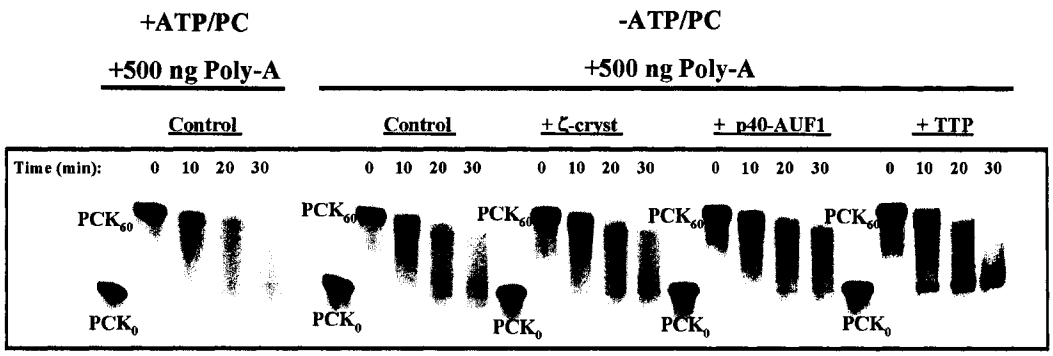

Fig. 7-3 Effect of recombinant proteins on the deadenylation and subsequent decay of the GemPCK6/7-A_{60} mRNA in the absence or presence of poly-A RNA. The GemPCK6/7-A_{60} mRNA was incubated with WKPT S100 cytoplasmic extracts for the indicated times in the absence or presence of the added recombinant proteins. The experiments were performed in the absence or presence of 500 ng Poly-A RNA and ATP/phosphocreatine (PC). The reaction products were analyzed on a 5% acrylamide-urea gel. Addition of poly-A RNA enhanced the rate of mRNA turnover. The addition of various proteins had little effect on the deadenylation and decay of the GemPCK6/7-A_{60} RNA in the presence of ATP/PC (**Panel a**). By contrast, the absence of ATP/PC decreased the rate of decay of GemPCK6/7-A_{60} RNA. Subsequent addition of TTP resulted in the accumulated of the deadenylated GemPCK6/7-A_0 product (**Panel b**).

7.3 Decay profile of GemPCK6/7-A_{60} in WKPT-ζ^+ cells

The addition of recombinant ζ-cryst in the *in vitro* deadenylation assay had little effect on the rate of deadenylation and turnover of the GemPCK6/7-A_{60} RNA. It may be possible that ζ-cryst requires a post-translational modification that occurs only in mammalian cells. In order to determine the possible role of ζ-cryst on mRNA turnover, WKPT-ζ^+ cells were tested. It was previously demonstrated that WKPT-ζ^+ cells over-express ζ-cryst by 36-fold in comparison to WKPT cells.

The GemPCK6/7-A_{60} mRNA was incubated with WKPT-ζ^+ S100 cytoplasmic extracts in the presence of 500 ng poly-A RNA, and the deadenylation pattern was compared to WKPT extracts (**Fig. 7-4**). As observed for the control substrates, Gem-A_{60} and GemARE-A_{60}, stimulation of deadenylation and accumulation of the deadenylated GemPCK6/7-A_0 product was observed in WKPT-ζ^+ cells.

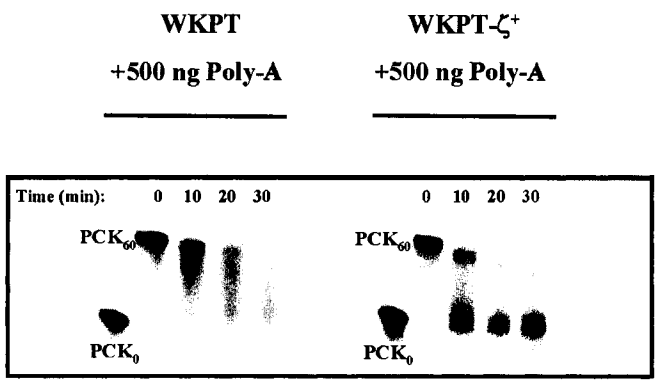

Fig. 7-4 Effect of over-expression of ζ-cryst on the deadenylation and subsequent decay of the GemPCK6/7-A_{60} mRNA in WKPT-ζ^+ cells. The GemPCK6/7-A_{60} mRNA was incubated with WKPT or WKPT-ζ^+ S100 cytoplasmic extract for the indicated time in the presence of 500 ng Poly-A RNA. The reaction products were analyzed on a 5% denaturing acrylamide gel. The deadenylation of GemPCK6/7-A_{60} was significantly enhanced in WKPT-ζ^+ cell extracts.

In the absence of poly-A RNA, the rate of decay of the GemPCK6/7-A_{60} substrate was minimal (**Fig. 7-5 panel a**). Addition of recombinant ζ-cryst did not effect on the turnover rate of GemPCK6/7-A_{60} RNA. However, a stabilizing effect of p40-AUF1 on GemPCK6/7-A_{60} RNA was observed in the absence of poly-A RNA, evidenced by a slower disappearance of GemPCK6/7-A_{60} substrate over time. The addition of recombinant TTP slightly enhanced the decay of the GemPCK6/7-A_{60} RNA as observed with WKPT cell extracts.

A significant increase in the rate of deadenylation and accumulation of the deadenylated product were observed in the presence of 500 ng poly-A RNA (**Fig. 7-5 panel b**). However, the stabilizing effect of p40-AUF1 was no longer observed. Again, the addition of TTP enhanced the accumulation of the deadenylated product. It is interesting to note that even though there was a significant increase in rate of deadenylation with the addition of poly-A RNA, the turnover process of GemPCK6/7-A_{60} mRNA was diminished as the deadenylated products were accumulated.

Surprisingly, the absence of added ATP/PC had little effect on the turnover of GemPCK6/7-A_{60} mRNA compared to that observed in the presence of ATP/PC (**Fig. 7-5 panel c**). Omission of ATP/PC should inhibit the exosome, and hence it was expected that omission of ATP/PC would result in greater accumulation of the deadenylated product. Thus, it is possible that the decay of the PEPCK mRNA occurs through decapping and a 5'→3' exonuclease activity with the processing bodies.

The experiments performed in WKPT-ζ^+ cells demonstrated that ζ-cryst may act as a destabilizing ARE binding protein, that may stimulate the turnover of mRNA. Further experiments need to be performed in order to further characterize ζ-cryst as a

possible trans-acting instability factor. Based on the results obtained through the *in* vitro deadenylation assay, TTP may act as a destabilizing trans-acting factor that may stimulate deadenylation and subsequent turnover of PEPCK mRNA. In contrast, p40-AUF1 may act as a stabilizing *trans*-acting factor to increase the stability of the PEPCK mRNA. AUF1 has been demonstrated to have a multiple roles in mRNA turnover. It functions as either stabilizing or destabilizing transacting factor. It has been suggested that differential role of AUF1 may be regulated by the relative abundance of each AUF1 isoform [Raineri et al, 2004]. Hence, the stabilizing effect of p40-AUF1 on the deadenylation and turnover of PEPCK mRNA observed in the current experiments may reflect the use of a single isoform. In addition, the bacterially expressed recombinant p40-AUF1 lacks potential post-translational modifications. Therefore, the stabilizing effect of p40-AUF1 may solely reflect the effect of over-expression of unphosphorylated p40-AUF1. Overall, these experiments demonstrate that the *in vitro* deadenylation assay can be used to characterize the role of ARE binding proteins on the deadenylation and turnover rate of PEPCK mRNA and the stabilization of PEPCK mRNA during metabolic acidosis.

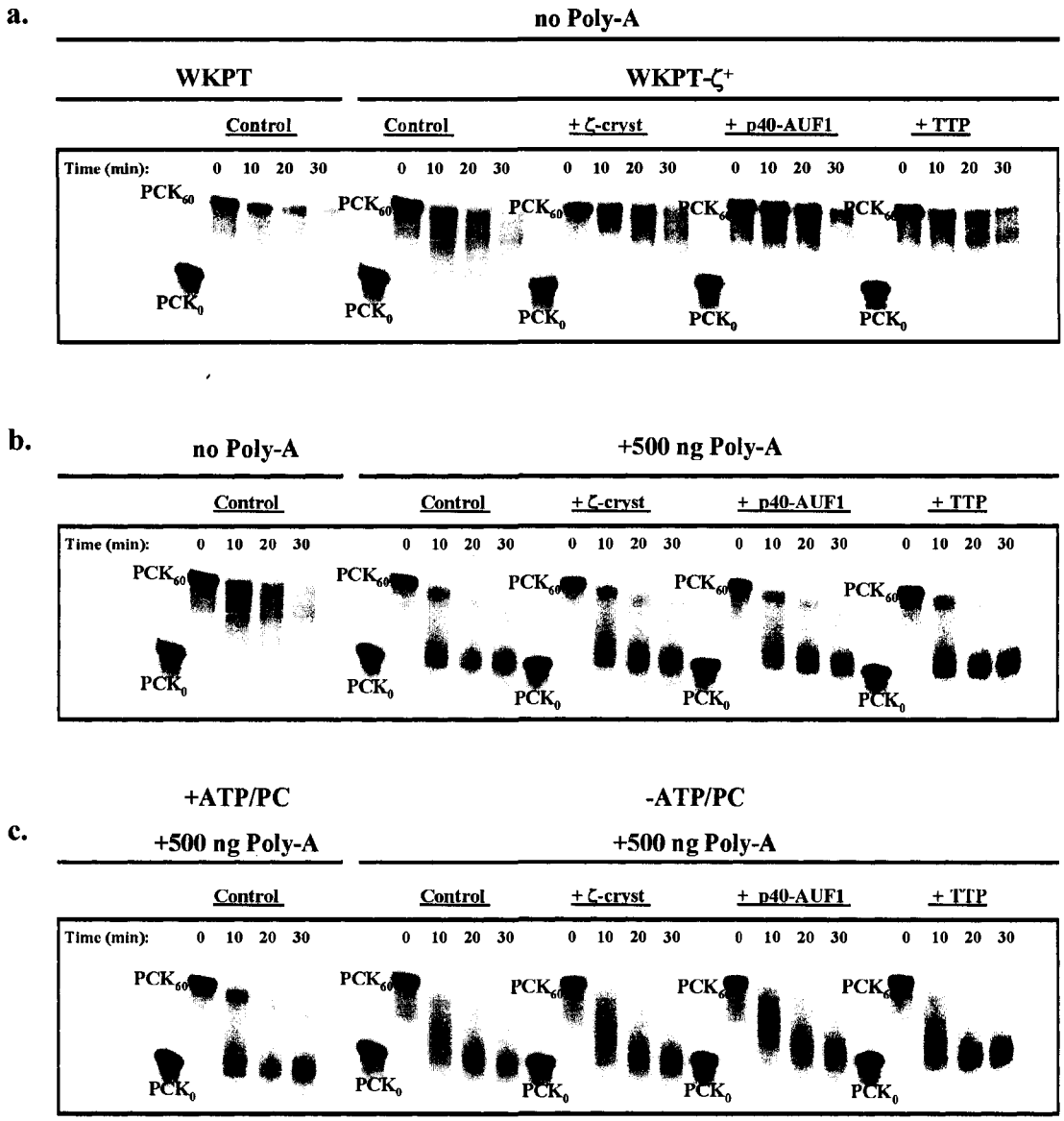

Fig. 7-5 Effect of recombinant proteins on the deadenylation and subsequent decay of the GemPCK6/7-A_{60} in WKPT-ζ^+ cells. The GemPCK6/7-A_{60} RNA was incubated with WKPT-ζ^+ S100 cytoplasmic extract for the indicated times in the absence or presence of the added recombinant proteins. The experiments were performed in the absence or presence of 500 ng poly-A RNA and of ATP/phosphocreatine (PC). The reaction products were analyzed on a 5% denaturing acrylamide gel. The deadenylation and subsequent decay of GemPCK6/7-A_{60} was significantly enhanced in WKPT-ζ^+ cells. The addition of p40-AUF1 stabilized GemPCK6/7-A_{60} mRNA in the absence of poly-A RNA (**Panel a**). By contrast, with addition of poly-A RNA the addition of TTP enhanced the accumulation of deadenylated product of the GemPCK6/7-A_{60} RNA (**Panel b and c**). The omission of ATP/PC had little or no effect on the accumulation of the deadenylated product (**Panel c**).

CHAPTER 8

DISCUSSION AND FUTURE DIRECTIONS

The mitochondrial glutaminase (GA) catalyzes the initial reaction in the renal catabolism of glutamine and is a key regulator of the increased renal ammoniagenesis and gluconeogenesis that occur in response to metabolic acidosis. Glutamine is extracted by the kidney and then deamidated and deaminated to yield two ammonium ions. The resulting increase in ammonium ion excretion conserves sodium and potassium ions and partially compensates the systemic acidosis. During chronic acidosis, this adaptive response is sustained by increased expression of the mitochondrial GA that results from selective stabilization of the GA mRNA [Curthoys et al, 2001].

Previous experiments identified an 8-base AU-sequence (UUAAAAUA or UUUAAAUA) within the 3'-UTR of the GA mRNA, which functions as a pH-response element (pHRE) in a chimeric reportor mRNA [Laterza et al , 1997]. This AU-sequence was used as an affinity ligand to purify and identify ζ-crystallin/NADPH:quinone reductase (ζ-cryst) as a pHRE-binding protein [Tang et al, 2001]. Recent experiments also demonstrated that p40-AUF1, a known ARE binding protein, binds to the pHRE with high affinity and specificity [Schroeder et al, 2006]. Hence, it was imperative to investigate the role of these ARE binding proteins in the stabilization of GA mRNA during metabolic acidosis.

The rate of mRNA turnover is determined by the presence of *cis*-acting elements within the mRNA, including the 5'-^{7met}guanosine cap, stem-loop structures, AU-rich elements (AREs), and the poly-A tail. Stabilization or destabilization of the transcript is

regulated by *trans*-acting factors, usually mRNA binding proteins, that interact with the cis-acting elements [Ross, 1995]. Specific AU-rich elements within the coding sequence or the 3'-UTR of the mRNA function as stability or instability elements [Chen, C-Y et al, 1995]. Under certain conditions, the AREs recruit proteins that remove the poly-A binding proteins and enhance 3'-deadenylation, which leads to rapid 3'→5' exonucleolytic degradation by the exosome [Mukherjee et al, 2002]. Alternatively, deadenylation can promote decapping and 5'→3' exonucleolytic degradation within processing bodies [van Dijk et al, 2002]. The AU-rich elements can also prevent the turnover of an mRNA if they recruit ARE binding proteins that act as stabilizing trans-acting factors. Alternatively, the turnover of mRNAs may be initiated by a site-specific endonucleolytic cleavage, which generates sites for rapid exonucleolytic degradation [Wang et al, 2000].

In order to identify the *trans*-acting factors that regulate GA mRNA turnover and stabilization, a 28-bp fragment, containing a direct repeat of the two AREs from the 3'-UTR of the GA mRNA, was cloned into a β-globin reporter construct. Analysis of this construct and various mutant constructs demonstrated that the individual pHREs were both necessary and sufficient to impart a pH-response stabilization [Laterza et al, 2000]. In order to characterize the role of ARE binding proteins in stabilization and turnover of GA mRNA, an *in vitro* deadenylation assay was used to compare the rates of deadenylation and degradation of the GA mRNA. Cytoplasmic extracts from rat WKPT and porcine LLC-PK_1-F^+, two lines of renal proximal tubule cells, were analyzed.

As controls, Gem-A_{60} and GemARE-A_{60} substrates were utilized in the *in vitro* deadenylation assay. The Gem-A_{60} mRNA contains a 5' cap and a 60-nt poly-A tail.

The GemARE-A_{60} mRNA additionally contains the AU-rich element from TNF-α mRNA. The *in vitro* deadenylation assay was initially developed with Gem-A_{60} and GemARE-A_{60} mRNAs using S100 cytoplasmic extracts of LLC-PK_1-F^+. The reactions were optimized by titrating different amounts of poly-A RNA, by varying the $MgCl_2$ concentration, and by preparing the cytoplasmic extracts using different KCl concentrations. In all of the conditions tested, the LLC-PK_1-F^+ extracts produced a relatively rapid but non-specific decay that failed to produce the fully deadenylated Gem-A_0 or GemARE-A_0 RNA, even as a transient intermediate. The reaction time was increased to 90 min, without observation of the deadenylated product. Therefore, the LLC-PK_1-F^+ cells may express a non-specific RNase that is not inhibited by RNasin or other general RNase inhibitors that were tested.

Hence WKPT, another line of renal proximal tubules cells, were utilized in the *in vitro* deadenylation assay. In contrast to the results obtained with the LLC-PK_1-F^+ extracts, progressive deadenylation and formation of the fully deadenylated product was observed using WKPT extracts. Therefore, the WKPT cells must express sufficient levels of the *trans*-acting factors that regulate mRNA turnover and are necessary to reproduce the deadenylation process in *in vitro*. Therefore, it was important to establish if the WKPT cells lines are a pH-responsive line of renal proximal tubules, prior to performing a detailed molecular analysis of the mechanism mediating the enhanced expression of the GA gene during the onset of metabolic acidosis.

The induction of the endogenous kidney-type GA mRNA was measured using real-time RT-PCR to analyze RNA isolated from WKPT and LLC-PK_1-F^+ cells. Both cell lines expresses a 4.5-kb GAC mRNA and a 5.0-kb KGA mRNA. In the rat, both GA

mRNAs contain one or more pHREs, whereas in the pig only the GAC isoform is pH-responsive [Porter et al, 2002]. A quantitative real-time RT-PCR assay was developed using specific primer sets and differentially labeled Taqman probes to quantify the different kidney-type GA mRNA in LLC-PK_1-F^+ cells. Total RNA harvested on different days post split demonstrated that expression of the GAC mRNA was increased 2-fold, but only when 2-d post split LLC-PK_1-F^+ cells were transferred to acidic medium for 24 h. The analysis of the WKPT cells harvested at different stages of confluency demonstrated that both KGA (1.9-fold) and GAC (1.5-fold) mRNAs are increased when subconfluent (25%) cells are transferred to acidic medium for 24 h. Additionally, real-time RT-PCR analysis of RNA from WKPT cells following prolonged treatment with acidic medium demonstrated a pronounced and reproducible increase in KGA mRNA. The WKPT cells transferred to acidic medium for 4 or 5 d demonstrated a 1.9-fold induction of KGA mRNA. This correlated with the observation that the rat renal GA mRNA and activity are increased gradually and reached a plateau after 7 days of acidosis [Curthoys et al, 1995]. Hence prolonged treatment of WKPT cells may reflect the physiological changes of renal GA mRNA that occurs in rat kidneys during metabolic acidosis. On the other hand, the GAC isoform of rat kidney-type GA mRNA did not exhibit a pH-responsive increase following prolonged treatment of WKPT cells with acidic medium. Preliminary experiments using antibodies that are specific for the GAC isoform indicate that this protein is not up-regulated in rat kidney during acidosis [T. Bacon, unpublished data].

Once WKPT cells were established as a pH-responsive renal proximal tubule cell line, western blot analysis was performed to characterize the distribution of various ARE

binding proteins and proteins that were known to be involved in mRNA turnover process. WKPT and WKPT-ζ^+ cells were treated with normal medium (pH 7.4, 25 mM HCO_3^-) or acidic medium (pH 6.9, 10 mM HCO_3^-) for 24 h before harvesting, and S10 post-nuclear or S100 cytoplasmic extracts were prepared. WKPT-ζ^+ cells over-express ζ-cryst by 36-fold in comparison to wild type WKPT cells. Although the levels of many of proteins were nearly identical in the two extracts, there were some exceptions to this finding. For example, HuR was primarily recovered in the S10 post-nuclear extracts, which is likely to include the stress granules and P-bodies, complexes that have M_r >500 kDa. It was also interesting to find that higher amounts of Brf1 and Brf2 were present in cells grown with normal than acidic medium, suggesting that the two proteins may be pH-responsive. Western blots also indicated that Dcp1a and Pm/Scl-75 were expressed at a higher level in cells grown in normal medium compared to cells treated with pH 6.9 medium. These observations are consistent with a higher rate of RNA turnover for general mRNA during normal acid-base balance. It was also interesting to note that under acidic conditions, there may be a diminished level of cap-dependent translation of some proteins due to the decreased level of eIF4E and the increased level of phosphorylated PARN to bind to the 5'-cap. However, it was previously demonstrated that the stabilization of GA mRNA under acidotic condition is not due to changes in its rate of translation [Tong et al, 1987]. Thus, the possible decrease in cap-dependent translation may effect other mRNAs in WKPT cells, but may exclude the translation of GA mRNA.

Once the steady state levels of the RNA binding proteins were determined, RNA electrophoretic mobility shift and *in vitro* deadenylation assays were used to characterize the role of ARE binding proteins in the regulation of GA mRNA deadenylation and

subsequent turnover. A 28-nt segment of containing the pHRE of GA mRNA ($^{5'}$CTAGTGCTAGCTC**TTTAAATA**AA**TTAAAATA**ATTACTAAT$^{3'}$) was cloned into the pGem-A_0 and pGem-A_{60} vectors to yield pGemGA-A_0 and pGemGA-A_{60}, respectively. When transcribed using SP6 RNA polymerase in the presence of [α-^{32}P]-UTP and 500 μM ^{7met}GppG, the plasmids produced capped mRNAs that either lack or contain a 60-nt poly-A tail.

Previous RNA electrophoretic mobility shift assays (EMSA) were performed, using S100 cytoplasmic extracts prepared from rat kidney cortex and LLC-PK_1-F^+ cells. Since the WKPT cells line was demonstrated to be pH-responsive rat proximal tubule cells, it was important to test whether the cytoplasmic extracts of WKPT cells also contain the various pHRE binding proteins. RNA-EMSA demonstrated the presence of pHRE binding proteins in both the S10 post-nuclear and S100 cytoplasmic extracts of WKPT and WKPT-ζ^+ cells. In order to determine the specific pHRE binding proteins expressed in WKPT-ζ^+ cells, antibodies to known RNA-binding proteins were used in a RNA gel super-shift assay. Pre-incubation of S10 post-nuclear extracts from WKPT-ζ^+ cells with ζ-cryst and HuR antibodies resulted in RNA:protein complexes that were retained in the wells. However, super-shifted RNA:protein complexes were observed for the addition of AUF1 and TTP antibodies. In contrast, antibody against Brf1 had little effect on the RNA:protein complex formation. This experiment demonstrated the pHRE binding protein complexes may contain ζ-cryst, AUF1, TTP, and HuR. It was previously demonstrated that the pHRE binds ζ-cryst and AUF1 in LLC-PK_1-F^+ extracts with high affinity and specificity [Tang et al, 2001; Schroeder et al, 2006]. The reported experiments demonstrate that these proteins are also present in WKPT extracts and bind

to the pHRE. More importantly, this was the first demonstration that TTP and HuR, two well-characterized ARE binding proteins, also bind to the pHRE of the GA mRNA. This was significant because TTP is a well-characterized destabilizing *trans*-acting factor [Carballo et al, 1998; Raghavan et al, 2001; Sully, G. et al, 2004], while HuR is known to be a stabilizing *trans*-acting factor [Fan et al, 1998; Dean et al, 2001; Ming et al, 2001; Sully et al, 2004].

To test the hypothesis that TTP and HuR may also bind to the pHRE of the GA mRNA, $(His)_6$-tagged recombinant TTP and HuR were purified using Nickel column chromatography and tested in RNA gel shift assay using capped GemGA-A_0 mRNA as the substrate. As a control, the binding of recombinant ζ-cryst and p40-AUF1 were also performed. The gel shift assays demonstrated that indeed ζ-cryst, p40-AUF1, TTP, and HuR bind to the pHRE of the GA mRNA. The gel shift assays were performed in the absence of EDTA in the running buffers, since EDTA may chelate Zn^{+2} and disrupt the zinc-binding motifs of the proteins [Nyborg and Peersen, 2004]. In fact, the RNA:TTP interaction is abolished with the addition of EDTA to the gel running buffer. Therefore, these results suggest zinc-binding motif of TTP [Carballo et al, 1998] is necessary for the RNA binding. However, the RNA:ζ-cryst interaction is not affected by addition of EDTA. ζ-cryst is a member of Zn^{+2} containing alcohol dehydrogenase family [Jornvall et al, 1993], but lacks the CCCH zinc finger domain found in ARE binding proteins such as TTP, Brf1, and Brf2.

Competition assays were performed to determine if the ARE-binding proteins share the same binding site or bind to different binding sites within the pHRE of GA mRNA. The competition assays indicated that ζ-cryst and TTP bind to the same binding

site. However, ζ-cryst and p40-AUF1 did not compete for binding, and hence may bind to different sites within the GemGA-A_0 mRNA.

The RNA gel shift assays produced several additional insights and conclusions. It was interesting to note that capped and uncapped GemGA-A_0 mRNA formatted different complexes with p40-AUF1. This suggested that p40-AUF1 may interact with the cap structure when it is bound to an AU-rich element. Hence, increasing amounts of cap analog were titrated into the binding reaction with the purified recombinant proteins. This experiment indicated that ζ-cryst and p40-AUF1 may interact with the 5'-cap structure.

The gel shift analysis demonstrated that multiple ARE binding proteins can bind to the pHRE. However, RNA gel shift analysis only determines the binding affinity and specificity of the ARE binding proteins to the pHRE. Hence, it was important to further characterize the role of the individual ARE binding proteins in the regulation of GA mRNA turnover. The *in vitro* deadenylation assay was developed to characterize the effect of each ARE binding protein on the rate of deadenylation and decay of the GemGA-A_{60} mRNA.

In vitro deadenylation was performed in the absence or presence of 0.86 μM ζ-cryst, 0.79 μM p40-AUF1, 0.20 μM TTP, or 0.63 μM HuR. Minimal deadenylation and turnover of GemGA-A_{60} mRNA observed in WKPT cell extracts in the absence or presence of poly-A RNA. In contrast, a significant increase in the rate of deadenylation and turnover of GemGA-A_{60} mRNA was observed in WKPT-ζ^+ cells. The stabilizing effects of p40-AUF1 and HuR on the deadenylation and subsequent turnover of GemGA-A_{60} mRNA were observed in the absence of poly-A RNA. The addition of poly-A RNA

stimulated the deadenylation and turnover of the GemGA-A_{60} mRNA. Addition of TTP also enhanced the rates of deadenylation and decay of GemGA-A_{60} mRNA in either the absence or presence of added poly-A RNA. These experiments demonstrated that HuR and p40-AUF1 may act as stabilizing *trans*-acting factors that regulate of GA mRNA deadenylation and turnover, while TTP and ζ-cryst may function as destabilizing *trans*-acting factors.

The *in vitro* deadenylation assay was also used to investigate whether the exosome may play a role in the turnover process of GemGA-A_{60} mRNA. ATP is required for the catalytic activity of the exosome, hence the omission of ATP/PC should inhibit the function of the exosome and cause accumulation of the deadenylated product of the GemGA-A_{60} mRNA. With the omission of ATP/PC, accumulation of the deadenylated product, GemGA-A_0 mRNA, was observed. This effect was most apparent with addition of TTP to the reaction. Therefore, the *in vitro* deadenylation assay demonstrated that the turnover of GemGA-A_{60} mRNA involves deadenylation and possibly followed by subsequent 3'→5' decay pathway. Therefore, the exosome may participate in the turnover of the deadenylated GA mRNA.

At least four different deadenylases have been identified, including Pan2 and Pan3, CCR4 and nocturnin, CAF1, and PARN. Pan2 and Pan 3 are cytoplasmic deadenylases that are activated by Pab1p [Uchida et al, 2004]. Pan2 has an intrinsic 3'→5' exoribonuclease activity and requires Mg^{+2} for the enzyme activity, whereas Pan3 interacts with PABP to simulate Pan2 nuclease activity. This complex is thought to participate in the initial shortening of long poly-A tails. CCR4 and nocturnin complexes have been shown to have a distinct spatial and temporal expression from PARN and are

localized in P-bodies [Baggs et al, 2003]. CAF1 is a component of the CCR4 and nocturnin complex, that has 3'→5'exoribonulcease activity with a preference for poly-A substrates in *in vitro* assays. However, in yeast the deadenylase function of CAF1 is not required for poly-A removal [Viswanathan et al, 2004]. PARN is a cap-dependent deadenylase [Dehlin et al, 2000] that has been shown to be modulated by ARE-binding proteins [Lai et al, 2003]. In order to test whether PARN was the deadenylase responsible for the deadenylation process in WKPT-ζ^+ extracts, cap analog was titrated into the deadenylation reaction mixture. Deadenylation was inhibited by the addition of cap analog, indicating that the observed deadenylation is cap-dependent and that PARN contributes to the 3'→5' decay in WKPT-ζ^+ cell extracts.

The role of poly-A binding proteins in the deadenylation process was also demonstrated by adding increasing amounts of cap analog in the absence or presence of poly-A RNA. Without the addition of poly-A RNA, the rate of deadenylation is slow and the intermediates of the deadenylation process accumulate gradually over 30 min. The addition of cap analog decreased the rate of deadenylation, even in the absence of poly-A RNA polymers, again indicating that PARN is responsible for the deadenylation observed in WKPT-ζ^+ cell extracts.

In order to investigate whether the stabilization of GA mRNA during metabolic acidosis is due to a slower deadenylation rate of GA mRNA, WKPT and WKPT-ζ^+ cells were treated with either normal or acidic medium for 24 h. A significant increase in the deadenylation and turnover rate was observed in WKTP-ζ^+ cell extracts compared to WKTP extracts. However, the rate of deadenylation of the GemGA-A_{60} mRNA occurred at comparable rates in pH 6.9 extracts compared to pH 7.4 extracts. This observation

suggests that the recruitment of stabilizing ARE binding proteins, and not changes in the rate of deadenylation, may be the rate determining factor that leads to stabilization of the GA mRNA during metabolic acidosis. Alternatively, factors that contribute to the pH-responsive stabilization are modified or not retained in an activated form when extracts are prepared.

Recently, processing–bodies (P-bodies) have been identified as the cytoplasmic loci that contains the decapping enzymes [Ingelfinger et al, 2002], Xrn1 (5'→3' exonuclease) [Bashkirov et al, 1997], and Lsm1-7 heptamers [Ingelfinger et al, 2002]. ARE binding proteins such as HuR [Anderson et al, 2006], TTP [Stoecklin et al, 2004], and Brf1 [Kedersha et al, 2005] were shown to interact with both the exosome and the factors in involved in decapping and 5'→3' decay. Since TTP and HuR were shown to bind to the pHRE, it was important to investigate whether the 5'→3' decay pathway also contributed to the turnover of the GA mRNA. Several decapping products were observed in the *in vitro* decapping assay, including ^{7met}GpppG, ^{7met}GDP, ^{7met}GDP. ^{7met}GpppG is produced by 3'→5' degradation of a transcript by the exosome. Subsequently, ^{7met}GMP is produced by, DcpS, the scavenger decapping enzyme, that acts on the ^{7met}GpppG product of exosomal decay. Following deadenylation, the hydrolysis of the transcript's ^{7met}GpppG cap by Dcp1a/Dcp2 generates ^{7met}GDP. The resulting decapped transcript is then subjected to 5'→3' decay pathway by Xrn1. Addition of cap analog results in appearance of ^{7met}GpppG, by inhibiting DcpS action on the final product of the exosomal decay pathway. In addition, the decapping reaction occurred at a faster rate in S10 post-nuclear extracts than in S100 cytoplasmic extracts. This finding correlates with the previous report suggesting that the S100 cytoplasmic extracts may be deficient in the

factors involved in 5'→3' decay pathway, since protein complexes of M_r >500 kDa, including the stress granules and P-bodies are pelleted by cenfugation of at 100,000 xg [Seal et al, 2005]. The performed experiments indicate that the S100 cytoplasmic extracts do contain the protein complexes involved in 5'→3' decay pathway, but to a lesser extent compared to the S10 post-nuclear extracts. The *in vitro* decapping assay demonstrated that indeed 5'→3' decay pathway is involved in the turnover of GemGA-A_{60} mRNA, as well as 3'→5' decay pathway. Determination of whether the 5'→3' or 3'→5' decay pathway predominate *in vivo* will require further analysis.

ARE binding proteins frequently shuttle between the nucleus and the cytoplasm TTP, Brfl, and AUF1 bind to proteins of the 14-3-3 family, that function to regulate the subcellular localization of the bound proteins [Stoecklin et al, 2004; He et al, 2006]. Hence it was important to characterize the distribution of the ARE binding proteins that may be involved in GA mRNA turnover in WKPT-ζ^+ cells. Nuclear and cytoplasmic extracts were prepared using NE-PER Nuclear and Cytoplasmic Extraction Kit (Pierce) and the distribution of the ARE binding proteins were analyzed by western blot analysis. The p37, p40, p42, and p45 isoforms of AUF1 were detected in the nuclear fraction of WKPT-ζ^+ cells, while only the p37 and p40 isoforms were detected in the cytoplasmic fraction. The majority of the HuR and TTP proteins were also localized in the nuclear fraction, with minor amounts in the cytoplasmic fraction. This distribution is indicative of nuclear-cytoplasmic shuttling of the proteins. Interestingly, ζ-cryst was shown to be localized solely in the nuclear fraction, even though it was reported to be a soluble cytoplasmic protein [Wang, W. et al, 1998].

It was expected that proteins that are associated with P-bodies would localize in both nuclear and cytoplasmic fractions, depending on their shuttling activity. This was demonstrated for many of the proteins involved in the mRNA turnover, including Dcp1a, Dcp2, DcpS, PARN, and Pm/Scl-75. The proteins that may be associated with stress granules were also analyzed. The phosphorylation of eIF2α served as marker for the stress granules. Surprisingly, phosphorylated eIF2α was found only in the nuclear fraction, while total eIF2α was found in both the nuclear and cytoplasmic fractions. Therefore, the NE-PER Nuclear and Cytoplasmic Kit may leave the ER membrane intact and associated with the nuclear fraction. Hence, stress-granule-associated proteins may partition into the nuclear fraction with the intact nucleus. This may explain why known stress-granule-associated proteins such as Brf1 and phospho-eIF2α were recovered in the nuclear fraction.

Based upon the western blot analysis of the protein distribution in the nuclear and cytoplasmic fractions, it became imperative to further characterize the localization the ζ-cryst. Hence immunostaining experiments were performed using ζ-cryst antibody and Hoechst dye to stain the nucleus. Immunostaining experiments revealed that ζ-cryst was present in both the nucleus and the cytoplasm, with the majority of the ζ-cryst residing in the cytoplasm. A closer examination of the data revealed that a small proportion of ζ-cryst was clustered into cytoplasmic loci near the nucleus. Thus, further experiments were performed to identify the cytoplasmic loci that contained ζ-cryst.

Antibodies against ζ-cryst, total eIF-2α and phospho-eIF2α were used for immunostaining along with the ER-tracker Blue/White DPX staining dye to examine whether phospho-eIF2α and ζ-cryst may co-localize in stress granules. WKPT-ζ^+ cells

were grown with normal medium or treated with acidic medium for 2 h, 24 h, or 5 d, before harvesting. Immunostaining experiment using ζ-cryst and total eIF2α revealed that within 24 h of pH 6.9 treatment, ζ-cryst is localized in stress granules and co-localizes with the total eIF2α staining. Control experiment using phospho-eIF2α and total-eIF2α indicated that the cytoplasmic loci were indeed stress granules. Unfortunately, no mouse monoclonal anti-phospho-eIF2α antibody was available. Thus, it was not possible to perform co-localization of phospho-eIF2α and ζ-cryst. When treated with pH 6.9 medium for 5 d, ζ-cryst redistributed into the cytoplasm and was no longer localized in stress granules. In contrast, phospho-eIF2α and total eIF2α remained localized in stress granules even after 5 d of treatment with acidic medium. It should also be noted that activation of ER stress signaling pathway required 24 h of treatment with acidic medium, which is significantly slower than the activation of ER stress signaling pathway observed with other environmental stress conditions [Dang et al, 2006]. The finding that metabolic acidosis may trigger the ER stress signaling pathway is both novel and potentially significant. These data also indicate that ζ-cryst initially enters and then leaves the stress granules. Thus, this ARE binding protein may cause a transient arrest of translation of the GA during acute onset of acidosis. **Fig. 8-1** illustrates a possible model for the activation of ER stress signaling pathway during metabolic acidosis.

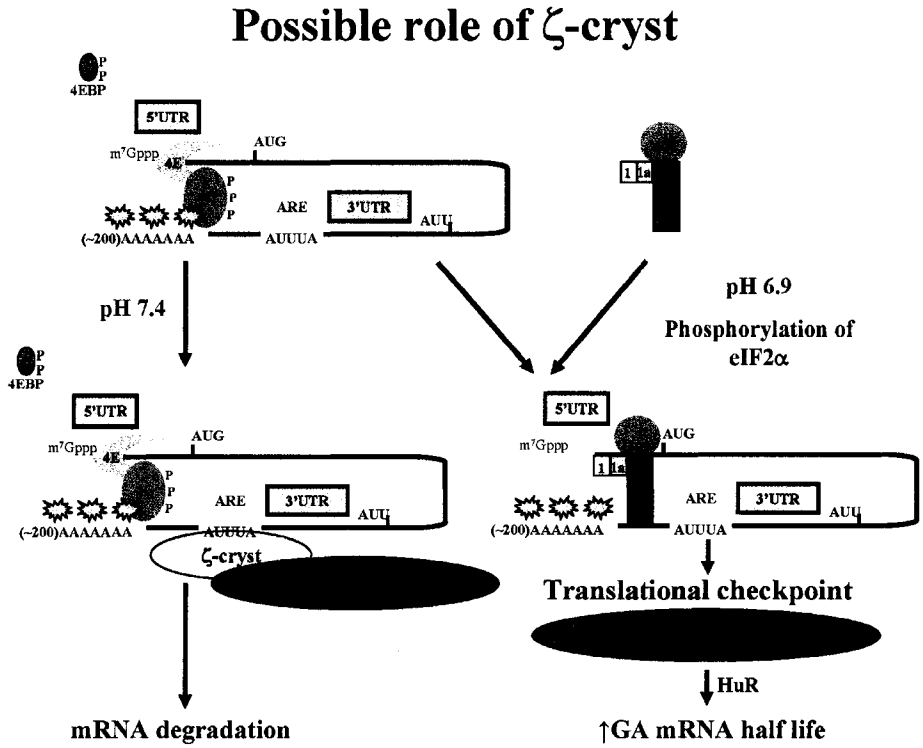

Fig. 8-1 Possible model for activation of ER stress signaling pathway during metabolic acidosis. Under normal conditions, the eIF2-GTP-tRNA^{met} ternary complex is able to form a canonical 48S preinitiation complex at the 5' end of the transcript. Binding of destabilizing ARE binding proteins to the GA mRNA, such as ζ-cryst and TTP, may recruit the machinery involved in mRNA turnover. Under metabolic acidosis, phosphorylation of eIF2α depletes eIF2-GTP-tRNA^{met}, and leads to the formation of a noncanonical 48S preinitiation complex. Binding of an unknown factor, possibly TIAR or TIA-1, recruits stalled translation-initiation complex to stress granules, where the GA mRNA may bind HuR to enhance its stability.

The completed experiments raise more questions to address in the future. Previous experiments performed in the lab using LLC-PK_1-F^+ cells showed over-expression or knock-down of ζ-cryst using siRNA had no effect on the turnover or the pH-responsive stabilization of a β-globin-GA reporter mRNA (H. Ibrahim, Ph.D. Thesis). These data indicate that ζ-cryst is not the rate limiting factor in the turnover or pH-responsive stabilization of GA mRNA. Alternatively over-expression of mouse ζ-cryst in porcine kidney proximal tubule cell lines may not elicit the appropriate response due to the lack of a required modification of the exogenous ζ-cryst. Furthermore, the knock-down of porcine ζ-cryst to 10-20 % of normal expression in LLC-PK_1-F^+ may not sufficient to block the function of the endogenous ζ-cryst. By contrast, the WKPT cells are a rat kidney proximal tubule cell line. Thus, they may contain the necessary enzymes to appropriately modify the over-expressed mouse ζ-cryst. This could explain why extracts of WKPT-ζ^+ cells that over-express mouse ζ-cryst by 36-fold exhibit an enhanced rate of deadenylation and the turnover of GemGA-A_{60} mRNA.

Since the extracts prepared from WKPT or WKPT-ζ^+ cells grown in normal or acidic medium exhibit the same rates of deadenylation and turnover of GemGA-A_{60} mRNA, the deadenylation process may not be the rate limiting steps regulating the stabilization of GA mRNA during metabolic acidosis. Hence it is hypothesized that recruitment of different ARE binding proteins to the pHRE may regulate the fate of GA mRNA. Different ARE binding proteins were tested for their role in the regulation of deadenylation and turnover process of GemGA-A_{60} mRNA. It is hypothesized at pH 6.9, stabilizing proteins such as HuR and AUF1 may bind to the pHRE of the GA mRNA and

stabilize the message, whereas under normal conditions destabilizing proteins such as ζ-cryst and TTP may preferentially bind.

In COS7 cells, activation of the MAPK-activated kinase 2 (MK2) pathway leads to the phosphorylation of TTP and assembly of a phophorlyated-TTP:14-3-3 complex that causes exclusion of TTP from stress granules and inhibits TTP-dependent degradation of ARE-containing transcripts [Stoecklin et al, 2004]. It is important to emphasize that exclusion of phospho:TTP:14:3:3 protein occurred only under FCCP-induced energy deprivation, but not arsenite-induced oxidative stress. Therefore the exclusion of the phospho-TTP:14:3:3 complex is dependent upon the nature of environmental stress. Treatment of LLC-PK_1-F^+ cells with acidic medium results in activation of the p38-MAPK and phosphorylation and activation of the downstream MK2 [O'Hayre et al, 2006]. Therefore, activation of MK2 pathway in kidney cells may lead to phosphorylation of TTP and the formation of phopho-TTP:14:3:3 complex. Hence it is important to determine if treatment with acidic medium results in formation of a phospho-TTP:14:3:3 complex and its subsequent exclusion from stress granules. Such a process could contribute to the pH-responsive stabilization of the GA mRNA.

In contrast, the nuclear-cytoplasmic shuttling of p37-AUF1 is not dependent on the phosphorylation state of AUF1. It was recently demonstrated that p37-AUF1 binding to the 14-3-3-α scaffolding protein leads to the shuttling of AUF1 to cytoplasm [He, 2006]. Hence it will be important to determine if 14-3-3-α is also responsible for the translocation of p40-AUF1, and possibly for ζ-cryst, in WKPT and WKPT-ζ^+ cells. It should also be noted that western blot analysis of the distribution of AUF1 in the nuclear and the cytoplasmic fractions indicated that the steady state distribution of AUF1 is not

altered following treatment with acidic medium. Therefore, it is unlikely that nuclear-cytoplasmic shuttling of AUF1 is responsible for the stabilization of GA mRNA. However, it will be important to characterize the localization of AUF1 within the cytoplasm under normal and acidic conditions. There may be several challenges in addressing this question. First, because there are multiple isoforms of AUF1 and antibody against AUF1 recognized all four isoforms, it is hard to distinguish which of the cytoplasmic isoforms, p37 or p40, might be involved in GA mRNA turnover. For this reason, many studies that have characterized the functions of AUF1 have utilized a single recombinant isoform. Thus, the resulting data should be interpreted as the effect of over-expression of one isoform. However, *in vivo* the differential effects of AUF1 may result from changes in the relative abundance of the multiple isoforms [Raineri et al, 2004].

The pHRE of the GA mRNA has been shown to bind multiple ARE binding proteins that are both stabilizing and destabilizing *trans*-acting factors. Even though the possible functions of the ARE binding proteins have been demonstrated through the *in vitro* deadenylation assay, it is important to determine whether there is a preferential binding of a stabilizing *trans*-acting factor to the GA mRNA during acidotic conditions. This experiment can be performed using a ribonucleoprotein immunoprecipitation (RNP)-immunoprecipitation assay [Niranjanakumari et al, 2002; Zielinski et al, 2006] of WKPT and WKPT-ζ^+ cells maintained in normal medium or treated with acidic medium for 24 h or 5 d. It is hypothesized that a stabilizing ARE binding protein binds to the pHRE of the GA mRNA within 24 h of acidic treatment, while the same pHRE may bind a destabilizing ARE binding protein in non-treated cells. However, a more pronounced increase in GA mRNA in WKPT cells is not observed only after 4-5 d of treatment with

acidic medium, hence differential binding of ARE binding proteins may also occur between 1d and 5d of treatment with acidic medium.

It is also possible that changes in medium pH will not effect the proteins that are bound to the pHRE. In this case, post-translational modifications of the ARE binding proteins may effect the translocation of the GA mRNA to different loci in the cytoplasm that determine the fate of GA mRNA. For example, under normal and acidotic conditions, TTP may be bound to the pHRE of GA mRNA with the same affinity and degree of saturation. However, phosphorylation of TTP may effect the localization of the GA mRNA:TTP complex. As mentioned previously, under certain conditions, the phospho-TTP:14:3:3 complex is excluded from stress granules. Hence, the post-translational modification of the ARE binding proteins may determine the localization of the RNA:protein complexes within the cytoplasm. Therefore, even though the GA mRNA may be bound to TTP under both normal and acidotic condition, the GA mRNA:TTP protein complex may be excluded from stress granules only under acidotic condition. Phosphoprotein purification experiments indicated that ζ-cryst is not a phopho-protein. Thus it will be also important to determine if ζ-cryst undergoes an alternative post-translational modification.

Stress granules are the cytoplasmic loci where stalled, translation-initiation complexes accumulate in response to various environmental stress. Proteins that are known to be involved in mRNA turnover process, including HuR [Gallouzi et al, 2000] and TTP [Stoecklin et al, 2004], also accumulate in stress granules. Immunostaining experiments demonstrated that ζ-cryst is clustered in stress granules under acidotic conditions, indicating that the ER-stress signaling pathway is activated during metabolic

acidosis. It is important to emphasize that the localization of a protein is not sufficient to determine its function, especially when both stabilizing and destabilizing ARE binding proteins are known to accumulate in stress granules. However, the transient association of ζ–cryst with stress granules may indicate that the GA mRNA is also transiently recruited to stress granules following initial transfer to acidic medium. Such an association could result in a transient arrest of translation of the GA mRNA. This might explain why during onset of acidosis there is a 8-10 h lag before an increase in GA mRNA is observed and 1-2 d lag before an increase in glutaminase activity occurs [Hwang et al, 1991a].

It is known that deadenylases and the exosome that are involved in the 3'→5' decay pathway along with some of ARE binding proteins, such as AUF1, are not localized in P-bodies or stress granules. Under normal conditions, ζ-cryst is distributed throughout the cytoplasm, where the 3'→5' decay machinery resides, while it is localized in stress granules following treatment with acidic medium. This observation suggests that ζ-cryst may act as a destabilizing *trans*-factor under normal conditions by interacting with a deadenylase and/or the exosome to promote 3'→5' decay. When it is recruited to the stress granules by treatment with acidic medium, the ζ-cryst is sequestered and may no longer associate with the GA mRNA. The resulting inability to recruit the GA mRNA to the exosome could account for its increased stability. Alternatively, ζ-cryst may act similar to TIA-1 and TIAR and recruit GA mRNA to stress granules during metabolic acidosis and promote the association of stabilizing trans-acting factors with GA mRNA. The *in vitro* decay experiments performed with WKPT-ζ^+ cell extracts suggest that ζ-cryst may play a destabilizing role in the deadenylation and subsequent turnover of the

GA mRNA. Whether the observed destabilizing role of ζ-cryst is due to ubiquitous localization of ζ-cryst throughout cytoplasm, where the 3'→5' decay machinery resides and how accumulation of ζ-cryst in stress granules during metabolic acidosis may effect the stabilization of GA mRNA still need to be determined.

It is imperative to determine whether ζ-cryst also localizes with P-bodies that contain the decapping enzymes and the proteins involved in 5'→3' decay pathway. This can be accomplished through immunostaining experiments with Dcp1a, Dcp2, and other proteins that are known to be localized in P-bodies but not in stress granules. There are dynamic interactions between stress granules and P-bodies [Kedersha et al, 2005]. This may explain why many proteins involved in mRNA turnover process co-localize in stress granules and P-bodies. Immunostaining experiments may reveal the differential localization of ARE binding proteins and proteins involved in mRNA turnover process under normal or acidotic conditions. It will be necessary to follow the localization of GA mRNA under the normal or acidotic condition, in order to directly correlate the localization of the regulatory proteins with GA mRNA. This can be established by designing a chimeric GA mRNA that contains multiple MS2 protein binding elements in the 3'UTR. A chimeric MS2 coat protein containing a GFP (green fluorescence protein) domain, can be co-expressed and used to trace the movement of GFP-tagged GA mRNA under normal and acidotic conditions. This approach has been previously used to follow the initial processing and subsequent decay of chimeric mRNAs [Janicki et al, 2004; Shav-Tal et al, 2004].

A new model is proposed for the mechanisms that may lead to the stabilization of the GA mRNA during metabolic acidosis. Under normal condition, the binding of TTP

or ζ-cryst to the pHRE of GA mRNA leads to the recruitment of PARN. After deadenylation, exoribonucleases are recruited to ARE containing transcripts, leading to more rapid degradation of GA mRNA. 5'→3' decay of GA mRNA can occur in P-bodies, where decapping enzymes and 5'→3' exonuclease (Xrn1) are localized. Additionally, the 3'→5' decay of GA mRNA can occur in cytoplasm, where the exosome, a 3'→5' exonuclease complex, is recruited to the transcript and degrades the transcript in 3'→5' direction (**Fig. 8-2**).

In contrast, during metabolic acidosis the activation of MK2 pathway may lead to the phosphorylation of TTP. Phopho-TTP:14:3:3 complex may be excluded from stress granules under certain environmental stress. This will allow stabilizing *trans*-acting factors such as HuR to interact with GA mRNA in stress granules. In contrast, in the cytoplasm the transcripts may interact with stabilizing *trans*-acting factors such as HuR and AUF1, leading to the stabilization of the GA mRNA. Additionally, ζ-cryst is recruited to stress granules during metabolic acidosis. Whether ζ-cryst is recruiting GA mRNA to stress granules, and if it is involved in translational regulation of GA mRNA are yet to be determined. It is also possible the recruitment of ζ-cryst to stress granules may hinder its interaction with GA mRNA in the cytoplasm, allowing other stabilizing trans-acting factors to bind to the pHRE of GA mRNA (**Fig. 8-3**).

The experiments performed demonstrated the complexity and intricacy of the mRNA turnover process and its regulation. It has been demonstrated the differential role of ARE binding proteins in the regulation of GA mRNA, and the importance of localization of RNA:protein complexes as a possible determining factor of mRNA turnover process. It is anticipated that the suggested experiments will define, at least in

part, the regulatory mechanism that leads to the stabilization of the GA mRNA during metabolic acidosis.

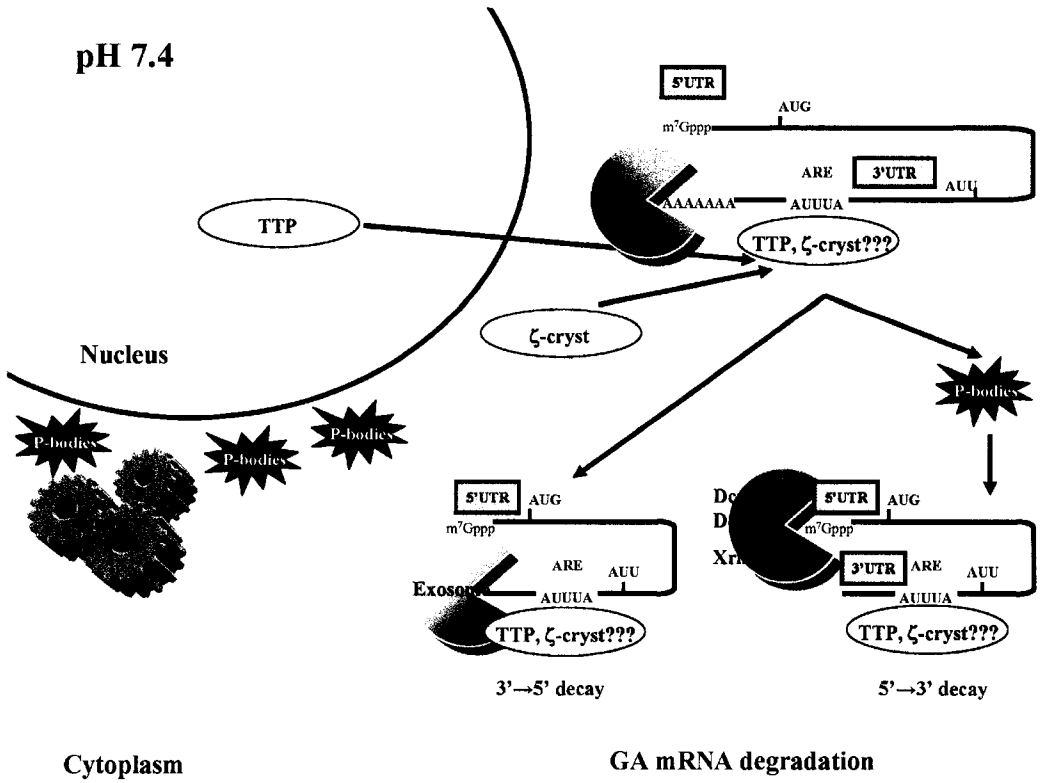

Fig. 8-2 Model depicting a possible mechanism that leads to degradation of the GA mRNA under the normal condition (pH 7.4, 25 mM HCO_3^-). At pH 7.4, the binding of TTP or ζ-cryst to the pHRE of GA mRNA leads to the recruitment of PARN. After deadenylation, exoribonucleases are recruited by the ARE-binding proteins, leading to more rapid degradation of GA mRNA. 5'→3' decay of GA mRNA can occur in P-bodies, where decapping enzymes and 5'→3' exonuclease (Xrn1) are localized. Additionally, the 3'→5' decay of GA mRNA may occur in cytoplasm, where exosome, a 3'→5' exonuclease complex, is recruited to the transcript and degrades the transcript in 3'→5' direction.

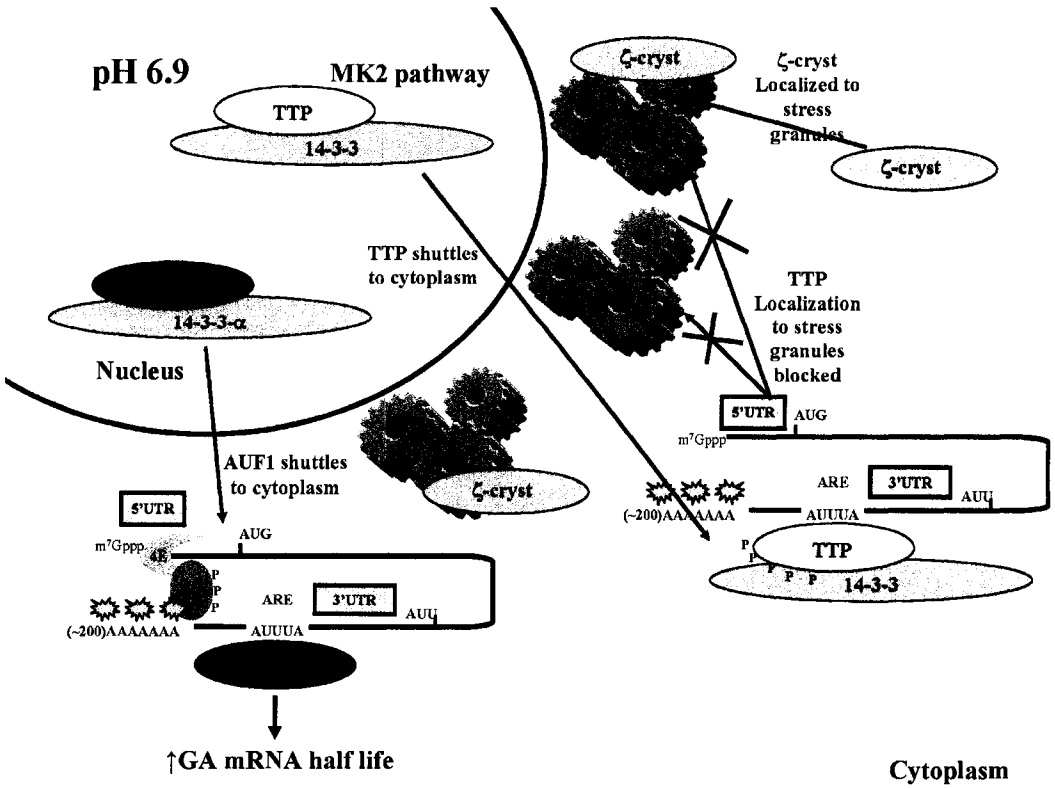

Fig. 8-3 Model depicting a possible mechanisms that lead to the stabilization of the GA mRNA under acidic condition (pH 6.9, 10 mM HCO_3^-). At pH 6.9, the activation of MK2 pathway leads to the phosphorylation of TTP. Phopho-TTP:14:3:3 complex may be excluded from stress granules. This would allow stabilizing *trans*-acting factors, such as HuR, to interact with GA mRNA in the stress granules. Alternatively, the transcript may interact with stabilizing trans-acting factors such as HuR and AUF1 in the cytoplasm, leading to the stabilization of the GA mRNA. Additionally, ζ-cryst is recruited to stress granules during metabolic acidosis. Whether ζ-cryst is recruiting GA mRNA to stress granules and is involved in translational regulation of GA mRNA are yet to be determined. It is also possible that recruitment of ζ-cryst to stress granules may hinder its interaction with GA mRNA, allowing other stabilizing *trans*-acting factors to bind to the pHRE of GA mRNA.

Previous experiments using a tet-regulated promoter system demonstrated that the 3' UTR of the PEPCK mRNA contains multiple instability elements [Hajarnis et al, 2006] AUF1 was shown to bind with high affinity and specificity to the PCK-2, PCK-6 and PCK-7 segments of the 3' UTR that contribute to the rapid turnover of the PEPCK mRNA. It was also determined that the primary destabilizing elements were located within the PCK6/7 segment that constitutes the final 73-nt of the PEPCK 3'-UTR. To further characterize the potential functions of the ARE-binding proteins in the turnover of the PEPCk mRNA, an *in vitro* deadenylation assay was developed.

The *in vitro* deadenylation of the GemPCK6/7-A_{60} mRNA was first analyzed using extracts of LLC-PK_1-F^+ cells, since the previous experiments using a tet-regulated promoter system were performed in LLC-PK_1-F^+ cells. Cytoplasmic extracts from LLC-PK_1-F^+ cells were not suitable for the *in vitro* deadenylation assay since the GemPCK6/7-A_{60} mRNA was rapidly degraded without accumulation of the deadenylated product. Perhaps the LLC-PK_1-F^+ cells express a non-specific RNase that is not inhibited by RNasin or other general RNase inhibitors that were tested. Hence, extracts of WKPT cells, a rat proximal tubule cell line that were previously used to study the *in vitro* deadenylation of GemGA-A_{60} mRNA, were used to determine the effect of recombinant proteins on the PEPCK mRNA turnover.

The addition of poly-A to compete for the binding of poly-A binding proteins, stimulated the deadenylation of the GemPCK6/7-A_{60} mRNA (**Fig. 7-3 panel a**). The addition of recombinant ζ-cryst and p40-AUF1 had little effect on the rate of decay of the GemPCK6/7-A_{60} mRNA. The addition of TTP slightly stimulated the decay of the GemPCK6/7-A_{60} substrate, but this also occurred without the accumulation of

deadenylated product. Omission of ATP/PC increased the rate of decay of the GemPCK6/7-A_{60} RNA and also resulted in appearance of the deadenylated product (**Fig. 7-3 panel b**). The addition of recombinant ζ-cryst and p40-AUF1 in the absence of ATP/PC again had little or no effect on the decay pattern. In contrast, the addition of recombinant TTP now resulted in significant accumulation of deadenylated product and its subsequent degradation. Since the exosome should be non-functional in the absence of ATP/PC, this may indicate that alternative decay pathways are involved in the turnover of the GemPCK6/7-A_{60} mRNA.

The addition of recombinant ζ-cryst to the *in vitro* deadenylation assay had little effect on the rate of deadenylation and turnover of the GemPCK6/7-A_{60} RNA. To further characterize the possible role of ζ-cryst in PEPCK mRNA turnover, extracts of WKPT-ζ^+ cells were tested. It was previously demonstrated that WKPT-ζ^+ cells over-express ζ-cryst by 36-fold in comparison to WKPT cells. As observed for the control substrates, Gem-A_{60} and GemARE-A_{60}, a significant stimulation of decay and accumulation of the deadenylated GemPCK6/7-A_0 product was observed in the WKPT-ζ^+ extracts.

In the absence of poly-A RNA, the rate of decay of the GemPCK6/7-A_{60} substrate was minimal (**Fig. 7-5 panel a**). Addition of recombinant ζ-cryst did not effect the turnover rate of GemPCK6/7-A_{60} RNA. However, a stabilizing effect of p40-AUF1 on GemPCK6/7-A_{60} RNA was observed. The addition of recombinant TTP slightly enhanced the decay of the GemPCK6/7-A_{60} RNA as observed with WKPT cell extracts. A significant increase in the rate of deadenylation and accumulation of the deadenylated product were observed in the presence of 500 ng poly-A RNA (**Fig. 7-5 panel b**). However, the stabilizing effect of p40-AUF1 was no longer observed. Again, the

addition of TTP enhanced the accumulation of the deadenylated product. It is interesting to note that even though there was a significant increase in the rate of deadenylation with the addition of poly-A RNA, the deadenylated products accumulated and the further decay of the GemPCK6/7-A_0 mRNA was diminished.

Surprisingly, with the WKPT-ζ^+ extracts the absence of ATP/PC had little effect on the turnover of GemPCK6/7-A_{60} mRNA compared to that observed in the presence of ATP/PC (**Fig. 7-5 panel c**). Omission of ATP/PC should inhibit the exosome, and hence it was expected that omission of ATP/PC would result in greater accumulation of the deadenylated product. Thus, it is possible that the decay of the PEPCK mRNA occurs through decapping and a 5'→3' exonuclease activity in the processing bodies. Hence, it will be important to investigate whether 5'→3'decay pathway is involved in the turnover of GemPCK6/7-A_{60} mRNA using the *in vitro* decapping assay.

The experiments performed in WKPT-ζ^+ cells demonstrated that ζ-cryst may act as a destabilizing ARE binding protein, that may stimulate the turnover of mRNA. Further experiments need to be performed in order to further characterize ζ-cryst as a possible trans-acting instability factor. Based upon the results obtained through the *in* vitro deadenylation assay, TTP may also act as a destabilizing *trans*-acting factor that may stimulate deadenylation and subsequent turnover of PEPCK mRNA. In contrast, p40-AUF1 may act as a stabilizing trans-acting factor to increase the stability of the PEPCK mRNA. AUF1 has been demonstrated to have a multiple roles in mRNA turnover. It functions as either a stabilizing [Kiledjian et al, 1997; Chen et al, 2004; Xu et al, 2001] or destabilizing [Loflin et al, 1999; Sarkar et al, 2003] *trans*-acting factor. It has been suggested that the differential role of AUF1 may be regulated by the relative

abundance of each AUF1 isoform [Raineri et al, 2004]. Hence, the stabilizing effect of p40-AUF1 on the deadenylation and turnover of PEPCK mRNA observed in the current experiments may reflect the use of a single isoform. In addition, the bacterially expressed recombinant p40-AUF1 lacks potential post-translational modifications. Therefore, the stabilizing effect of p40-AUF1 may reflect the effect of over-expression of only the unphosphorylated form of p40-AUF1. Overall, these experiments demonstrate that the *in vitro* deadenylation assay can be used to characterize the role of ARE binding proteins on the deadenylation and turnover rate of PEPCK mRNA and the stabilization of PEPCK mRNA during metabolic acidosis. Treatment of LLC-PK_1-F^+ cells with acidic medium results in activation of the p38-MAPK and phosphorylation and activation of the downstream MK2 [O'Hayre et al, 2006]. Thus it will be important to determine if the treatment with acidic medium results in shuttling of the ARE binding proteins into the cytoplasm and/or exclusion from stress granules. Further experiments need to be performed to define the regulatory mechanism that leads to the stabilization of the PEPCK mRNA during metabolic acidosis.

Appendix

DOWNSTREAM ELEMENTS CONTRIBUTES TO THE pH-RESPONSIVE INDUCTION OF RENAL PHOSPHO*ENOL*PYRUVATE CARBOXYKINASE

This chapter will be re-submitted for publication.

Yeon J. Lee, Lynn Taylor, Norman Curthoys.

Appendix. 1. Abstract

Metabolic acidosis causes an increased expression of numerous proteins in the kidney that participate in the catabolism of glutamine, partially restore acid-base balance, and promote hypertrophy. Transcription of the phospho*enol*pyruvate carboxykinase (PEPCK) gene is rapidly activated following the onset of acidosis and thus serves as a paradigm to identify the elements that mediate this response. Luciferase (Luc) constructs containing either 490 or 2300 bp of the PEPCK promoter were expressed in LLC-PK_1-$FBPase^+$ cells. Neither construct exhibited increased activity when the cells were transferred to acidic medium (pH 6.9, 10 mM HCO_3^-). Integrated copies of both chimeric constructs and adenovirus constructs of PCK_{-2300}Luc also failed to exhibit a pH-responsive increase even though the endogenous PEPCK mRNA was increased 2- to 3-fold. As a control, Luc mRNA levels were quantified by Northern analysis and shown to be unchanged. By contrast, the CRC362 transgene, when stably transfected into LLC-PK_1-$FBPase^+$ cells and assayed by real-time RT-PCR, exhibits a 2-fold pH-responsive increase in expression. This construct contains the entire rat PEPCK gene, including 362 bp of promoter, but has a 485-bp insert of chicken sequence in the 3'-UTR. Thus, a reporter construct containing only 362 bp of the promoter along with the downstream exons and introns is sufficient to recapitulate the pH-responsive induction. Systematic

deletions of the CRC362 gene were analyzed to partially map the downstream segments that contribute to induction of the PEPCK gene in the kidney.

Appendix 2. Introduction

The maintenance of blood acid-base balance is essential for survival. Increased renal ammoniagenesis and gluconeogenesis from plasma glutamine contribute to the adaptive response that partially restores acid-base balance during metabolic acidosis [Taylor et al, 2004]. Renal catabolism of glutamine is sustained during chronic acidosis, at least in part, by increased expression of the genes that encode the cytoplasmic phospho*enol*pyruvate carboxykinase (PEPCK) [Burch et al, 1978], the mitochondrial glutaminase [Curthoys et al, 1973], glutamate dehydrogenase [Wright, 1990] and glutamine transporter [Sastrasihn et al, 1989], the apical Na^+H^+ exchanger [Preisig et al, 1988], and the basolateral glutamine transporter [Karinch et al, 2002] and $Na^+3HCO_3^-$ cotransporter [Preisig et al, 1988]. The level of PEPCK mRNA in rat kidney is rapidly increased following acute onset of acidosis [Hwang et al, 1991b]. The increase is initiated within 1 h and reaches a maximum within 7 h at a level that is 6-fold greater than normal. The 6-fold induced level of PEPCK mRNA is sustained in rats that are made chronically acidotic for 7 d [Hwang et al, 1991a]. Transcription run off experiments were conducted using isolated rat renal nuclei [Hwang et al, 1991b; Hwang et al, 1991a]. The relative rate of transcription of the PEPCK gene increased 3-fold within 2 h after acute onset of acidosis, reached a maximum of 4-fold induction by 6 h, and then decreased slightly by 20 h. The initial increase in transcription exceeded the initial increase in PEPCK mRNA. Therefore, enhanced transcription can account for the initial induction of PEPCK mRNA. The observed changes in PEPCK mRNA levels closely correlated with earlier data that measured changes in the relative rates of PEPCK protein synthesis in normal and acidotic

rats [Iynedjian et al, 1975]. Thus, regulation of the translation of the PEPCK mRNA is unlikely to contribute to the observed changes in PEPCK gene expression.

Various segments of the PEPCK promoter, as well as the core promoter (-460 to +73 bp) containing specific block mutations in regulatory elements, have been extensively analyzed in transgenic animals to determine their role in controlling PEPCK gene expression [Hanson et al, 1994]. The wild type core promoter fused to the bovine growth hormone (bGH) gene contains all of the information necessary to insure appropriate expression and hormonal regulation in liver [McGrane et al, 1990; McGrane et al, 1988]. A larger 2.3-kb segment of the PEPCK promoter was required to drive expression of the transgene in adipose tissue [McGrane et al, 1990; McGrane et al, 1988]. However, both of these constructs were expressed at low levels in the kidney. In contrast, the CRC362 transgene, that contains only 362 bp of the promoter but all of the downstream exons and introns of the rat PEPCK gene, was expressed with the correct developmental profile and at normal levels in the kidney [Eisenberger et al, 1992]. This transgene differed from the endogenous gene only by the substitution of a segment of the chicken PEPCK gene into the portion of the final exon that encodes the 3'-untranslated region of the PEPCK mRNA. Furthermore, only the latter construct exhibited a significant renal-specific induction when the transgenic mice were made acidotic [Cassuto et al, 2003]. These data suggest that the PEPCK gene may contain a downstream element that is essential for full expression and pH-responsive induction in the kidney.

Previous experiments demonstrated marked differences in the foot-printing patterns observed with nuclear extracts prepared from rat liver and kidney [Roesler et al,

1989], suggesting that kidney and liver may utilize different *trans*-acting factors to regulate the PEPCK gene. Further characterization of the specific *cis/trans* interactions that mediate the pH-responsive activation of the PEPCK gene required the identification of a renal cell line that accurately models this adaptation. Compared to the parental LLC-PK_1 cells, the LLC-PK_1-F^+ cells exhibit an enhanced rate of glutamine catabolism [Gstraunthaler et al, 1987] and a higher basal rate of ammonia production [Gstraunthaler et al, 2000]. Most importantly, when transferred to acidic medium (pH 6.9, 10 mM HCO_3^-), the LLC-PK_1-F^+ cells respond with a pronounced increase in ammonium ion production that correlates with a similar increase in glutaminase activity [Gstraunthaler et al, 2000]. In addition, the level of the pH-responsive cytosolic PEPCK mRNA was increased 2- to 3-fold while the level of the constitutively expressed mitochondrial PEPCK mRNA was unchanged [Holcomb et al, 1995]. Thus, the gluconeogenic LLC-PK_1-F^+ strain is a pH-responsive renal proximal tubule-like cell line.

In the current study, we demonstrate that an element downstream of the proximal promoter is essential for the pH-responsive induction of the PEPCK gene in LLC-PK_1-F^+ cells. Various PEPCK promoter-luciferase constructs, that were transiently or stably transfected into LLC-PK_1-F^+ cells, failed to exhibit a pH-responsive induction. However, the CRC362 gene, when stably transfected and assayed by real-time RT-PCR analysis, produced a 2-fold increase in expression when the cells were transferred to an acidic medium. Thus, a reporter construct containing only 362 bp of the promoter along with the downstream exons and introns is sufficient to recapitulate the pH-responsive induction. Systematic deletions of the CRC362 gene were analyzed in order to partially map the downstream segments that contribute to induction of the PEPCK gene.

Appendix 3. Materials and Methods

3.1 Materials

Geneticin (G418) and Hygromycin B were obtained from Mediatech. Dulbecco's modified Eagle's medium/F-12 base medium and cloning rings were purchased from Sigma-Aldrich. Formazol was purchased from Molecular Research Center. Mini-RNA isolation kit was ordered from Zymo Research. [α-^{32}P]dCTP (3,000 Ci/mmol) was purchased from MP Biomedicals. The oligo-labeling kit was from obtained from Ambion. The avian myeloblastosis virus-reverse transcriptase was purchased from Promega. Platinum qPCR SuperMix-UDG was purchased from Invitrogen. Dual-labeled Taqman Probes were ordered from Biosearch Technologies.

3.2 Plasmids

The CRC362 plasmid [Eisenberger, 1992] was obtained from Dr. Lea Reshef (Department of Biochemistry, Hadassah Medical School, Hebrew University, Israel). It was digested with *Sma*I and religated to yield the Δ_1*Sma*I construct. Digestion with *Bgl*II and religation yielded Δ_1BglII. Blunt-end ligation of the 1.6-kb *Sma*I fragment into the *Bgl*II restricted vector yielded Δ_2*Sma*I, whereas insertion of the isolated 0.6-kb *Bgl*II fragment yielded Δ_2*Bgl*II. Insertion of the 1.4-kb *Bgl*II fragment isolated from PCK10 cDNA [Cimbala, 1982] yielded the -362cDNA construct that contained the complete exon sequence but lacks all the introns of the PEPCK gene.

3.3 Cell culture and transfections

LLC-PK_1-F^+ cells [Gstraunthaler et al, 1987] were grown in a 50:50 mixture of Dulbecco's modified Eagle's and Ham's F-12 medium containing 5 mM glucose, 25 mM $NaHCO_3$, 100 units/ml penicillin, 100 mg/ml streptomycin, and 10% fetal bovine serum at 37 °C in a 5% CO_2 atmosphere. Samples containing 5 μg of the CRC362 plasmid or the various deletion constructs were co-transfected with 1 μg of pRSV-neo using a calcium phosphate protocol [Chen, C. et al, 1987]. The transfected cells were selected for growth in Dulbecco's modified Eagle's medium/F-12 medium containing 0.5 mg/ml G418. The cells were allowed to select for 2-3 weeks. The resulting colonies were isolated with cloning rings and the clonal lines were expanded in medium containing 0.2 mg/ml G418. Confluent LLC-PK_1-F^+ cells were treated with either normal medium (pH 7.4, 25 mM HCO_3^-) or acidic medium (pH 6.9, 10 mM HCO_3^-) for 24 h before isolating total RNA.

3.4 Luciferase assays

The various luciferase constructs were assembled in pGL2-Basic (Promega) that encodes the firefly luciferase gene. The $PEPCK_{-2300}CAT$ and $PEPCK_{-490}CAT$ plasmids were restricted with *Bam*HI and *Bgl*II to excise the either -2300 or -490 to +73-bp fragments of the rat PEPCK promoter. The purified fragments were then cloned into pGL2-Basic that had been restricted with *Bgl*II to produce the $PEPCK_{-2300}Luc$ and $PEPCK_{-490}Luc$ constructs, respectively. LLC-PK_1-F^+ cells were grown for 7 d in 6-well plates to achieve confluence. The cells were transiently co-transfected with 0.6 μg of either $PEPCK_{-2300}Luc$ or $PEPCK_{-490}Luc$ and 0.1 μg of pRL-null (Promega) per well by

calcium phosphate precipitation [Chen, C. et al, 1987]. The cells were cultured for an additional 24 h in normal or acidic medium and then washed twice with phosphate-buffered saline. Cell extracts were prepared and assayed using the reagents contained in the Dual Luciferase™ Reporter Assay Kit (Promega). The firefly luciferase activities obtained from the various PEPCK-Luc plasmids were divided by the corresponding *Renilla* luciferase activities to correct for differences in transfection efficiency. The mean of the ratio of the luciferase activities measured in extracts of cells grown in normal medium (pH 7.4, 25 mM HCO_3^-) was normalized to a value of 1. Reported values are the mean of data obtained from triplicate samples.

3.5 RNA extraction and Reverse transcription

Total cellular RNA was isolated using the TRIzol® reagent or Mini-RNA Isolation Kit from Zymo Research and the RNA concentration was determined by measuring the absorbance at 260 nm. The initial strand of cDNA was synthesized using avian myeloblastosis virus-reverse transcriptase and an Oligo-dT_{15} primer for 60 min at 42 °C. The cDNAs prepared from the reverse transcription reactions were used directly for quantitative real-time RT-PCR analysis.

3.6 Northern blot analysis

A 485-bp segment of chicken PEPCK sequence was excised by restricting the CRC362 plasmid with *Eco*RI and *Sph*I. A 1.9-Kb fragment of PEPCK cDNA was excised by restricting pBS-PCK with *Xba*I and *Eco*RI. A plasmid encoding the porcine GAPDH was generously provided Dr. David Silversides (Veterinary Medicine,

University of Montreal, Canada). It was restricted with *Hind*III and *Sac*I to yield a 475-bp fragment of GAPDH cDNA. A 2.0-kb fragment of the 18 S ribosomal RNA cDNA from *Acanthamoeba castellanii* was excised by restricting pAr2 [D'Alessio et al, 1981] with *Hind*III and *Eco*RI. The fragments were separated on a 1% agarose gel, excised, and purified using the GeneClean kit (Bio101). The synthesis of oligo-labeled cDNA probes and Northern analysis were performed as described previously [Laterza et al, 2000]. The blots were exposed to a PhosphorImager screen, and the intensities of the resulting digital images were quantified using Molecular Dynamics software. The level of the endogenous PEPCK mRNA was divided by the corresponding level of 18 S rRNA or GAPDH mRNA to correct for errors in sample loading.

3.7Real-time RT-PCR

The purified 485-bp segment of chicken PEPCK cDNA was serially diluted from 10^{-2} ng/μl to 10^{-7} ng/μl. Real-time RT-PCR was performed using a forward primer, $^{5'}$TCAACTGCCATAGGTTACATCC$^{3'}$, and a reverse primer, $^{5'}$CTGTTTGATTTCTT CCACCTCC$^{3'}$, that amplify the region from bp 27 to 155 within this segment of the CRC362 transgene. The reaction also included a FAM-labeled Taqman Probe, $^{5'}$FAM-CTGACACTGCTTTGAACTTGAAGGGTTTAGAA-BHQ1$^{3'}$ that is complementary to the region from bp 52 to 84 of the chicken sequence. The purified 475-bp fragment of porcine GAPDH plasmid was serially diluted from 1 ng/μl to 10^{-5} ng/μl. A primer set was designed to amplify the region from bp 731 to 875 within the coding region. The forward primer, $^{5'}$GATGGGCATGAACCATGAGA$^{3'}$, and the reverse primer, $^{5'}$GGCATGGACTGTGGTCATGA$^{3'}$, were used in real-time RT-PCR along with a

Taqman Probe, $^{5'}$CAL-Red^{TM}-TGCCTCCTGTACCACCAACTGCTTGG-BHQ2$^{3'}$, that is complementary to region from bp 783 to 807 of the porcine GAPDH coding region. The quantitative real-time PCR reaction was performed using Platinum qPCR Supermix-UDG in the presence of 100 nM primers, 200 nM Taqman Probes, and 9 mM $MgCl_2$. The fold induction was calculated using a mathematical model of relative expression in real-time PCR [Pfaffl, 2001] to quantify the relative levels of the CRC362 mRNA in comparison to the GAPDH mRNA. Quantitative real-time PCR reactions were performed in triplicate. The reported values are the mean ± S.E. of data obtained from triplicate samples of multiple clonal lines of cells that stably express the CRC362 construct or each of the deletion constructs.

Appendix 4. Results

LLC-PK_1-FBPase$^+$ cells were transiently transfected with pRL_{null}, that expresses a *Renilla* luciferase from a minimal promoter, and either pPEPCK$_{-490}$Luc or pPEPCK$_{-2300}$Luc and assayed using a dual-luciferase assay. The former activity was used as an internal standard to correct for minor differences in transfection efficiency. All of the Luc reporter constructs produced a strong signal when transfected into subconfluent or confluent cultures of LLC-PK_1-F^+ cells. The two luciferase constructs proved very effective in characterizing the cAMP-dependent activation of PEPCK transcription in LLC-PK_1-F^+ cells [Liu et al, 2001]. However, neither construct produced a significant increase in luciferase activity when the confluent cells were transferred to acidic medium (**Appendix Fig. 1 panel a**). Since subconfluent cultures of LLC-PK_1-F^+ cells fail to exhibit a pH-responsive induction of the endogenous PEPCK gene [Holcomb et al, 1995], it was initially hypothesized that following transfection of confluent cultures, the luciferase activity was primarily expressed in the small population of poorly differentiated LLC-PK_1-F^+ cells that continued to grow and divide rapidly. Thus, stable cell lines that express integrated copies of the two PEPCK-Luc constructs were isolated and tested for a pH-response in confluent cultures. Again, neither construct exhibited a pH-responsive increase in luciferase activity, even though the endogenous PEPCK mRNA levels were still increased 3-fold following transfer to acidic medium (data not shown). As a control to insure that a decrease in intracellular pH had not caused an irreversible denaturation of the firefly luciferase, the levels of the Luc mRNA were quantified by Northern analysis and shown to be unchanged in the stably transformed cells that had been treated with acidic medium (**Appendix Fig. 1 panel b**). An adenovirus construct that expresses the

a.

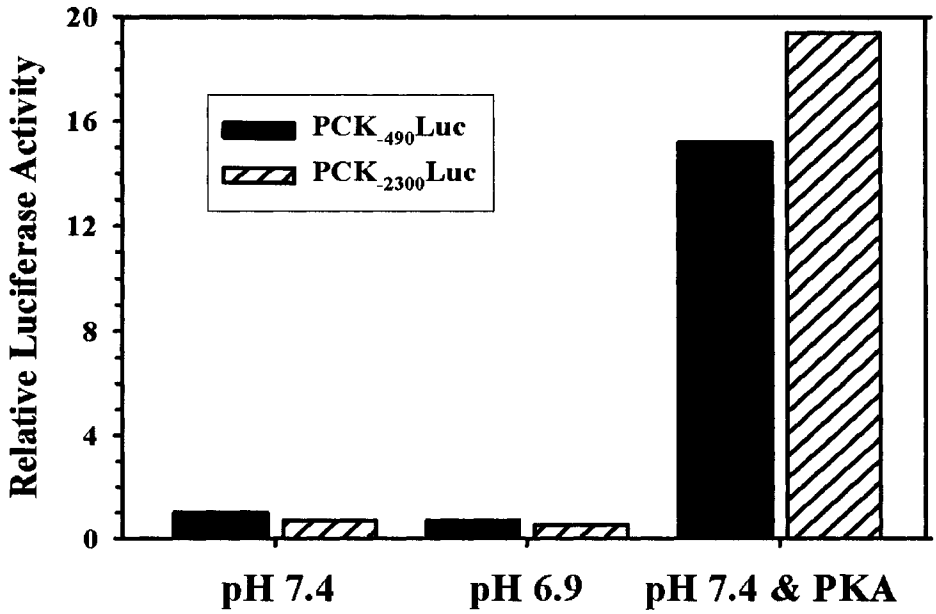

b.

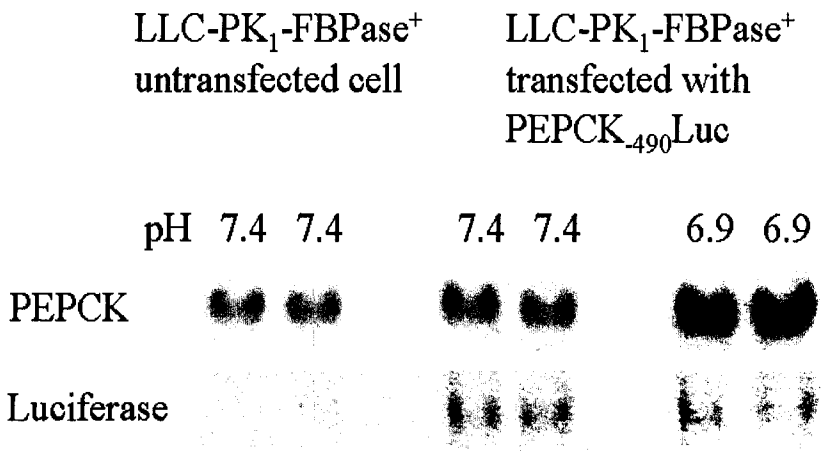

Appendix Fig. 1 Expression of PEPCK-Luc constructs. Panel A. Effect of acidic medium (pH 6.9) or co-expression of catalytic subunit of protein kinase A (PKA) on the $PEPCK_{-490}Luc$ (solid bars) and $PEPCK_{-2300}Luc$ (shaded bars) activities expressed in LLC-PK_1-F^+ cells. Panel B. RNA was isolated from wild type and stably transfected LLC-PK_1-F^+ cells grown in normal (pH 7.4) or acidic medium (pH 6.9) and hybridized with ^{32}P-labeled cDNAs to quantify the PEPCK and $PEPCK_{-490}Luc$ mRNAs.

$PCK_{-2300}Luc$ gene was developed and used to infect LLC-PK_1-F^+ cells. Control experiments using an adenovirus that expresses green fluorescent protein indicated that nearly all the LLC-PK_1-F^+ cells are rapidly infected. This protocol also produced very high luciferase activity in the LLC-PK_1-$FBPase^+$ cells, but again this activity was not pH-responsive (data not shown). Thus, the combined data indicate that the proximal segment of the PEPCK promoter is not sufficient to produce a pH-responsive luciferase construct. Therefore, an element located either upstream or downstream of the proximal promoter may also contribute to the pH-responsive expression of the PEPCK gene.

Eisenberger, *et al.* [Eisenberger et al, 1992] demonstrated that the CRC362 transgene is expressed with a normal developmental profile and at normal adult levels in kidney and is induced when the transgenic mice were made acidotic [Cassuto et al, 2003]. This construct differed from the normal rat gene only by the removal of a 465-bp *Eco*RI/*Sph*I fragment from the 3'-untranslated region and insertion of the corresponding 485-bp segment from the chicken PEPCK gene (**Appendix Fig.2**). Thus, the CRC362 construct was cotransfected with pRSV-neo into LLC-PK_1-F^+ cells. Northern analysis indicated that the three isolated clonal lines exhibit a 2.0 +/- 0.4 fold induction of the endogenous PEPCK mRNA when the LLC-PK_1-F^+ cells are transferred to acidic medium for 24 h (**Appendix Fig. 3**). The level of the CRC362 mRNA was too low to detect using northern blot analysis. However, expression of the CRC362 mRNA was verified by RT-PCR.

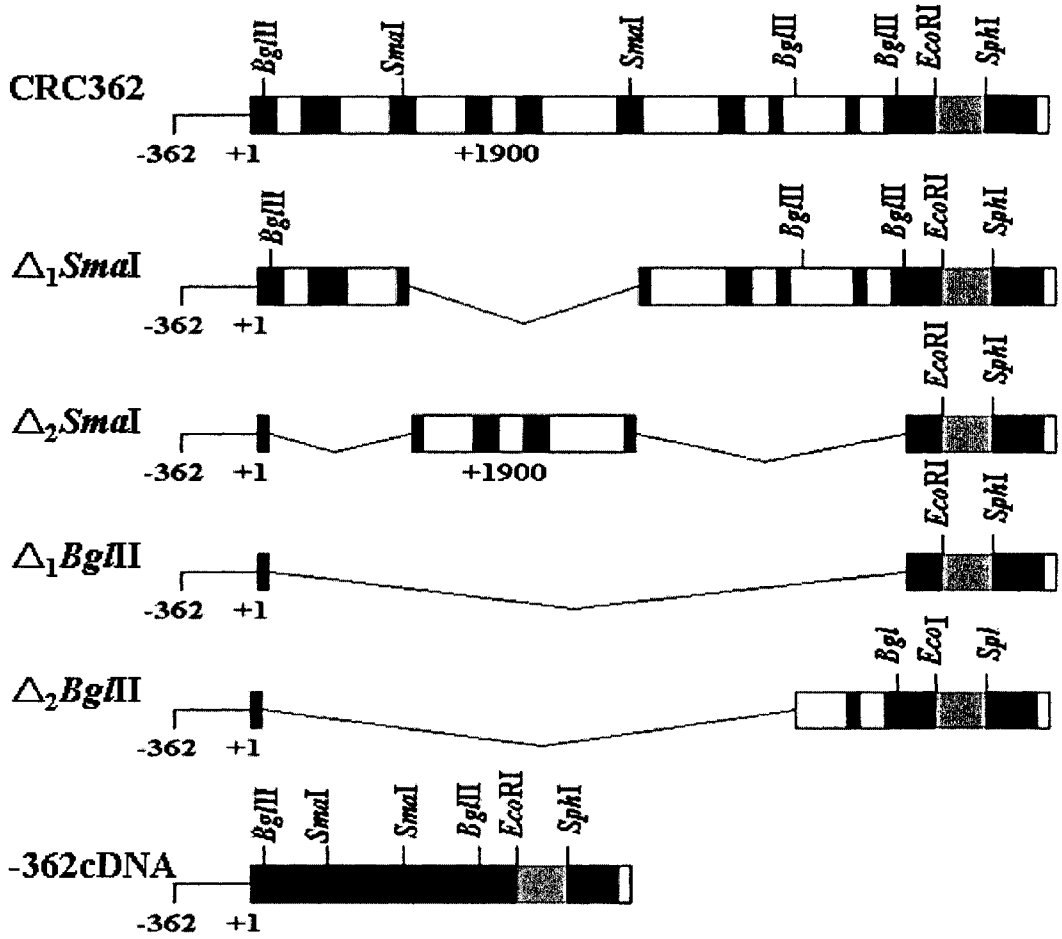

Appendix Fig. 2 Schematic of the CRC362 gene and deletion constructs. The CRC362 gene contains 362 bp of promoter sequence and all of the exons (solid bars) and introns (open bars) of the rat PEPCK gene. The shaded area corresponds to the unique chicken sequence that was amplified in the real-time PCR assay. The CRC362 plasmid was digested with *Sma*I and religated to yield the Δ_1*Sma*I construct. Digestion with *Bgl*II and religation produced the Δ_1*Bgl*II. Blunt-end ligation of the 1.6-kb *Sma*I fragment into the *Bgl*II restricted vector yielded Δ_2*Sma*I, whereas insertion of the isolated 0.6-kb *Bgl*II fragments yielded Δ_2*Bgl*II, respectively. Insertion of the 1.4-kb *Bgl*II fragment isolated from the PCK10 cDNA produced the –362cDNA construct that contains the complete exon sequence but lacks all the introns of the PEPCK gene.

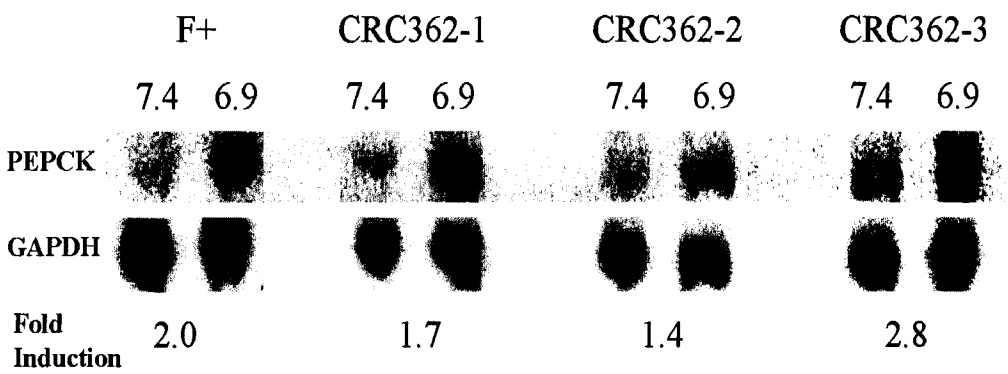

Appendix Fig. 3 pH-responsive induction of endogenous PEPCK mRNA. RNA was isolated from LLC-PK_1-F^+ cells and from three clonal lines of cells that stably express the CRC362 gene that were treated with normal (pH 7.4) or acidic (pH 6.9) medium. The levels of the endogenous PEPCK and GAPDH mRNAs were determined by northern blot analysis.

To determine if the chimeric CRC362 transgene exhibits a pH-responsive induction, a quantitative real-time RT-PCR assay was developed using specific primer sets and differentially labeled Taqman probes to quantify the CRC362 and glyceraldehyde 3-phosphate dehydrogenase (GAPDH) mRNAs (**Appendix Fig. 4 panel a**). The excitation and emission wavelengths of the two Taqman fluorescent probes do not overlap. Thus, the levels of the two mRNAs were quantified using the same reaction mixture and the same RNA samples used in the northern analysis of the endogenous PEPCK. Purified restriction fragments obtained from the CRC362 and porcine GAPDH cDNAs were used to generate standard curves and to calculate the relative levels of the two mRNAs in each sample. Comparison of the ratio of CRC362 mRNA to GAPDH mRNA in the total RNA samples isolated from triplicate plates of LLC-PK_1-FBPase$^+$ cells treated with normal or acidic medium were used to calculate the fold induction for each clonal line that expresses the CRC362 mRNA (**Appendix Fig. 4 panel b**). The analysis of the clonal lines that stably express the CRC362 transgene demonstrated that expression of the integrated CRC362 gene exhibits a highly significant (2.1 +/- 0.3 fold) and reproducible induction when the LLC-PK_1-F^+ cells are transferred to acidic medium for 24 h (**Appendix Fig. 5**). Control samples in which the reverse transcriptase was omitted were performed in order to establish that none of the resulting signal was generated from contaminating genomic DNA. The specificity of the analysis was also demonstrated by including RNA samples isolated from non-transfected LLC-PK_1-F^+ cells (data not shown).

In order to identify the segment of the PEPCK gene that contains the downstream pH-responsive element, systematic deletions of the CRC362 construct were generated

a. **CRC362 FAM labeled probe**

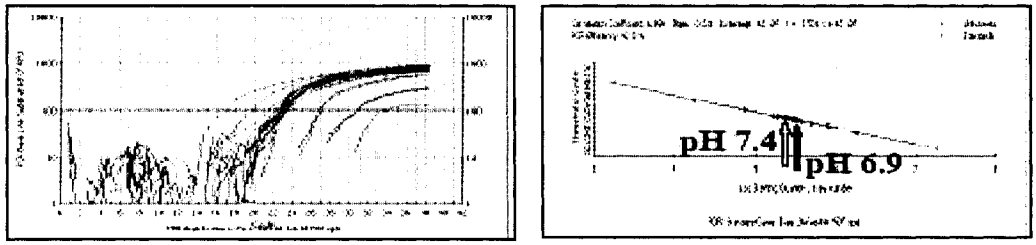

GAPDH CAL-Red labeled probe

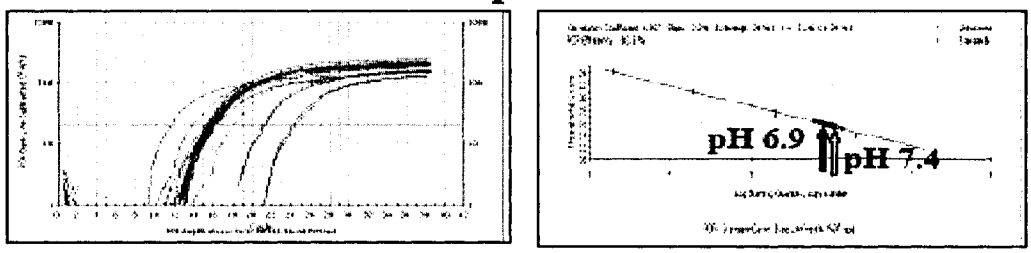

b.

$$\text{Ratio} = \frac{(E_{target})^{\Delta CP_{target}\,(control_{pH\,7.4}-sample_{pH\,6.9})}}{(E_{ref})^{\Delta CP_{ref}\,(control_{pH\,7.4}-sample_{pH\,6.9})}}$$

$$E = 10^{[-1/slope]}$$

- E_{target} = PCR efficiency of target gene
- E_{ref} = PCR efficiency of a reference gene
- ΔCP_{target} = CP dev of control – sample of target gene
- ΔCP_{ref} = CP dev of control – sample of reference gene
- CP = Threshold Crossing point

Appendix Fig. 4 Quantitative real-time RT-PCR analysis of CRC362 mRNA levels. Panel A. Time profiles and standard curves for RT-PCR amplification of CRC362 and GAPDH mRNAs. The arrows indicate RNA samples from cells treated with normal (pH 7.4) or acidic (pH 6.9) medium. Panel B. Calculation of fold induction using data obtained from the CRC362 and GAPDH Taqman probes. The fold induction was calculated using an equation that corrects for differences in PCR efficiency, where: E_{target} is the PCR efficiency for amplification of the purified CRC362 cDNA; E_{ref} is the PCR efficiency for amplification of the purified GAPDH cDNA; ΔCP_{target} is the difference in threshold cycle measured for the CRC362 mRNA isolated from cells treated with normal and acidic media; and ΔCP_{ref} is the difference in threshold cycle measured for the GAPDH mRNA isolated from cells treated with normal and acidic media. The PCR efficiencies were calculated as $E = 10^{[-1/slope]}$.

(**Appendix Fig. 2**). Clonal lines that express each of the deletion constructs were derived and analyzed by quantitative real-time PCR (**Appendix Fig. 5**). The level of the mRNA expressed from the -362cDNA construct, which lacks all of the introns, exhibited a 1.9 +/- 0.5 fold induction when transferred to acidic medium for 24 h. Thus, a necessary downstream element may reside within the exons. The $\triangle_1$*Bgl*II construct, which contains portions of exons 1 and 10, exhibited a decreased expression (0.61 +/- 0.15 fold) when transferred to acidic medium. By contrast, the $\triangle_2$*Bgl*II construct, which adds exon 9 and the remainder of exon 10, exhibits a slightly reduced, but significant 1.5 +/- 0.2 fold induction. Thus, an element within exon 9 or the 5'-end of exon 10 may contribute to the pH-responsive induction. The $\triangle_1$*Sma*I construct, which adds exons 7 and 8 and a portion of exon 6, also exhibited a pH-responsive induction (2.2 +/- 0.3 fold) that is equal to that of the full length CRC362 transgene. However, the greatest induction (3.7 +/- 1.3 fold) was observed in the clonal lines that express the $\triangle_2$*Sma*I construct. This construct incorporates exons 4 and 5 and includes the region around +1900 bp that contains a nuclease hypersensitive site that is unique to genomic DNA isolated from kidney [Cissell, 1999]. Thus, a kidney specific trans-acting factor may bind to the nuclease hypersensitive region and interact with another trans-acting factor that binds further downstream in exon 9 or 10 to mediate the pH-responsive induction of PEPCK in the kidney.

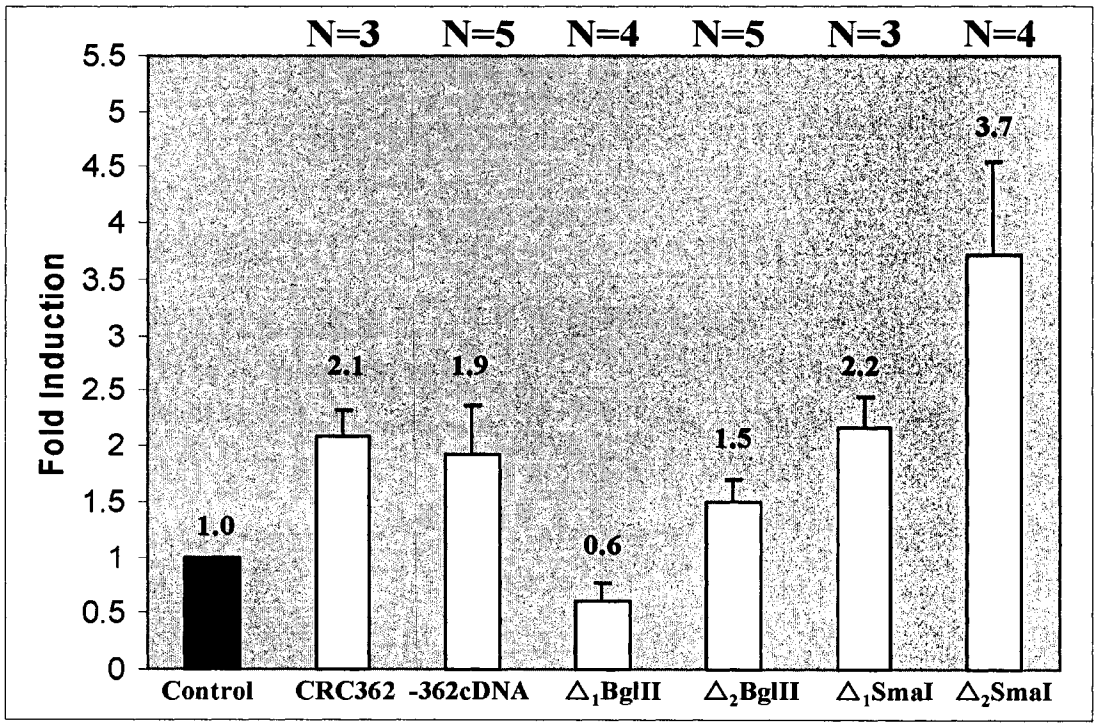

Appendix Fig. 5 Summary of the real-time RT-PCR analysis of the pH-responsive induction of the various CRC362 constructs. The CRC362 deletion constructs were stably transfected into LLC-PK_1-FBPase$^+$ cells and triplicate RNA samples from three to five clonal lines (N) were assayed for induction following treatment for 24 h in acidic medium (pH 6.9).

Appendix 5. Discussion

Analysis of the pH-responsive induction of PEPCK expression and the associated signal transduction pathway provide an excellent paradigm to characterize the molecular mechanism by which transcription of a gene is activated during metabolic acidosis. Confluent and well-differentiated cultures of LLC-PK_1-F^+ cells exhibit a 2- to 3-fold increase in PEPCK mRNA when transferred to acidic medium (pH 6.9, 10 mM HCO_3^-) for 18-24 h [Holcomb et al, 1995]. Previous experiments using chloramphenicol acetyltransferase (CAT) reporter constructs indicated that elements within the proximal promoter region mediate this response in LLC-PK_1-F^+ cells. Confluent cultures transfected with PEPCK$_{-490}$CAT exhibited a 2- to 3- fold increase in CAT activity when shifted to acidic medium for 48 h [Holcomb et al, 1996]. Mutation of the P3(II) or CRE1 element caused a 50% decrease in the pH-response, whereas mutation of the other well-characterized elements in the PEPCK promoter had no effect on this response. Cassuto, *et al.* [Cassuto et al, 1997] generated a PEPCK$_{-597}$CAT construct along with various deletions and site-specific mutations. They also found that the wild type construct exhibited a 2.5-fold increase in CAT activity when the cells were transferred to acidic medium. However, this response was retained in a deletion construct that lacked the entire P3 region suggesting that the P3(II) element was not necessary. A mutation in CRE-1 again caused a partial reduction in the fold response. Mutation of the P2 element significantly reduced basal activity and also had a lower pH-response (1.6-fold). Thus, they concluded that the binding of hepatic nuclear factor-1 (HNF-1) to the P2 element contributes to both basal and pH-responsive activation of PEPCK expression in kidney cells. Finally, Drewnowska, *et al.* [Drenowska et al, 2002] compared the pH-response of

PEPCK$_{-490}$CAT and PEPCK$_{-2300}$CAT constructs in subconfluent LLC-PK$_1$-F$^+$ cells. They reported that a 2.7-fold pH-response was observed only with the construct containing the longer promoter element, suggesting that an element upstream of the shorter -490-bp segment was essential for the pH-response. Given the divergence of these results and the fact that the measured CAT activity approached the lower limits of the sensitivity of this assay, the -490 and -2300 promoter segments were cloned into pGL2-Basic (Promega), a firefly luciferase (Luc) expression vector.

Transient expression of the PEPCK$_{-490}$Luc and PEPCK$_{-2300}$Luc constructs in confluent cultures of LLC-PK$_1$-F$^+$ cells produced a high level of luciferase activity that was easily quantified. The activities of the two constructs are activated nearly 20-fold by coexpression of the catalytic subunit of PKA (**Appendix Fig. 1 panel a**). However, neither construct exhibited a pH-responsive activation. Cells in which the PEPCK-Luc gene was either stably integrated or expressed from an adenovirus also failed to exhibit a response even though the endogenous PEPCK mRNA was significantly increased. Therefore, elements outside the proximal promoter are also required for the pH-responsive induction of the PEPCK gene.

Previous experiments with transgenic mice also indicated that the proximal promoter of the PEPCK gene is not sufficient to produce a pH-responsiveness induction in the kidney [Hanson et al, 1994]. Of the various constructs tested, only the CRC362 gene exhibits a normal pattern of renal expression [Eisenberger et al, 1992] and a pH-responsive induction [Cassuto et al, 2003]. This construct contains the entire rat PEPCK gene including 362 bp of 5'-promoter region and 0.5 kb of 3'-flanking sequence. It differed from the normal rat gene only by the removal of a 465-bp *EcoRI/SphI* fragment

from the 3'-untranslated region and insertion of the corresponding segment from the chicken PEPCK gene. When stably expressed in LLC-PK_1-F^+ cells, the CRC362 gene exhibited a pH-responsive induction that was equivalent to that of the endogenous PEPCK gene.

In order to measure the induction of the chimeric CRC362 transgene, quantitative real-time RT-PCR assays were developed using specific primer sets and differentially labeled Taqman probes to quantify the CRC362 and GAPDH mRNAs. Analysis of three clonal lines that stably express the integrated CRC362 gene demonstrated that expression of the CRC362 is increased 2.1 +/- 0.3 fold when the LLC-PK_1-F^+ cells are transferred to acidic medium for 24 h (**Appendix Fig. 5**). Northern blot analysis of the same RNA samples determined that the level of endogenous PEPCK mRNA is increased 2.0 +/- 0.4 fold. Thus, a reporter construct containing only 362 bp of the promoter along with all of the downstream exons and introns of the PEPCK gene is sufficient to recapitulate the full pH-responsive induction of the PEPCK gene. In an attempt to identify the segment of the PEPCK gene that contains the necessary downstream element, systematic deletions of this construct were also analyzed by quantitative real-time RT-PCR.

The analysis of quantitative real-time RT-PCR of -362 cDNA construct revealed that a necessary downstream element may reside within an exon (**Appendix Fig. 5**). The 3'-end of the sequence encoded in exon 10 contains elements that mediate the rapid turnover of the PEPCK mRNA [Hajarnis et al, 2005]. A minimal spacing between the 3'-untranslated region and the proximal promoter region may be crucial for normal turnover. This could explain the decreased expression of the very short $\triangle_1$*Bgl*II construct when the LLC-PK_1-FBPase$^+$ cells were transferred to acidic medium (0.61 +/- 0.15 fold). Analysis

of the $\triangle_2$*Bgl*II and $\triangle_1$*Sma*I deletion constructs suggested a downstream element is contained in either exon 9 or the 5'-end of exon 10. However, the $\triangle_2$*Sma*I construct lacks this region and it exhibits an even greater fold induction (3.7 +/- 1.3). Thus, an additional element may be located in the segment that contains introns 3, 4 and 5. This segment includes the region around +1900 bp that exhibits a nuclease hypersensitive region in chromatin isolated from rat kidney, but not from rat liver [Cissell et al, 1999]. Therefore, a kidney specific trans-activator may bind within this nuclease hypersensitive region. Alternatively, the regions deleted from the $\triangle_2$*Sma*I construct may contain a binding site for a transcriptional repressor. Deletion of a repressor element in $\triangle_2$*Sma*I could also result in the greater pH-responsive activation compared to the CRC362 construct. Thus, there may be multiple downstream cis-acting elements that are required to recapitulate the pH-response of the PEPCK gene.

The binding of C/EBP$_\beta$ [Liu et al, 2001], HNF-1 [Cassuto et al, 2003; Cassuto et al, 1997], and possibly activating protein-1 (AP-1), to the CRE-1, P2 and P3(II) elements, respectively, may account for the basal transcription of the PEPCK gene in kidney [Curthoys et al, 2001]. Transfer of LLC-PK$_1$-F$^+$ cells to an acidic medium leads to activation of the p38 mitogen-activated protein kinase (p38 MAPK) pathway and the phosphorylation of activating transcription factor ATF-2 [Feifel et al, 2002; O'Hayre et al, 2006]. The binding of phosphorylated ATF-2 to the CRE-1 element along with the binding of an unidentified factor to a downstream element may enhance the recruitment of a coactivator and polymerase II (Pol II), leading to activated transcription of PEPCK gene **(Appendix Fig. 6)**. Further studies are required to identify the specific downstream

elements and transcription factors that are necessary for the pH-responsive induction of renal PEPCK.

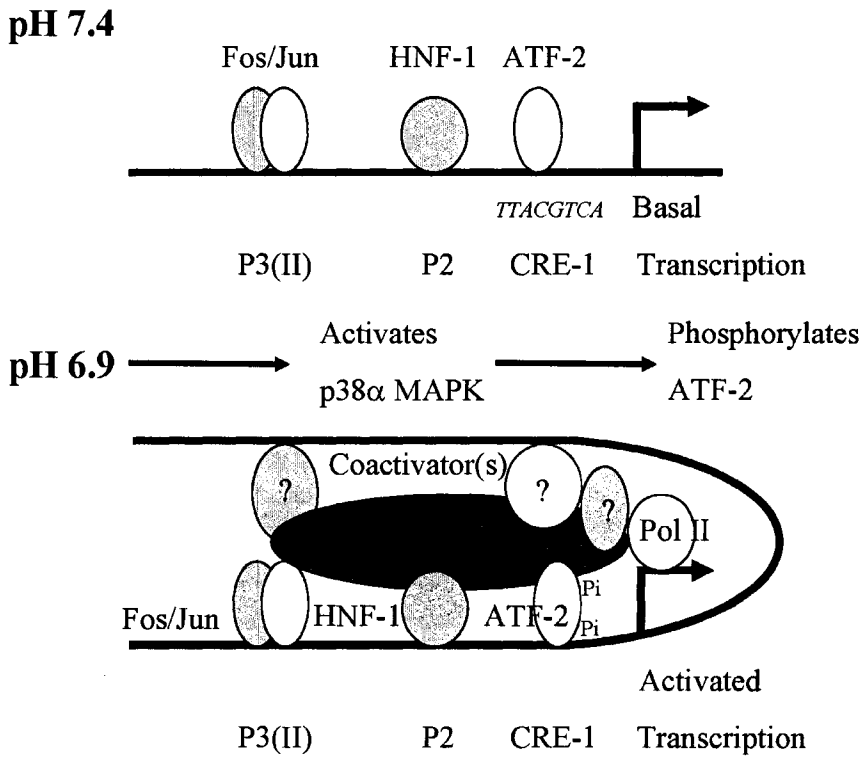

Appendix Fig. 6 Model of the pH-responsive induction of PEPCK mRNA transcription during metabolic acidosis. At pH 7.4, basal transcription of the PEPCK is mediated by binding of hepatocyte nuclear factor-1 (HNF-1) and possibly by c-Fos/c-JUN to the P2 and P3(II) elements, respectively. The CRE-1 site of the PEPCK promoter is occupied with either nonphosphorylated ATF-2 or C/EBP$_\beta$. The latter transcription factor mediates the cAMP-dependent activation of transcription [26]. A decrease in intracellular pH causes the activation of p38α MAPK and phosphorylation of ATF-2 [32, 33]. The activated ATF-2 may interact with one or more transcription factors that bind downstream. The resulting complex then recruits a coactivator that facilitates the recruitment of RNA polymerase II (Pol II) or modifies the nucleosomes that bind near the transcription start site, leading to activated transcription of the PEPCK mRNA.

Appendix 6. Acknowledgement

We wish to thank Dr. Leah Reshef (Developmental Biochemistry, Hebrew University-Hadassah Medical School, Jerusalem, Israel) and Dr. David Silversides (Veterinary Medicine, University of Montreal, Saint-Hyacinthe, Quebec, Canada) who generously provided the CRC362 construct and the porcine GAPDH plasmid (AF017079), respectively.

This research was supported in part by National Institute of Diabetes and Digestive and Kidney Diseases Grant DK-43704 awarded to N. P. Curthoys.

Appendix 7. Other experiments performed

Appendix 7.1 Transient transfection of genomic CRC362 construct

Transient transfection of the PEPCK transgene CRC362 was also performed to determine whether a pH-responsive induction could be quantified following transient transfection in LLC-PK_1-F^+ and LLC-PK_1-F^+-8C cells. LLC-PK_1-F^+-8C cells (8C) are a clonal line of LLC-PK_1-F^+ cells that were selected following transfection of a hygromycin resistance expression vector. In order to account for the differences in transfection efficiencies among the samples, 5 μg of RSV-β-globin was co-transfected with 5 μg CRC362. Expression of the CRC362 mRNA was verified by RT-PCR and quantified by real-time RT-PCR. A multiplex real-time PCR reaction with three different probes was extensively optimized, and the level of CRC362 mRNA was normalized to the level of the βG mRNA and the GAPDH mRNA. However, the pH-responsive induction (0.62 +/- 0.36) of the CRC362 was too variable to draw a conclusion (**Appendix Fig. 7 panel a**). This may be due to the large variation in the transfection efficiencies or alternatively, integration into chromatin as occurs in a stable transfection may be required to observe a pH-responsive induction.

Therefore, mixed populations of cells containing stably integrated CRC362 gene were also tested for the induction of the transgene following transfer to acidic medium for 24 h. Such cells exhibit a 1.40 +/- 0.14 fold induction of the transgene (**Figure 7 panel b**). These data indicate that indeed appropriate chromatin configuration may be required to recapitulate the pH-responsive induction of the PEPCK gene in LLC-PK_1-F^+ cells. Hence clonal lines that stably express the genomic CRC362 construct and the deletions

constructs were derived in LLC-PK_1-F^+ and tested using quantitative real-time PCR as described in the results section.

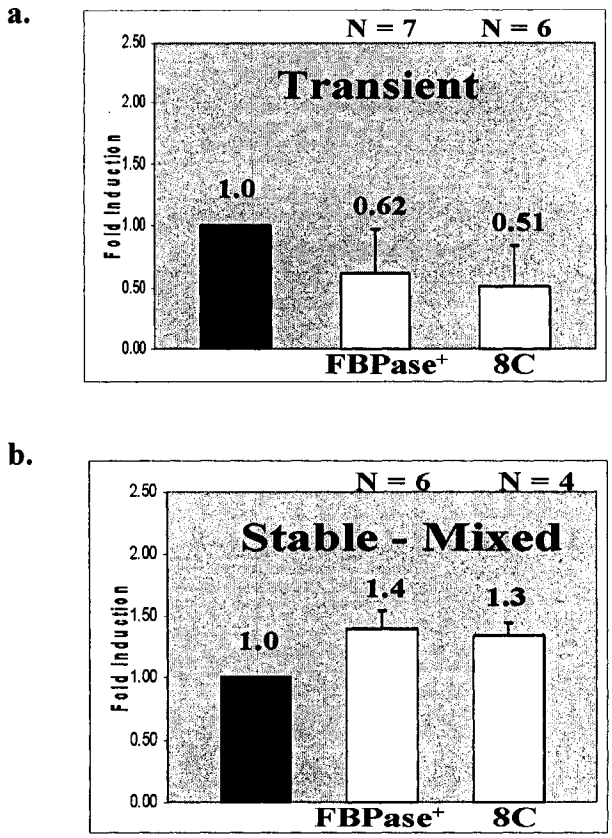

Appendix Fig. 7 Quantitative real-time RT-PCR analysis of CRC362 mRNA levels in transiently transfected and stably transfected mixed populations in LLC-PK_1-F^+ and LLC-PK_1-F^+-8C cells. **(Panel a)** The genomic CRC362 construct was transiently transfected into LLC-PK_1-F^+ cells or clonal LLC-PK_1-F^+-8C cells, and treated with normal (pH 7.4) or acidic (pH 6.9) medium. The levels of chimeric CRC362 and GAPDH mRNAs were determined using real-time RT-PCR. **(Panel b)** The levels of the chimeric CRC362 and GAPDH mRNAs, in mixed population of LLC-PK_1-F^+ and LLC-PK_1-F^+-8C cells, that stably express the genomic CRC362 construct were measured by real-time RT-PCR.

Appendix 7.2 Northern analysis of CRC362 deletion constructs

In order to identify the segment of the PEPCK gene that contains the downstream pH-responsive element, systematic deletions of the CRC362 construct were generated. Clonal lines that express each of the deletion constructs were derived and induction of the endogenous PEPCK mRNA was analyzed by northern blot analysis (**Appendix Fig. 8 panel a**). The cumulative northern blot data demonstrated that induction of the endogenous PEPCK mRNA in clonal cell lines of ranged from 1.2- to 2.5-fold induction, a level that is comparable to that previously observed in LLC-PK_1-F^+ cells (**Appendix Fig. 8 panel b**).

Appendix 7.3 TransFac analysis

The binding of phosphorylated ATF-2 to the CRE-1 element along with the binding of an unidentified factor to a downstream element may enhance the recruitment of a coactivator and polymerase II (Pol II), leading to activated transcription of PEPCK gene (**Appendix Fig. 6**). Hence, TransFac analysis was performed in order to identify putative transcription binding sites within exons 4-6 and exons 9-10 (**Appendix Fig. 9**). Western blot analysis of nuclear extracts prepared from LLC-PK_1-F^+ cells revealed the presence of high levels of both Sp1 and Sp3 transcription factors (**Appendix Fig. 10**). Treatment of THP-1 and 2F7 cells with SB203580, a p38 MAPK inhibitor, resulted in inhibition of Sp1 [Ma et al, 2001; Vega et al, 2004]. Therefore, it will be important to examine whether activation of p38 MAPK pathway in LLC-PK_1-F^+ cells by treatment with acidic medium leads to an increase level of Sp1. In addition, C/EBP_β and Sp1 act synergistically to fully trans-activate expression of the insulin-like growth factor II (IGF-II) gene [Palamarchuk et al, 2001]. Hence, Sp1 bound to a downstream element may interact with

C/EBP$_\beta$ at the proximal promoter to form a loop structure and trans-activate the basal and/or pH-responsive expression of PEPCK in LLC-PK$_1$-F$^+$ cells. TransFac analysis failed to identify potential transcriptional elements within introns 3, 4 or 5. Thus, further studies are required to test these hypotheses and to identify the specific downstream elements and transcription factors that are necessary for the pH-responsive induction of renal PEPCK.

a.

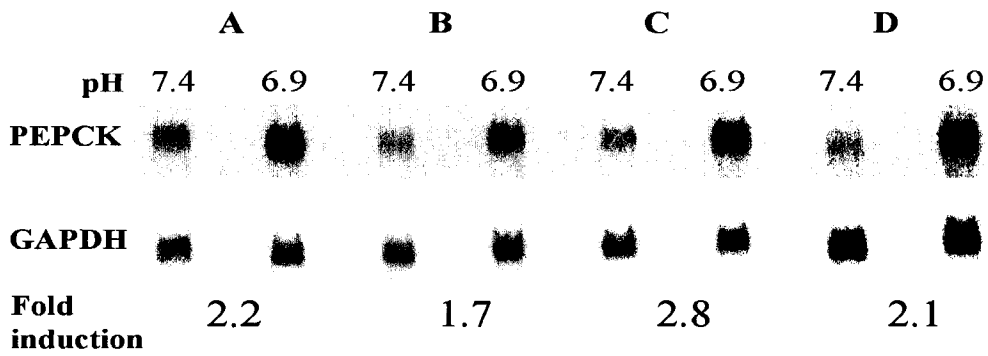

b.

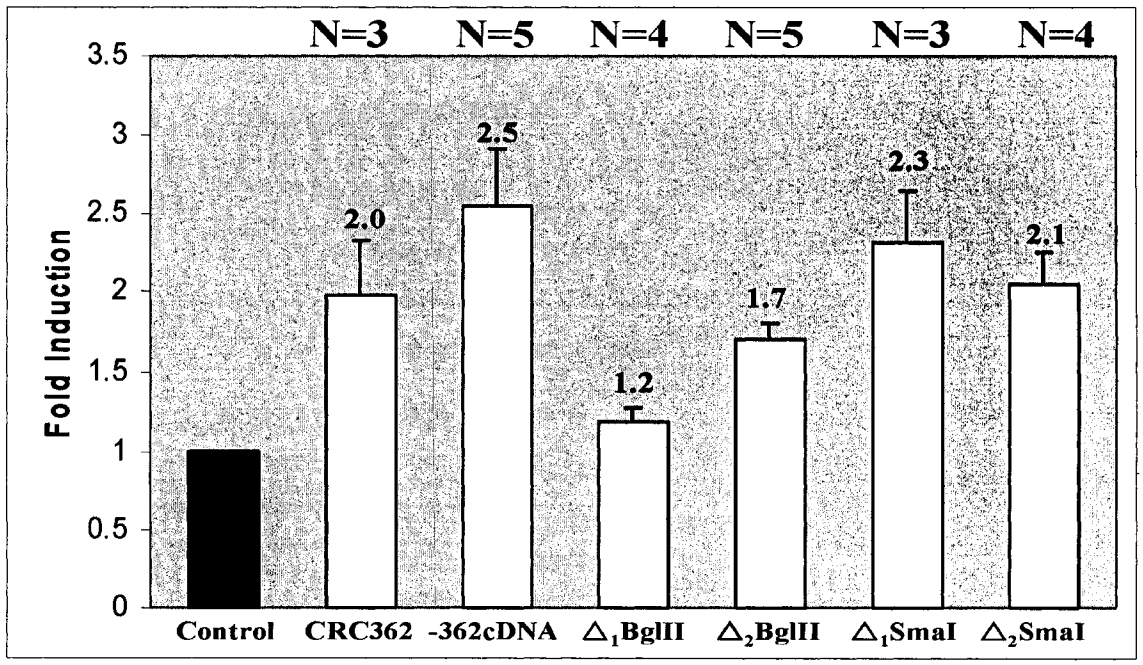

Appendix Fig. 8 Summary of the northern blot analysis of the pH-responsive induction of the endogenous PEPCK gene. The CRC362 deletion constructs were stably transfected into LLC-PK1-FBPase+ cells, and treated with normal (pH 7.4) or acidic (pH 6.9) medium for 24 h. The levels of the endogenous PEPCK and GAPDH mRNA were determined by northern blot analysis in clonal cells. The northern blot analysis of the Δ_2SmaI construct is shown as an example. Clonal lines are labeled as A-D (**Panel a**). A summary of the induction of the endogenous PEPCK mRNA in clonal cells that stably express the various CRC362 deletion constructs. N equals the number of cell lines analyzed (**Panel b**).

	Transcription factor	Sequence	Begin	End
Exon 4	**SP1**	TGGTGGCCAG	1744	1753
Exon 5	**C/EBPα, CREB**	CCTGCAACCC	2147	2156
	SP1	AGGAAGGGTG	2285	2294
	NF-1	GGGTGGCTGG	2290	2299
Exon 6	**CREB**	TGGCCATGAT	2971	2980
	T3R	ATGAACCCCA	2979	2988
Exon 9	**c-Jun**	CCATGAGATC	4701	4710
Exon 10	**SP1**	GGCCTGGGG	5160	5168

Appendix Fig. 9 TransFac Analysis. Comparison of the conserved sequence region of exons 4-6 and exons 9-10 from 3 species (mouse, rat, and human) revealed several putative sites for transcription factors that may enhance the recruitment of a coactivator, leading to activated transcription of PEPCK gene.

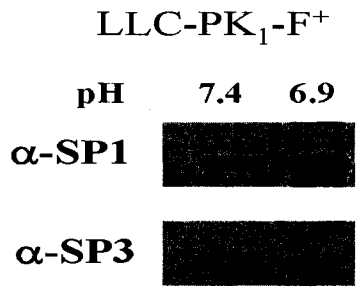

Appendix Fig. 10 Western blot analysis of Sp1 and Sp3 in LLC-PK$_1$-F$^+$ cells. Nuclear extracts harvested from LLC-PK$_1$-F$^+$ cells that had been grown in normal medium (pH 7.4, 25 mM HCO_3^-) or transferred to acidic medium (pH 6.9, 10 mM HCO_3^-) for 24 h, and subjected to western blot analysis using α-Sp1 and α-Sp3 antibodies.

References

Ackerman, J.J., Lowry, M, Radda, G.K., Ross, D., and Wong, G.G. The role of intrarenal pH in regulation of ammoniagenesis: [^{31}P]NMR studies of the perfused rat kidney. *J. Physiol.* 1981 319:65-79.

Anderson P, Kedersha N. RNA granules. *J Cell Biol.* 2006 Mar 13;172(6):803-8. Epub 2006 Mar 6.

Aruga S, Wehrli S, Kaissling B, Moe OW, Preisig PA, Pajor AM, Alpern RJ. Chronic metabolic acidosis increases NaDC-1 mRNA and protein abundance in rat kidney. *Kidney Int.* 2000 Jul;58(1):206-15.

Baggs JE, Green CB. Nocturnin, a deadenylase in Xenopus laevis retina: a mechanism for posttranscriptional control of circadian-related mRNA. *Curr Biol.* 2003 Feb 4;13(3):189-98.

Banner, C., Hwang, J-J., Shapiro, R.A., Wenthold, R.J., Lampel, K.A., Nakatani, Y., Thomas, J.W., Huie D., and Curthoys, N.P. Isolation of a cDNA for rat brain glutaminase. *Molec. Brain Res.* 1988 3:247-254.

Barreau C, Paillard L, Osborne HB. AU-rich elements and associated factors: are there unifying principles? *Nucleic Acids Res.* 2006 Jan 3;33(22):7138-50.

Bashkirov VI, Scherthan H, Solinger JA, Buerstedde JM, Heyer WD. A mouse cytoplasmic exoribonuclease (mXRN1p) with preference for G4 tetraplex substrates. *J Cell Biol.* 1997 Feb 24;136(4):761-73.

Bianchin C, Mauxion F, Sentis S, Seraphin B, Corbo L. Conservation of the deadenylase activity of proteins of the Caf1 family in human. *RNA.* 2005 Apr;11(4):487-94.

Binder R, Horowitz JA, Basilion JP, Koeller DM, Klausner RD, Harford JB. Evidence that the pathway of transferrin receptor mRNA degradation involves an endonucleolytic cleavage within the 3' UTR and does not involve poly(A) tail shortening. *EMBO J.* 1994 Apr 15;13(8):1969-80.

Bradford MM. A rapid and sensitive method for the quantitation of microgram quantities of protein utilizing the principle of protein-dye binding. *Anal Biochem.* 1976 May 7;72:248-54.

Brandsch, M., Brandsch, C., Prasad, P., Ganapathy, V., Hopfer, U. And Leibach, F. Identification of a renal cell line that constitutively expresses the kidney-specific high-affinity H^+/peptide cotransporter. *FASEB Journal.* 1995 Nov;9(14):1489-96.

Brosnan, J.T., P. Vinay, A. Gougoux, and M.L. Halperin. Renal ammonia production and its implications for acid-base balance. In. *pH Homeostasis-Mechanism and Control,* edited b D. Haussinger. New York: Academic Press, 1988 28-304.

Brown CE, Tarun SZ Jr, Boeck R, Sachs AB. PAN3 encodes a subunit of the Pab1p-dependent poly(A) nuclease in Saccharomyces cerevisiae. *Mol Cell Biol.* 1996 Oct;16(10):5744-53

Burch, H. B., Narins, R. G., Chu, C., Fagioli, S., Choi, S., McCarthy, W. and Lowry, O. H. Distribution along the rat nephron of three enzymes of gluconeogenesis in acidosis and starvation. *Am J Physiol* 1978 235, F246-F253.

Caput D, Beutler B, Hartog K, Thayer R, Brown-Shimer S, Cerami A. Identification of a common nucleotide sequence in the 3'-untranslated region of mRNA molecules specifying inflammatory mediators. *Proc Natl Acad Sci* U S A. 1986 Mar;83(6):1670-4.

Cassuto, H., Olswang, Y., Livoff, A. F., Nechushtan, H., Hanson, R. W. and Reshef, L. Involvement of HNF-1 in the regulation of phosphoenolpyruvate carboxykinase gene expression in the kidney. *FEBS Lett* 1997 412, 597-602.

Cassuto, H., Olswang, Y., Heinemann, S., Sabbagh, K., Hanson, R. W. and Reshef, L. The transcriptional regulation of phosphoenolpyruvate carboxykinase gene in the kidney requires the HNF-1 binding site of the gene. *Gene* 2003 318, 177-184.

Carballo E, Lai WS, Blackshear PJ. Feedback inhibition of macrophage tumor necrosis factor-alpha production by tristetraprolin. *Science.* 1998 Aug 14;281(5379):1001-5.

Chen, C. and Okayama, H. High-efficiency transformation of mammalian cells by plasmid DNA. *Mol. Cell Biol.* 1987 7, 2745-2752.

Chen, CY.A. and Shyu, AB. AU-rich elements: characterization and importance in mRNA degradation. *Trends Biochem. Sci.* 1995 20:465-470.

Chen CY, Xu N, Zhu W, Shyu AB. Functional dissection of hnRNP D suggests that nuclear import is required before hnRNP D can modulate mRNA turnover in the cytoplasm. *RNA.* 2004 Apr;10(4):669-80.

Chen CY, Gherzi R, Ong SE, Chan EL, Raijmakers R, Pruijn GJ, Stoecklin G, Moroni C, Mann M, Karin M. AU binding proteins recruit the exosome to degrade ARE-containing mRNAs. *Cell.* 2001 Nov 16;107(4):451-64.

Chen J, Rappsilber J, Chiang YC, Russell P, Mann M, Denis CL. Purification and characterization of the 1.0 MDa CCR4-NOT complex identifies two novel components of the complex. *J Mol Biol.* 2001 Dec 7;314(4):683-94.

Cimbala, M.A., Lamers, W.H., Nelson, K. and Monahan J.E., Yoo-Warren, H. and Hansen, R.W. Rapid change in the concentration of phosphoenolpyruvate carboxykinase mRNA in rat liver and kidney. Effects of insulin and cyclic AMP. *J. Biol. Chem.* 1982 257:7629-7636.

Cissell, M. A. and Chalkley, R. Characterization of a kidney-specific pattern of chromatin structure in the rat phosphoenolpyruvate carboxykinase gene. *Biochim Biophys Acta* 1999 1445, 299-31328.

Curthoys, N. P. and Lowry, O. H. The distribution of glutaminase isoenzymes in the various structures of the nephron in normal, acidotic and alkalotic rat kidney. *J. Biol. Chem.* 1973 248, 162-168.

Curthoys, N. P. and M. Watford. Regulation of glutaminase activity and metabolism. *Annu. Rev. Nutr. 1995* 15:133-159.

Curthoys, N. P. and Gstraunthaler, G. Mechanism of increased renal gene expression during metabolic acidosis. *Am J Physiol Renal Physiol 2001* 281, F381-F390.

D'Alessio, J. M., Harris, G. H., Perna, P. J. and Paule, M. R. Ribosomal ribonucleic acid repeat unit of Acanthamoeba castellanii: cloning and restriction endonuclease map. *Biochemistry* 1981 20, 3822-3827.

Dang Y, Kedersha N, Low WK, Romo D, Gorospe M, Randal K, Anderson P, Liu JO. Eukaryotic initiation factor 2alpha independent pathway of stress granule induction by the natural product pateamine A. *J Biol Chem.* 2006 Sep 2;

de Moor CH, Richter JD. Translational control in vertebrate development. *Int Rev Cytol.* 2001;203:567-608.

Dean JL, Wait R, Mahtani KR, Sully G, Clark AR, Saklatvala J. The 3' untranslated region of tumor necrosis factor alpha mRNA is a target of the mRNA-stabilizing factor HuR. *Mol Cell Biol.* 2001 Feb;21(3):721-30. Erratum in: *Mol Cell Biol.* 2005 Apr;25(8):3400.

Dehlin E, Wormington M, Korner CG, Wahle E. Cap-dependent deadenylation of mRNA. *EMBO J.* 2000 Mar 1;19(5):1079-86.

DeMaria CT, Brewer G. AUF1 binding affinity to A+U-rich elements correlates with rapid mRNA degradation. *J Biol Chem.* 1996 May 24;271(21):12179-84.

Dember LM, Kim ND, Liu KQ, Anderson P. Individual RNA recognition motifs of TIA-1 and TIAR have different RNA binding specificities. *J Biol Chem.* 1996 Feb 2;271(5):2783-8.

Denis CL, Chen J. The CCR4-NOT complex plays diverse roles in mRNA metabolism. *Prog Nucleic Acid Res Mol Biol.* 2003;73:221-50.

Drewnowsk, K., Craig, M., Digiovanni, S., McCarty, J., Moorman, A., Lamars, W. and Schoolwerth, A. C. PEPCK mRNA localization in proximal tubule and gene regulation during metabolic acidosis. *J. Physiol. Phram.* 2002 53, 3-20.

Eisenberger, C. L., Nechushtan, H., Cohen, H., Shani, M. and Reshef, L Differential regulation of the rate phosphoenolpyruvate carboxykinase gene expression in several tissues of transgenic mice. *Mol. Cell Biol.* 1992 12, 1396-1403.

Fan XC, Steitz JA. Overexpression of HuR, a nuclear-cytoplasmic shuttling protein, increases the in vivo stability of ARE-containing mRNAs. EMBO J. 1998 Jun 15;17(12):3448-60.

Feifel, E., Obexer, P., Andratsch, M., Euler, S., Taylor, L., Tang, A., Wei, Y., Schramek, H., Curthoys, N. P. and Gstraunthaler, G. p38 MAPK mediates the acid-induced transcription of phospho*enol*pyruvate carboxykinase in LLC-PK_1-$FBPase^+$ cells. *Am J Physiol Renal Physiol* 2002 283, F678-F688.

Fenger-Gron M, Fillman C, Norrild B, Lykke-Andersen J. Multiple processing body factors and the ARE binding protein TTP activate mRNA decapping. *Mol Cell.* 2005 Dec 22;20(6):905-15.

Ford, L.P., Bagga, P.S. and Wilusz, J.. The poly-A tail inhibits the assembly of a 3' to 5' exonuclease in an in vitro RNA stability system. *Mol. Cell. Biol.* 1997 17:398-406.

Ford, L.P. and Wilusz, J. An in-vitro system using HeLa cytoplasmic extracts that reproduces regulated mRNA stability. *Methods* 1999 17:21-27.

Gagna CE, Chen JH, Kuo HR, Lambert WC. Binding properties of bovine ocular lens zeta-crystallin to right-handed B-DNA, left-handed Z-DNA, and single-stranded DNA. *Cell Biol Int.* 1998;22(3):217-25.

Gallouzi IE, Brennan CM, Stenberg MG, Swanson MS, Eversole A, Maizels N, Steitz JA. HuR binding to cytoplasmic mRNA is perturbed by heat shock. Proc Natl Acad Sci U S A. 2000 Mar 28;97(7):3073-8.

Gao M, Fritz DT, Ford LP, Wilusz J. Interaction between a poly(A)-specific ribonuclease and the 5' cap influences mRNA deadenylation rates in vitro. *Mol Cell.* 2000 Mar;5(3):479-88.

Gao M, Wilusz CJ, Peltz SW, Wilusz J. A novel mRNA-decapping activity in HeLa cytoplasmic extracts is regulated by AU-rich elements. *EMBO J.* 2001 Mar 1;20(5):1134-43.

Gringhuis SI, Garcia-Vallejo JJ, van Het Hof B, van Dijk W. Convergent actions of I kappa B kinase beta and protein kinase C delta modulate mRNA stability through phosphorylation of 14-3-3 beta complexed with tristetraprolin. *Mol Cell Biol.* 2005 Aug;25(15):6454-63.

Gstraunthaler, G. and Handler, J. S. Isolation, growth and characterization of a gluconeogenic strain of renal cells. *Am. J. Physiol.* 1987 252, C232-C238.

Gstraunthaler, G., Holcomb, T., Feifel, E., Liu, W., Spitaler, N. and Curthoys, N. P. Differential expression and acid-base regulation of glutaminase mRNAs in gluconeogenic LLC-PK_1-$FBPase^+$ cells. *Am. J. Physiol. Renal Physiol.* 2000 278, F227-237.

Guyton-Arthur, C.I. and Hall, John E. In: *Medical Physiology.*, edited by W.B. Saunders. New York: Harcourt Health, 9th ed., 1996 Chap. 30, 385-403.

Hajarnis, S., Schroeder, JM, Curthoys, NP. 3'-Untranslated region of phosphoenolpyruvate carboxykinase mRNA contains multiple instability elements that bind AUF1.*J Biol Chem.* 2006Aug 5;280(31):28272-80.

Hansen, W.R., Barsic-Tress, N., Taylor, L and Curthoys, N.P. The 3' untranslated region of the rat renal glutaminase mRNA contains a pH-responsive stability element. *Am. J. Physiol.* 1996 271:F126-F131.

Hanson, R. W. and Patel, Y. M. Phosphoenolpyruvate carboxykinase (GTP): The gene and the enzyme. *Adv. Enzymol. Relat. Areas Mol. Biol.* 1994 69, 203-281.

He, C., and Schneider, R. 14-3-3a is a p37 AUF1j-binding protein that facilitates AUF1 transcport and AU-rich mRNa decay. *The EMBO Journal.* 2006 25, 3823-3831.

Holcomb, T., Curthoys, N. P. and Gstraunthaler, G. Subcellular localization of PEPCK and metabolism of gluconeogenic substrains of renal cell lines. *Am. J. Physiol.* 1995 268, C449-C457.

Holcomb, T., Liu, W., Snyder, R., Shapiro, R. and Curthoys, N. P. Promoter elements which mediate the pH-response of phosphoenolpyruvate carboxykinase mRNA in LLC-PK_1-F^+ cells. *Am. J. Physiol.* 1996 271, F340-F346.

Horie S, Moe O, Tejedor A, Alpern RJ. Preincubation in acid medium increases Na/H antiporter activity in cultured renal proximal tubule cells. *Proc Natl Acad Sci* U S A. 1990 Jun;87(12):4742-5.

Hughey, R.P., B.B. Rankin, N.P. Curthoys. Acute acidosis and renal arteriovenous differences of glutamine in normal and adrenalectomized rats. *Am. J. Physiol.* 1980 238:F199-F204.

Hwang, J-J., Perera, S., Shapiro, R.A., Curthoys, N.P. Mechanism of altered renal glutaminase expression in response to chronic acidosis. *Biochemistry* 1991a 30:7522-7526.

Hwang, J.J. and Curthoys, N.P. Effect of acute alterations in acid-base balance on rat renal glutaminase and phosphoenolpyruvate carboxykinase gene expression. *J. Biol. Chem.* 1991b 266:9892-9896.

Karinch, A. M., Lin, C. M., Wolfgang, C. L., Pan, M. and Souba, W. W. Regulation of expression of the SN1 transporter during renal adaptation to chronic metabolic acidosis in rats. *Am. J. Physiol. Renal Physiol.* 2002 283, F1011-F1019.

Khanna R, Kiledjian M. Poly(A)-binding-protein-mediated regulation of hDcp2 decapping in vitro. *EMBO J.* 2004 May 5;23(9):1968-76.

Kedersha N., Stoecklin G., Ayodele M., Yacono P., Lykke-Andersen J., Fitzler M.J., Scheuner D., Kaufman R.J., Golan D.E., Anderson P. Stress granules and processing bodies are dynamically linked sites of mRNP remodeling. *J Cell Biol.* 2005 Jun 20;169(6):871-84.

Kiledjian M, DeMaria CT, Brewer G, Novick K.Identification of AUF1 (heterogeneous nuclear ribonucleoprotein D) as a component of the alpha-globin mRNA stability complex. *Mol Cell Biol.* 1997 Aug;17(8):4870-6.

Kushner SR. mRNA decay in prokaryotes and eukaryotes: different approaches to a similar problem. *IUBMB Life.* 2004 Oct;56(10):585-94.

Hentze MW. Enzymes as RNA-binding proteins: a role for (di)nucleotide-binding domains? *Trends Biochem Sci.* 1994 Mar;19(3):101-3.

Ingelfinger D, Arndt-Jovin DJ, Luhrmann R, Achsel T. The human LSm1-7 proteins colocalize with the mRNA-degrading enzymes Dcp1/2 and Xrnl in distinct cytoplasmic foci. *RNA.* 2002 Dec;8(12):1489-501.

Iynedjian, P.B., Ballard, F.J. and Hanson, R.W. The regulation of phosphoenolpyruvate carboxykinase (GTP) synthesis s in rat kidney cortex. The role of acid-base balance and glucocorticoids. *J. Biol. Chem.* 1975 250:5596-5603.

Janicki SM, Tsukamoto T, Salghetti SE, Tansey WP, Sachidanandam R, Prasanth KV, Ried T, Shav-Tal Y, Bertrand E, Singer RH, Spector DL. From silencing to gene expression: real-time analysis in single cells. *Cell.* 2004 Mar 5;116(5):683-98.

Jornvall H, Persson B, Jeffery J. Characteristics of alcohol/polyol dehydrogenases. The zinc-containing long-chain alcohol dehydrogenases. *Eur J Biochem.* 1987 Sep 1;167(2):195-201.

Jornvall H, Persson B, Du Bois GC, Lavers GC, Chen JH, Gonzalez P, Rao PV, Zigler JS Jr. Zeta-crystallin versus other members of the alcohol dehydrogenase super-family. Variability as a functional characteristic. *FEBS Lett.* 1993 May 17;322(3):240-4.

Labow, B., Souba, W. Glutamine, *World J. Surg.* 2000 24, 1503-1513.

Lai WS, Kennington EA, Blackshear PJ. Tristetraprolin and its family members can promote the cell-free deadenylation of AU-rich element-containing mRNAs by poly(A) ribonuclease. *Mol Cell Biol.* 2003 Jun;23(11):3798-812.

Laterza, O.F., Hansen, W. R., Taylor, L., and Curthoys, N.P. Identification of an mRNA-binding protein and the specific elements that may mediate the pH-responsive induction of renal glutaminase mRNA. *J. Biol. Chem.* 1997 272:22481-22488.

Laterza, O. F. and Curthoys, N. P. Specificity and functional analysis of the pH-responsive element within renal glutaminase mRNA. *Am. J. Physiol. Renal Physiol.* 2000 278, F970-F977.

Liu H, Rodgers ND, Jiao X, Kiledjian M. The scavenger mRNA decapping enzyme DcpS is a member of the HIT family of pyrophosphatases. *EMBO J.* 2002 Sep 2;21(17):4699-708.

Liu J, Hanson RW. Regulation of phosphoenolpyruvate carboxykinase (GTP) gene transcription. *Mol Cell Biochem.* 1991 May 29-Jun 12;104(1-2):89-100.

Liu J, Valencia-Sanchez MA, Hannon GJ, Parker R. MicroRNA-dependent localization of targeted mRNAs to mammalian P-bodies. *Nat Cell Biol.* 2005a Jul;7(7):719-23.

Liu J, Rivas FV, Wohlschlegel J, Yates JR 3rd, Parker R, Hannon GJ. A role for the P-body component GW182 in microRNA function. *Nat Cell Biol.* 2005b Dec;7(12):1261-6.

Liu, X., Wall, Q. T., Taylor, L. and Curthoys, N. P. C/EBP$_\beta$ mediates cAMP-activated transcription of phosphoenolpyruvate carboxykinase in LLC-PK$_1$-F$^+$ cells. *Am. J. Physiol. Renal. Physiol.* 2001 281, F649-F657.

Loflin P, Chen CY, Shyu AB. Unraveling a cytoplasmic role for hnRNP D in the in vivo mRNA destabilization directed by the AU-rich element. *Genes Dev.* 1999 Jul 15;13(14):1884-97.

Lowry M, Ross BD. Activation of oxoglutarate dehydrogenase in the kidney in response to acute acidosis. *Biochem J.* 1980 Sep 15;190(3):771-80.

Lykke-Andersen J. Identification of a human decapping complex associated with hUpf proteins in nonsense-mediated decay. *Mol Cell Biol.* 2002 Dec;22(23):8114-21.

Lykke-Andersen J, Wagner E. Recruitment and activation of mRNA decay enzymes by two ARE-mediated decay activation domains in the proteins TTP and BRF-1. *Genes Dev.* 2005 Feb 1;19(3):351-61.

Ma W, Lim W, Gee K, Aucoin S, Nandan D, Kozlowski M, Diaz-Mitoma F, Kumar A. The p38 mitogen-activated kinase pathway regulates the human interleukin-10 promoter via the activation of Sp1 transcription factor in lipopolysaccharide-stimulated human macrophages. *J Biol Chem.* 2001 Apr 27;276(17):13664-74. Epub 2001 Jan 26.

Martinez J, Ren YG, Nilsson P, Ehrenberg M, Virtanen A. The mRNA cap structure stimulates rate of poly(A) removal and amplifies processivity of degradation. *J Biol Chem.* 2001 Jul 27;276(30):27923-9.

McGrane, M. M., Yun, J. S., Moorman, A. F., Lamers, W. H., Hendrick, G. K., Arafah, B. M., Park, E. A., Wagner, T. E. and Hanson, R. W. Metabolic effects of developmental, tissue-, and cell-specific expression of a chimeric phosphoenolpyruvate carboxykinase (GTP)/bovine growth hormone gene in transgenic mice. *J. Biol. Chem.* 1990 265, 22371-22379.

McGrane, M. M., de Vente, J., Yun, J., Bloom, J., Park, E., Wynshaw-Boris, A., Wagner, T., Rottman, F. M. and Hanson, R. W. Tissue-specific expression and dietary regulation of a chimeric phosphoenolpyruvate carboxykinase/bovine growth hormone gene in transgenic mice. *J. Biol. Chem.* 1988 263, 11443-11451.

Medina, MA. Glutamine and cancer. *J Nutr.* 2001 Sep;131(9 Suppl):2539S-42S; discussion 2550S-1S.

Ming XF, Stoecklin G, Lu M, Looser R, Moroni C. Parallel and independent regulation of interleukin-3 mRNA turnover by phosphatidylinositol 3-kinase and p38 mitogen-activated protein kinase. *Mol Cell Biol.* 2001 Sep;21(17):5778-89.

Mithieux, G. New data and concepts on glutamine and glucose metabolism in the gut. *Curr Opin Clin Nutr Metab Care.* 2001 Jul;4(4):267-71.

Mukherjee D, Gao M, O'Connor JP, Raijmakers R, Pruijn G, Lutz CS, Wilusz J. The mammalian exosome mediates the efficient degradation of mRNAs that contain AU-rich elements. *EMBO J.* 2002 Jan 15;21(1-2):165-74.

Neu, J., Shenoy, V., Chakrabarti, R. Glutamine nutrition and metabolism: where do we go from here? *Faseb J.* 1996 10:829-837.

Newsholme P. Why is L-glutamine metabolism important to cells of the immune system in health, postinjury, surgery or infection? *J Nutr.* 2001 Sep;131(9 Suppl):2515S-22S; discussion 2523S-4S.

Niranjanakumari S, Lasda E, Brazas R, Garcia-Blanco MA. Reversible cross-linking combined with immunoprecipitation to study RNA-protein interactions *in vivo*. *Methods.* 2002 Feb;26(2):182-90

Nyborg, J., and Peersen, Olve. That zincing feeling: the effects of EDTA on the behavior of zinc-binding transcriptional regulators. *Biochem. Journal* 2004 381, e3-e4.

O'Hayre, M., Taylor, L., Andratsch, M., Feifel, E., Gstraunthaler, G. and Curthoys, N. P. Effects of constitutively active and dominant negative MKK3 and MKK6 on the pH-responsive increase in phosphoenolpyruvate carboxykinase mRNA. *J. Biol. Chem.* 2006 281, 2982-2988.

Palamarchuk AY, Kavsan VM, Sussenbach JS, Holthuizen PE. The chum salmon insulin-like growth factor II promoter requires Sp1 for its activation by C/EBPbeta. *Mol Cell Endocrinol.* 2001 Feb 14;172(1-2):57-67.

Pastori RL, Moskaitis JE, Schoenberg DR. Estrogen-induced ribonuclease activity in Xenopus liver. *Biochemistry.* 1991 Oct 29;30(43):10490-8.

Peng, Y., Amemiya, M., Yang, X., Fan, L., Moe, O. W., Yin, H., Preisig, P. A., Yanagisawa, M., and Alpern, R. J. (2001) *Am J Physiol Renal Physiol* 280(1), F34-42.

Peng SS, Chen CY, Xu N, Shyu AB. RNA stabilization by the AU-rich element binding protein, HuR, an ELAV protein. *EMBO J.* 1998 Jun 15;17(12):3461-70.

Perera, S.Y., Chen, T.C., Curthoys, N.P. Biosynthesis and processing of renal mitochondrial glutaminase in cultured proximal tubular epithelial cells and in isolated mitochondria. *J. Biol. Chem.* 1990 265:17764-70.

Perera, S.Y., Voith, D.M., Curthoys, N.P. Biosynthesis and processing of mitochondrial glutaminase in HTC hepatoma cells. *Biochem. J.* 1991 273:265-270.

Petersen DD, Magnuson MA, Granner DK. Location and characterization of two widely separated glucocorticoid response elements in the phosphoenolpyruvate carboxykinase gene. *Mol Cell Biol.* 1988 Jan;8(1):96-104.

Pfaffl M.W. A new mathematical model for relative quantification in real-time RT-PCR. *Nucleic Acids Res.* 2001 May 1;29(9):e45.

Phillips RS, Ramos SB, Blackshear PJ Members of the tristetraprolin family of tandem CCCH zinc finger proteins exhibit CRM1-dependent nucleocytoplasmic shuttling. *J Biol Chem.* 2002 Mar 29;277(13):11606-13.

Porter LD, Ibrahim H, Taylor L, Curthoys NP. Complexity and species variation of the kidney-type glutaminase gene. *Physiol Genomics*. 2002 9(3):157-66. Epub 2002 Apr 16.

Preisig, P. A. and Alpern, R. J. Chronic metabolic acidosis causes adaptation in the apical membrane Na/H antiporter and basolateral Na(HCO_3)3 symporter in the rat proximal convoluted tubule. *J. Clin. Invest.* 1988 82, 1445-1453.

Raineri I, Wegmueller D, Gross B, Certa U, Moroni C. Roles of AUF1 isoforms, HuR and BRF1 in ARE-dependent mRNA turnover studied by RNA interference. *Nucleic Acids Res*. 2004 Feb 19;32(4):1279-88.

Raijmakers R, Egberts WV, van Venrooij WJ, Pruijn GJ. Protein-protein interactions between human exosome components support the assembly of RNase PH-type subunits into a six-membered PNPase-like ring. *J Mol Biol*. 2002 Nov 1;323(4):653-63.

Raijmakers R, Schilders G, Pruijn GJ. The exosome, a molecular machine for controlled RNA degradation in both nucleus and cytoplasm. *Eur J Cell Biol*. 2004 Jul;83(5):175-83.

Rao PV, Gonzalez P, Persson B, Jornvall H, Garland D, Zigler JS Jr. Guinea pig and bovine zeta-crystallins have distinct functional characteristics highlighting replacements in otherwise similar structures. *Biochemistry*. 1997 May 6;36(18):5353-62.

Raghavan A, Robison RL, McNabb J, Miller CR, Williams DA, Bohjanen PR. HuA and tristetraprolin are induced following T cell activation and display distinct but overlapping RNA binding specificities. *J Biol Chem*. 2001 Dec 21;276(51):47958-65.

Ren YG, Kirsebom LA, Virtanen A. Coordination of divalent metal ions in the active site of poly(A)-specific ribonuclease. *J Biol Chem*. 2004 Nov 19;279(47):48702-6.

Rigby WF, Roy K, Collins J, Rigby S, Connolly JE, Bloch DB, Brooks SA. Structure/function analysis of tristetraprolin (TTP): p38 stress-activated protein kinase and lipopolysaccharide stimulation do not alter TTP function. *J Immunol*. 2005 Jun 15;174(12):7883-93.

Rognstad R. Rate-limiting steps in metabolic pathways. *J Biol Chem*. 1979 Mar 25;254(6):1875-8.

Roesler, W. J., Vandenbark, G. R. and Hanson, R. W. Identification of multiple protein binding domains in the promoter-regulatory region of the phosphoenolpyruvate carboxykinase (GTP) gene. *J. Biol. Chem.* 1989 264, 9657-9664.

Ross, J. mRNA stability in mammalian cells. *Microbiol. Rev.* 1995 59:423-450.

Rutkowski DT, Kaufman RJ. A trip to the ER: coping with stress. *Trends Cell Biol.* 2004 Jan;14(1):20-8

Sahai, A., Laughrey, E. and Tannen, R.L. Relationship between intracellular pH and ammonia metabolism in LLC-PK_1 cells. *Am. J. Physiol.* 1990 258:F103-F108.

Sarkar B, Xi Q, He C, Schneider RJ.Selective degradation of AU-rich mRNAs promoted by the p37 AUF1 protein isoform. *Mol Cell Biol.* 2003 Sep;23(18):6685-93.

Sastrasinh, S. and Sastrasinh, M. Glutamine transport in submitochondrial particles. *Am. J. Physiol.* 1989 257, F1050-F1058.

Schroeder JM, Ibrahim H, Taylor L, Curthoys NP. Role of deadenylation and AUF1 binding in the pH-responsive stabilization of glutaminase mRNA. Am J Physiol Renal Physiol. 2006 Mar;290(3):F733-40.

Seal, R., Temperley, R., Wilusz, J., Lightowlers R. and Chrzanowska-Lightowlers, M. A. Serum-deprivation stimulates cap-binding by PARN at the expense of eIF4E, consistent wih the observed decrease in mRNA stability. *Nucleic Acids Research.* 2005 Vol. 33. No. 1: 376-387.

Sen GL, Blau HM. Argonaute 2/RISC resides in sites of mammalian mRNA decay known as cytoplasmic bodies. *Nat Cell Biol.* 2005 Jun;7(6):633-6.

Shav-Tal Y, Darzacq X, Shenoy SM, Fusco D, Janicki SM, Spector DL, Singer RH. Dynamics of single mRNPs in nuclei of living cells. *Science.* 2004 Jun 18;304(5678):1797-800.

Sheth U, Parker R. Decapping and decay of messenger RNA occur in cytoplasmic processing bodies. Science. 2003 May 2;300(5620):805-8.

Silbernagl S. Tubular reabsorption of L-glutamine studied by free-flow micropuncture and microperfusion of rat kidney. *Int J Biochem.* 1980;12(1-2):9-16.

Squires, E.J., D.E. Hall and J.T. Brosnan. Arterovenous differences for amino acids and lactate across kidneys of normal and acidic rats. *Biochem. J.* 1996 160:125-128.

Stoecklin, G., Stubbs, T., Kedersha, N., Wax, S., Ribgy, W., Balckwell, T. and Anderson, P. MK2-induced tristetraprolin:14-3-3 complexes prevent stress granule association and ARE-mRNA binding decay. *The EMBO Journal.* 2004 23, 1313-1324.

Sully G, Dean JL, Wait R, Rawlinson L, Santalucia T, Saklatvala J, Clark AR. Structural and functional dissection of a conserved destabilizing element of cyclo-oxygenase-2 mRNA: evidence against the involvement of AUF-1 [AU-rich element/poly(U)-binding/degradation factor-1], AUF-2, tristetraprolin, HuR (Hu antigen R) or FBP1 (far-upstream-sequence-element-binding protein 1). *Biochem J.* 2004 Feb 1;377(Pt 3):629-39.

Sun HW, Plapp BV. Progressive sequence alignment and molecular evolution of the Zn-containing alcohol dehydrogenase family. *J Mol Evol.* 1992 Jun;34(6):522-35.

Tang, A. and Curthoys, N.P.. Identification of □-crystallin/NADPH:quinone reductase as a renal glutaminase mRNA pH-response element binding protein. *J. Biol. Chem.* 2001 276:21375-21380.

Tannen, R. L. Renal ammonia production and excretion. In: *Handbook of Physiology. Renal Physiology*, edited by J. Orloff and R.W. Berliner. Oxford, UK: Oxford Univ. Press, 1993 Vol. I, Sect. 8, Chap. 23, 1017-1059.

Taylor GA, Thompson MJ, Lai WS, Blackshear PJ. Phosphorylation of tristetraprolin, a potential zinc finger transcription factor, by mitogen stimulation in intact cells and by mitogen-activated protein kinase in vitro. *J Biol Chem.* 1995 Jun 2;270(22):13341-7.

Taylor, L. and Curthoys, N. P. Glutamine metabolism: role in acid-base balance. *Biochem. Molec Biol. Ed.* 2004 32, 291-304.

Tchen CR, Brook M, Saklatvala J, Clark AR. The stability of tristetraprolin mRNA is regulated by mitogen-activated protein kinase p38 and by tristetraprolin itself. *J Biol Chem.* 2004 Jul 30;279(31):32393-400

Tharun S, Muhlrad D, Chowdhury A, Parker R. Mutations in the Saccharomyces cerevisiae LSM1 gene that affect mRNA decapping and 3' end protection. *Genetics.* 2005 May;170(1):33-46.

Tong, J., Harrison, J. and Curthoys, N.P. The effect of metabolic acidosis on the synthesis s and turnover of rat renal phosphate-dependent glutaminase. *Biochem. J.* 1986 233:139-144.

Tucker M, Staples RR, Valencia-Sanchez MA, Muhlrad D, Parker R. Ccr4p is the catalytic subunit of a Ccr4p/Pop2p/Notp mRNA deadenylase complex in Saccharomyces cerevisiae.*EMBO J.* 2002 Mar 15;21(6):1427-36.

Uchida N, Hoshino S, Katada T. Identification of a human cytoplasmic poly(A) nuclease complex stimulated by poly(A)-binding protein. *J Biol Chem.* 2004 Jan 9;279(2):1383-91. Epub 2003 Oct 28.

van Dijk E, Cougot N, Meyer S, Babajko S, Wahle E, Seraphin B. Human Dcp2: a catalytically active mRNA decapping enzyme located in specific cytoplasmic structures. *EMBO J.* 2002 Dec 16;21(24):6915-24.

Vega MI, Huerta-Yepaz S, Garban H, Jazirehi A, Emmanouilides C, Bonavida B. Rituximab inhibits p38 MAPK activity in 2F7 B NHL and decreases IL-10 transcription: pivotal role of p38 MAPK in drug resistance. *Oncogene.* 2004 Apr 29;23(20):3530-40.

Viswanathan P, Ohn T, Chiang YC, Chen J, Denis CL. Mouse CAF1 can function as a processive deadenylase/3'-5'-exonuclease in vitro but in yeast the deadenylase function of CAF1 is not required for mRNA poly(A) removal. *J Biol Chem.* 2004 Jun 4;279(23):23988-95. Epub 2004 Mar 23.

Wang W, Liu LQ, Higuchi CM, Chen H. Induction of NADPH:quinone reductase by dietary phytoestrogens in colonic Colo205 cells. *Biochem Pharmacol.* 1998 Jul 15;56(2):189-95.

Wang, Z., Kiledjian, M. The poly-A biding protein and an mRNA stability protein jointly regulate an endoribonuclease activity. *Molec. Cell Biol.* 2000 20:6334-6341.

Wang Z, Jiao X, Carr-Schmid A, Kiledjian M. The hDcp2 protein is a mammalian mRNA decapping enzyme. *Proc Natl Acad Sci U S A.* 2002 Oct 1;99(20):12663-8.

Wagner BJ, DeMaria CT, Sun Y, Wilson GM, Brewer G. Structure and genomic organization of the human AUF1 gene: alternative pre-mRNA splicing generates four protein isoforms. *Genomics.* 1998 Mar 1;48(2):195-202.

Wek RC, Jiang HY, Anthony TG. Coping with stress: eIF2 kinases and translational control. *Biochem Soc Trans.* 2006 Feb;34(Pt 1):7-11.

Wilson GM, Brewer G. Identification and characterization of proteins binding A + U-rich elements. *Methods.* 1999 Jan;17(1):74-83.

Wilusz CJ, Wilusz J. Bringing the role of mRNA decay in the control of gene expression into focus. *Trends Genet.* 2004 Oct;20(10):491-7.

Wright, P.A. and M.A. Knepper. Glutamate dehydrogenase activities in microdisected rat nephron segments: Effects of acid-base loading. *Am. J. Physiol. 1990* 259, F53-F59.

Woost, P., Orosz, D., Jin, W., Frisa, P., Jacobberger, J., Douglas, J., and Hopper, U. Immortalization and characterization of proximal tubule cells derived form kidneys of spontaneously hypertensive and normotensive rats. *Kidney International.* 1996 50:125-134.

Xu N, Chen CY, Shyu AB.Versatile role for hnRNP D isoforms in the differential regulation of cytoplasmic mRNA turnover. *Mol Cell Biol.* 2001 Oct;21(20):6960-71.

Yamashita A, Chang TC, Yamashita Y, Zhu W, Zhong Z, Chen CY, Shyu AB. Concerted action of poly(A) nucleases and decapping enzyme in mammalian mRNA turnover. *Nat Struct Mol Biol.* 2005 Dec;12(12):1054-63.

Yaman I, Fernandez J, Sarkar B, Schneider RJ, Snider MD, Nagy LE, Hatzoglou M. Nutritional control of mRNA stability is mediated by a conserved AU-rich element that

binds the cytoplasmic shuttling protein HuR. *J Biol Chem.* 2002 Nov 1;277(44):41539-46.

Yang F, Peng Y, Schoenberg DR. Endonuclease-mediated mRNA decay requires tyrosine phosphorylation of polysomal ribonuclease 1 (PMR1) for the targeting and degradation of polyribosome-bound substrate mRNA. *J Biol Chem.* 2004 Nov 19;279(47):48993-9002.

Yu JH, Yang WH, Gulick T, Bloch KD, Bloch DB. Ge-1 is a central component of the mammalian cytoplasmic mRNA processing body. *RNA.* 2005 Dec;11(12):1795-802

Zielinski J, Kilk K, Peritz T, Kannanayakal T, Miyashiro KY, Eiriksdottir E, Jochems J, Langel U, Eberwine J. *In vivo* identification of ribonucleoprotein-RNA interactions. *Proc Natl Acad Sci U S A.* 2006 Jan 31;103(5):1557-62.